1993

Late Wisconsinan And Holocene Sedimentation Of Silverhope Valley, British Columbia

James Rodney Goff

LATE WISCONSINAN AND HOLOCENE SEDIMENTATION OF SILVERHOPE VALLEY, BRITISH COLUMBIA

by

James R. Goff

Department of Geology

Submitted in partial fulfilment
of the requirements for the degree of
Doctor of Philosophy

Faculty of Graduate Studies
The University of Western Ontario
London, Ontario
May 1993

ISBN 0-315-83990-2

Canada

ABSTRACT

Sixty eight bedrock and sediment exposures, six lake bottom cores, and twenty six bulk samples of river gravels were studied by various stratigraphic methods including: radiocarbon and caesium dating, tephrochronology and lithofacies analysis to interpret late Wisconsinan and Holocene deposits in the Silverhope Creek drainage basin.

Late Wisconsinan evidence suggests that during the downwasting and retreat of the Cordilleran Ice Sheet between approximately 11 500 and 11 000 years BP, there was one minor readvance and two smaller standstill/oscillations. During deglaciation a dead ice-dammed lake formed in front of the retreating ice mass. Partial lake drainage occurred initially by catastrophic flooding through dead ice into the contiguous Chilliwack valley over a low pass. Subsequent lake levels were controlled by dead ice decay, hummocky terrain, ice marginal drainage and height of the retreating ice mass. Final drainage occurred as a small outburst into the Fraser valley. Tributary glaciers appear to have retreated at different rates and to be, at times, temporarily covered by water.

Burial of Mazama tephra found in paraglacial alluvial fans suggests that following deglaciation, meltwater reworking of glacial sediments was more rapid on the west side of the drainage basin.

Landslide-damming (probably not seismic-generated) of Silver Lake appears to have taken place around 1100 A.D. Radiocarbon ages indicate that

sedimentation in the lake occurred at a rate of about 0.14 cm a^{-1} until 1946, with Silverhope Creek forming a delta into the southwest side of the lake. In 1946, diverted flows built a new delta into the southeast side of Silver Lake at the commencement of major logging activity and road construction around and to the south of Silver Lake. Caesium-137 traces indicate that post-1946 sedimentation rates have increased to approximately 2.75 cm a^{-1}. Rates do not appear to have declined significantly in the last twenty to thirty years.

Analysis of in-channel gravels from Silverhope Creek indicates that human activity (logging and road construction) has site specific influences on particle size distribution. However, most disequilibriums in the general trend of downstream fining have been inherited from previous glaciation and the landslide-damming of Silver Lake. A tentative model of Holocene sedimentation for this unique drainage basin indicates that sediment yield is both episodic (lake-forming mass movement event and human impact) and perhaps subject to climatic asymmetry.

ACKNOWLEDGEMENTS

The author wishes to convey his sincere appreciation to several individuals. First, I am deeply indebted to Stephen Hicock for his guidance, encouragement, financial and logistical support above and beyond the call of duty, and for the hours of patient assistance talking through all those problems associated with an ageing graduate student. John Clague (GSC), Bruce Thompson (MOF) and Russ Knutson (MOF) were all extremely helpful during my field research, and provided invaluable logistical support. Many thanks are due to Dr. Tark Hamilton at the PGC on Vancouver Is., who not only carried out Caesium analyses on my lake cores quickly and efficiently, but also gave me many helpful comments on the vagaries of this type of work. Similarly, Bob Barnett and Dave Kingston of microprobe fame were fountains of knowledge. Rick Linden, Lynne Strickland, and the M.V. Pilea were all an integral part of my field work and we now know a lot about getting boats out of lakes. Many geologic conundrums were solved during discussions with Jon Riedel, and numerous geographic and ecologic queries were answered by Jack Delair.

I am particularly indebted to the rangers from the North Cascades National Park and to the members of the Seattle City Light "team". I would like to thank Betty Delair for providing a welcome "home from home" in Hope during those few periods of civilised life. In Vancouver, Jack and Winnie Hicock offered an oasis of sanity during two hectic field seasons, for which I am extremely grateful.

Catherine Chagué has been a constant source of support; bread, cheese, wine, proof reading and encouragement, I will be forever in her debt. In the office, Olav Lian and Jon North provided hours of discussion, irreverent debate, beer and wine, they were essential to my sanity and I thank them. In a similar vein both Ian and the late Seguin Besch were definite humanising influences. I guess it needs to be said that my sanity was preserved by many, many games of squash - thanks are especially due to Don Boyes for all the hits received and given.

This thesis could never have completed without the support of my mother and brother back in the old country, they are always in my thoughts. To Kelly, a special thanks - for everything.

Finally, my thanks to the townsfolk of Hope, B.C., it wasn't exactly Rambo, but they tolerated another invasion without complaint.

This thesis was financially supported by an NSERC Grant, two UWO Vice President's Awards, and grants from the Habitat Conservation Fund and the Skagit Environmental Endowment Commission to Dr. S.R. Hicock. I would also like to acknowledge the support of the Pacific Geoscience Centre/Geological Survey of Canada for providing me with Caesium data from the Silver Lake cores.

TABLE OF CONTENTS

LIST OF TABLES

LIST OF FIGURES

LIST OF FIGURES (Continued):

LIST OF FIGURES (Continued):

LIST OF FIGURES (Continued):

LIST OF FIGURES (Continued):

LIST OF PLATES

LIST OF APPENDICES

CHAPTER ONE

INTRODUCTION

1.1. Purpose and Organisation

The purpose of this study is to interpret late Wisconsinan and Holocene deposits within the Silverhope Creek drainage basin (Figure 1.1) which has not been previously studied in detail; and to ascertain whether the depositional history of the valley has been punctuated by periods of disequilibrium (deglaciation, the landslide-damming of Silver Lake, and human disturbance (logging activity and road construction)).

Lithofacies analysis, glacial, fluvial and lacustrine geologic techniques, radiocarbon and caesium isotope analyses and tephrochronology are used to reconstruct paleosedimentary environments. Aerial photographs and maps were used to assist in morphological interpretation (Appendix IVc). Where necessary, descriptions of methodology are given in the Appendices, with a brief overview in Section 1.6.

68 slide scar, gravel pit, bedrock, river and road cut exposures; six lake bottom sediment cores and 26 bulk samples of on-bar river gravels were examined. Section localities are plotted on Figure 1.2. (See Appendix I for list of sections and elevation data; see Chapter Five for maps of lake bottom sediment core and Silverhope Creek in-channel gravel sample sites). Plates 1.1 and 1.2 provide aerial photographic coverage of the study area for comparison.

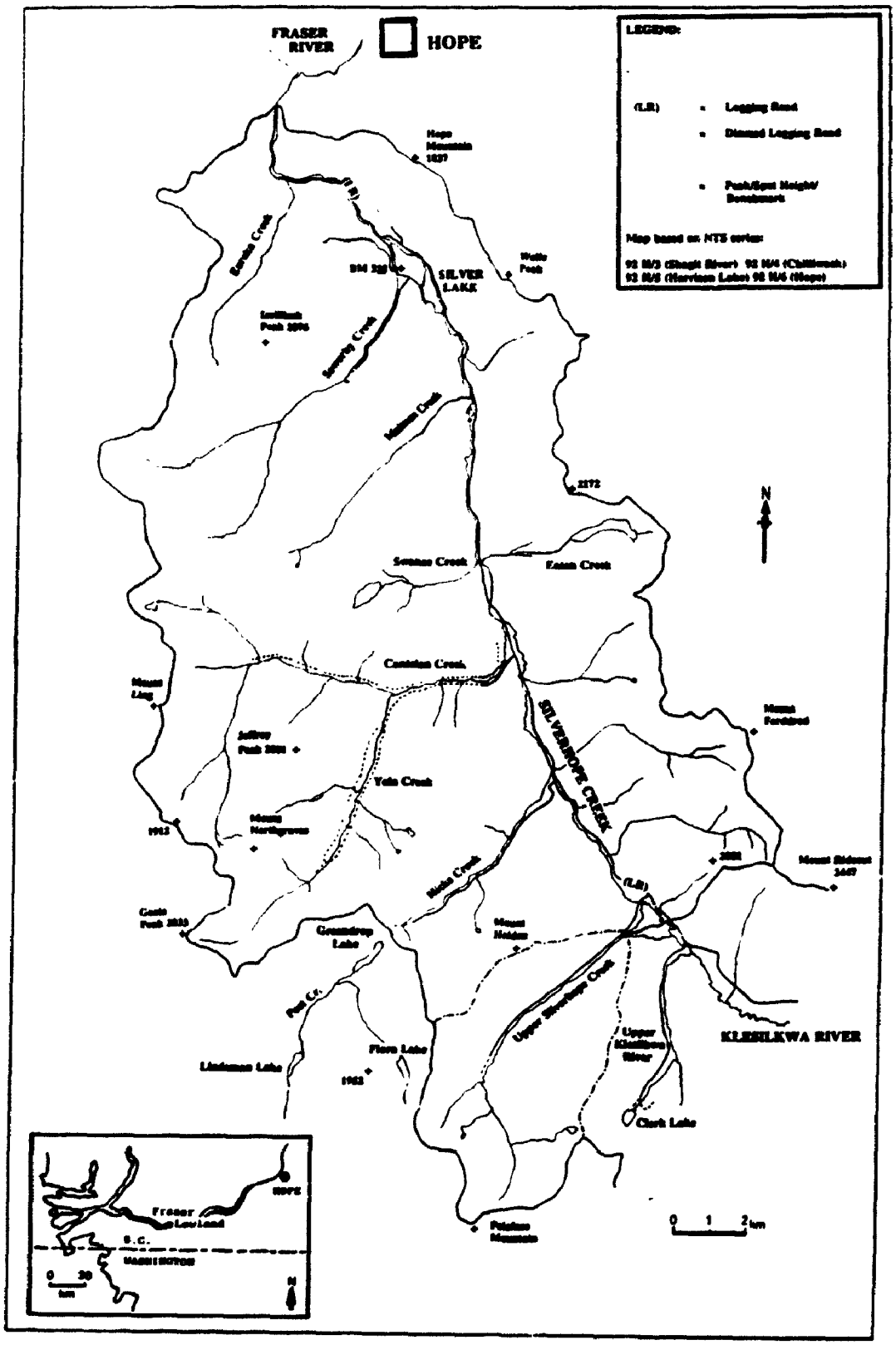

Figure 1.1 **SILVERHOPE CREEK DRAINAGE BASIN (Including portions of contiguous catchments discussed in the text, elevations in m)**

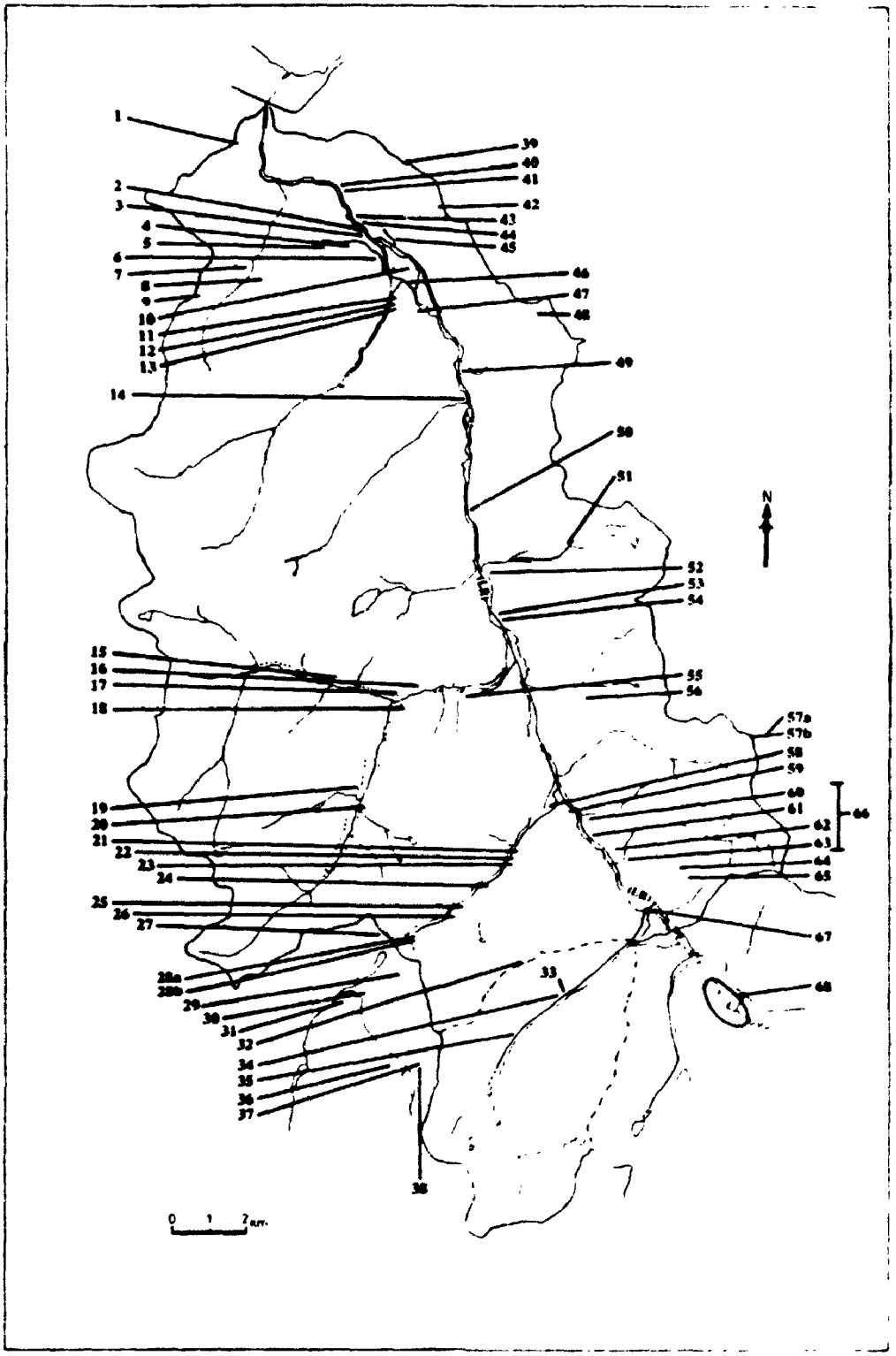

Figure 1.2 SILVERHOPE CREEK DRAINAGE BASIN - Location of study sites (see Figure 1.1 for legend)

Plate 1.1 AIRPHOTO MOSAIC OF SILVERHOPE BASIN (BC88073, 237 -238; BC88078, 266-267; Approximate Scale, 1 : 70 000)

Plate 1.2 AIRPHOTO OF NORTHERN PORTION OF SILVERHOPE BASIN
(BCB91079, 91; Approximate Scale, 1 : 60 000)

In this chapter the physical character of the study area is described and previous work is summarised. In Chapter Two, the sedimentary record of glaciation and deglaciation in the drainage basin are described. Chapter Three contains detailed site interpretations of information given in Chapter Two. Site interpretations are considered in a local and regional context of late Wisconsinan sedimentation in Chapter Four. The Holocene record is discussed in Chapter Five and concentrates on three main events, deposition of Mazama tephra, landslide-damming of Silver Lake, and recent human disturbance. Chapter Six comprises a brief summary and conclusions.

1.2. General Physiography

The northern Cascade Mountains possess the features typically associated with alpine glaciation. Nunataks and horns rise to a maximum of 2500 m and most of the land below 2000 m has been rounded by ice. Valleys in the region display deeply-eroded cross-sections and contain truncated spurs, arêtes and cirques (Saunders, 1986).

Silverhope valley trends approximately N-S along the Ross Lake Fault (Monger, 1989). The main valley is about 29 km long, and is occupied by Silverhope Creek which flows north into the Fraser River (Figure 1.1, Plates 1.1 and 1.2) near the town of Hope, a drainage area of approximately 320 km^2. At the southern end of the Silverhope drainage basin there is an area of poorly-drained, low-lying terrain. The valley system extends further south into the Skagit River basin, but this portion is occupied by the southward flowing Klesilkwa River

(Figure 1.1, Plate 1.1). Highland areas fringing the valley have a maximum elevation in excess of 2470 m (8100 ft) and would probably have risen above the Cordilleran Ice Sheet (Østrem, 1966; Waitt and Thorsen, 1983). Several tributary streams that feed Silverhope Creek have headwater lakes formed by glacial activity. The adjacent Chilliwack valley is connected by a low pass (about 1020 m) between Hicks Creek (part of the Silverhope drainage basin) and Post Creek (Chilliwack basin).

Silverhope Creek has a considerably steeper long profile than Klesilkwa River to the south with a mean main valley gradient of 0.023, as opposed to 0.005 for Klesilkwa. The longitudinal profile of the river has three generally concave sections 7 (Upper Silverhope Creek), 19, and 8 km long. The upper two sections (7 and 19 km in length) are separated by a 2.5 km convex alluvial fan situated where the headwaters enter the main valley. An intermediate base level is controlled by Silver Lake, which forms the headwaters for the final concave section (8 km in length). Drainage is characterized by steep, energetic mountain streams, in an environment that is inherently unstable. Although discharge data are not available for Silverhope Creek, the flow appears to exhibit alpine characteristics.

Adjacent Chilliwack valley appears to possess an analogous regime in which monthly and daily discharges are dominated by spring snowmelt. In general, maximum monthly and daily discharges occur in May and June, and minimum figures are recorded between October and April (Saunders, 1985). Storm runoff is an important influence on the short term regime of the lower

Chilliwack valley, causing some fluctuations from the general trend. In Silverhope valley, Silver Lake generally mitigates flood discharges, although breaching of lake ice dams in early spring have caused catastrophic outbursts, the most recent in 1990 (Hope Chamber of Commerce, 1991).

Silverhope Creek flows into Silver Lake, situated near the north end of the valley (Figure 1.1, Plate 1.1). This landslide-dammed lake possesses two deltas at its southern end, which reflect the effects of stream diversion following the commencement of logging activities within the valley (section 1.5.2.). To the north of Silver Lake, valley sides steepen and a marked 'V-shape' develops before valley mouth expansion into the Fraser valley. To the south of Silver Lake, the main valley possesses a marked 'U-shape', which widens adjacent to each major tributary valley confluence point, then gradually narrowing again between these points.

Tributary streams generally flow in steep bedrock-dominated channels incised through thick valleyside surficial deposits. No tributary has completely graded to the main Silverhope valley, and most issue, to varying degrees, from hanging valleys. Alluvial fans emanate from many of the major west valleyside tributaries, overlying late Wisconsinan deposits (Ryder, 1971a, b). (For future reference, when the term 'paraglacial' is used in this thesis for alluvial deposits laid down by flows emanating from non-glacial sources during the period immediately following deglaciation, when sediment supply exceeded flow competence). A few tributaries on the east side of Silverhope valley appear to

have deposited paraglacial alluvial fans, although much smaller in extent than their west valley counterparts.

All of the streams in the area carry abundant coarse bed load and fine suspended sediment. Bank stability is generally poor, although in the main valley it has been enhanced in places to protect the adjacent road. Tributary streams and the upper and lower reaches of Silverhope Creek still possess mainly single channel flow characteristics, primarily due to lateral confinement although recent logging activities have reduced bank stability. The 19 km central section exhibits patterns which vary from short reaches of single channelled flow to a braided regime. Aggradation immediately upstream of Silver Lake appears to be encouraging the development of a braided network.

1.3. Bedrock Geology

A bedrock map of the valley contains three dominant belts trending approximately NW/SE with some peripheral rock formations (Monger, 1989); (Figure 1.3.). The oldest rocks in the study area are probably late Palaeozoic/early Mesozoic ultramafic rocks of the Hozameen Complex, which form the southeast valley side and valley floor. They have been intruded by early Tertiary granodiorite which comprise the majority of the east valley side.

The west valley side is defined by the Ross Lake Fault. The Custer Gneiss complex, situated to the west of the fault, comprises mainly pegmatitic granite gneiss and pelitic schist, and appears to have originated from regional metamorphism of the Hozameen strata (McTaggart and Thompson, 1967). Custer

Q. Quaternary	Thick drift; alluvium; glaciofluvial and lacustrine deposits, till, colluvium, landslides
1. Miocene - Mgd	Granodiorite (MOUNT BARR BATHOLITH)
2. Oligocene - Ogd	Granodiorite (CHILLIWACK BATHOLITH)
3. Eocene a. Egd b. Es	Granodiorite (NEEDLE PEAK, MOUNT OUTRAN PLUTONS) PRINCETON GROUP: Sandstone, conglomerate, argillite (includes ALLENBY FORMATION OF PRINCETON GROUP)
4. Early Tertiary - eTgd,i	Intrusions of granodioritic (gd) and intermediate (i) composition
5. Cretaceous and/or Tertiary a. KTc b. Ms	CUSTER GNEISS: pegmatitic granite gneiss; pelitic schist and amphibolite, minor marble and ultramafic rocks Garnet-biotite, staurolite, kyanite and sillimanite schist (in part, SETTLER SCHIST), local amphibolite, minor ultramafic rock and siliceous schist
6. Late Early, Early Late Cretaceous - Kp	(a) undifferentiated sandstone, conglomerate, argillite; (b) 'winthrop facies': probably a non-marine facies equivalent of the upper part of the JACKASS MOUNTAIN GROUP
7. Early, Middle Cretaceous a. Kj b. Kgd,d	JACKASS MOUNTAIN GROUP Sandstone, argillite, conglomerate; marine and non-marine; upper part is probably facies equivalent of PASAYTEN GROUP Quartz granodiorite (gd), diorite (d), (SPUZZUM PLUTON); local gneissic phases
8. Late Jurassic and Early Cretaceous - JKg	Muscovite-biotite granite and pegmatite (EAGLE PLUTONIC COMPLEX)
9. Early and Middle Jurassic a. Jl b. JD	LADNER GROUP Argillite, slate, siltstone, tuff; includes minor amounts of Upper Jurassic sandstone and conglomerate, possibly correlative with 'Thunder Lake sequence' DEWDNEY CREEK FORMATION of LADNER GROUP: sandstone, argillite; local mafic to intermediate volcanics
10. Late Triassic and/or Early Jurassic a. Tjgd	Granodiorite (gd) (ALLISON LAKE, BROMLEY, CAHILL CREEK PLUTONS, part of MOUNT LYTTON COMPLEX)
b. Tjd	Small dioritic plutons in NICOLA GROUP; diorite and amphibolite of MOUNT LYTTON COMPLEX: dioritic HEDLEY INTRUSIONS
11. Triassic - PMu	Ultramafic rock, local gabbro
12. Permian to Jurassic a. PJH b. PJHv	HOZAMEEN COMPLEX Undifferentiated chert, pelite, limestone, gabbro and ultramafic rock Mafic volcanics
c. PJBr	BRIDGE RIVER COMPLEX Siliceous and chlorite schist, phyllite; correlative with HOZAMEEN COMPLEX but west of Fraser River
d. Pju	Ultramafic rock and local gabbro, associated with HOZAMEEN and BRIDGE RIVER COMPLEXES
	Approximate Geologic Boundary

N.B. A Late Cretaceous granodiorite of the Skuzzy Pluton (lKgd) appears on the map, but not in the legend which details bedrock types relevant to clast provenance data only (lKgd was not found).

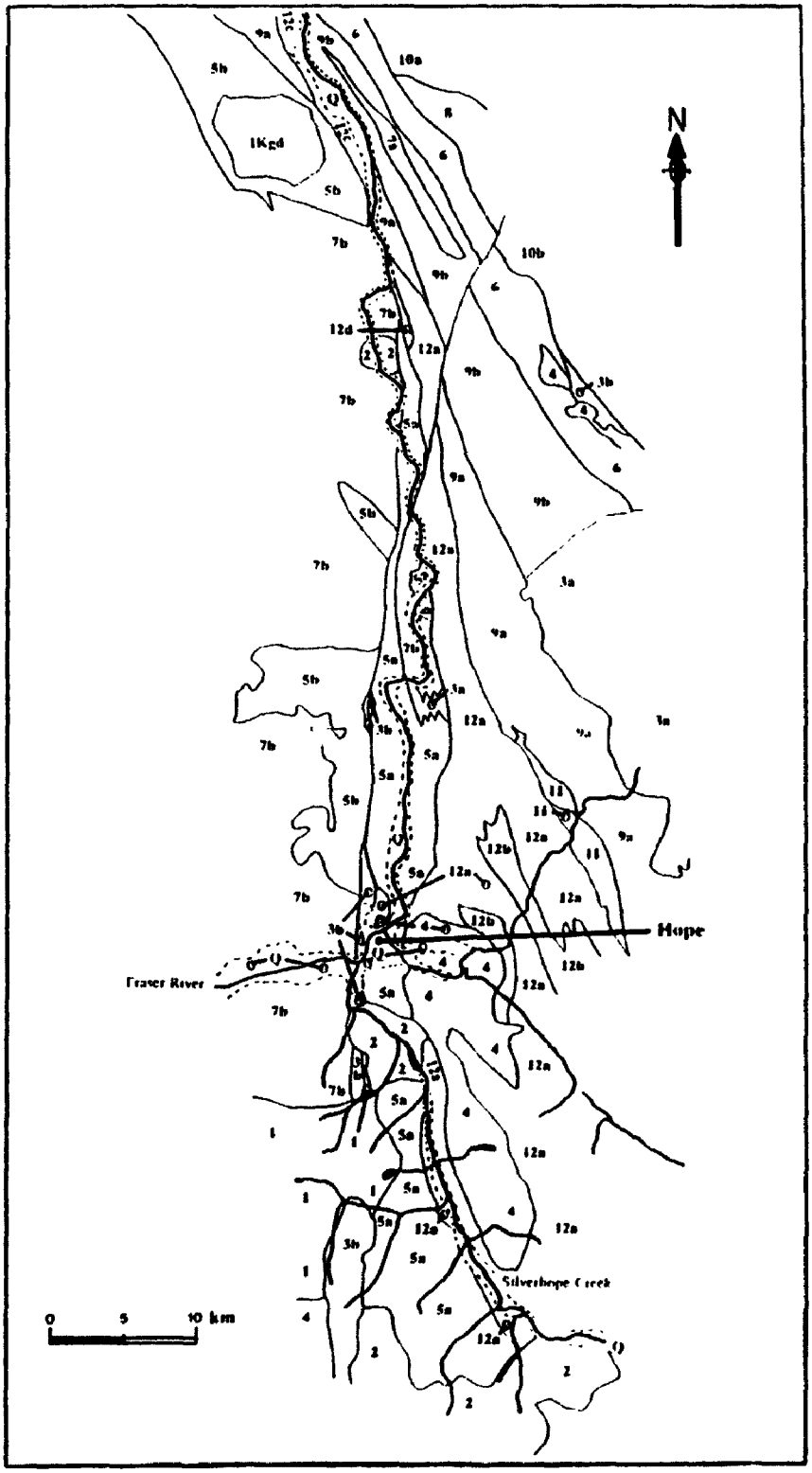

Figure 1.3 HOPE AREA - Simplified Bedrock Geology and Legend (based on Monger, 1989)

rocks are probably derived from early Mesozoic, and possibly Palaeozoic and Precambrian rocks, and were metamorphosed in the late Cretaceous and early Tertiary Periods. The Spuzzum Pluton (late Cretaceous), comprises quartz diorite, diorite and granodiorite, and is situated to the northwest. Custer Gneiss and Spuzzum Pluton are of similar age but separated by a N-S trending thrust fault, preserving conglomerates and argillite of the Allenby Formation (Eocene). Later intrusions by the Chilliwack (Oligocene granodiorite) and Mount Barr Batholiths (Miocene granodiorite) comprise the remainder of the fault-bounded western side of the drainage basin.

1.4. Surficial Geology

Unconsolidated Late Wisconsinan and Holocene sediments occur throughout the study area and are preserved on the main valley sides, in tributary valleys, and as a thick valley fill upstream of Silver Lake. Mass wasting is active within the study area, particularly in the recently-logged headwater valleys and main valley sides (Plate 1.1). Ancient mass movement activity, mainly debris avalanches, are evident in several main valley locations and are discussed below.

1.5. Previous Research

1.5.1. Late Wisconsinan and Early Holocene

1.5.1.1. Regional

A simplified stratigraphic history of the Fraser Lowland since the middle of the late Wisconsinan (16 000 years BP) is given in Table 1.1. This information is

^{14}C Years BP ($x10^3$)	Chronostratigraphic Units	Geologic - Event Units		Lithostratigraphic Units	
0 -				Salish Sediments	
5 -	Holocene	Postglacial			
10 -				Capilano Sediments	Sumas Drift
			Sumas Stade		
12 -			Everson Int.		Ft. Langley Fm.
14 -	Late Wisconsin	Fraser Glaciation	Vashon Stade	Vashon Drift	
16 -					

Table 1.1 LATE WISCONSINAN AND HOLOCENE STRATIGRAPHY OF THE FRASER LOWLAND (modified after Clague, 1989)

largely derived from work carried out in the central and western Fraser Lowland, although some notable data have been included from the lower Fraser canyon (Mathewes *et al.*, 1972).

Silverhope valley is just south of the Fraser Lowland, and it has long been recognised that the use of the time divisions listed in Table 1.1 outside the Fraser Lowland is dubious (Clague, 1981; Hicock *et al.*, 1982). However, interactions between the Silverhope and Chilliwack valleys caused by Cordilleran Ice Sheet decay necessarily link the study area to the Fraser Lowland regime. However, Silverhope valley may possess a less complex stratigraphic history similar to south-central British Columbia (Fulton and Smith, 1978).

Many authors have provided comprehensive summaries of the Quaternary geology of the general region (Armstrong *et al.*, 1965; Crandell, 1965; Richmond *et al.*, 1965; Armstrong, 1981; Clague, 1981; Waitt and Thorson, 1983; Hicock and Armstrong, 1985; Saunders *et al.*, 1987; Jackson and Clague, 1991; Ryder *et al.*, 1991) which is briefly recounted below.

Immediately prior to the time interval covered by this study, Cordilleran ice retreated from a maximum coverage stretching as far as Olympia, Washington (Heusser, 1973), at which time it reached a height of up to 2100 masl in the Fraser Lowland (Mathews *et al.*, 1970). During the Everson Interstade (13 000 - 12 000 years BP) most of the Fraser Lowland was ice-free, with only the eastern part occupied by a piedmont lobe (Armstrong, 1981). Complex subaerial and submarine ice margin fluctuations are recorded in the deposits of the Capilano Sediments and Fort Langley Formation at this time.

Desloges and Gilbert (1991) found no evidence for inundation by the sea recorded within Harrison Lake sediments even though Armstrong (1981) proposed a sea level rise of up to 200 m. However, Gilbert and Desloges (1992) reported possible glaciomarine sediments in Stave Lake approximately 30 km to the southwest. Clague (1981) suggested that the absence of marine clay overlying Sumas Drift shows that the land had emerged prior to sea level rise in that area. It is also possible that the piedmont glacier effectively blocked the Fraser Lowland somewhere between Harrison Lake and Fort Langley.

At approximately 12 000 - 11 500 years BP a minor ice readvance occurred, terminating in the Fraser Lowland near Sumas, Washington. Clague (1981) doubted whether this could be termed a stadial period since it appears to have occurred only locally. The Sumas Stade may have been a minor advance induced by the grounding of the ice lobe as sea level dropped, and not from climatic change. Estimating the time taken for ice retreat, standstills and ice margin oscillations from this final maximum has become a major problem in interpreting the deglaciation of the region. Radiocarbon ages offer apparently conflicting evidence about ice conditions at this time (Table 1.2).

Broecker & Kulp (1957) provided a radiocarbon age for Sumas Drift near Mission of 11 950 $\pm$ 200 years BP (L-331C). Additional data from Mission, Cultus Lake and Abbotsford indicate that ice was still present, albeit possibly stagnant, until as late as approximately 11 000 years BP (Armstrong, 1960). However, South (1989) found ice-free conditions in the southeast Coast Mountains as early as 12 255 $\pm$ 770 years BP (at 838 masl) and 11 485 $\pm$ 185 years BP (at 1060 masl),

No.	^{14}C ages (years BP)	Laboratory No.	Locality	Source
1	11 000 ± 170	I-6068	Pinecrest Lake, Nr. Yale	Mathewes *et al.*, 1972
2	11 000 ± 900	L-221E	Near Abbotsford	Lowdon and Blake, 1973
3	11 140 ± 260	I-5346	Squah Lake, Nr. Yale	Mathewes *et al.*, 1972
4	11 300 ± 100	GSC-2623	Cultus Lake	Lowdon and Blake, 1973
5	11 400 ± 140	GSC-3308	Sleese Cr., Chilliwack	Saunders *et al.*, 1987
6	11 430 ± 160	I-6067	Pinecrest Lake, Nr. Yale	Mathewes *et al.*, 1972
7	11 485 ± 185	S-2935	Kokwaskey Lake, SE coast Mts.	Souch, 1989
8	11 600 ± 280	GSC-1675	Near Abbotsford	Lowdon and Blake, 1975
9	11 700 ± 100	GSC-2966	Sleese Cr., Chilliwack	Saunders *et al.*, 1987
10	11 950 ± 200	L-331C	Mission	Broecker & Kulp, 1957
11	12 285 ± 770	S-3010	Kwoiek Lake, SE Coast Mts.	Souch, 1989

Table 1.2 RADIOCARBON AGES RELEVANT TO THE DEGLACIATION OF THE EASTERN FRASER LOWLAND-HOPE AREA

Mathewes *et al.* (1972) found similar cases in the Fraser Canyon between 11 430 ± 150 years BP and 11 000 ± 170 years BP (at 320 masl). To account for these apparent anomalies, it has been suggested that there was another ice source for the Fraser Lowland (Roberts and Mark, 1970; Armstrong *et al.*, 1971). Clague (1989) considers the most popular possibility, the Cascades, unlikely because the lower Chilliwack valley became ice-free by 11 700 ± 100 years BP, prior to ice retreat in the Fraser Lowland (Saunders *et al.*, 1987). Two subsequent minor advances by the main Fraser valley ice into the lower Chilliwack valley have been recorded at about 11 500 and 11 200 years BP (Saunders *et al.*, 1987). Recognition of minor readvances and ice-free conditions in the area is hampered by the paucity of dateable material in many valleys. It is likely that many of the smaller valleys were not ice-free long enough for vegetation to develop, a problem encountered in the Silverhope.

The Fraser River appears to have been completely ice-free by 11 000 years BP or soon after. Ice-free conditions existed north of Pemberton by 10 600 years BP (Mathewes and King, 1989) and the climate was as warm as today by approximately 9 120 years BP (Clague *et al.*, 1987). Rapid ice retreat, at rates of up to 50-100 km in 300 years is suggested by this evidence (Clague, 1981; Ryder *et al.*, 1991). Most of the preserved depositional units in the region are the products of this unusual, short-lived event, which is catastrophic in a geological sense (Clague, 1986). Swanson and Pankaj (1992) are currently attempting to resolve this problem of apparently non-synchronous ice retreat. They are calculating Chlorine-36 ages of samples taken from erratics and eroded bedrock

associated with the Puget and Okanogan lobes of the Cordilleran Ice Sheet, and with alpine glaciers in the eastern Cascades.

These events appear to have been triggered by rapid climatic amelioration (Clague, 1989). Deglaciation occurred by downwasting, frontal retreat and stagnation, starting in the ice marginal mountain ranges (Davis and Mathews, 1944; Mathews, 1944; Fulton, 1967; Slaymaker and McPherson, 1977; Clague, 1981; Saunders 1985). While the downwasting process has been shown to be significant in both the north Cascade and east Coast Mountains, researchers have not demonstrated a similar process for the main Fraser Lowland ice. Downwasting may explain active, stagnant and dead ice deposits over considerable distances, accounting for apparently anomalous radiocarbon ages and rapid ice "retreat".

Postglacial sedimentation has consisted mainly of fluvial and mass movement reworking of glacial deposits. A central problem in denudation processes in a watershed is the role of sediment storage between point of provenance and mouth of basin (Meade, 1982). Rapid aggradation generated by abundant sediment supply led to the development of floodplains, alluvial fans and lacustrine deposits during a period of prolonged paraglacial activity (Ryder, 1971a; b; Church and Ryder, 1972; Clague *et al.*, 1987). Mazama tephra is normally found within the top 2 to 3 m of regional deposits indicating that the majority of this deposition occurred prior to 6.8 ka (Ryder, 1971a; Church and Slaymaker, 1989). Clague (1981) suggested that initial postglacial resedimentation had waned within a few hundred years of deglaciation because of slope

stabilisation by vegetation. A second phase of "paraglacial activity" was generated by declining sediment input and a drop in base level with isostatic rebound. Massive downcutting and terracing washed sediments into the major lowland valley systems and generally marked the end of paraglacial activity in upland valleys (Church and Slaymaker, 1989).

1.5.1.2. Local

General reconnaissance of surficial deposits has been carried out in most major valleys of Canada and the United States. While Daly (1912) omitted Silverhope valley from his examination of the geology of the North American Cordillera at the forty-ninth parallel, he recognised the significance of a "bouldery recessional moraine" in the adjacent Chilliwack valley. Cairnes (1924) carried out a cursory reconnaissance, concurring with Daly (1912) that ice thickness had been about 1200-1500 m at the height of glaciation.

The "bouldery recessional moraine" in Chilliwack valley was later identified as a catastrophic flood deposit originating from the Silverhope valley (Munshaw, 1976). More recently, Gourlay (1977), Clague and Luternauer (1982), and Saunders (1985) working in the Chilliwack valley, have proposed alternative theories for the origin of the catastrophic flood deposit. Saunders' (1985) study of Chilliwack valley is the only detailed Quaternary and/or Holocene sedimentary study carried out in this region of the Cascade Mountains. He tentatively suggested that an ice-dammed lake formed in the Silverhope valley between ice

masses advancing in opposite directions; Skagit ice from the south-east and Silverhope ice from the north-west. To date, this problem remains unsolved.

Minor readvances of Fraser Lowland ice into lower Chilliwack valley appear to have occurred about 11 500 and 11 200 years BP, in a complex environment at the margin of the Cordilleran Ice Sheet. These results add to a growing number of studies which indicate that minor regional ice readvances were generally non-synchronous or localised (Armstrong *et al.*, 1965; Armstrong, 1981; Hicock *et al.*, 1982; Saunders *et al.*, 1987).

To the east of Silverhope valley, a complex valley system exists, comprising the Sumallo River, Nicolum Creek and Skagit River. Mathews (1968) reported a westerly diversion of meltwater by the Cordilleran Ice Sheet in an area immediately to the southeast of Silverhope valley.

To the south, Barksdale (1941) provided evidence of regional glaciation up to 7260 ft. This concurs with Waitt and Thorson (1983) who concluded that the Chilliwack valley was covered by ice up to an elevation of 2000 m thick at the peak of the Fraser Glaciation, and Østrem (1966) who proposed a local ice elevation of approximately 2000 m.

Waitt and Thorsen (1983), working mainly to the south, proposed that the Silverhope was the first valley in the Cascades Range adjacent to the Fraser Lowland that was not influenced by late Wisconsinan sea level fluctuations. Ice flowed down the Silverhope and Skagit valleys and was confined by their narrow walls causing a local increase in ice thickness to 2600 m at the International border (Waitt, 1977). Researchers generally agree that the Skagit valley north of

Ross Lake acted as a confluence point for several valley glaciers (Barksdale, 1941; Weis, 1969; Waitt, 1972). However, in the late sixties and early seventies there was some debate concerning the direction of ice sheet movement. Weis (1969) and Coates (1974) both proposed a north-flowing ice sheet. Weis (1969) envisioned the ice emanating from the Ross Lake basin and flowing north through the Klesilkwa-Silverhope pass into the Fraser River at Hope. Coates (1974) suggested a Hozameen Ice Sheet terminating in the Hozameen Range to the east of Silverhope valley. Waitt (1977) highlighted the inconsistencies of those proposals based on limited research in the Klesilkwa-Silverhope pass identifying numerous north-derived erratics from the Spuzzum Pluton (Figure 1.3). He concluded that the pass had channelled ice to the south, and had probably been shaped by it.

There is almost a complete absence of any local research on paraglacial sedimentation, except for Saunders (1985) who made brief mention of some features in Chilliwack valley. Reference is made to terraces formed by lower valley lake drainage, a temporary mid-valley lake formed by landslide-damming, and a poorly-defined upper valley delta. Paraglacial deposits in Silverhope valley remained unexamined until now.

1.5.2. Mid- and Late Holocene

Post-paraglacial sediments in the Silverhope region consist mainly of mass movement, lacustrine and fluvial deposits. Little research has been carried out in the immediate Silverhope area, although the Hope Slide in the adjacent eastern

valley is an exception. Mathews and McTaggart (1978) identified two minor earthquakes immediately prior to the slide and discussed possible seismic triggering. Many areas of the Canadian Cordillera are prone to slope failure and mass movements because of the combined effects of geological weakness, glacial oversteepening of slopes, high precipitation and seismic activity (Eisbacher, 1979; Brooks and Hickin, 1991; Evans and Brooks, 1991). In recent years human-use of mountain environments has increased in British Columbia. This region has a high hazard potential for rapid slope failures, damming of drainage systems, and eventual dam failures (Eisbacher and Clague, 1984; Gallino and Pierson, 1985; Butler *et al.*, 1991). Failures of landslide-dammed lakes have cost lives and produced considerable property damage (Schuster and Costa, 1986; Hope Chamber of Commerce, 1991).

Several landslide-dammed lakes have been identified in the region and these may have been formed by seismic-generated landslides (Adams, 1981; Swanson *et al.*, 1986; Costa and Schuster, 1988). It has been suggested that some of these lakes in the Olympic Mountains area, about 250 km southwest of Silver Lake, were products of a large earthquake which occurred in the Seattle area sometime between 1000 and 1100 years ago (Logan and Schuster, 1991). Subaqueous mass movement structures preserved in such lakes are proving to be useful for dating seismic events (Sims, 1975; Doig, 1986; 1990; 1991). However, identification of seismic-generated events by morphology alone (without an historical record) is still controversial (Sims, 1975; Clague *et al.*, 1989). Recent

work by Clague and Shilts (in press) suggests that the formation of Silver Lake may just postdate the Seattle event (Section 5.5.2.).

In forested mountain areas, rapid slope failures have a recurrence rate 6.5 times greater on logged slopes (Slaymaker and McPherson, 1977). In Oregon, suspended sediment increased 40% over 4 years in a catchment 25% patch-cut, mainly due to local mass movement near forest roads, but after an 80% clear-cut it increased three-fold (Beschta, 1978). Similar effects on sediment yield and mass movement activity have been reported in several lowland areas primarily due to reduced bank stability and water release brought about by root and biomass removal (Pierce *et al.*, 1973; Trimble, 1975; Trimble and Lund, 1982). Furthermore, deforestation releases overburden pressure and decreases substrate cohesion.

It is generally accepted that even controlled logging in forested catchments increases sediment yield and peak discharge significantly, although the effect may be relatively short-lived if regrowth is rapid (Sopper & Lynch, 1973; Langford, 1976).

Considerable controversy has been generated by logging activities, and Judge Kroninger's ruling over forest logging and related sediment problems in California is indicative of the debate (from Wolman, 1977):

> "While numerous expert witnesses in the field of geology, forestry, engineering and biology were presented, their conclusions and the opinions they derived from them are hopelessly irreconcilable on such critical questions as how much and how far solid particles will be moved by any given flow of surface water. They were able to agree only that sediment will not be transported upstream."

This situation normally arises because of limited data available for analysis, but the well preserved late Holocene sedimentary record of the Silverhope valley should permit less controversial conclusions to be drawn.

Desloges and Church (1987) found that alluvial processes in the Bella Coola River, B.C., were controlled by sediments which had accumulated by late glacial and Holocene events. In British Columbia generally, the problems associated with mass movement and logging are exacerbated by, or subordinate to, a regional topography, gross valley form, and boundary sediments inherited from the past glaciation (Church and Slaymaker, 1989; Brown, 1990; Jordan and Slaymaker, 1991). This inheritance exerts a certain degree of spatial control over Holocene fluvial processes on a drainage basin scale, as part of what Ferguson (1981) terms 'persistent passive disequilibrium'.

An inherent part of this disequilibrium are fluctuations in the downstream decrease of particle size. In western Canada, different sedimentation processes (tributary input, past glaciations and logging activities) play a crucial role in determining the degree of downstream fining (Church and Gilbert, 1975; Dawson, 1988). In some cases these processes can be sufficient to cause downstream particle size increase (Fahnestock, 1963; Bradley *et al.*, 1972), especially in glaciated mountain areas of British Columbia and Alberta (Kellerhals, 1982; Shaw and Kellerhals, 1982; Dawson, 1988). In general, mountain valleys in western Canada have inherited downstream changes in particle size related to major depositional events of the past (Shaw and Kellerhals, 1982).

Jackson and Clague (1991) summed up the problems of Late Wisconsinan and Holocene research by stating that:

> "In order to understand the significance of past glaciations, mass movement activity, fluvial processes and modern land-use practices, sedimentary sequence studies in mountain valleys require an interdisciplinary 'basin analyses' approach".

This is what is attempted in this thesis for the Silverhope drainage basin.

1.6. Methodology

Sedimentary sequences were defined using structural elements (bedding, fissility, fractures and folds), texture, provenance, lateral continuity, paleodirectional indicators, contacts, altitude and age (radiocarbon ages and caesium dating - see Appendix IV); (cf. Goudie, 1981; Gardiner and Dackombe, 1983). Systematic classification and description of measured sections followed the basic guidelines of Miall (1978) and Eyles *et al.* (1983). Altitude (in metres above sea level) is shown on the left side of facies diagrams in Chapter Two.

Particle size was determined using the Wentworth Classification. Laboratory analysis was carried out by the sieve and hydrometer method (ASTM, 1972). For samples with large clasts, field sieving was carried out on the coarse fraction greater than 8 mm. Samples were dried on tarpaulins and measurements were taken using a particle size template (256 mm - 8 mm) and weighed on field scales accurate to the nearest tenth of a gram. Sample size criteria were:

a) < 2 mm size fraction - 100 g samples were analysed by hydrometer.

b) > 2 mm size fraction - sample weights were based on bulk sampling standards established by Church *et al.* (1987), and Yuzyk (1986). Logistical constraints prohibited statistically significant weights to be gathered for samples with a largest particle size ranging from 180-256 mm (180-400 kg), although more than 100 kg were analysed in each case.

Data were processed using Lotus 1-2-3 and Planperfect 5.0 spreadsheets, and particle size distributions were produced for sand-silt-clay and gravel-sand-mud comparisons. Individual phi-size percentage distributions were also produced. Accurate identification of clast provenance was achieved by matching samples with data provided by J.W.H. Monger (GSC) in Vancouver and by petrographic microscopy. Where possible, at least 50 clasts were analysed from each unit. Graphic interpretation of granulometric analyses were prepared using Grapher. Paleodirectional indicators and fabric data were amalgamated in summary form for diagrammatic display adjacent to section models (summary data are detailed in Appendix II). Fabric measurements were taken from both diamictons and gravels. A base diagram incorporating fabric data was prepared using Stereo software (McEachran, 1988). This plot represents equal area, lower hemisphere spherical projections of points plotted within 10% density areas. Where recorded, poles to fracture planes are indicated on the plot (general paleomovement direction is indicated on the circumference). For sites possessing paleomovement indicators only, annotated rose diagrams are used.

CHAPTER TWO

LATE WISCONSINAN SITES

2.1. Introduction

This chapter systematically describes the major exposures of late Wisconsinan and early Holocene deposits in the Silverhope drainage basin. Study sections and their elevations are listed in Appendix I, relevant map locations are shown in Figure 1.2. Lithofacies coding, texture and contact illustrations, the sedimentary and fabric structure system, and rose diagram legend are detailed in Tables 2.1, 2.2, 2.3 and 2.4, respectively. Stratigraphic models (including general paleomovement direction and altitude) and annotated rose diagrams are presented in the text (Figures 2.1a - 2.1ba). Summaries of paleodirection and particle size data are detailed in Appendices II and III respectively. Pebble source lithology information is given in Table 2.5. (reference is made in the text to the legend abbreviations, e.g. Ogd; and their reference number, e.g. Ogd - 2).

The term 'dropstone' is used in some site descriptions for both interpretation and description. This refers to clasts that appear to have been released from ice (floating iceberg or ice margin) into standing water. These are normally subrounded, appear to either be imbedded in underlying sediments or to have downwarped them, and overlying sediments may drape the clast. They sometimes possess striae on either upper or lower surfaces or both. The term is used to differentiate observed features from either boulder scours (Shaw, 1983) or clasts (usually angular) deposited from snow-avalanches onto lake ice in winter

GENERAL CLASSIFICATION	
D	Diamicton
F	Fines (silt and clay)
G	Gravel
Gy	Gyttja
IMB	Imbrication
Maz	Mazama tephra
Org	Organics
S	Sand
COARSE-SEDIMENT SUBSCRIPTS	
Dmm	Matrix-supported massive diamicton
Gcf	Clast-supported foreset gravel
Gcm	Clast-supported massive gravel
Gcp	Clast-supported gravel, planar cross-stratification
Gcs	Clast-supported stratified gravel
Gmm	Matrix-supported massive gravel
Gms	Matrix-supported stratified gravel
FINE-SEDIMENT SUBSCRIPTS	
Sc/Fc	Channel/scour fills
Sf	Foreset sand
Sh	Horizontal stratification
Sm/Fm	Massive
Sp	Planar cross-stratification
Sr	Ripples
Ss	Stratified
S-d/F-d	Containing dropstones
Fl	Laminated
SORTING	
WS	Well sorted
MS	Moderately sorted
PS	Poorly sorted
ROUNDING OF CLASTS	
R	Rounded
SR	Subrounded
SA	Subangular

Table 2.1 Lithofacies Coding (modified after Miall, 1978; Eyles *et al.*, 1983)

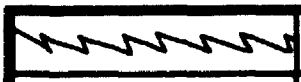	Interbedded	Contacts
	Loaded	
	Erosional	
	Conformable	
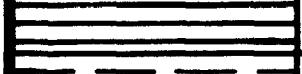	Clay, silt	Predominant Textures
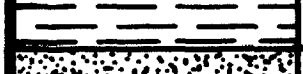	Silt, fine sand	
	Fine and medium sand	
	Medium and coarse	
	Pebble gravel	
	Cobble and boulder gravel	
	Diamicton	

Table 2.2 **Textures and Contacts**

	Paleoflow direction
▪	Pole to shear surface
+ 1000 ± 70	Wood sample, with ^{14}C age
• 1964	Gyttja sediment with ^{137}Cs age
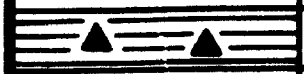	Interbedded unit (example)
U U	Deformation structures
● ● ●	Dropstones
	Channel scour/fill (example)
	Lens (example)
	Irregular/wavy bedding
	Cross-bedding
	Foreset bedding
	Horizontal bedding
	Organics in general
	Gyttja
+ + +	Tephra

Where interbedded units are too thin to portray diagrammatically they are shown as superimposed textures.

N.B. Paleoflow arrows inferred from Rose Diagram data (Table 2.5 and Appendix II) for Sites 3 - *Unit 4a/4b* and 20 - *Unit 1* are shown on the rim of the respective stereonets. Differences in inferred paleoflow direction are noted in the text.

Table 2.3 Sedimentary and Fabric Structure System

Striae are grouped in 5° intervals:	
striae on top surface - Nt (open)	----
striae on bottom surface - Nb (filled)	___
OTHER FEATURES:	
Boulder mounds	O
Chattermarks (one set)	C
Clay smudges (thickest end)	©
Paleoflow (ice/meltwater) direction	⇨
Stoss end of Stoss/lee feature (one)	●

Table 2.4 Rose Diagrams - Legend

Q. Quaternary	Thick drift; alluvium; glaciofluvial and lacustrine deposits, till, colluvium, landslides
1. Miocene - Mgd	Granodiorite (MOUNT BARR BATHOLITH)
2. Oligocene - Ogd	Granodiorite (CHILLIWACK BATHOLITH)
3. Eocene a. Egd b. Ea	Granodiorite (NEEDLE PEAK, MOUNT OUTRAN PLUTONS) PRINCETON GROUP: Sandstone, conglomerate, argillite (includes ALLENBY FORMATION OF PRINCETON GROUP)
4. Early Tertiary - eTgd,i	Intrusions of granodioritic (gd) and intermediate (i) composition
5. Cretaceous and/or Tertiary a. KTc b. Ms	CUSTER GNEISS: pegmatitic granite gneiss; pelitic schist and amphibolite, minor marble and ultramafic rocks Garnet-biotite, staurolite, kyanite and sillimanite schist (in part, SETTLER SCHIST), local amphibolite, minor ultramafic rock and siliceous schist
6. Late Early, Early Late Cretaceous - Kp	(a) undifferentiated sandstone, conglomerate, argillite; (b)'winthrop facies': probably a non-marine facies equivalent of the upper part of the JACKASS MOUNTAIN GROUP
7. Early, Middle Cretaceous a. KJ b. Kgd,d	JACKASS MOUNTAIN GROUP Sandstone, argillite, conglomerate; marine and non-marine; upper part is probably facies equivalent of PASAYTEN GROUP Quartz granodiorite (gd), diorite (d), (SPUZZUM PLUTON); local gneissic phases
8. Late Jurassic and Early Cretaceous - JKg	Muscovite-biotite granite and pegmatite (EAGLE PLUTONIC COMPLEX)
9. Early and Middle Jurassic a. Jl b. JD	LADNER GROUP Argillite, slate, siltstone, tuff; includes minor amounts of Upper Jurassic sandstone and conglomerate, possibly correlative with 'Thunder Lake sequence' DEWDNEY CREEK FORMATION of LADNER GROUP: sandstone, argillite; local mafic to intermediate volcanics
10. Late Triassic and/or Early Jurassic a. TJgd b. TJd	 Granodiorite (gd)(ALLISON LAKE, BROMLEY, CAHILL CREEK PLUTONS, part of MOUNT LYTTON COMPLEX) Small dioritic plutons in NICOLA GROUP; diorite and amphibolite of MOUNT LYTTON COMPLEX: dioritic HEDLEY INTRUSIONS
11. Triassic - PMu	Ultramafic rock, local gabbro
12. Permian to Jurassic a. PJH b. PJHv c. PJBr d. PJu	HOZAMEEN COMPLEX Undifferentiated chert, pelite, limestone, gabbro and ultramafic rock Mafic volcanics BRIDGE RIVER COMPLEX Siliceous and chlorite schist, phyllite; correlative with HOZAMEEN COMPLEX but west of Fraser River Ultramafic rock and local gabbro, associated with HOZAMEEN and BRIDGE RIVER COMPLEXES
	Approximate Geologic Boundary

N.B. A Late Cretaceous granodiorite of the Skuzzy Pluton (lKgd) appears on the map, but not in the legend which details bedrock types relevant to clast provenance data only (lKgd was not found).

Site	eTgd	KTc	Mgd	Ogd	PJB	Sgd	Se	JD	Jl	Kgd,d	Ma	PJBv	PJu	PMu	eTl	JEg	EJ	Ep	PJBr	TJgd	TJd	Total	Sample Roundness
2 Unit 1	19	11	11	6	27		9	2		13							1	1				100	SR
Unit 2	11	5	11	15	29		11		1	17												100	SR
3 Unit 1		3		3			1			1												8	SA
Unit 2	3	17		22			33	3	4	4	3		5				2	2	1	1		100	SR
Unit 3	4	21	1	11			25	2	3	21	2	1	2			2	1		2	1	1	100	SA
Unit 4		22	2	20			47			5			1				2		1			100	SA
6 Unit 1	2	20	3	11	27		26	1		5	1	1			1		1				1	100	SR
Unit 2	5	25	6	7	13	1	13	3		11	3	2	3	5				1	1		1	100	SA
7 Unit 1	3	11	21	5	17		9			27	3						2	1	1			100	SR/SA
8 Unit 1	26	15	2	7	9		27			10	1			2		1						100	SR
11 Unit 1		13	33	13	1		26			14												100	SA
Unit 2		27	5	11						7												50	SA
Unit 3		6	90				2			2												100	SR
Unit 4		1																				1	SR
Unit 5	1	7	44	4	2		5			27	1		2	3		1	1	1	1			100	SR
12 Unit 1		26	12	18			18			24	2											100	SA
Unit 2		24	22	20	10			3		11	3	2					3			1	1	100	SR
13 Unit 1		36	24	8			16			16	1					1						100	SR
Unit 2		17	48	18						17												100	SA
14 Unit 1	1	47	24		27		1															100	SA
15 Unit 1		29	34	1			33			3												100	SA
16 Unit 1		45	22	1			31			1												100	SR
Unit 3	1	50	17		3		27			2												100	SR
Unit 4		1																				1	SR
Unit 5		2		1			3															6	SA
17 Unit 2			48	1			45			3	2								1			100	SR
19 Unit 1		60		4	16		12			8												100	SR
Unit 3		70		3	4		23															100	SR
20 Unit 1	2	69	8		5		16															100	SA
22 Unit 1		6																				6	SA
23 Unit 1		81			18					1												100	SR
25 Unit 1	8	38	8	8	8			1	1	16	9						1	2				100	SA
26 Unit 1	5	13			5						1											26	SA
Unit 2a	5	85		2	5			1									1		1			100	SR
Unit 2b	36	17		1	43		2			1	1								1			100	SR
30 Unit 1	12	39	5	14	7	4	7	5		4	2					1						100	SR
Unit 2	7	17	3	21	33		5	4	6	2	1					1						100	SA
33 Unit 1	11	45		9	31		4															100	SA
Unit 2		7		2	5																	14	SA
Unit 3	1	90		6	3																	00	SA
34 Unit 1		67		22	10		1															100	SA/SR
39 Unit 1	1	45		38	16																	100	SA
Unit 2		7									1											9	SR
41 Unit 1	12	21	7	15	31		5			4			1	1		1	1	1				100	SR
Unit 2	4	13	3	10	3		12			3	1								1			50	SR
Unit 3	2	3		5			2															12	SR
Unit 4	9	10	7	5	12		31	1	2	2			5	15						1		100	SR
43 Unit 1	2	21	1	25	12		17			15	4						2	1				100	SR
Unit 3	5	14		16	2	2	21		1	23	7		2	5			1		1			100	SR
45 Unit 1	2	29	1	31	13		2			21							1					100	SR
46 Unit 1	2	28	27	15	5		9			11	2						1					100	SA
49 Unit 1	7	17	4	21	31		14		2	1	2						1					100	SA/SR
50 Unit 1	25	14	2	6	28	1	15	1		3	2	1						1		1		100	SA
52 Unit 1	26	9	3	11	25		2	1	1	17	1						2	2				100	SR
53 Unit 1	21	26		1	37		2		4	1	1		2				2			2	1	100	SA/SR
54 Unit 1	5	17	1	11	12	1	7	1	1		1								1			58	SA
56 Unit 1	11	5	1	2	7					2												28	SA
58 Unit 1	15	22	1	17	12		7	3	4	3	5						1	1	8		1	100	SA
61 Unit 1					5																	5	SR
62 Unit 1a	52	2			46																	100	SR
Unit 1b	46	3			50		1															100	SR
Unit 1c	45	10	1	2	39		3															100	R/SR
65 Unit 1	16	17		13	32		7	1	1		4						3	6				100	SA/SR
Unit 1a	9	21	1	19	43		3		1	2								1				100	SR
67 Unit 3		44		28	25		1			1	1											100	SR
68 Unit 1	14	23	2	6	35		13	1		1	3	1					1					100	SR

Table 2.5 Pebble Source Lithologies - Legend on Facing Page (See Figure 1.2 for site locations) N.B. Site 67 is discussed in Chapter 6.

(Luckman, 1975). However, the presence of glaciofluvial or glacial dropstones alone may not be conclusive evidence of glacier proximity, the depositional context must also be considered.

2.2. Site Descriptions

2.2.1. Site 1

This site is a low pass located approximately 1.5 km southwest of the mouth of Silverhope Creek. Air photo analysis indicates that an alluvial fan entering the Fraser valley emanated from this low pass. Imbrication structures show a northerly paleoflow direction (Figure 2.1a), and the high eigenvalue indicates a strong unimodal pattern. The height of the breach on the Silverhope valley side is 263.8 m and boulders up to 10 m in diameter can be found in the deposit.

2.2.2. Site 2

The exposure is a slide scar adjacent to the Silver Lake campground branch of the main logging road approximately 7.0 km from the mouth of Silverhope Creek (Figure 2.1b).

Unit 1 is about 1.0 m thick. It is composed of a compact, grey, laminated mud with striated, subrounded dropstones. There are no apparent deformation structures. The unit was not sampled. The upper contact appears to be conformable. Dropstones are of locally-derived pelite (Hozameen Complex - 'PJH' - 12a), but over 25% of clasts are of distant origin.

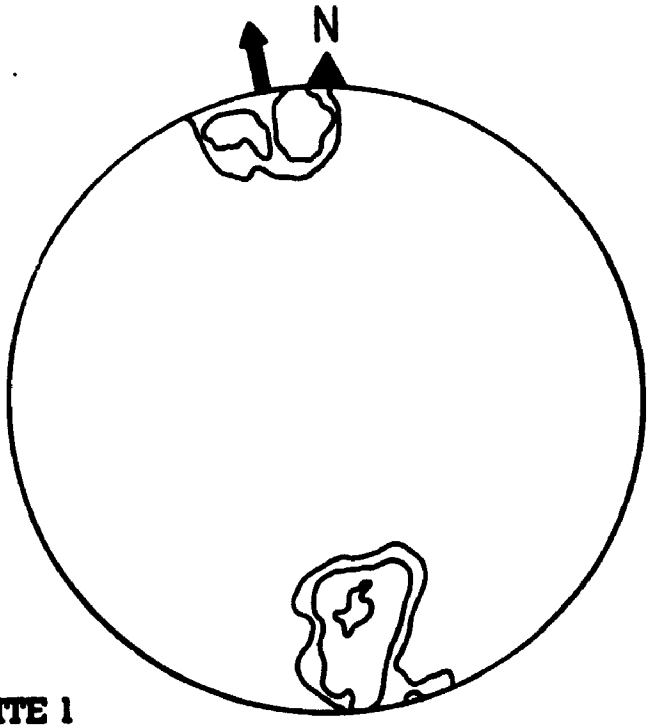

Figure 2.1a SITE 1

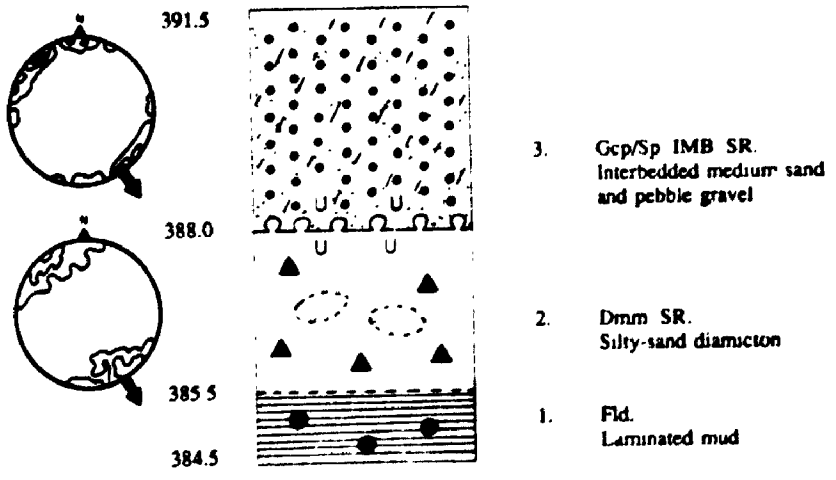

Figure 2.1b SITE 2

Unit 2 is approximately 2.5 m thick. It consists of a compact, grey, silty-sand diamicton with subrounded clasts. In the central part of the unit there are several sand lenses which do not appear to have mixed with the surrounding diamicton. Subrounded clasts have no visible striae or stoss-lee features. Clast orientation within the diamicton indicates paleomovement from the northwest. There is a strong eigenvalue, but some spreading around the girdle in the stereo plot suggests that a weak bimodal pattern might exist, with a second mode oriented north-south. The upper contact appears to be deformed and several flame structures are visible rising up in a southeast orientation into the overlying unit. Structures that may be water escape features, delimited by fine sand and clay infills, are also visible in the top of the unit, rising up to the deformed contact. These features appear to dissipate at the contact. Dominant clast lithology is locally-derived pelite (PJH - 12a) and more distantly-derived quartz granodiorite (Spuzzum Pluton - 'Kgd' - 7b).

Unit 3 is 3.5 m thick. It is composed of a non-compacted, buff-grey, interbedded medium sand and pebble gravel. Planar cross-bedding appears to dip at about 7° southeast, and clast orientation and imbrication indicate a similar paleomovement direction. The eigenvalue is the same as *Unit 2*, but fabric data appear to girdle the rim of the stereonet. Subrounded clasts possess no apparent striae or stoss-lee features, but some have percussion markings. At the lower contact, flames of diamicton intrude into the lowest gravel layer. It appears that most of the deformation at this contact has been caused by diamicton squeezing into this unit creating a more compact, matrix-supported gravel in this part of the

unit. Dominant clast lithology appears to be locally-derived pelite (PJH - 12a) and more distantly-derived quartz granodiorite (Spuzzum Pluton - 'Kgd' - 7b), but were not sampled.

2.2.3. Site 3

The exposure is a large slide scar adjacent to the Silver Lake campground branch of the main logging road approximately 7.2 km from the mouth of Silverhope Creek (Figure 2.1c).

Unit 1 is about 9.0 m thick. The unit is a grey, compact, laminated silty-mud with dropstones. Small, subrounded dropstones retain poorly-preserved fine striae on lower surfaces, and are predominantly composed of locally-derived pegmatitic granite gneiss (Custer Gneiss - 'KTc' - 5a) and granodiorite (Chilliwack Batholith - 'Ogd' - 2). The upper contact appears to be deformed.

Unit 2, 11.9 m thick, is composed of a grey, compact, sandy-silt diamicton. At the lower contact, muddy flame structures appear to be forced up into the unit along sand-filled fractures which dip north. Fine sand inclusions are also visible just above the lower contact, and fine sand interbeds near the top of the unit. Numerous sets of parallel striae are detectable on the top surfaces of predominantly subrounded clasts. Stoss-lee and bimodal fabric data indicate dominant paleomovement from north to south although some clasts are transverse to inferred paleoflow direction, the eigenvalue is correspondingly low at 0.66. There appear to be less fines in this unit than in the ones above and below. Several clay smudges are preserved throughout the unit and pinch out south. The

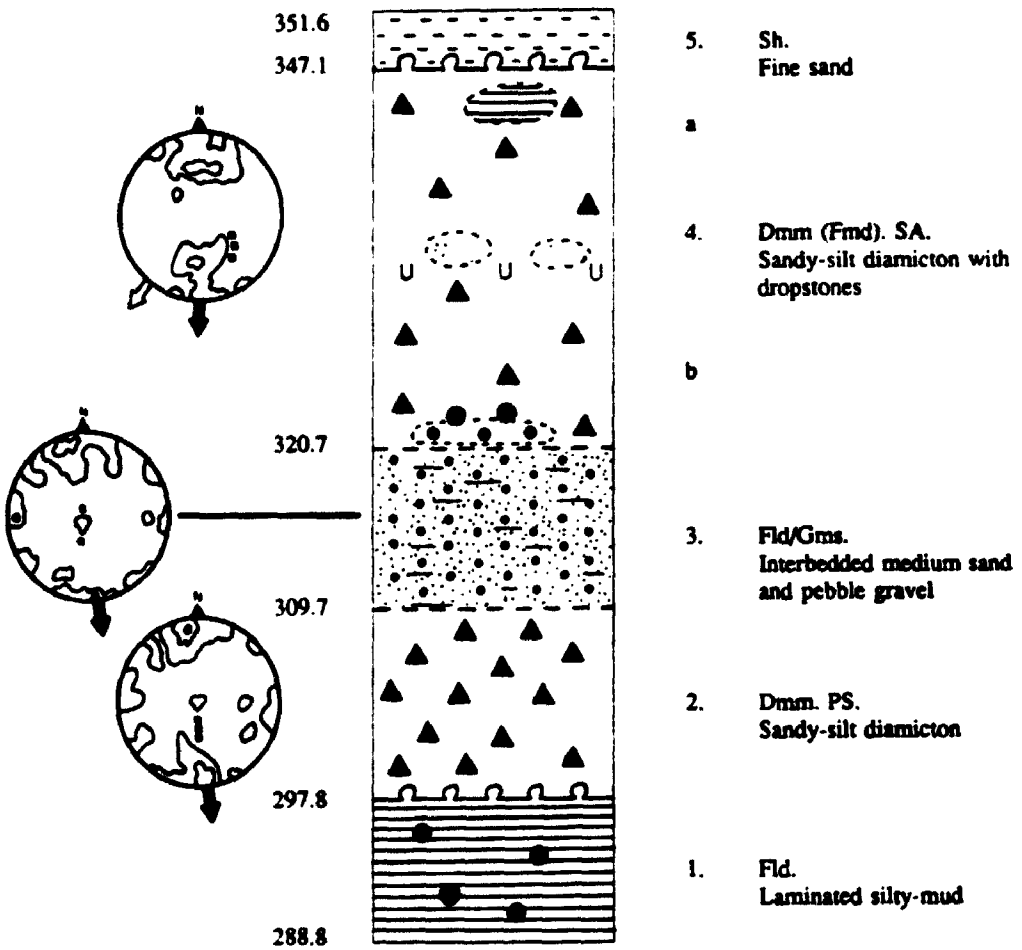

Figure 2.1c SITE 3

upper contact appears to be conformable. Clast lithology is mainly locally-derived argillite (Princeton Group - 'Es'- 3b), with some distantly-derived gabbro (Hozameen and Bridge River Complexes - 'PJu' -12d) and garnet-biotite (Settler Schist - 'Ms' - 5b).

Unit 3 attains a thickness of 11.0 m. This is a saturated, compact, interbedded medium sand and pebble gravel unit. In the lower part, gravels appear to form a conformable contact with the underlying unit. The unit appears to be composed of a sequence of horizontally-bedded gravel and mud (the beds of fine, laminated mud with dropstones (?) are very thin and not included in Figure 2.1c other than by general classification), the latter containing subangular clasts, possibly dropstones. These clasts have no apparent striae and are generally covered by mud drapes. Trimodal fabric data indicate paleoflow to the south, although there are numerous transverse clasts in the upper half of the unit, which produces an eigenvalue of only 0.55. The gravel is supported by a mud matrix. The upper contact appears to be conformable. Clast lithology is predominantly locally-derived argillite (Es - 3b) and pelitic schist (KTc - 5a) and diorite (Spuzzum Pluton - 'Kgd,d' - 7b) of more distant origin. Subangular clasts (dropstones?) are of locally-derived argillite (Es - 3b).

Unit 4 is approximately 26.4 m thick. This unit is made up of a grey, compact, saturated, massive sandy-silt diamicton with dropstones, which fines upwards. Near the base there is a lens of fairly well sorted, subrounded, non-striated cobble clasts oriented southeast which conformably overlie the interbedded sand and gravel of *Unit 3.* Striated, subrounded dropstones in the

top of the lens form a series of pebble clusters. The lens pinches out to the south and clast imbrication and generally unimodal fabric (an eigenvalue of 0.70) indicates a south-southwest paleoflow direction. Sand-filled shear planes, trending south, are visible rising diagonally over these clusters. Near the middle of the unit, south-trending flames of gravelly diamicton (Appendix III: Site 3 - *Unit 4a*) are intruded into the finer, overlying diamicton (Appendix III: Site 3 - *Unit 4b*). At the same level, a lens of fine diamicton appears to be squeezed down into a cavity-fill behind a boulder, and rare medium sand lenses are also visible here. Clay smears are found in the diamicton immediately above these deformations.

In the upper part of the unit, there is a mud lens, and clay drapes over several striated clasts. Bottom striae on clasts are generally oriented northeast-southwest (stoss ends are to the northeast). The upper contact appears to be deformed and occurs at a point of water seepage. Clast lithology in the coarser, lower part of the unit is mainly locally-derived argillite (Es - 3b) and more distantly-derived diorite (Kgd,d - 7b). In the finer, upper part, provenance is predominantly locally-derived argillite (Es - 3b), amphibolite (KTc - 5a) and granodiorite (Ogd - 2).

Unit 5 is about 4.5 m thick. The unit is composed of loose, horizontally-stratified fine sand. There are no apparent structures and paleoflow direction is unclear.

2.2.4. Site 4

This bedrock outcrop on the west valley side 2 km northwest of Silver Lake is at a height of 536.1 m. Striae, stoss-lee and chattermark features indicate paleoflow was from the northwest (Figure 2.1d).

2.2.5. Site 5

This is a bedrock outcrop situated 3 km west-northwest of Silver Lake. Striae, stoss-lee and chattermarks suggest paleoflow from the northwest (Figure 2.1e). It is located between Sites 4 and 7, but no elevation was recorded.

2.2.6. Site 6

This is a small road cut situated on the Eureka Creek logging road approximately 0.8 km from the junction with the main logging road (Figure 2.1f).

Unit 1 is up to 2.0 m thick. This is a compact coarse gravel composed of subrounded clasts, with poorly-defined massive bedding planes. Weakly bimodal fabric and dip of bedding indicate dominant paleoflow to the southeast, although there appear to be some clasts transverse to the dominant paleoflow direction. The eigenvalue is 0.73. Preserved striae on the underside of some clasts are oriented west-northwest - east-northeast. All striated clasts possess a smooth upper side, with no visible stoss-lee features. Clast lithology is predominantly locally-derived gabbro (PJH - 12a) and sandstone (Es - 3b). The upper contact appears to be deformed and fine gravels are diapirically intruded into *Unit 2*.

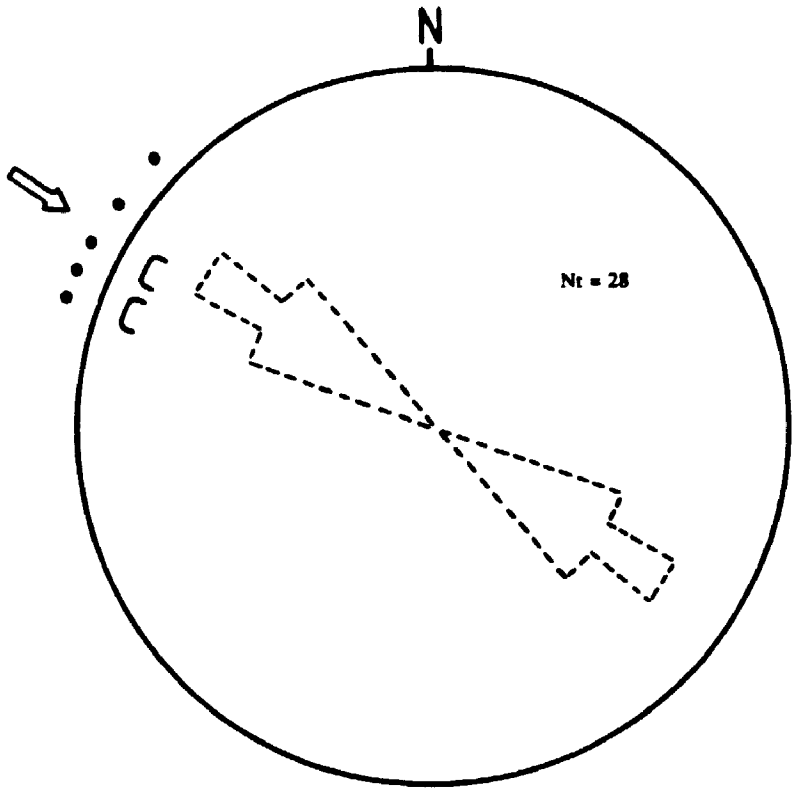

Figure 2.1d SITE 4

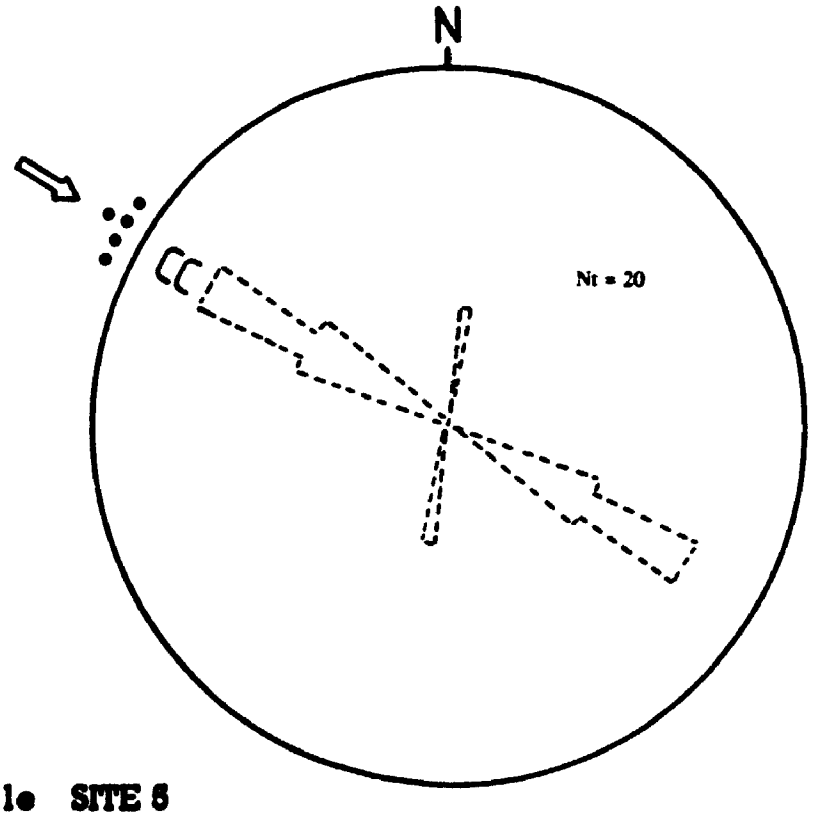

Figure 2.1e SITE 5

Unit 2 attains a maximum thickness of 0.5 m. The unit consists of a compact, laminated mud with dropstones. The dropstones possess many parallel sets of striae oriented in several directions, and are mainly of locally-derived pegmatitic granite gneiss (KTc - 5a), although lithology is diverse. Deformation structures are diapiric and appear to dip east. The upper contact appears to be deformed.

Unit 3 is approximately 5.9 m thick. It is composed of a massive, compact pebble gravel, more compact than underlying units. Clast orientation and imbrication are scattered, and weakly bimodal fabric data (eigenvalue 0.73) suggest an eastward paleoflow. Most larger clasts (pebbles and cobbles) form pebble clusters, although some individual clasts appear to be oriented transverse to these features. There are many subrounded clasts, some of which possess fine striae. There appear to be few fines. The dominant lithology (not analysed) appears to be locally-derived pegmatitic granite gneiss (KTc - 5a - mostly subangular clasts). There is no apparent upper contact.

2.2.7. Site 7

This is a small exposure situated approximately 5.0 km west of the junction between the Eureka Creek and main logging roads (Figure 2.1g).

Unit 1 has a maximum thickness of about 4.2 m. There are no apparent contacts. This is composed of a compact, grey, pebble gravel to gravelly-mud. The upper part of the unit has 90% gravel, and the lower, 70%. Mud lenses with rare sub-angular clasts (dropstones?) are visible in the lower part of the unit.

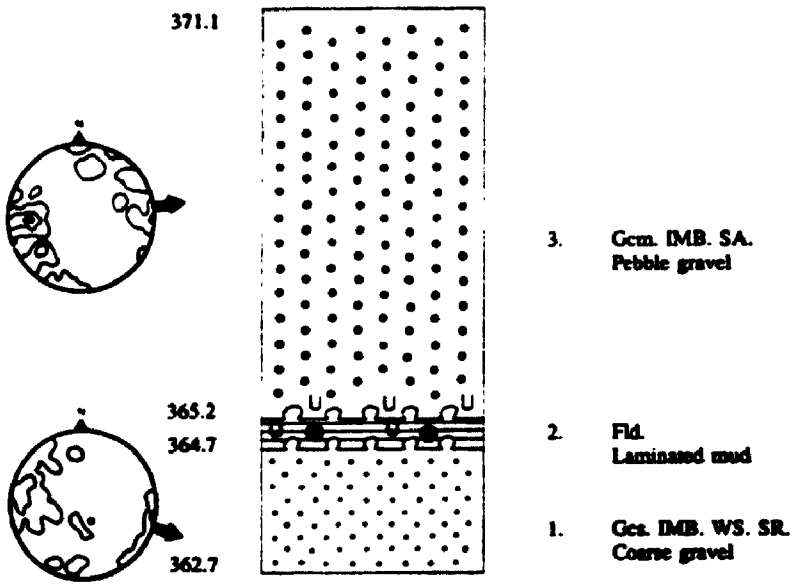

Figure 2.1f SITE 6

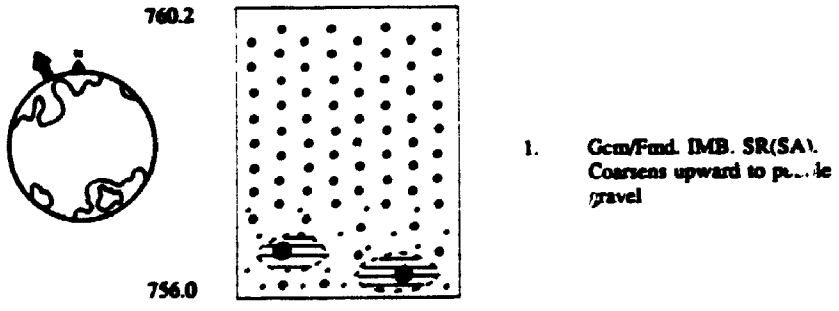

Figure 2.1g SITE 7

Clast orientations and imbrications are weakly bimodal (eigenvalue 0.77) and indicate a northwest paleoflow. Dominant subangular clast lithology is locally-derived granodiorite (Kgd - 7b). Gravel lithology is predominantly locally-derived granodiorite (Mount Barr Batholith - 'Mgd' - 1).

2.2.8. Site 8

This exposure is located in a small slide scar approximately 3.8 km west of the junction between the Eureka Creek and main logging roads (Figure 2.1h).

Unit 1 reaches a maximum thickness of 20.0 m. There are no apparent contacts. The unit is composed of a compact, grey, pebble gravel to gravelly-mud. The unit coarsens upwards and the upper half consists of 90% gravel, and the lower half, 42% with a high percentage of fines. Mud lenses with dropstones are visible in the lower half of the unit. There are an increasing number of imbrication structures apparent toward the top of the unit, which indicate a northwesterly paleoflow. However, fabric data are dispersed and weakly trimodal, with an eigenvalue of 0.66. Subrounded clasts predominate and there are no apparent striae. Dropstone lithology is predominantly locally-derived granodiorite ('eTgd' - 4) and argillite (Es - 3b). Gravel lithology is mainly locally-derived pelitic schist (KTc - 5a) and pelite (PJH - 12a), with many distantly-derived lithologies.

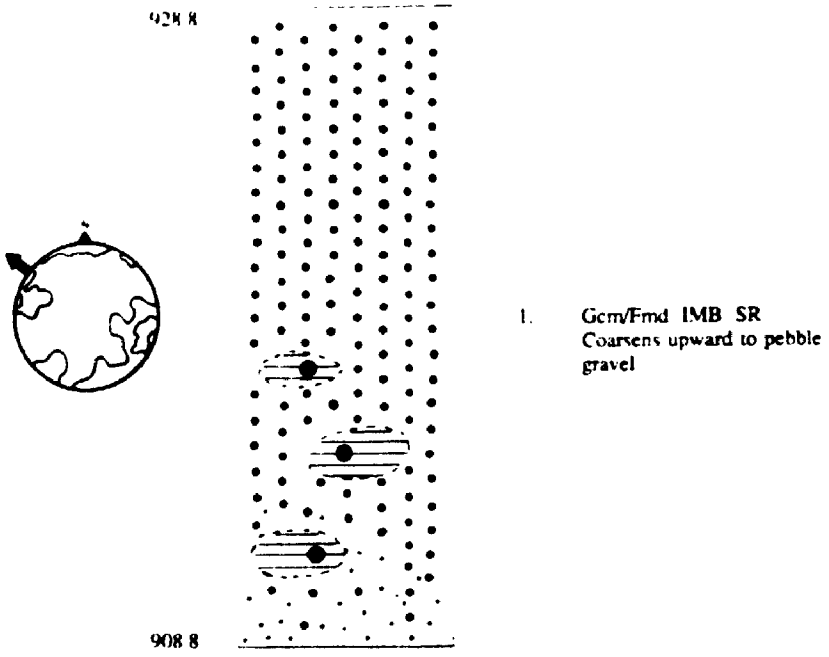

Figure 2.1h SITE 8

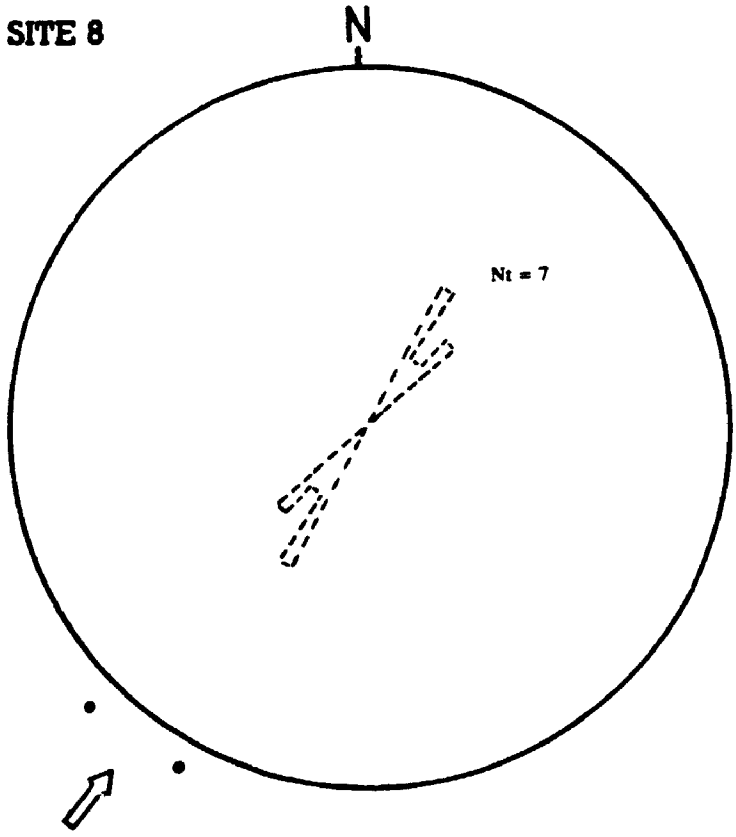

Figure 2.1i SITE 9

2.2.9. Site 9

This is a bedrock exposure located on the north side of Eureka Creek. It is about 8.0 km from the junction with the Silver Lake campground branch of the main logging road. Striae and stoss-lee features indicate paleoflow from the southwest (Figure 2.1i).

2.2.10. Site 10

In a central valley location at the northwest end of Silver Lake, this roche moutonée has striae, stoss-lee and chattermark features indicating paleoflow from the northwest (Figure 2.1j).

2.2.11. Site 11

The exposure is a small slide scar adjacent to the Sowerby Creek logging road approximately 0.5 km from the junction with the Silver Lake campground branch of the main logging road (Figure 2.1k).

Unit 1 is about 1.7 m thick. The unit is composed of a compact, poorly-sorted, grey, sandy-silt diamicton and muddy gravel. The mud content appears to increase upward within the unit. Near the base, clasts possess several sets of poorly-preserved striae (top and bottom surfaces - not studied). Massive bedding near the base possesses slightly scattered stone imbrication structures (eigenvalue 0.83) which indicate northward paleoflow. The upper contact appears to be conformable. Clast lithology is locally-derived granodiorite (Mgd - 1) and argillite (Es - 3b).

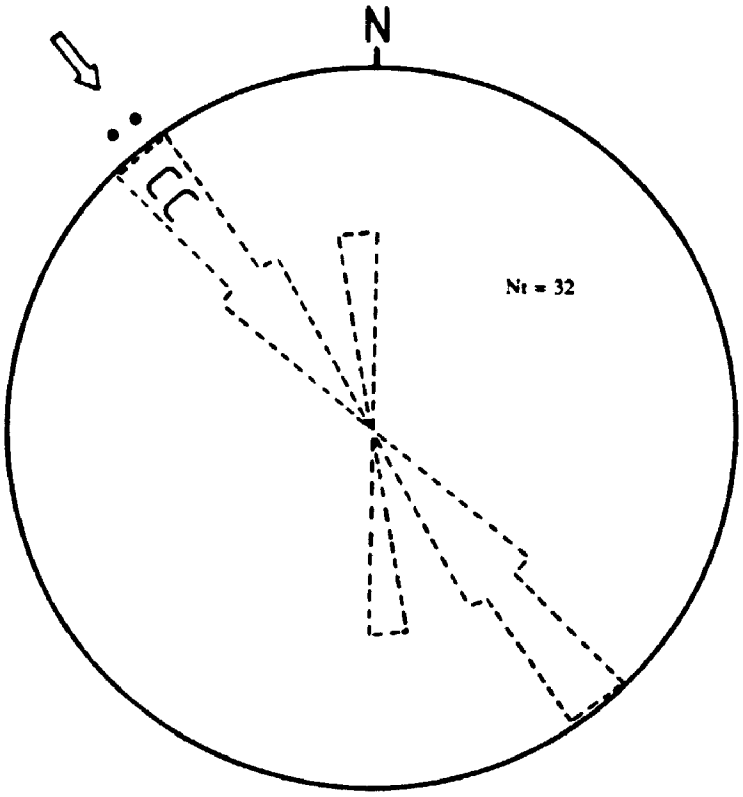

Figure 2.1j SITE 10

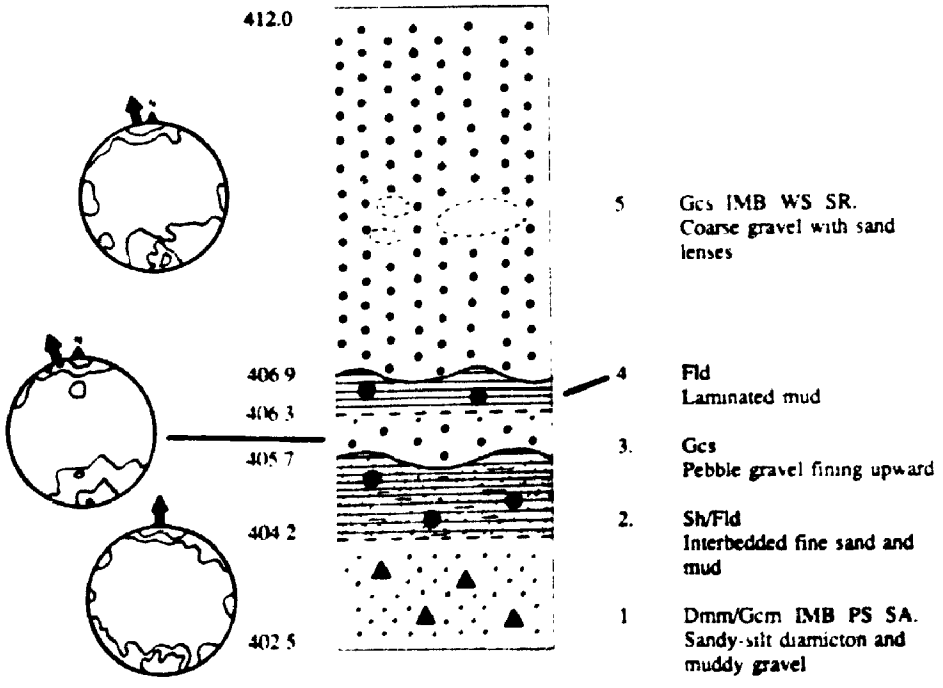

Figure 2.1k SITE 11

Unit 2 attains a thickness of 1.5 m. The unit incorporates a compact, horizontally-interbedded fine sand and mud unit with dropstones, which is coarser than the upper part of *Unit 1*. The upper contact, in the form of a gravel lag, appears to be erosional. Dropstones are subangular and possess several non-parallel striae. They are dominated by locally-derived pegmatitic granite gneiss (KTc - 5a).

Unit 3, 0.6 m thick, is a non-compacted, weakly-bedded pebble gravel. The unit attenuates to the north and the particle size appears to fine upwards. A bed of medium gravel forms the basal erosional contact. Clast orientation of the gravel indicates a dominant northward paleomovement, although there is some dispersal and a weak bimodality (eigenvalue 0.82). The upper contact appears to be conformable. Dominant lithology of the clasts in the lower part of the unit is a locally-derived granodiorite (Mgd - 1).

Unit 4, 0.60 m thick, and appears to be a compact, grey, laminated mud (not sampled). The unit possesses one heavily-striated, subangular dropstone of locally-derived pegmatitic granite gneiss (KTc - 5a). The upper contact appears to be erosional.

Unit 5 attains a maximum thickness of 5.1 m. This is a compact, well-sorted, subrounded coarse gravel with beds dipping gently north. Clast imbrication and orientation possess bimodal fabric, with an eigenvalue of 0.77 in a northerly paleoflow direction. Particle size coarsens towards the base. Sand lenses are visible in the middle of the unit. Clast lithology is mainly locally-derived granodiorite (Mgd - 1) and diorite (Kgd,d - 7b) of more distant origin.

2.2.12. Site 12

The exposure is a slide scar adjacent to the Sowerby Creek logging road, approximately 0.7 km from the junction with the Silver Lake campground branch of the main logging road (Figure 2.11).

Unit 1, 1.5 m thick, is a compact, saturated, grey, sandy-silt diamicton. Rare dropstones are present in the finer, lower part of the unit, and they have no apparent striae. Many subrounded clasts have basal striae and some have stoss-lee features indicating a northward paleomovement. Fabric suggests northward paleomovement although there is some dispersal and evidence of clast rotation (eigenvalue 0.78). Preserved clay smudges which pinch out northwards are visible in the central part of the unit, these immediately overlie several small sand lenses. The upper contact appears to be erosional. Dominant lithologies are locally- (KTc - 5a) and distantly-derived granodiorite (Kgd - 7b).

Unit 2 is about 1.0 m thick. This unit is a gradational sequence of saturated sediments which commence at the base as a pebble gravel lag forming the lower contact. Rippled, fine sands overlie the gravel, and these in turn are overlain by laminated fines. Ripples suggest a northerly flow direction. There is no apparent upper contact. Clast lithology is mainly locally-derived amphibolite (KTc - 5a) and granodiorite (Mgd - 1 and Ogd - 2), with several clasts from more distant source areas.

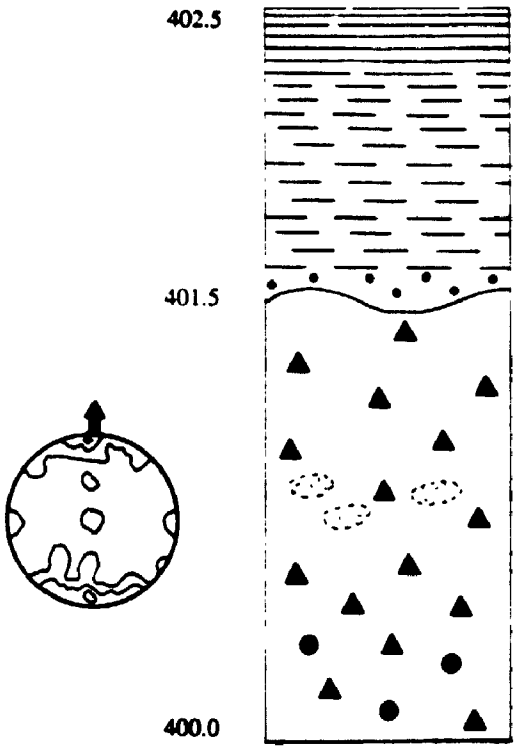

2. Sr/Fl
Rippled fine sand with
gravel lag grading into fines

1 Dmm. SR.
Sandy-silt diamicton

Figure 2.11 SITE 12

2.2.13. Site 13

The exposure is a slide scar adjacent to the Sowerby Creek logging road, approximately 1.0 km from the junction with the Silver Lake campground branch of the main logging road (Figure 2.1m).

Unit 1 is about 0.5 m thick. There is no visible lower contact and the upper one appears to be deformed. The unit is a compact, grey, massive, sandy-silt diamicton with no dropstones. There are many large clasts, but they possess no apparent striae or stoss-lee features. Clast orientation indicates a north-northeast paleoflow, although there is a distinct bimodality in the fabric data, with a weak eigenvalue of 0.64. There appears to be a concentration of larger clasts near the top part of the unit, but they do not form agglomerated clusters. This feature pinches out to the north. Muddy flame structures are visible attenuating northwards into the overlying unit. Some muddy diapiric structures appear to be intruded into the upper part of the unit from the overlying unit. Dominant clast lithologies are locally-derived pegmatitic granite gneiss (KTc - 5a) and granodiorite (Mgd - 1), and argillite (Es - 3b) and quartz granodiorite (Kgd - 7b) from more distant source areas.

Unit 2 is approximately 1.5 m thick. There is no visible upper contact and the lower one appears to be deformed. The unit is a compact, grey, massive, sandy-silt diamicton with no dropstones, and appears to be more compact than the underlying sediments. There are many large clasts with striae on upper and lower surfaces, and stoss-lee features indicating a north-northeast paleomovement. Water escape and shear structures are present on the lower

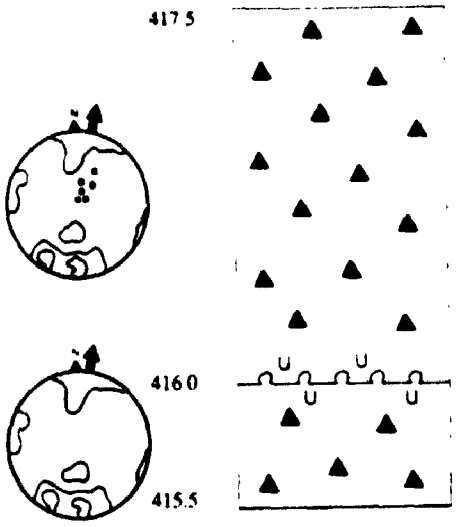

2 Dmm SA/SR
Sandy-silt diamicton
Contortions near base of unit

1. Dmm SA/SR
Sandy-silt diamicton
Contortions near top of unit

Figure 2.1m SITE 13

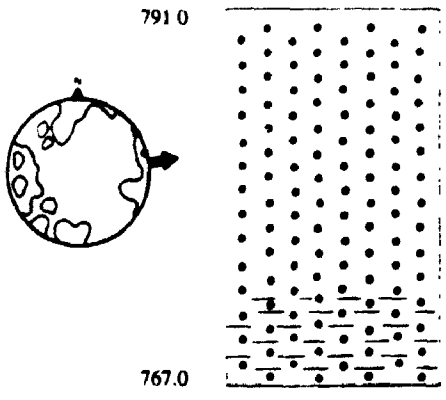

1 Gmm (Fm) MS SA
Muddy pebble gravel

Figure 2.1n SITE 15

part of the section and orientations generally coincide with an inferred paleomovement north-northwest, with distinct bimodality of fabric. Fine diamicton appears to be squeezed into the underlying unit, attenuating a concentration of large clasts. Dominant lithologies are two types of locally-derived granodiorite (Mgd - 1, Ogd - 2) and more distant-derived quartz granodiorite (Kgd,d - 7b).

2.2.14. Site 15

This is a road cut situated on the Cantelon Creek logging road approximately 5.4 km from the junction with the main logging road (Figure 2.1n).

Unit 1, 24.0 m thick, has no apparent contacts. The unit is composed of a compact, grey, massive, muddy pebble gravel. In the central part of the unit, numerous clasts in a sandy matrix, possess striated top surfaces (trending west - east). Pebble clusters and clast orientations overlying these clasts are scattered but suggest an easterly paleoflow (an eigenvalue of 0.65). The striated clasts appear to be *in situ*, and stoss-lee orientations coincide with inferred paleomovement direction. There is a finer, muddy matrix in the lower part of the unit. Clasts are predominantly subangular, with some in the upper part of the unit lying transverse to inferred paleoflow direction. Clast lithology is mainly locally-derived granodiorite (Mgd - 1) and pegmatitic granite gneiss (KTc - 8a), and more distantly-sourced argillite (Es - 3b) and diorite (Kgd,d - 7b).

2.2.15. Site 16

This is a road cut situated on the Cantelon Creek logging road approximately 3.0 km from the junction with the main logging road (Figure 2.1o).

Unit 1 is up to 0.5 m thick. This is a grey, compact, poorly-sorted sandy-silt diamicton. Loading structures and water escape structures (diapers and flames) in the upper part of the unit, protrude into the overlying sand and mud. These features are oriented northeast. Fine striae are visible on the bottom surfaces of a few clasts. Unimodal clast orientation indicates paleomovement to the northeast, with an eigenvalue of 0.82. Horizontal fine sand inclusions are visible in the lower half of the unit. There is an apparent contorted upper contact. Clast lithology is mainly locally-derived pegmatitic granite gneiss (KTc - 5a) and more distantly-derived argillite (Es - 3b).

Unit 2, about 39.5 m thick, is composed of a compact, sandy-grey, interbedded fine sand and mud. Deformation structures are visible (diapirs) in the lower part of the unit. A medium sand lens in the lowest mud layer pinches out northeast and fines upward. The sand beds have weak stratification and deformation structures appear to gently upwarp and pinch out toward the northeast. Some shearing is evident at the lower contact with *Unit 1*, although this apparently is not extensive (shown in *Unit 1* stereonet). Fine sand infills the shear planes which rise both to the northwest and northeast.

Unit 3 is approximately 1.0 m thick. This is a unit of grey, compact, poorly-sorted diamicton. There are deformation structures in the upper part of the unit, but no shear planes. Subrounded clasts have no discernible striae. Horizontal

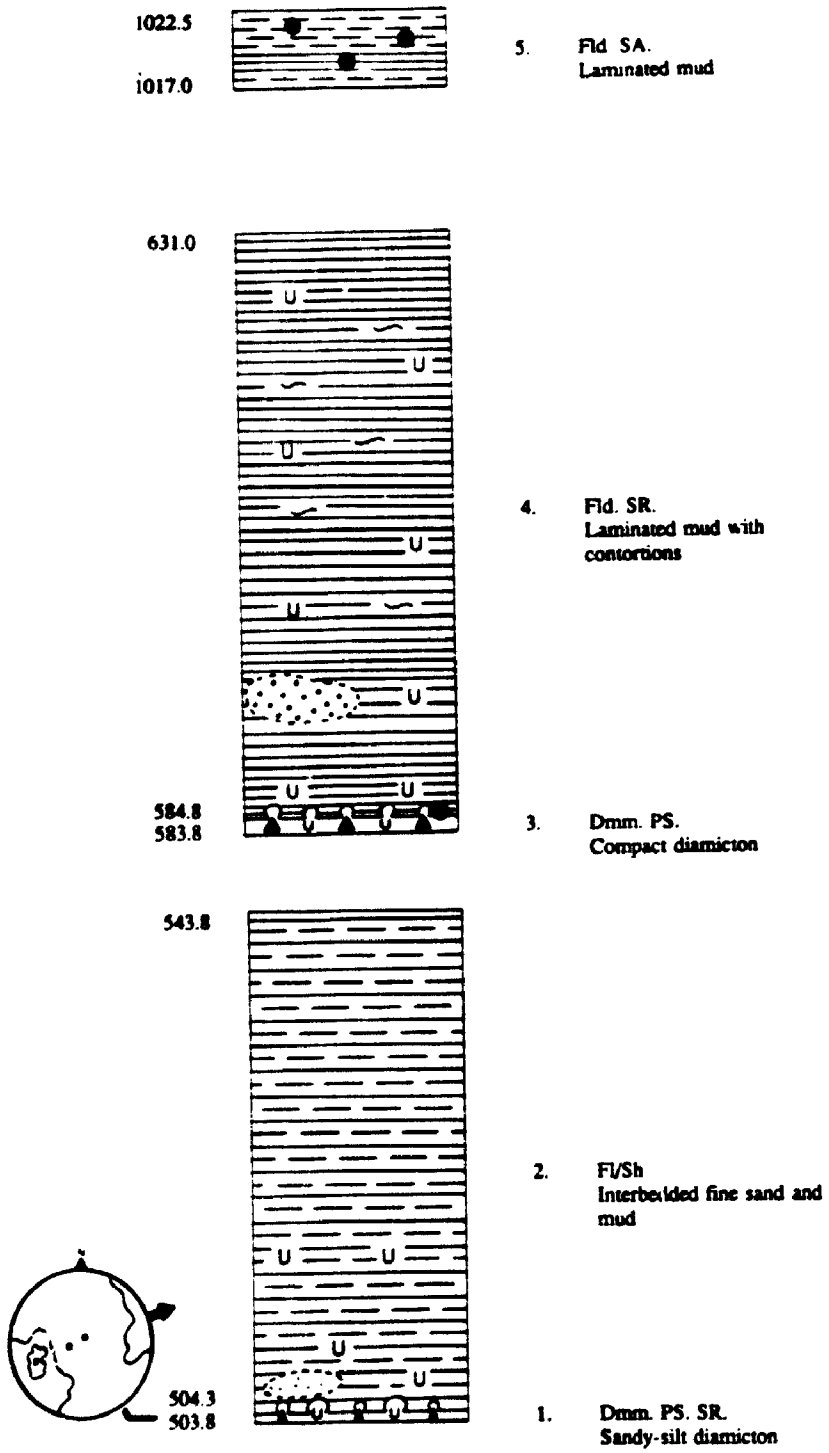

Figure 2.1o SITE 16

fine sand inclusions are visible near the top of the unit. The upper contact appears to be deformed, but structures do not indicate a definite paleomovement direction. Clast lithology is mainly locally-derived pelitic schist (KTc - 5a) and argillite (Es - 3b) of more distant origin, although there are also some locally-derived gabbros (PJH - 12a).

Unit 4 attains a thickness of 46.2 m. T.is is a grey, compact, laminated mud with deformation structures trending northwest. A medium sand and gravel inclusion in the lower part of the unit pinches out northeast and fines upwards. A subrounded dropstone of locally-derived pegmatitic granite gneiss (KTc - 5a) in the lower part of the unit intrudes into the underlying diamicton. It has striae on both top and bottom surfaces, and laminated muds are visibly warped beneath the dropstone and fine mud drapes the upper surface.

Unit 5, about 5.5 m thick, is a compact, sandy-grey, laminated mud with subangular distantly-derived argillite (Es - 3b) dropstones. These clasts have no apparent striae, and the unit has no apparent deformation structures or contacts.

2.2.16. Site 17

This is a road cut situated on the Cantelon Creek logging road approximately 3.9 km from the junction with the main logging road (Figure 2.1p).

Unit 1 is approximately 4.5 m thick. This is a compact, grey, massive, matrix-supported subangular cobble gravel. There is no apparent stratification visible. There is an apparent erosional upper contact.

Unit 2, 4.0 m thick, consists of a compact, grey, stratified coarse gravel with beds dipping gently at about 3°. Clast imbrications and unimodal orientation indicate paleoflow from the northwest, although rare transverse clasts reduce the eigenvalue to 0.75. Clasts are subrounded and the majority of the fines appear to have been winnowed out. Clast lithology is locally-derived granodiorite (Mgd - 1) and conglomerate (Es - 3b) of more distant origin.

2.2.17. Site 18

This is a road cut situated on the Yola Creek logging road approximately 3.8 km from the junction with the main logging road.

Unit 1 is approximately 2.0 m thick. It is composed of a grey, laminated fine mud with no apparent dropstones. Deformation structures are visible in the unit. There are no apparent contacts.

2.2.18. Site 19

This is a road cut situated on the Yola Creek logging road approximately 5.3 km from the junction with the main logging road (Figure 2.1q).

Unit 1 is about 2.0 m thick. It is composed of a compact, grey, matrix-supported, sandy-silt diamicton. The unit possesses some fissility. A few of the dominantly subrounded clasts have parallel bottom sets of striae and stoss-lee features, indicating mainly north-south paleomovement. Clast orientation suggests a similar paleoflow pattern (from the southwest), but fabric is dispersed and weakly bimodal with an eigenvalue of 0.76. Some fine sand layers are visible in

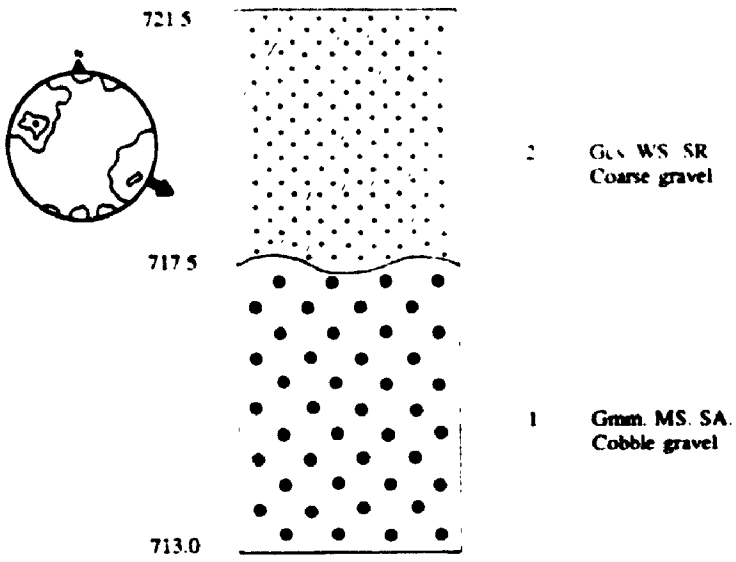

Figure 2.1p SITE 17

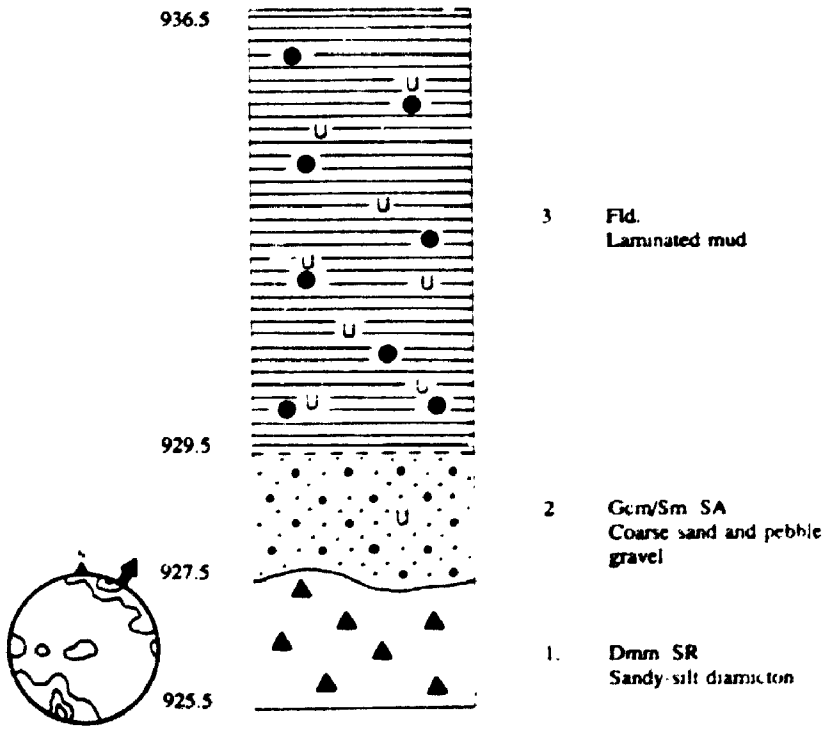

Figure 2.1q SITE 19

the upper part of the unit. The are no apparent deformation structures, and the upper contact seems to be erosional. Dominant lithology is locally-derived pelitic schist (KTc - 5a) and pelite (PJH - 12a), with some distantly-derived argillite (Es - 3b).

Unit 2 is approximately 2.0 m thick. This is composed of a non-compacted, grey, massive coarse sand and pebble gravel. In the middle of the unit there appears to be a deformation structure rolled by paleomovement from the west. The particle size appears to become finer toward the top of the unit. Subangular clasts have no visible striae or stoss-lee structures. The upper contact appears to be conformable. Dominant lithology was not recorded.

Unit 3, 7.0 m thick, is a fine grey laminated mud with dropstones. There are several diapiric structures, most having a dropstone core. There are no apparent shear structures, but the majority of dropstones have striae (not recorded) on the bottom surface only. Dominant dropstone lithologies are locally-derived pelitic schist (KTc - 5a), and distantly-sourced sandstone (Es - 3b) and argillite (Es - 3b).

2.2.19. Site 20

This is a road cut situated on the Yola Creek logging road approximately 6.1 km from the junction with the main logging road (Figure 2.1r).

Unit 1 is about 8.0 m thick. It comprises a grey, massive, sandy-silt diamicton with a medium sand and gravel lens. Immediately beneath the unit is an exposure of striated, pelitic schist bedrock with stoss-lee orientation indicating

paleoflow from the southwest. Clast orientation in the overlying diamicton shows a similar trend, with an eigenvalue of 0.84. The predominantly subangular clasts in the diamicton possess rare bottom surface striae and stoss-lee features, but those recorded mainly suggest paleomovement to the north. The sand and gravel lens is visible in this unit because it appears to be cleaner, with many subrounded clasts. There appears to be little mud. There are no apparent contacts. Dominant lithology is a locally-derived pelitic schist (KTc - 5a).

2.2.20. Site 21

This is in a road cut situated on the Hicks Creek logging road approximately 2.1 km from the junction with the main logging road. It represents the lowest exposure of lacustrine sediments in Hicks Creek valley. No analyses were carried out.

2.2.21. Site 22

This is a road cut situated on the Hicks Creek logging road approximately 2.7 km from the junction with the main logging road.

Unit 1 is up to 30.1 m thick. There are no apparent contacts This is a compact, grey, laminated silty mud with rare dropstones. The dropstones are subrounded, locally-derived pelitic schist (KTc - 5a), with fine non-parallel striae (not recorded).

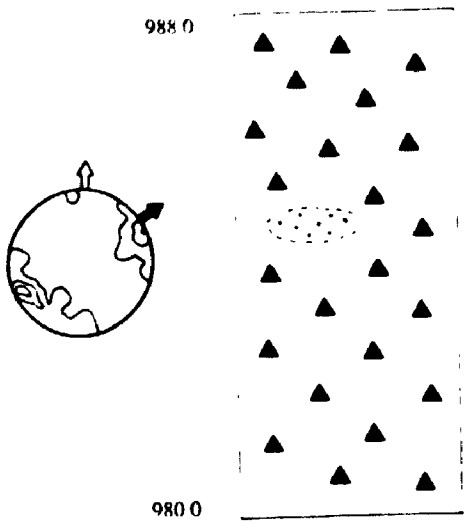

Figure 2.1r SITE 20

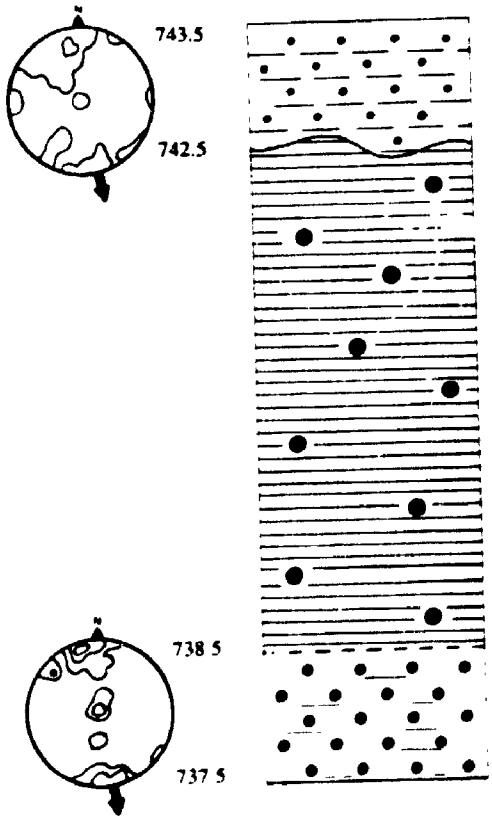

Figure 2.1s SITE 23

2.2.22. Site 23

This is a road cut situated on the Hicks Creek logging road approximately 3.0 km from the junction with the main logging road (Figure 2.1s).

Unit 1, about 1.0 m thick, is a compact, grey, clast-supported stratified cobble gravel, with few fines. Clast imbrication and pebble clusters suggest that paleomovement was to the south, although fabric is dispersed and is has closely-grouped bimodality (the eigenvalue is 0.73). There is some pinching out of the unit to the south. Subrounded clasts possess no visible striae or stoss-lee features. The upper contact appears to be conformable. Dominant lithology is a locally-derived pelitic schist (KTc - 5a).

Unit 2 is approximately 4.0 m thick. It is a compact, grey, laminated mud with dropstones. There are no apparent deformation structures, and dropstones have no visible striae. Dropstones appear to be of locally-derived pelite (PJH - 12a), but were not analysed. The upper contact appears to be erosional.

Unit 3 attains a maximum thickness of 1.0 m. It is a non-compacted, grey, massive, muddy pebble gravel. Clast imbrications are dispersed and weakly bimodal (an eigenvalue of 0.74), but together with pebble clusters indicate paleoflow to the south. Particle size appears to be finer than *Unit 1*, but fabric measurements yield similar data. There is no apparent upper contact. Dominant lithology appears to be a locally-derived granodiorite (Ogd - 2), but was not analysed.

2.2.23. Site 24

This is in a road cut situated on the Hicks Creek logging road approximately 3.6 km from the junction with the main logging road.

No facies diagram is prepared for this section which is about 0.5 m thick. It contains a roll-up deformation structure dissected by a low-angle fault. This is located in a compact, grey, laminated mud sequence which appears to be similar to *Unit 2* at Site 23. Both shear and roll-up structure are oriented southwest, the shear dipping at about 10° NE. The feature is situated at 868 masl. Fine sand appears to fill the shear plane. Across the 1.0 m section width, several near-vertical threads of fine sand diverge upwards from the shear plane, dissipating into the surrounding muds. There are no visible dropstones.

2.2.24. Site 25

This exposure is located in a road cut on the Hicks Creek logging road approximately 4.3 km from the junction with the main logging road.

Unit 1 is about 3.5 m thick. It is composed of a laminated sandy mud with small dropstones and diamicton lenses. The predominantly subangular dropstones possess no striae or stoss-lee features. Two diamicton lenses are visible in the centre of the exposure. There appears to be some mixing with the surrounding mud, but no water escape structures are visible. Laminae beneath these lenses show signs of deformation and are slightly downwarped. Clasts were too small for imbrication analysis, but dominant lithologies are locally-

derived pelitic schist (KTc - 5a) and quartz granodiorite (Kgd - 7b) of distant-origin. There are no apparent contacts.

2.2.25. Site 26

This is a road cut situated on the Hicks Creek logging road approximately 4.8 km from the junction with the main logging road (Figure 2.1t).

Unit 1 is 0.8 m thick. The upper contact in this compact, grey, laminated silty-mud appears to be erosional. There are small, subangular dropstones of mainly locally-derived pelitic schist (KTc - 5a) and gabbro (PJH - 12a) lithology visible mostly in the upper part of the unit. However, one clast, a garnet-biotite schist, is of Fraser valley origin (Settler Schist), several kilometres northwest of Hope.

Unit 2, 1.2 m thick, is a compact, well sorted, pebble gravel with massive bedding. Percussion marks are visible on several clasts. Clast imbrication and orientation possess a unimodal fabric in the lower part of the unit and indicate paleoflow to the southwest (an eigenvalue of 0.91). Some gravel is imbedded in the upper contact with *Unit 1*. The upper part of the unit has dispersed bimodal fabric (an eigenvalue of 0.68), indicating probable paleoflow to the southwest. Clasts appear to lie along a bedding dip of 3-5°, and some of them possess fine striae (not recorded). Clast lithology in the lower part of the unit is mainly locally-derived chert (PJH - 12a), gabbro (PJH - 12a) and granodiorite (eTgd - 4). In the upper part, lithology is predominantly locally-derived pelitic schist (KTc - 5a). There is no apparent upper c ntact.

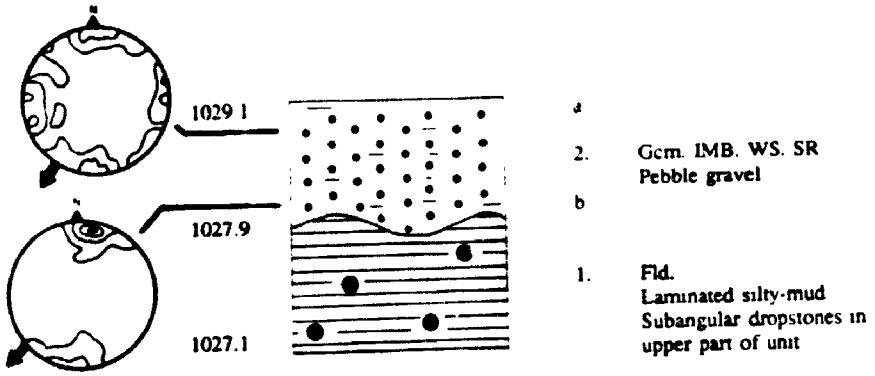

Figure 2.1t SITE 26

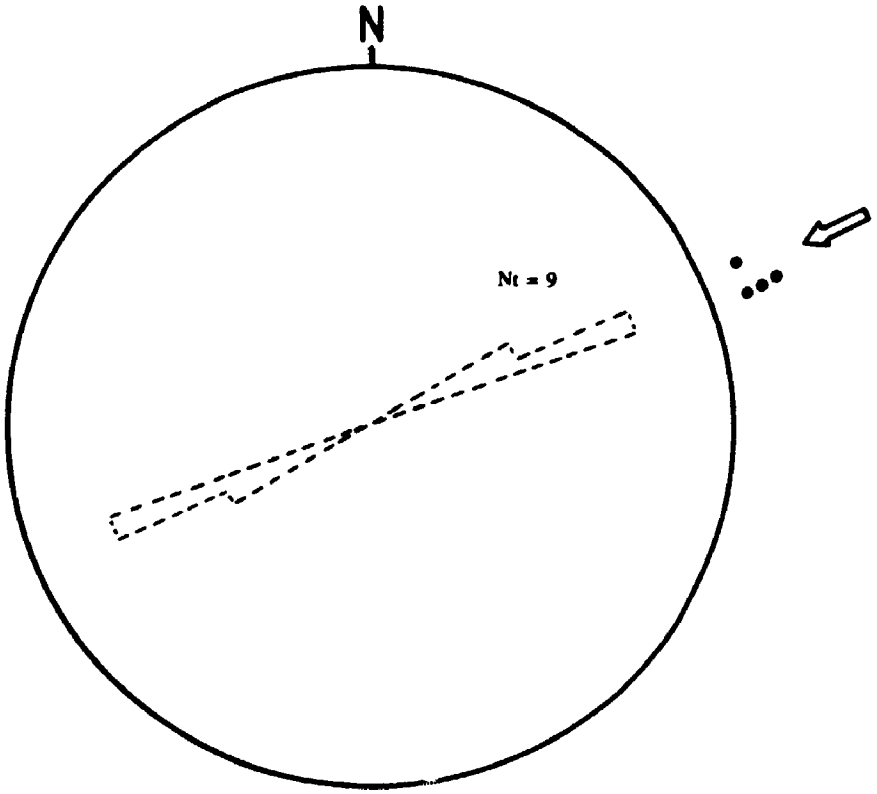

Figure 2.1u SITE 27

2.2.26. Site 27

This bedrock outcrop located on the valley side about 0.7 km north of Greendrop Lake has striae and stoss-lee features indicating paleomovement from t east-north st (Figure 2.1u).

2.2.27. Site 28a

This exposure is located in a gully cut on the Hicks Creek logging road approximately 6.1 km from the junction with the main logging road (Figure 2.1v).

Unit 1 is about 0.7 m thick. It is composed of a compact, grey laminated sandy-mud interbedded with fine sand. There are no dropstones. There are no paleomovement indicators visible, no apparent lower contact and the upper contact appears to be conformable.

Unit 2, 0.3 m thick, appears to be a layer of tephra. There are no paleomovement indicators visible and the upper contact appears to be conformable. This is discussed in Section 5.2.3.

Unit 3, about 0.5 m thick appears to be a colluvial veneer and has not been studied.

2.2.28. Site 28b

The exposure is located in a road cut on the Hicks Creek logging road approximately 6.3 km from the junction with the main logging road.

Unit 1 is about 1.5 m thick. It is composed of a compact, grey, laminated and interbedded fine sand and mud with no dropstones. There are no

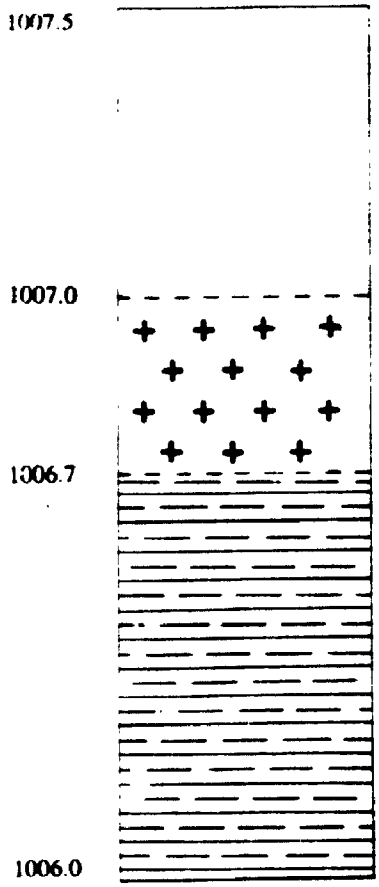

3. Colluvium

2. Maz.
Mazama tephra

1. Fl/Sm
Laminated and interbedded
fine sand and mud

Figure 2.1v SITE 28a

paleomovement indicators visible and no apparent contacts. Two small diamicton lenses are visible and downwarping of the underlying laminae suggest that these were deposited as 'dropstones'. These are composed of fine gravelly mud and possess no large clasts.

2.2.29. Site 29

This bedrock outcrop located on the valley side about 1.0 km southeast of Greendrop Lake has striae and stoss-lee features indicating paleomovement from the east-northeast (Figure 2.1w).

2.2.30. Site 30

This is a large slide scar section approximately 0.7 km south of Greendrop Lake and the Centennial Trail adjacent to the creek flowing north from Flora Lake (Flora Lake Creek), which forms a hanging valley at this point (Figure 2.1x).

Unit 1 is approximately 8.0 m thick. It is composed of a compact, grey, sandy-silt diamicton. Clasts are mostly subangular, bimodal orientation (an eigenvalue of 0.66) and basal striae (only) indicate paleomovement from the southeast. The unit is underlain by fissile bedrock (pelitic schist - KTc - 5a), which appears to possess predominantly horizontal fractures. In the upper part of the unit, shear planes, infilled with clay, and water escape features are evident, but there are no apparent diapiric loading structures. The upper contact appears to be erosional. Dominant lithology is a locally-derived granodiorite (Ogd - 2) and pelitic schist (KTc - 5a).

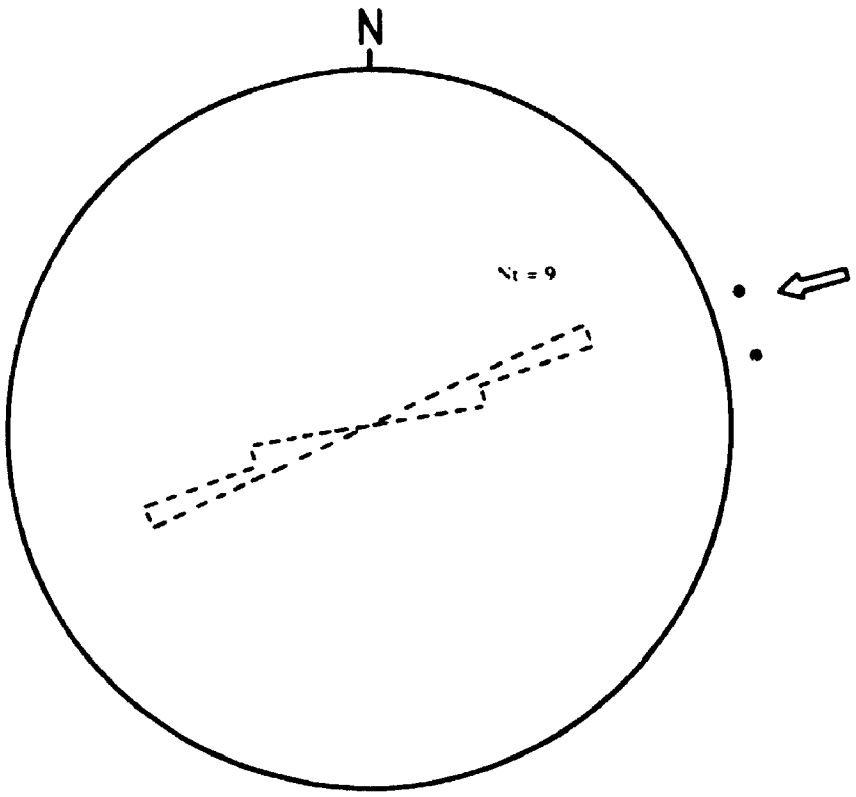

Figure 2.1w SITE 29

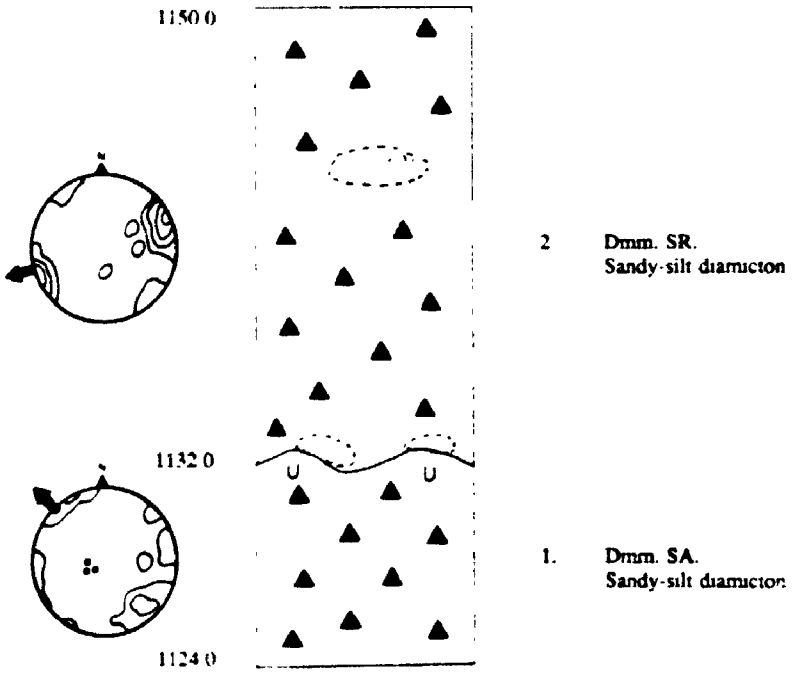

Figure 2.1x SITE 30

Unit 2, about 18.0 m thick, is a compact, grey, sandy-silt diamicton. This appears to have the same particle size distribution as *Unit 1* (taken from the lower part of the unit), but differs in fabric. Clasts are predominantly subrounded, with basal striae only (no stoss-lee features) and a weakly bimodal fabric (an eigenvalue of 0.83) indicating paleomovement from the east-northeast. At the lower contact with *Unit 1*, there are two medium sand lenses which grade into the surrounding diamicton. These are overlain by several clasts which appear to have been rolled transverse to the predominant paleomovement direction. A medium sand lens higher up in the unit shows no indication of mixing with the surrounding diamicton. There are no visible shear planes or water escape features. Clast lithology indicates predominantly locally-derived pelite (PJH - 12a) and granodiorite (Ogd - 2), although there are many distantly-derived clasts. The relative percentages suggest that these sources are to the east, whereas in *Unit 1* the source area appears to be to the south.

2.2.31. Site 31

This is a bedrock outcrop located on the west side of the interfluve between Post and Flora Lake Creeks, and is approximately 2.0 km north-northeast of Lindeman Lake. There are striae and stoss-lee features indicating paleomovement from the northeast (Figure 2.1y).

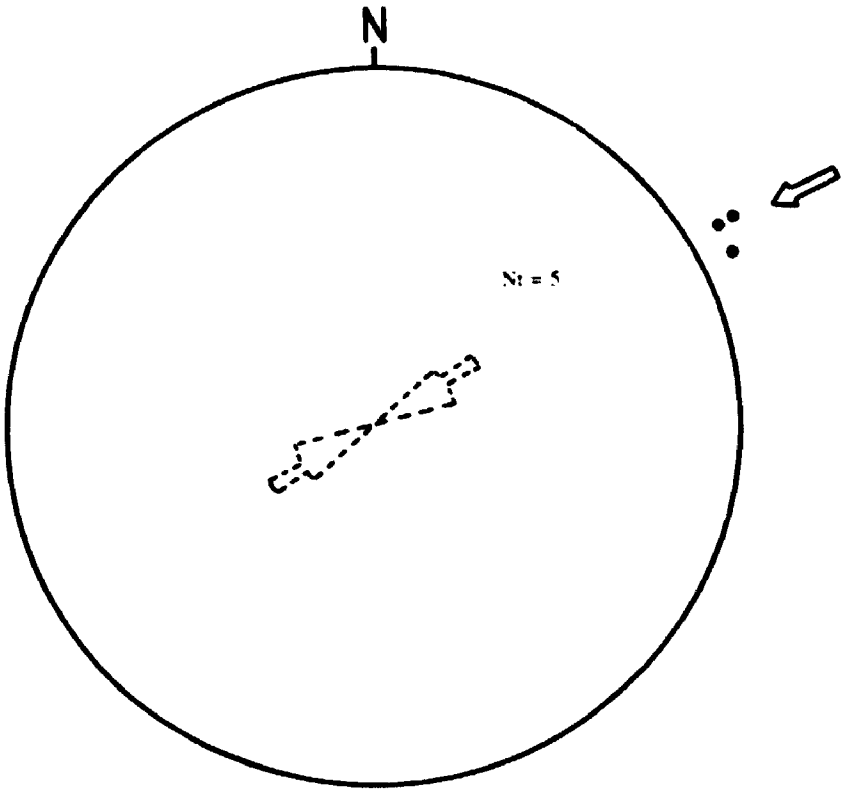

Figure 2.1y SITE 31

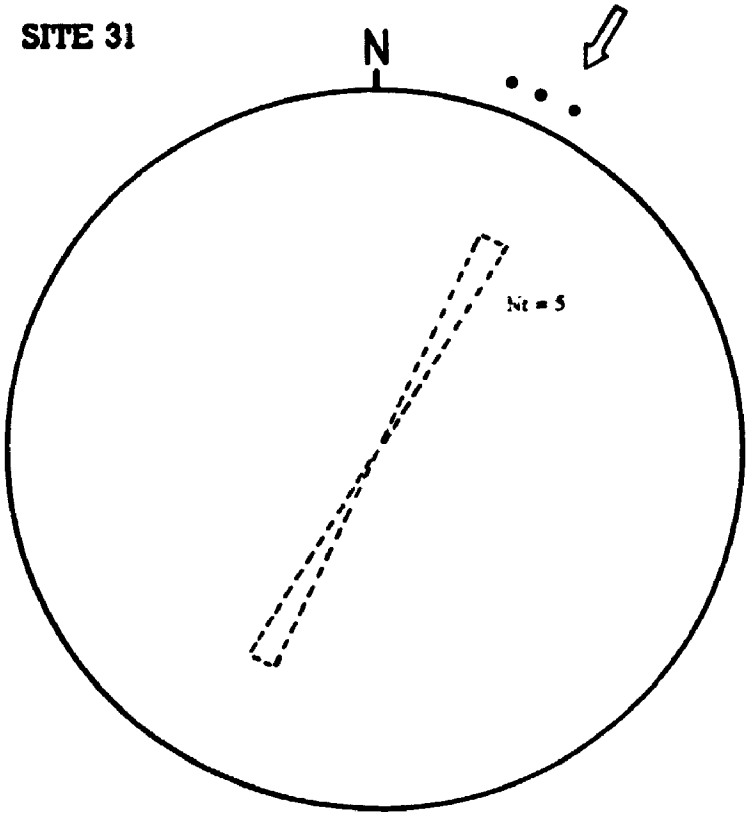

Figure 2.1z SITE 32

2.2.32. Site 32

This is a bedrock exposure located on the east side of Mount Holden. Striae and stoss-lee features indicate paleomovement from the northeast (Figure 2.1z).

2.2.33. Site 33

This is a slide scar situated on the Upper Silverhope Creek logging road approximately 4.4 km from the junction with the main logging road (Figure 2.1aa).

Unit 1 is 12.8 m thick. The unit is a compact, grey sandy-silt diamicton with rare massive medium gravel lenses near the upper contact. One lens overlies another with a thin interlens of diamicton. Both lenses pinch out to the east. They possess subangular, striated dropstones oriented mainly north-south. There are no apparent shear structures in this unit and clast orientation indicates dominant paleoflow to the west, although fabric is trimodal and possesses a weak eigenvalue of 0.60. Sand inclusions rise diagonally southwest in the upper part of the unit. The upper contact appears to be conformable. Clast lithology is mainly locally-derived gabbro (PJH - 12a) and pegmatitic granite gneiss (KTc - 5a), with some more distantly-derived granodiorite (eTgd - 4) .

Unit 2, 1.0 m thick, is a compact, grey, laminated sandy-mud. The lower part of this unit appears to have a mixture of finely striated and smooth, subrounded dropstones. Clast lithology is mainly locally-derived pegmatitic granite gneiss (KTc - 5a) and pelite (PJH - 12a).

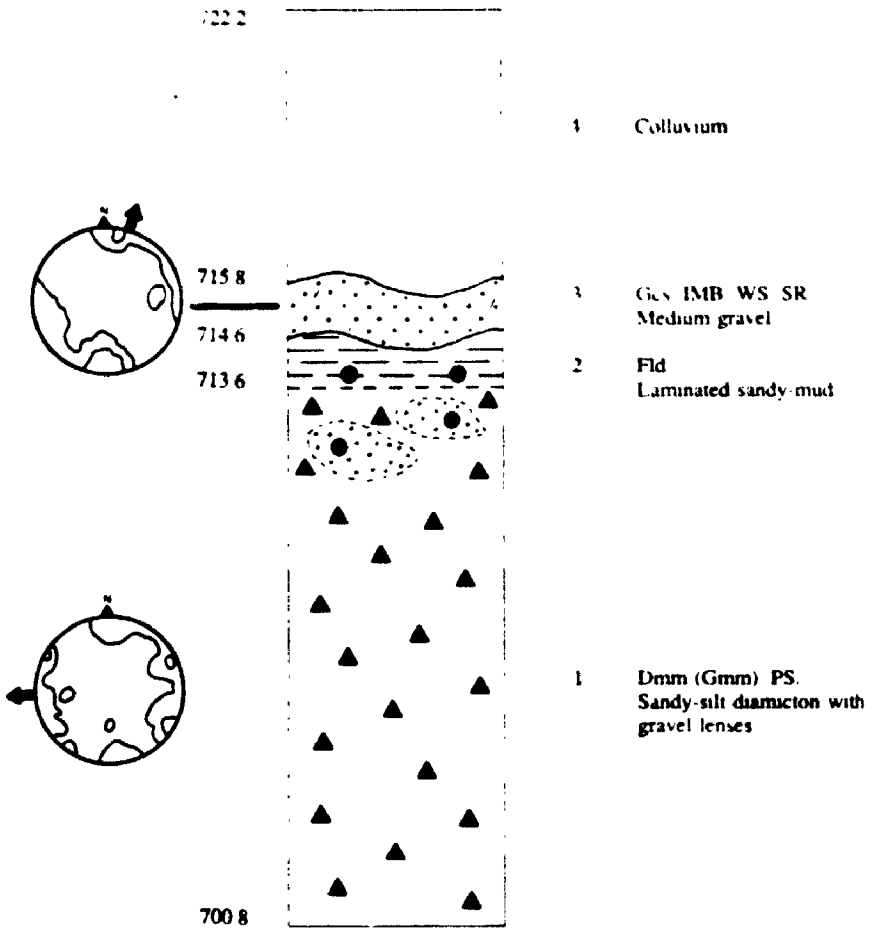

Figure 2.1aa **SITE 33**

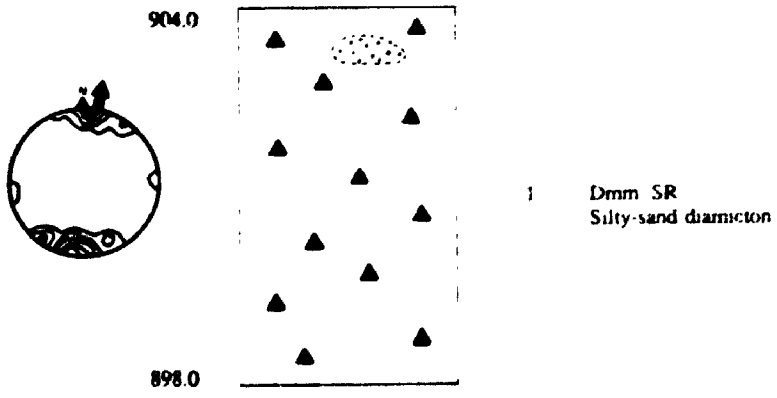

Figure 2.1ab **SITE 34**

Unit 3 is approximately 1.2 m thick. This is a non-compacted, well sorted medium gravel with massive beds dipping gently (3°) northwest. Clast imbrication and orientation indicate a north-northeast paleoflow, although there is some bimodality which reduces the eigenvalue to 0.74. The upper contact appears to be erosional and the unit has been truncated at the eastern end by colluvium. Clast lithology is mainly locally-derived pegmatitic granite gneiss (KTc - 5a) and pelitic schist (KTc - 5a).

Unit 4, 6.4 m thick, is colluvial and has not been studied.

2.2.34. Site 34

The exposure is a slide scar adjacent to the Upper Silverhope Creek logging road, 4.6 km from the junction with the main logging road (Figure 2.1ab).

Unit 1 is approximately 6.0 m thick. It is composed of a compact, grey, silty-sand diamicton with no apparent dropstones. The matrix seems to contain more mud than Site 35 discussed below. There seems to be no mixing between the medium sand lens in the upper part of the section and the surrounding unit. A pebble cluster (considered to be composed of pebble-sized clasts imbricated upstream of an obstacle stone, some finer clasts may be deposited in the lee-side zone of flow separation) is located in the diamicton about 0.5 m below the sand lens. There are no apparent striae or stoss-lee features. Strong fabric orientation (an eigenvalue of 0.89) of the dominantly subrounded clasts indicates paleomovement to the north. Dominant lithology is locally-derived pelitic schist (KTc - 5a) and amphibolite (KTc - 5a).

2.2.35. Site 35

The exposure is a slide scar adjacent to the Upper Silverhope Creek logging road, approximately 6.0 km from the junction with the main logging road (Figure 2.1ac).

Unit 1 is approximately 0.5 m thick. It is composed of large, subrounded, cobble clasts in a fine sand matrix. There appear to be no striae or stoss-lee features. Clast orientation appears to be the same as in the overlying unit. The upper contact appears to be erosional. Dominant lithology is locally-derived pelitic schist (KTc - 5a) and granodiorite (Ogd - 2).

Unit 2, 1.5 m thick, is a non-compacted, sandy-silt diamicton with a predominantly fine sand matrix. The subangular clasts are striated on their underside only. At the base of the unit a deformed lens of fine mud forms part of the erosional contact with *Unit 1*, where this is absent the contact is made by a thin layer of fine sand. Bimodal clast orientation (an eigenvalue of 0.68), striae and stoss-lee features indicate that paleomovement was from the south. There is no apparent upper contact. Clast lithology is local, specifically pegmatitic granite gneiss (KTc - 5a) and pelitic schist (KTc - 5a), except for one staurolite (Ms - 5b) of distant origin.

2.2.36. Site 36

This is a bedrock outcrop located on the valley side about 0.6 km northwest of Flora Lake. It has striae and stoss-lee features indicating paleomovement from the south (Figure 2.1ad).

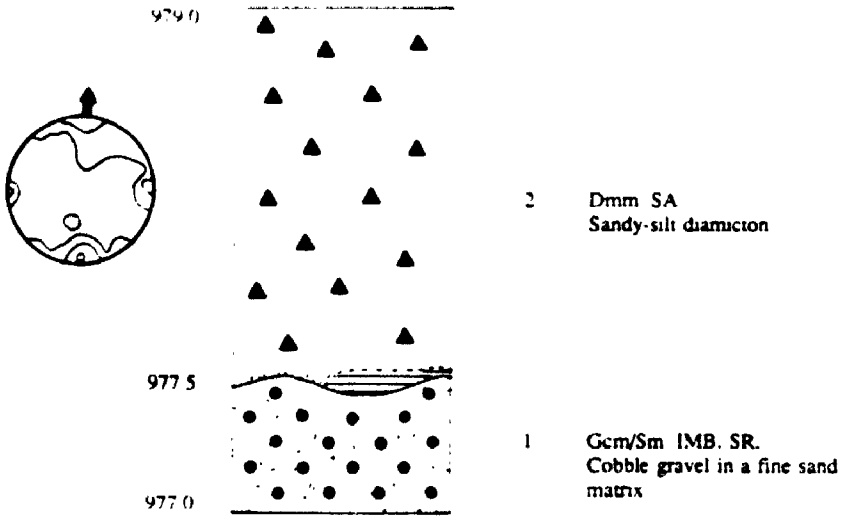

Figure 2.1ac **SITE 35**

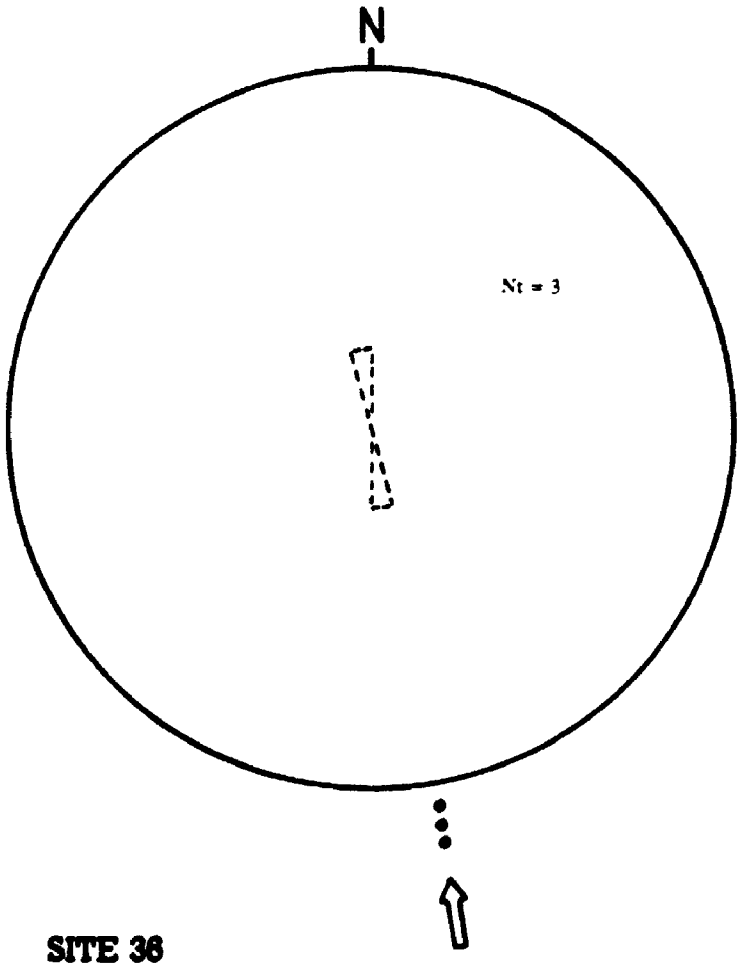

Figure 2.1ad **SITE 36**

2.2.37. Sites 37 and 38

These bedrock outcrops are located on the valley side about 0.4 km northeast of Flora Lake. They have striae and a stoss-lee feature indicating paleomovement from the south (Figure 2.1ae).

2.2.38. Site 39

This site is located in a high altitude, partially water-filled depression. It is located approximately 30 m south of Hope Mountain summit. Approximately 10 m northwest of this site preserved striae and a stoss-lee feature indicate paleomovement from the northwest (Figure 2.1af).

2.2.39 Site 40

This is a small slide scar adjacent to the main logging road 5.0 km from the mouth of Silverhope Creek (Figure 2.1ag).

Unit 1 is approximately 5.5 m thick. It is a compact, interbedded fine sand and coarse gravel unit with poorly-defined bedding planes dipping south at 2-5°. Strong clast orientations and imbrications (an eigenvalue of 0.98) indicate a southerly paleoflow. The upper contact appears to be conformable.

Unit 2 is about 5.0 m thick. The unit is composed of compact, fine laminated grey mud, with no visible dropstones. The upper contact appears to be erosional.

Unit 3 attains a maximum thickness of 19.1 m. It comprises a non-compacted, interbedded medium sand and gravel sequence with poorly-defined

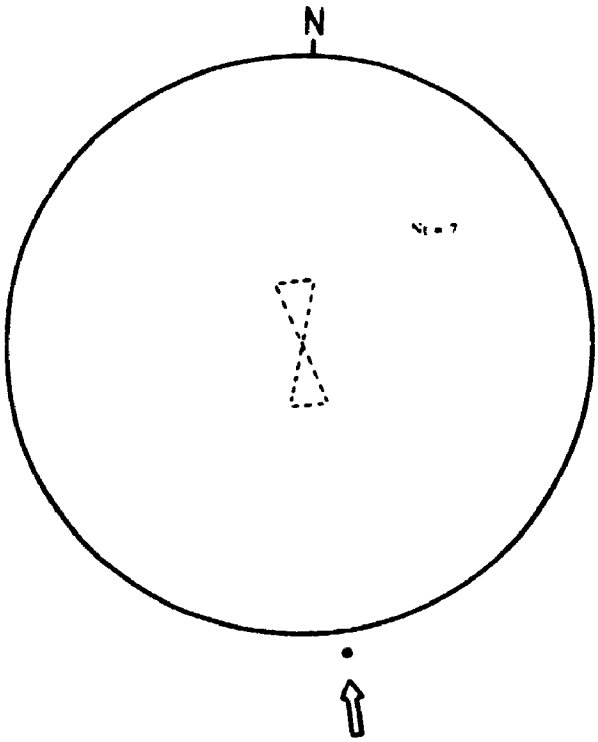

Figure 2.1ae **SITE 37/38**

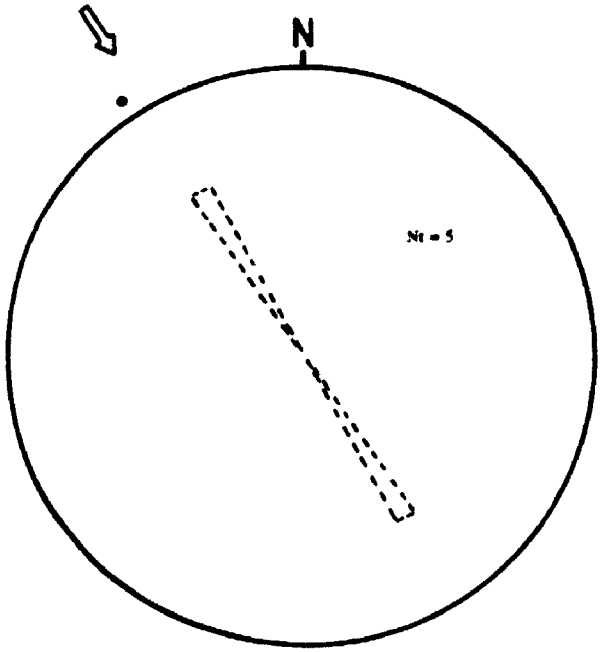

Figure 2.1af **SITE 39**

bedding planes dipping south at about 2°. It appears that paleoflow may have been to the south, but clast imbrications are rare.

2.2.40. Site 41

This is a small slide scar adjacent to the main logging road 5.2 km from the mouth of Silverhope Creek (Figure 2.1ah).

Unit 1 is compact and attains a maximum thickness of 3.5 m. It comprises interbedded medium sand and coarse gravel, with abundant sub-rounded clasts. There is poorly-defined planar cross-bedding, dipping north at 7-10°, most visible in the lower half of the unit. Imbrication indicates paleoflow to the north, although there is weak bimodality (an eigenvalue of 0.78). Deformation structures are visible in the upper half of the unit. The upper horizontal contact appears to be erosional. Gravel lithology is predominantly locally-derived pelite (PJH - 12a) and pelitic schist (KTc - 5a).

Unit 2 is approximately 0.5 m thick. It is composed of well sorted, compact, medium sand which fines upward. A layer of subrounded medium gravel appears to form an erosional contact with *Unit 1*. The unit pinches out to the south and possesses no distinct structures. An apparently erosional upper contact dips gently south at 3°. Gravel lithology is predominantly locally-derived pelitic schist (KTc - 5a) and argillite (Es - 3b).

Unit 3 is about 2.0 m thick, and has an upward colour change from sandy-yellow to grey. These fine, compact, laminated muds with dropstones possess deformation structures in the lower part of the unit. There also appears to be

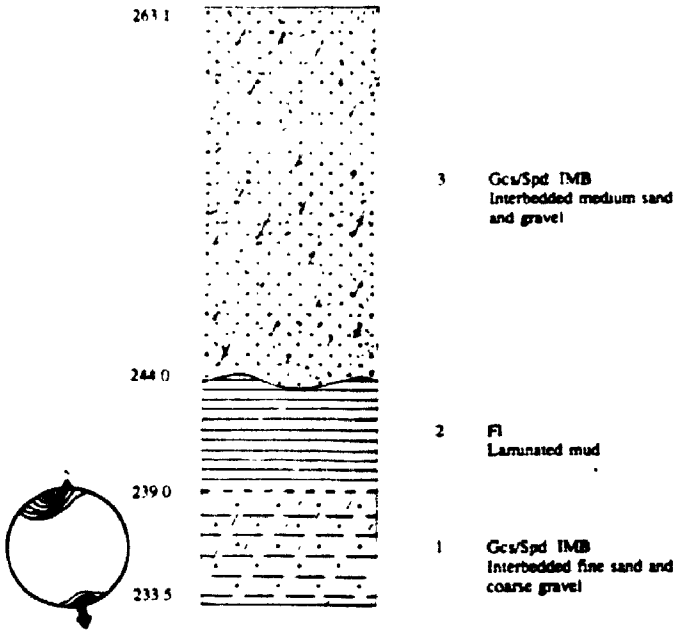

Figure 2.1ag **SITE 40**

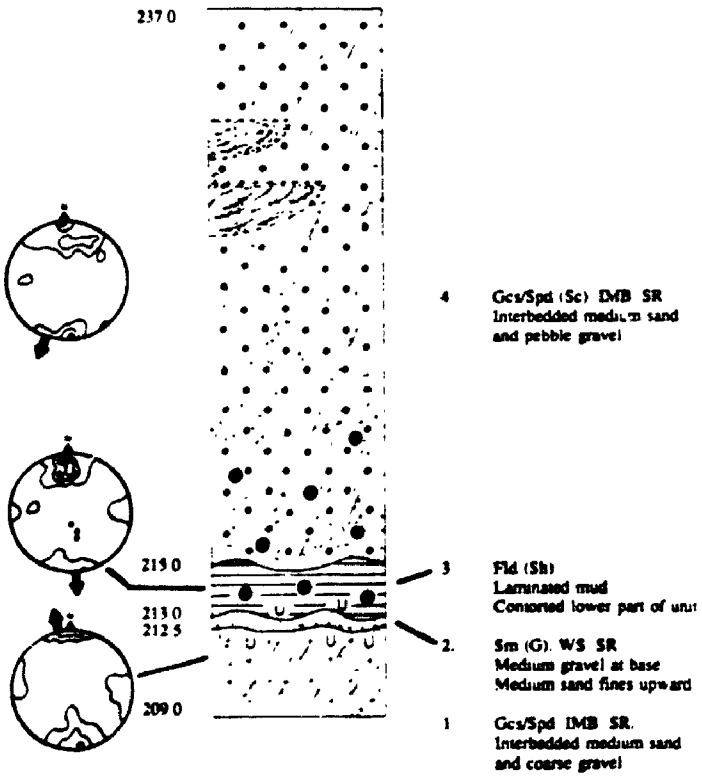

Figure 2.1ah **SITE 41**

several shear structures near the base of the unit. Dropstones appear to possess similar orientation to the south (an eigenvalue of 0.68). Most dropstones are of locally-derived granodiorite lithology (Ogd - 2), a few are of more distant origin. The upper contact appears to be erosional.

Unit 4 attains a thickness of 24.5 m. This is a compact, interbedded medium sand and pebble gravel, possessing crude bedding planes dipping south at 5-7°. Dropstones in a lower fine sand part of the unit are oriented in a similar direction to those found in *Unit 3.* Imbrication and orientation of the predominantly subrounded non-dropstone clasts indicate a southerly paleoflow direction, although there is some dispersal giving an eigenvalue of 0.79. There are some sandy channel fills in the upper part of the unit with apparent trough cross-bedding. Lithology is predominantly of locally-derived gabbro (PJH - 12a) and argillite (Es - 3b), with several distantly-derived gabbro (PMu - 11).

2.2.41. Site 42

This is a bedrock outcrop on the east valley side about 2 km north-northeast of Silver Lake. Striae and stoss-lee features are visible at a height of 1082.3 m and indicate paleomovement to be from the northwest (Figure 2.1ai).

2.2.42. Site 43

This is a small slide scar adjacent to the main logging road 5.8 km from the mouth of Silverhope Creek (Figure 2.1aj).

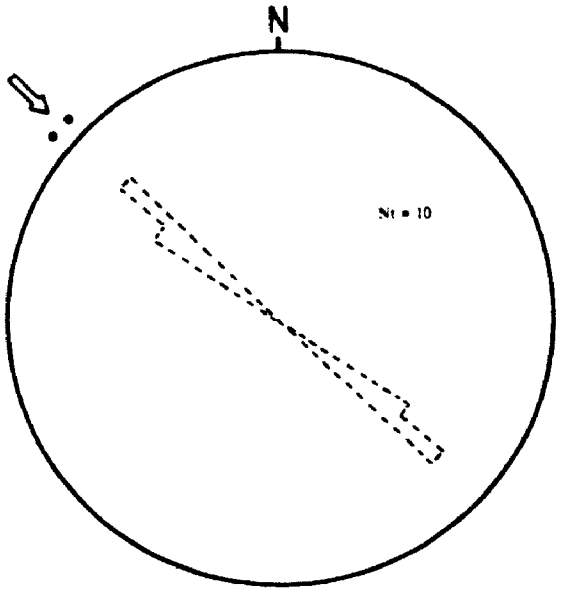

Figure 2.1ai **SITE 42**

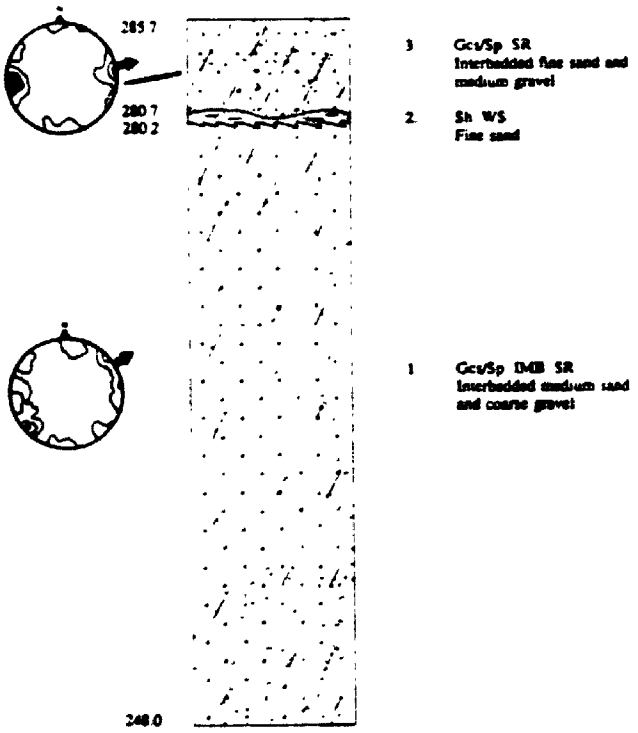

Figure 2.1aj **SITE 43**

Unit 1 is approximately 32.2 m thick. It comprises a non-compacted, interbedded medium sand and coarse gravel unit with subrounded clasts. Striae on the upper surfaces of larger clasts near the base of the unit are oriented west-east. Bedding dips gently (2-5°) to the east, but clast orientations and imbrications are strongly bimodal. Paleoflow appears to have been to the east-northeast, and the fabric has an eigenvalue of 0.71. Clast lithology is predominantly locally-derived granodiorite (Ogd - 2) and amphibolite (KTc - 5a). Locally-derived granodiorite (Ogd - 2) is the dominant lithology of the striated clasts. The upper contact appears to be gradational.

Unit 2 has a maximum thickness of 0.5 m. It consists of compact, horizontally-bedded, well sorted, fine sand. The upper contact appears to be erosional.

Unit 3 is approximately 5.0 m thick. It consists of a fine, non-compacted, interbedded fine sand and subrounded medium gravel. Beds dip east at 1-2°. Fabric is predominantly unimodal, with an eigenvalue of 0.82. Clast lithology is dominated by locally-derived diorite (Kgd,d - 7b) and argillite (Es - 3b).

2.2.43. Site 44

The exposure is in a small slide scar adjacent to the main logging road approximately 6.2 km from the mouth of Silverhope Creek (Figure 2.1ak).

Unit 1 attains a maximum thickness of 12.5 m. It consists of non-compacted, interbedded fine sand and medium gravel, with foreset beds dipping at 8° to the south. The upper contact appears to be erosional.

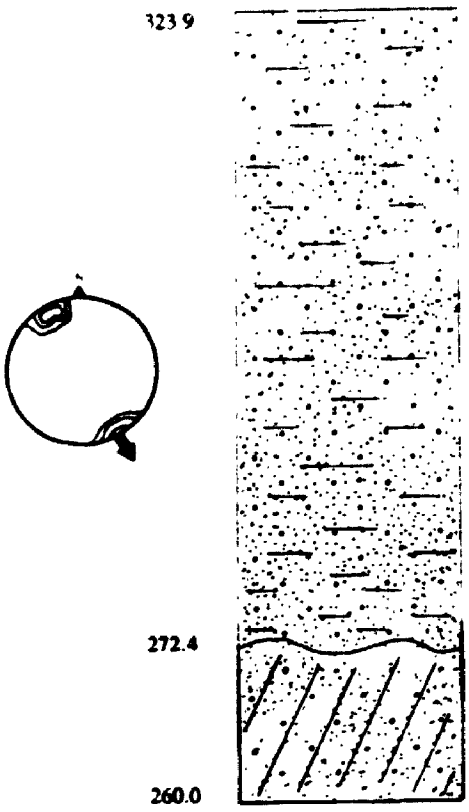

Figure 2.1ak **SITE 44**

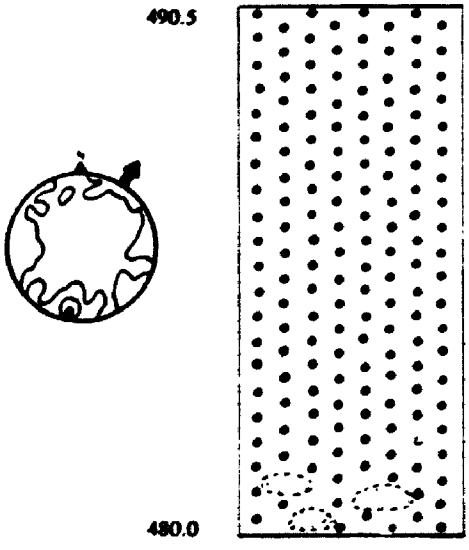

Figure 2.1al **SITE 45**

Unit 2 is about 50 m thick. It comprises a non-compacted, interbedded medium sand and gravel unit. There are horizontal topset beds with some ripples preserved. Strong clast imbrications and orientation (an eigenvalue of 0.99) indicate a southeast paleoflow. There is no apparent upper contact. Lithology was not studied.

2.2.44. Site 45

This is a small road cut exposure situated 0.2 km along an east valley logging road which leads off the main logging road about 7.7 km from the mouth of Silverhope Creek (Figure 2.1al).

Unit 1 is up to 10.5 m thick. There are no apparent contacts. This is a non-compacted pebble gravel with random stone fabric and an eigenvalue of 0.51. Three sand lenses are exposed near the base of the section. Parallel sets of striae, trending generally northwest - southeast, are visible on the underside of most subrounded clasts. Clast orientations indicate that paleoflow might be from either the west or south. There are several non-striated subangular clasts near the base of the exposed unit. The striated clasts are composed of only two lithologies, locally-derived granodiorite (Ogd - 2) and pegmatitic granite gneiss (KTc - 8a). Other clasts are dominated by locally-derived diorite (Kgd,d - 7b).

2.2.45. Site 46

The exposure is located in a disused gravel pit adjacent to the Silver Lake campground branch of the main logging road approximately 8.8 km from the mouth of Silverhope Creek (Figure 2.1am).

Unit 1 is about 2.5 m thick. There are no apparent contacts. It consists of a horizontally-bedded medium sand and pebble gravel unit, with bimodal imbrication structures and clast orientations to both the north and south. Several clasts are transverse to the principle eigenvector to the south, reducing the eigenvalue to 0.73. Large clasts are predominantly subangular with some poorly-preserved striae and numerous percussion marks. Near the base of the unit poorly-preserved bedding planes appear to dip gently south at 2-4°. Clast lithology is locally-derived granodiorite (Mgd - 1) and pelitic schist (KTc - 5a).

2.2.46. Site 47

This bedrock outcrop is situated on the west valley side adjacent to Silver lake. Striae and stoss-lee features suggest paleoflow from the northwest (Figure 2.1an).

2.2.47. Site 48

This bedrock outcrop located 3 km east of Silver Lake has striae and stoss-lee features indicating paleoflow to the south-southeast (Figure 2.1ao).

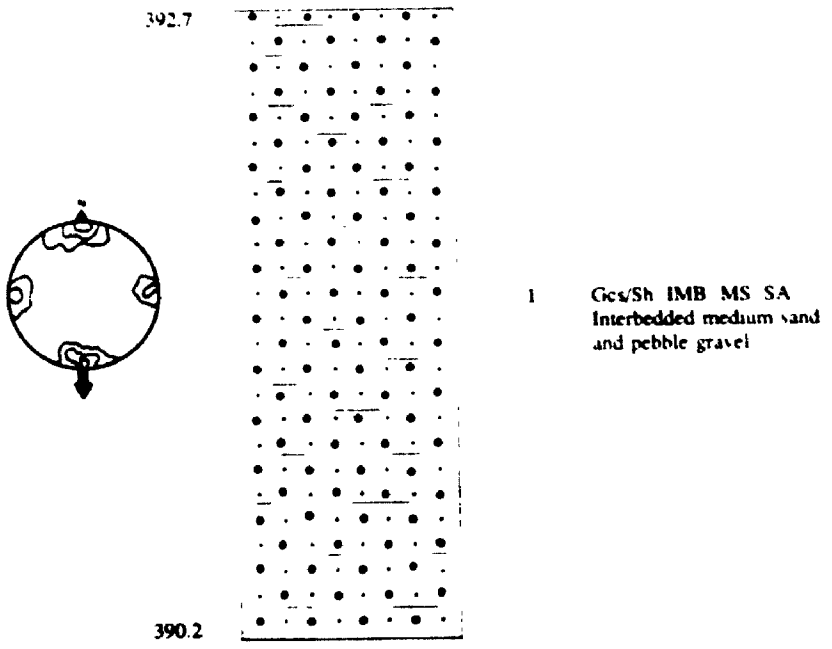

Figure 2.1am **SITE 46**

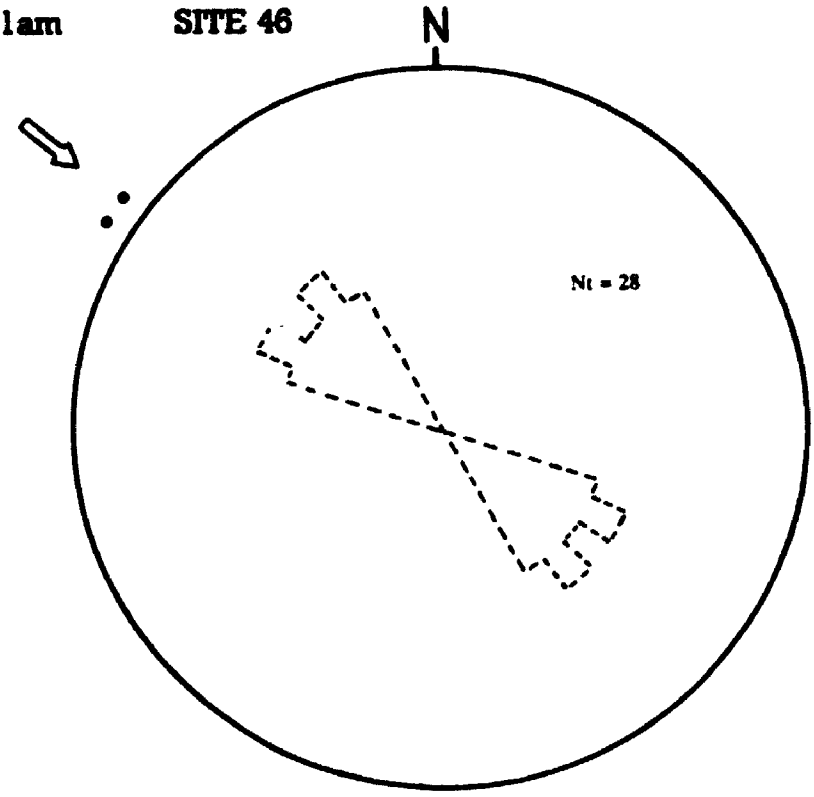

Figure 2.1an **SITE 47**

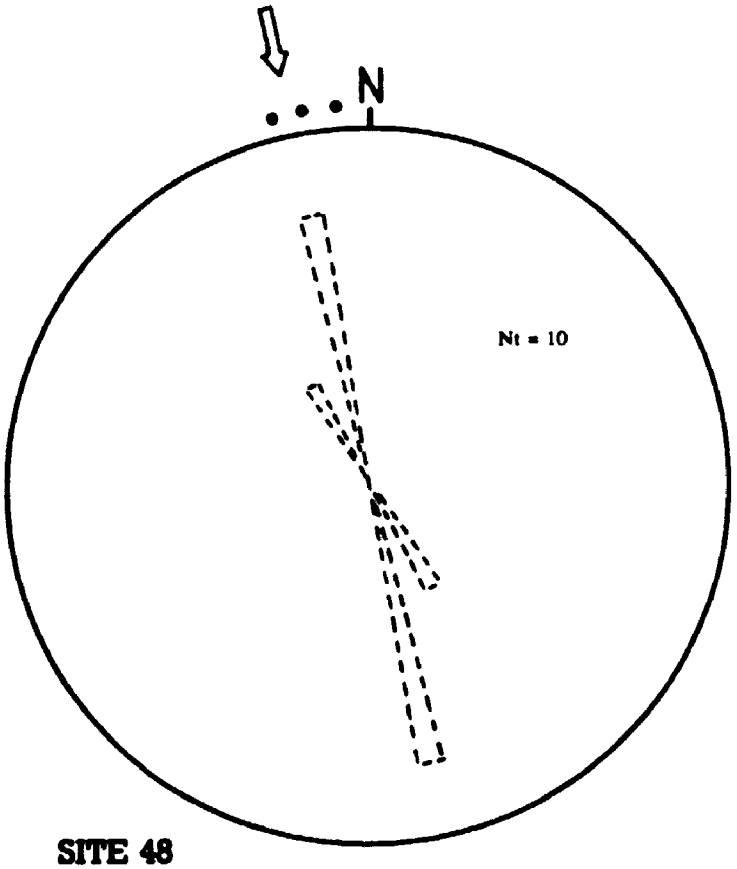

Figure 2.1ao **SITE 48**

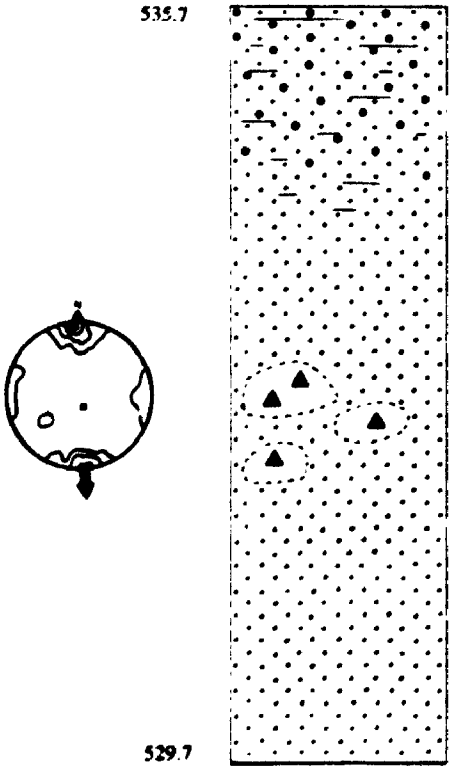

1. Gcm (Dmm). PS. SA. Medium gravel coarsening upward. Diamicton lenses in mud-unit

Figure 2.1ap **SITE 50**

2.2.48. Site 50

The exposure is located in a disused gravel pit adjacent to the main logging road approximately 15.1 km from the mouth of Silverhope Creek (Figure 2.1ap).

Unit 1, about 6.0 m thick, has no apparent contacts. This is a compact, massive medium gravel unit which coarsens upwards. The upper part of the unit possesses coarse horizontal bedding. Diamicton lenses are present in the lower half of the unit, where there is transition to a muddy gravel. Pitted, striated, bullet shaped clasts are visible in these diamicton lenses. Immediately beneath the diamicton lenses clast orientations are chaotic. In the upper part of the unit, clast imbrication and orientation are bimodal, but indicate general paleoflow to the south (an eigenvalue of 0.74). Dominant lithology of the pitted, striated, bullet-shaped clasts is locally-derived pegmatitic granite gneiss (KTc - 5a). Gravel lithology is mainly locally-derived granodiorite (eTgd - 4), gabbro (PJH - 12a) and sandstone (Es - 3b).

2.2.49. Site 51

This is a valley floor bedrock outcrop located on the western shore of Eaton Lake. Striae and stoss-lee indicate paleoflow from the east-northeast (Figure 2.1aq).

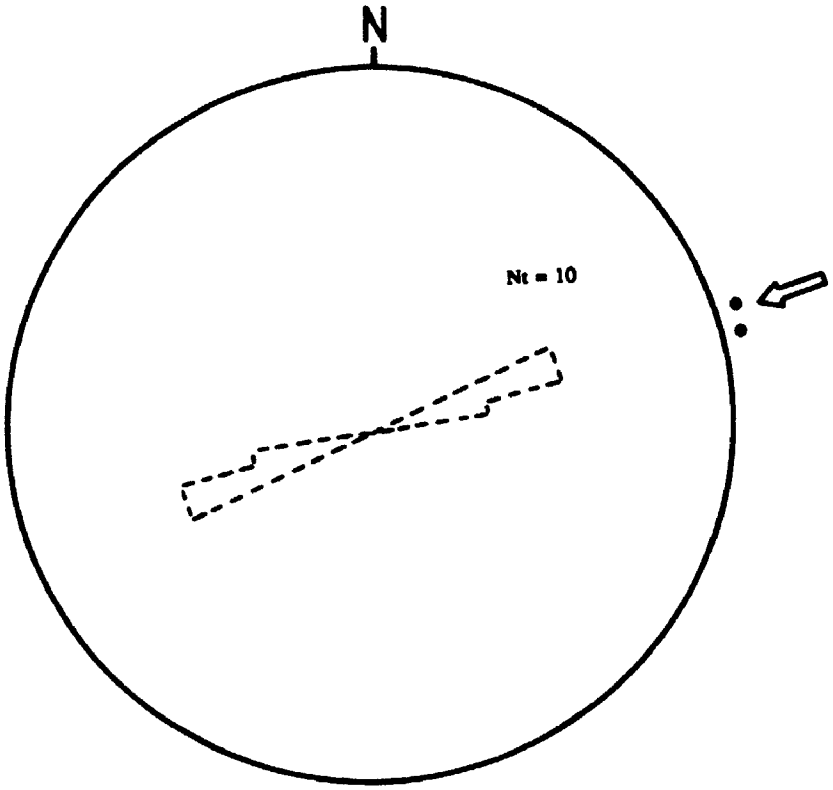

Figure 2.1aq SITE 51

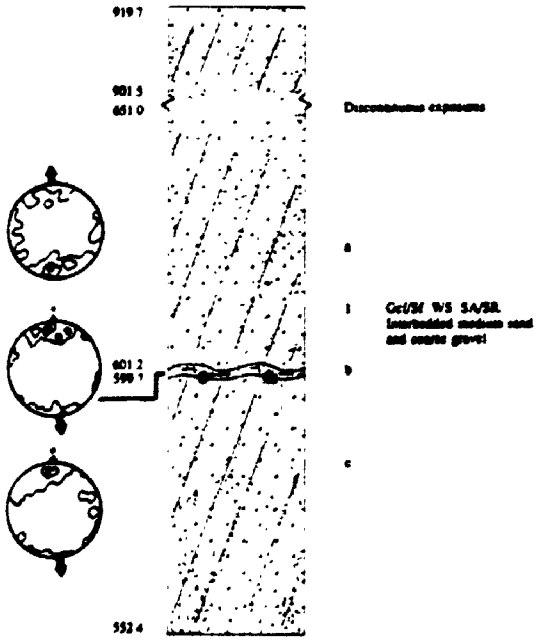

Figure 2.1ar SITE 53

2.2.50. Site 53

The exposure is a large slide scar and gravel pit adjacent to the main logging road approximately 18.3 km from the mouth of Silverhope Creek (Figure 2.1ar).

Unit 1 is discontinuously exposed but appears to retain similar texture over a thickness of about 367.3 m. The largest exposure, which attains a maximum thickness of 98.6 m, was studied in detail. This is a non-compacted, well sorted, interbedded medium sand and coarse gravel unit, with few fines. The lower part of the unit (*1c*) comprises foreset beds dipping south at 6-10°. In subunit *1c*, percussion marks and poorly-preserved fine striae are visible on many clasts. Several pebble clusters composed of horizontally imbricated stones are visible. Most clasts appear to have avalanched down foresets and stacked on top of each other. Imbrications are scattered but paleoflow appears to be generally southward (an eigenvalue of 0.77). Clasts appear to be coarser in subunit *1c* than in the overlying sediments. Rare dropstones, with preserved striae, are found near the base of a thin subunit of what appear to be topset beds in *1b*. Immediately beneath these topsets, foreset beds dip more steeply at an angle of 10-18°. The small topset subunit is about 1.5 m thick and is overlain by more foreset beds. Both the upper and lower contacts of the topset subunit appear to be erosional. The upper subunit (*1a*) is discontinuously exposed with the southerly dip of the foreset beds steepening upwards from 5 to 15°. Allowing for clast avalanching, scattered imbrication suggests southward paleoflow, eventhough indicators are oriented north. Dominant lithologies of the coarse,

subrounded lower subunit are locally-derived pelitic schists (KTc - 5a), granodiorite (eTgd - 4) and chert (PJH - 12a). Clast lithology of the finer, subangular, upper subunit is more diverse, but is dominated by locally-derived pelitic schist (KTc - 5a).

2.2.51. Site 54

This is a gully cut located on the east valley side adjacent to the main logging road approximately 18.5 km from the mouth of Silverhope Creek (Figure 2.1as).

Unit 1 is approximately 1.1 m thick. It is composed of a compact, grey, silty-sand diamicton. Clasts are predominantly subangular, and possess no apparent striae, stoss-lee features, or shear planes. Fabric data are strongly unimodal and indicate paleoflow from the north, with an eigenvalue of 0.95. Small clay lenses (not shown in diagram) are visible toward the upper part of the unit. The upper contact appears to be conformable. Dominant lithologies are locally-derived pegmatitic granite gneiss (KTc - 5a), pelitic schist (KTc - 5a) and pelite (PJH - 12a).

Unit 2, about 0.9 m thick, is composed of a grey, finely laminated mud with dropstones. The dropstones (apparently of distantly-derived argillite - Es - 3b, but not analysed) are subrounded and rest conformably on the surface of the lower contact. Many have upper surfaces covered by clay drapes. There are no apparent striae, stoss-lee features or deformation structures. There is no apparent upper contact.

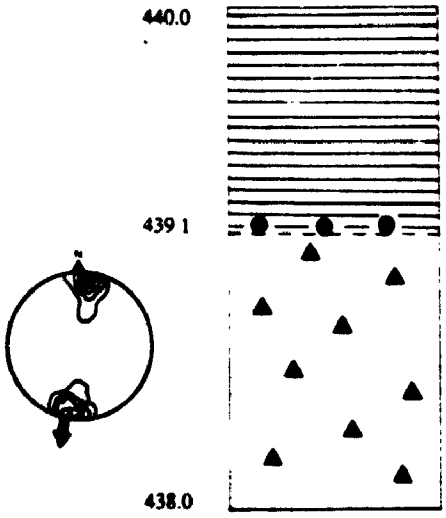

2. Fld.
Laminated mud

1. Dmm. SA.
Silty-sand diamicton

Figure 2.1as **SITE 54**

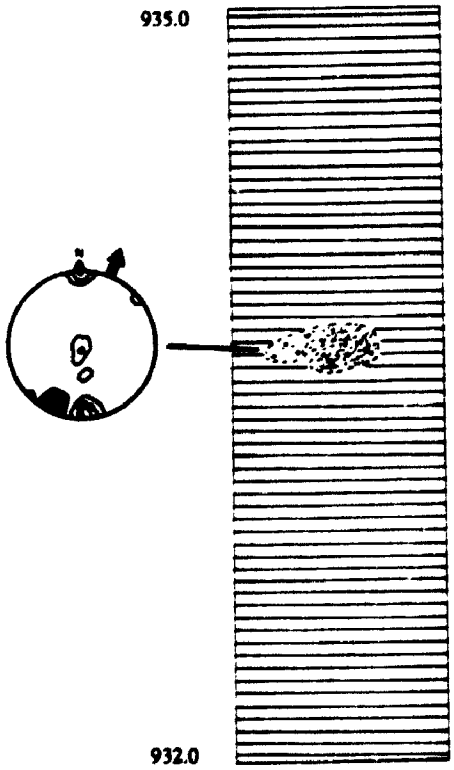

a

1. Fl.
Laminated mud
Roll-up structure in mud-unit

Figure 2.1at **SITE 56**

2.2.52. Site 55

This is a road cut situated on the Yola Creek logging road approximately 1.8 km from the junction with the main logging road.

Unit 1 attains a thickness of 3.0 m. It is composed of fine laminated mud with rare dropstones. No striae are visible on the subangular dropstones. There are no apparent deformation structures or contacts.

2.2.53. Site 56

This is a gully cut situated on the east valley side adjacent to the main logging road approximately 21.3 km from the mouth of Silverhope Creek (Figure 2.1at).

Unit 1 is about 3.0 m thick. It is composed of compact, fine, grey, laminated mud. In the middle of the unit is a medium sand and gravel lens (subunit *a*) which appears to thicken toward the southeast. Subrounded clasts incorporated within this feature appear to be oriented perpendicular to the direction of thickening. The feature terminates abruptly as a roll-up structure at the attenuated end. Clast orientation in the lens indicates paleoflow from the southwest (an eigenvalue of 0.77), if transverse it would suggest paleoflow from the southeast. The laminated muds possess no dropstones and within the sand and gravel lens there appear to be no striated clasts. There are no apparent contacts. Dominant lithology is locally-derived granodiorite (eTgd - 4), but some distantly-derived quartz granodiorite is present (Kgd - 7b).

2.2.54. Site 57

Site 57a is a bedrock exposure located on the west side of Mount Forddred. Striae and stoss-lee features indicate paleomovement from the north-northwest (Figure 2.1au). Site 57b, 58 m higher, is a bedrock exposure which possesses no paleomovement indicators.

2.2.55. Site 58

This exposure is a slide scar situated on the Hicks Creek logging road, approximately 0.4 km from the main logging road (Figure 2.1av).

Unit 1, 4.2 m thick, is a non-compacted, subrounded and subangular clast-supported medium sand and gravel with a diamicton lens. Beds dip at about 2° south, with strongly bimodal clast imbrication and pebble clusters. The principle eigenvalue suggests paleoflow from the south, although the eigenvector is only 0.55. There are no striae or stoss-lee features. The diamicton lens appears to be a compact, grey, muddy-gravel, beneath which there is some colour gradation into the sandy-yellow colour of *Unit 1*. There are no apparent contacts. Dominant lithology is locally-derived pelitic schist (KTc - 5a), but over 20% of the clasts analysed are of more distantly-derived lithology.

2.2.56. Sites 60, 63 and 66

This is a section of valley floor located in an area of clear cut forest adjacent to the main logging road about 26-28 km from the mouth of Silverhope Creek.

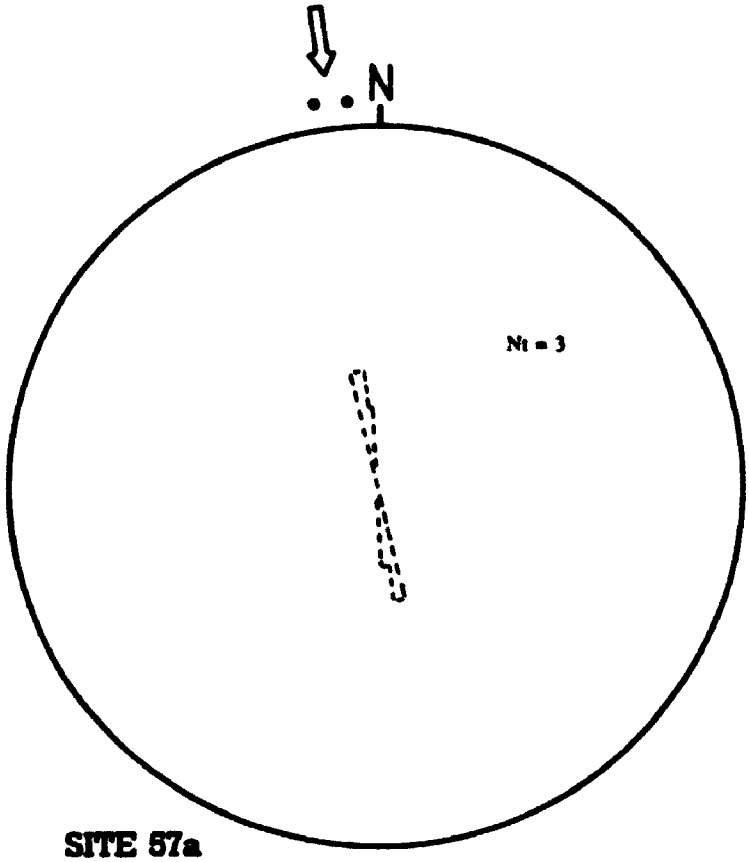

Figure 2.1au **SITE 57a**

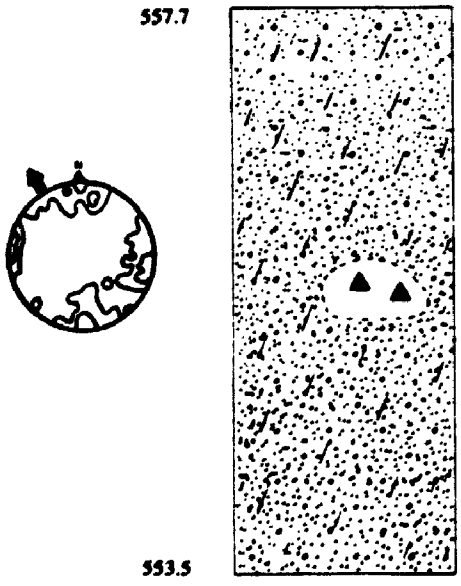

1. Gcp. IMB. SR.
Medium sand and gravel
with diamiction lens

Figure 2.1av **SITE 58**

There are a series of seven low hills with elevations between 614-630 masl. To the east of these hills are two clearly-defined terraces between about 570 and 580 masl. The elevations of these terraces coincide with ones cut into the northeast side of the most northerly hill. A narrow plain (approx. 618.6 masl), emanating from a small east side valley extends southward separating the most southerly hill from the rest of the group. Further south there appears to be an extensive plain of hummocky terrain (approx. 631.5 masl) covered by a series of fans emanating from the valley sides. Immediately to the south of this site are the headwaters of Silverhope Creek and Klesilkwa River. There appears to be a series of shallow water-filled depressions adjacent to a fan that emanates from the Upper Silverhope valley. The morphology of this area is discussed in more detail in Section 4.3.4., and the approximate topography is detailed in Figure 4.3.

2.2.57. Site 61

The exposure is in a road cut adjacent to the main logging road approximately 26.0 km from the mouth of Silverhope Creek (Figure 2.1aw).

Unit 1 is about 5.5 m thick. It is composed of a compact, grey, silty-sand diamicton. There is no apparent lower contact. Dispersed clast orientation of the predominantly subrounded clasts indicates paleomovement to the southeast (an eigenvalue of 0.70). Measurements of striae and stoss-lee features, including one bullet-shaped clast, concur. In the upper part of the unit there are deformation structures (clay smears, water escape features) which attenuate to the south, but immediately beneath these some of the subrounded clasts have clay drapes. A

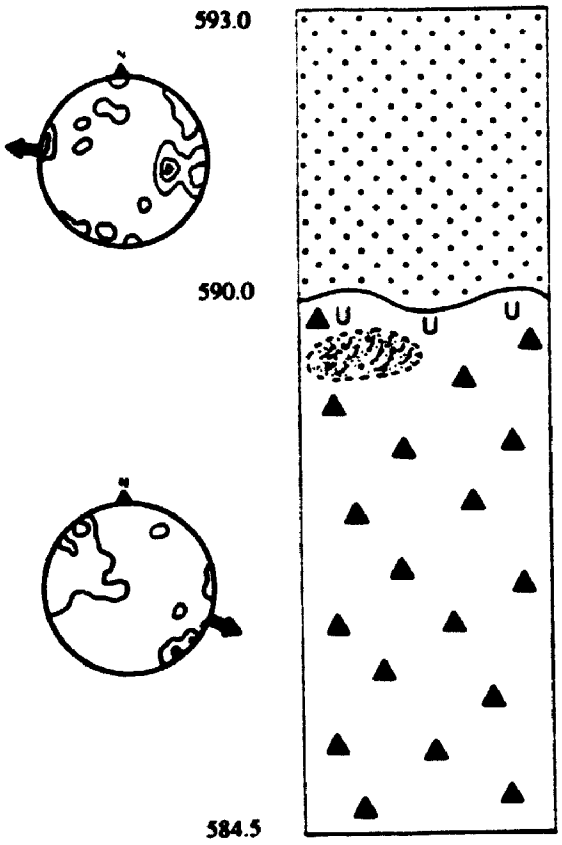

2. Gcm/Sm. SR.
Coarse sand and gravel

1. Dmm. SR.
Silty-sand diamicton

Figure 2.1sw **SITE 61**

large fine sand and medium gravel lens near the upper contact appears to be separate from the overlying unit and possesses trough-fill cross-stratification. Clasts in the upper half of the section dip more steeply than those beneath. There appears to be an upper erosional contact. Clast lithology is locally-derived gabbro (PJH - 12a).

Unit 2, 3.0 m thick, is a non-compacted, grey, massive coarse sand and gravel. Clasts are subrounded and a weakly bimodal orientation suggests paleomovement to the west-northwest (an eigenvalue of 0.64). There are no other visible paleomovement indicators or stratification. There is no apparent upper contact.

2.2.58. Site 62

The exposure is in a gravel pit adjacent to the main logging road approximately 26.6 km from the mouth of Silverhope Creek (Figure 2.1ax).

Unit 1 attains a maximum thickness of 17 m. This unit has no apparent lower contact, and appears to have been truncated at the upper contact by a thin colluvial veneer (not labelled on diagram). In the upper part of the unit (subunits *1a* and *1b*), non-compacted, interbedded medium sand and coarse gravel dips at 5-7°. In the lower subunit (*1c*), they are horizontal. Bimodal clast imbrication and orientation indicate two paleoflow directions, from the east-southeast (subunits *1a* and *1b*, with eigenvectors of 0.74 and 0.75 respectively) and southeast (subunit *1c* - an eigenvector of 0.67). Subunit *1c* appears to be coarser than the other subunits, with the larger clasts possessing no striae, but some fine striae are

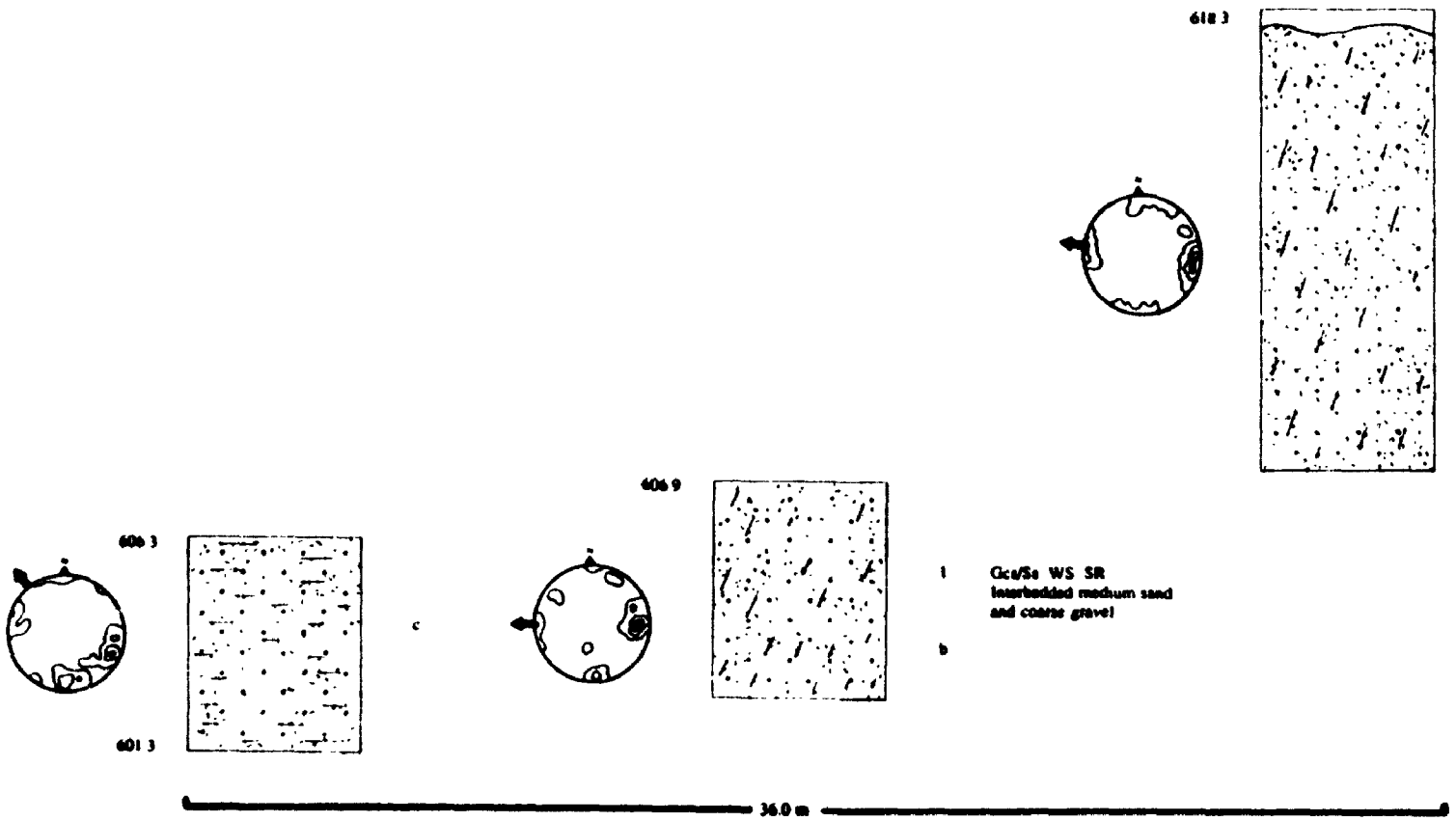

Figure 2.1ax **SITE 62**

evident on smaller clasts. Some clasts in subunit *1b* appear to dip downbed. Clast lithology in subunits *1a-c* is predominantly locally-derived granodiorite (eTgd - 4), gabbro (PJH - 12a) and pelite (PJH - 12a). Subunit *1c* has a higher percentage of locally-derived pegmatitic granite gneiss (KTc - 5a).

2.2.59. Site 64

This is a gully cut situated on the east valley side adjacent to the main logging road approximately 27.8 km from the mouth of Silverhope Creek.

Unit 1 is about 2.5 m thick. It is composed of compact, grey, fine laminated mud with rare, small dropstones. There are no apparent structures, or contacts. The lithologies of the two visible dropstones appear to be locally-derived pelite (PJH - 12a) and argillite (Es - 3b) of more distant origin, but these were not analysed in detail.

2.2.60. Site 65

This is a gully cut situated on the east valley side adjacent to the main logging road approximately 29 km from the mouth of Silverhope Creek (Figure 2.1ay).

Unit 1 is a non-compacted medium and coarse gravel with visible diamicton, sand, and mud lenses. There are no apparent contacts. In the upper part of the unit, a mud lens pinches out toward the south. Fine sand lenses are visible in the middle of the unit. Clast orientation and pebble clusters indicate paleomovement is generally to the south, although there is some dispersal (an

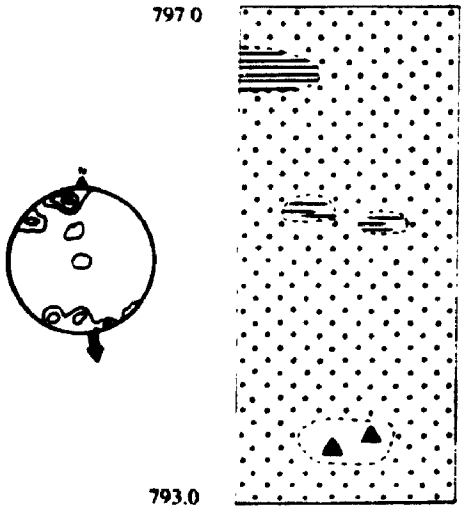

1. Gcs SR.
Medium and coarse gravel with diamicton, sand and mud lenses

a

Figure 2.1ay **SITE 68**

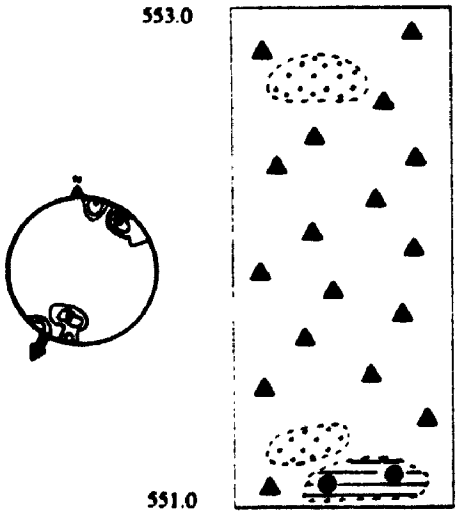

1. Dmm. SR.
Silty-clay diamicton

Figure 2.1az **SITE 68 *Unit 1***

eigenvalue of 0.76). The silty-sand diamicton lens in the lower part of the unit was sampled for particle size and lithology (*Unit 1a*). Dominant lithology of the diamicton lens is locally-derived pelite (PJH - 12a) and pelitic schist (KTc - 5a). The sand and gravel has a more diverse lithology, but is also dominated by locally-derived pelite (PJH - 12a) and pelitic schist (KTc - 5a).

2.2.61. Site 68

This is a section of valley floor located in an area of clear cut forest about 34-35 km from the mouth of Silverhope Creek. It is situated between the main logging road and Klesilkwa River at a point approximately 5-6 km southeast of the Silverhope Creek-Klesilkwa River confluence.

Unit 1 is approximately 2.0 m thick (Figure 2.1az). The unit is composed of a compact, yellow-grey, silty-clay diamicton. Near the base of the exposure is a lens of deformed, fine laminated mud with rare dropstones. Immediately above this is a coarse sand and gravel lens. Neither lens appears to have become disaggregated and incorporated into the surrounding diamicton. A similar coarse sand and gravel lens is situated near the top of the unit. Dispersed subrounded clast orientation within the diamicton indicates paleomovement from the northeast (an eigenvalue of 0.61). Paleocurrent indicators within the sand and gravel lenses were difficult to assess but appear to show west (lower lens) and southwest (upper lens) paleoflow directions. There are no visible striae, stoss-lee or deformation structures. Dominant clast lithology is locally-derived pelite (PJH - 12a), but distantly-derived sandstone (Es - 3b) is present.

The upper contact is formed by large subangular and subrounded clasts of locally-derived granodiorite (Ogd - 2), with no apparent matrix (*Unit 1a*). These clasts are agglomerated into boulder mounds up to 7.0 m above the underlying unit, and 12.0 m above adjacent depressions. Shallow depressions appear to separate these boulder mounds, some of which are water-filled, the remainder being linked by a meandering system of dry channels. Individual clasts attain a maximum long axis of about 10 m. Predominant clast orientation suggests paleomovement to the east, and boulder mound orientation concurs (Figure 2.1ba). There are no striae or stoss-lee features.

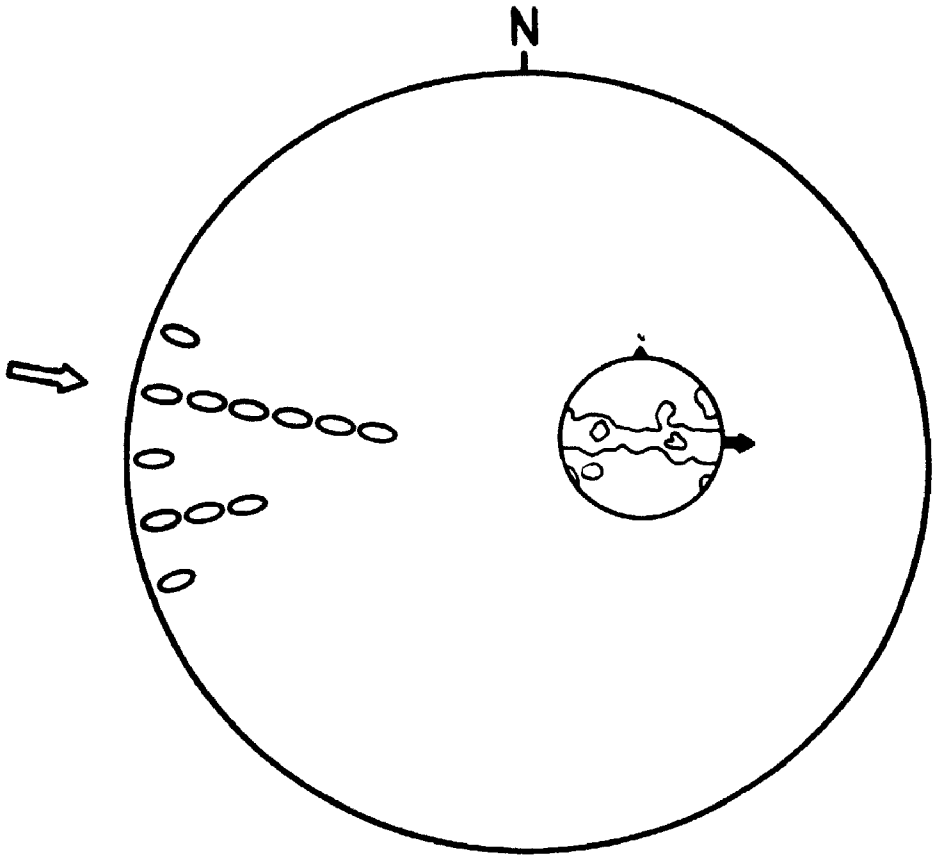

Figure 2.1ba **SITE 68**

CHAPTER THREE

LATE WISCONSINAN SITE FACIES INTERPRETATIONS

3.1. Introduction

Depositional environments are interpreted based upon the observations made at exposure sites in Chapter Two. This information is used in Chapter Four for the interpretation of the local and regional history of late Wisconsinan sedimentation.

Where reference is made to the reworking of sediments by meltwater, this includes water conductivity through sediment pore spaces as well as surface winnowing. The extent of reworking is dependent upon the degree of meltwater conductivity (i.e. meltwater conductivity is higher where most pore spaces are interconnected and surface runoff is unimpeded).

In this thesis a kame terrace is defined as a laterally extensive (not necessarily continuous) ridged valleyside landform, typically consisting of sand and gravel with generally unimodal fabric parallel to the valleyside. It is considered to have been laid down by meltwater at the junction between an ice mass and the valley wall (Allaby and Allaby, 1991). Kame terraces can be distributed in a step-like sequence along valley sides when ice downwastes in stages (Trenhaile, 1990). In the absence of topographic lows it is believed that drainage of ice-dammed lakes took place through kame terrace outlets, similar to the ice-marginal drainage paths discussed by Fulton (1969).

3.2. Depositional Environments

3.2.1. Site 1

Based upon analysis of aerial photographs of this site, it appears to be located on a proglacial alluvial outburst fan emanating from a low pass in the interfluve between Silverhope Creek and Fraser valley. Analysis of aerial photographs also shows that in Silverhope valley there appears to be a relict kame terrace feature forming a topographical ridge on the west valley side, just to the south of the low pass. The ridge only extends for about 50 m and there are no apparent exposures. Strong unimodal imbrication structures in clasts up to 10 m in diameter suggest an outburst origin.

3.2.2. Site 2

Based upon the presence of striated, subrounded dropstones (some of which are distantly-derived) in a laminated mud, *Unit 1* would appear to have been laid down in a distal glaciolacustrine environment. *Unit 2* is compact, and appears to be composed of reworked lacustrine sediment. It possesses a weak bimodal fabric of clasts rolled transverse to flow, several discrete sand lenses, water escape features and flame structures rising up into the overlying unit. Based upon these observations this unit appears to have been laid down in a subglacial, ice marginal environment, and to have been partially reworked by meltwater. Preservation of sand lenses suggests that the surrounding diamicton was frozen, and the environment most closely approximates a subglacial meltout till. Deposition appears to have occurred passively, from a stagnant ice mass (Dreimanis, 1990).

Deformation at the upper contact with *Unit 3* suggests that it may have been overlain by rapidly-deposited fluvial sediments, producing some squeeze-flowtill structures (Dreimanis, 1989) during ice melt, and reorienting some clasts into a closely-grouped bimodal pattern.

Based upon the sedimentary structures in *Unit 3* (planar cross-bedding), the presence of percussion marks on several clasts, and lithology, this appears to have been laid down rapidly in a proximal (?) glaciofluvial environment.

3.2.3. Site 3

Based upon the presence of a thick deposit of laminated silty-mud, dropstones with poorly-preserved striae, *Unit 1* appears to be a proximal glaciolacustrine environment, perhaps abutting a delta.

Unit 2 has a complex depositional history. It is a compact, muddy diamicton, with flame structures, fine sand inclusions, fine sand interbeds near the top of the unit, striae on the upper surfaces of clasts, stoss-lee features, bimodal fabric, preserved clay smudges which pinch out, and many distantly-derived clasts. This suggests at least two subglacial deposition processes, lodgement and meltout. Based upon the presence of numerous upper surface striae and flame structures at the lower contact, lodging of an entire sheet of debris-rich basal ice appears to have taken place (Dreimanis, 1990). During lodgement, the saturated sediment would have had a lower shear strength than overriding ice (Boulton and Paul, 1976), leading to deformation eventhough the bed was most likely frozen. Evidence can be found in some transverse striae which may reflect clast reorientation in a

viscous medium during lodgement. Proximity to the ice margin during deglaciation suggests that the ice may have been approaching stagnation. This might account for the settling of clasts in a bimodal fabric, one related to lodgement, the other to local depositional slope (Hicock, 1992). Later subglacial meltout of the entire sheet reworked much of the fine material and also preserved deformed clay smudges (Edwards, 1986). Lack of bottom striae might be related to several factors; clast rotation, local shear within the ice conferring striae on the upper surfaces of englacial debris, and the flow of meltwater in discrete channels (fine sand interbeds) smoothing the bottom surface of clasts. This frozen slab may have been previously lodged elsewhere upglacier.

Based upon the presence of a compact, horizontally-interbedded sand and gravel, with subangular dropstones *Unit 3* appears to have been laid down rapidly in an ice marginal glaciofluvial/glaciolacustrine environment. Sediments appear to have been laid down by an aggrading system, forming a conformable contact with the underlying unit. Sediment supply appears to have been greater than meltwater competence, and together with geomorphic evidence, the presence of subangular dropstones suggests that much of the material emanated from valley side sources. Mud drapes over these clasts, and the predominance of sand-sized material suggest that deposition may have been taking place on a low-lying delta in an ice marginal lake, with some larger clasts being slowly rolled along horizontal beds (bimodal fabric data). The presence of some distantly-derived clasts indicates that much of the sediment source was glacigenic.

Unit 4 appears to have a complex depositional history. Based upon the presence of a lens of fairly well sorted, subrounded, non-striated clasts at the base of the unit (conformably overlying *Unit 3*) there appears to have been meltwater drainage in an aggradational environment. Shear planes rising up from pebble clusters of striated (some on the upper surface), subrounded dropstones in the top of the lens suggest that lodgement by active ice may have proferred orientation and striae on the upper surface of a subglacial meltwater deposit. The presence of flame structures intruded into a finer, overlying diamicton in the middle of the unit, and a lens of finer diamicton squeezed down into a cavity-fill behind a boulder, at the same level suggests that passive subglacial meltout may have occurred (preserved clay smudges overlie this section), which may have been deformed later by density differences and/or overloading by stagnant ice. Further evidence for separate phases of lodgement and meltout can be inferred from the striae and stoss-lee record (Figure 2.1c). Probable lodgement-proffered top and bottom surface striae appear to be oriented north-south, as opposed to meltout-dominated striae and stoss-lee features which are oriented northeast-southwest.

Based upon the presence of a deformed lower contact and loose, horizontally-stratified fine sand *Unit 5* appears to be of glaciofluvial origin. A lack of mud suggests that this may have been deposited in a distal proglacial stream.

3.2.4. Site 6

Based on the presence of poorly-defined massive bedding planes, weakly bimodal fabric, preserved striae on the underside of some clasts and smooth upper

surfaces of clasts, in a compact gravel; *Unit 1* appears to be a glaciofluvial - ice marginal deposit. It is exposed in a topographical ridge along the west valleyside and appears most likely to be a kame terrace feature.

Unit 2 appears to have been deposited in an ice marginal glaciolacustrine environment. This is based on the presence of laminae, striated dropstones, deformation structures, and its association with kame terrace deposits. *Unit 3* appears to be similar to *Unit 1*. However, based upon the presence of larger clasts agglomerating in pebble clusters and a more diverse lithology, it appears to have been a more active glaciofluvial environment, and may represent a more established outlet for meltwater flows alongside the ice.

3.2.5. Site 7

This exposure is located on a topographical ridge similar in form to Site 6. Based on this information and the presence of a coarsening-upward weakly bimodal fabric, and mud lenses with rare sub-angular dropstones in the lower part of the unit; *Unit 1* appears to be a kame terrace feature. The presence of finer fabric and discrete mud lenses in the lower part of the unit suggests that flow was established through an ice marginal area zone with some supraglacial debris and frozen lacustrine deposits. More competent flow became established later.

3.2.6. Site 8

Unit 1 is located in an exposure on a third topographic ridge, above Sites 6 and 7. Based upon the similarity of sedimentary structures and texture between

this unit and Site 7 - *Unit 1*, this appears to be a kame terrace feature. Flow competence may have been higher than Site 7 because of the presence of several imbrication structures in the upper part of the unit. The presence of many distantly-derived lithologies indicates that the unit is composed of reworked glacigenic deposits.

3.2.7. Site 11

Based upon the presence of a diamicton with striated clasts near the base and a gradation into a muddy gravel near the top, *Unit 1* appears to consist of a subglacial diamicton which has been reworked by meltwater in the upper part of the unit. Bearing in mind that the unit is overlain by a glaciolacustrine sequence, it is suggested that *Unit 1* represents the inundation of retreating tributary ice by glaciolacustrine conditions caused by ice dams in the main valley. The ice may have been a stagnant glacier margin which became buried by successive sequences of glaciolacustrine and glaciofluvial sediments.

Unit 2 appears to be a glaciolacustrine sequence near an ice margin (a horizontally-interbedded sand and mud unit with subangular dropstones). Subangular dropstones appear to have emanated from the tributary glacier (either by rain-out from a floating ice margin, or from iceberg rafting). The glaciolacustrine sequence into *Unit 4* is interrupted by a non-compacted, fining-upwards, weakly-bedded gravel which pinches out. This forms an erosional contact with *Unit 2* and it is suggested that this represents a turbidity flow from the ice margin into the ice marginal lake.

Based upon the stratigraphic continuity of the exposure, *Unit 5* would appear to be of glaciofluvial origin. The presence of bimodal fabric, fining upward particle size, subrounded clasts and some distantly-derived lithologies together suggest that initial deposition of reworked glacigenic deposits was rapid. Flow competence diminished with a decline in meltwater supply. Reworked distantly-derived clasts being transferred from the southwest section of Sowerby Creek suggests that tributary ice was, at some point, overridden by the Cordilleran Ice Sheet.

3.2.8. Site 12

Based on the presence of subrounded clasts with basal striae, stoss-lee features, unimodal fabric with clast dispersal and settling, preserved clay smudges which attenuate northwards, several small sand lenses and some distantly-derived lithologies, this compact diamicton (*Unit 1*) appears to be a subglacial meltout till. Slow release of meltwater has preserved clay smudges and striae on the bottom of clasts (Shaw, 1985). More rapid meltwater release is confined to small sand lenses, and the lower part of the unit where small dropstones are preserved.

Unit 2 appears to have been glaciofluvially deposited, becoming gradually more distant from the ice margin. This is based on the presence of a gradational sequence of sediments from gravel lag, to rippled, fine sands and laminated mud.

3.2.9. Site 13

Based on the presence of large clasts with no apparent striae or stoss-lee features, distinct fabric bimodality, a concentration of larger clasts near the top part

of the unit (pinching out to the north), flame and diapiric structures at the upper contact; *Unit 1* appears to be a subglacial diamicton. Bearing in mind the reworking of fines in other units, resedimentation by meltwater appears to have removed fines from the upper part of the unit and smoothed the surfaces of large clasts. Overriding by ice appears to have conferred deformation structures on the upper part of the unit and may have contributed to clast rotation. *Unit 2* appears to be more compact than the underlying sediments. Based on the presence of many large clasts with striae on upper and lower surfaces, stoss-lee features, water escape and shear structures, some bimodality of fabric, the squeezing of fine diamicton into the underlying unit, and an abundance of distantly-derived clasts, this unit appears to be a lodgement till. It appears to have been deposited by tributary ice, which may have advanced over deposits laid down by the Cordilleran Ice Sheet.

3.2.10. Site 15

Based on the presence of numerous striated subangular clasts in a sandy matrix near the top of the unit with some transverse to inferred paleoflow, pebble clusters, and a finer matrix in the lower part of the unit, it appears that this is a proximal ice marginal glaciofluvial deposit. Rapid aggradation appears to have preserved striae, but also rolled some clasts as shown by stoss-lee orientations. There has been winnowing of fines in the upper part of the unit, perhaps during a degradational phase.

3.2.11. Site 16

Based on the presence of fine striae on some clasts, unimodal fabric, horizontal fine sand inclusions and some distantly-derived clasts in this sediment, *Unit 1* appears to be a glacial diamicton. Unimodal fabric and horizontal sand inclusions point to a subglacial meltout origin. The lack of many well-defined striae supports a meltout origin, and it seems likely that several processes were involved in the formation of this subglacial unit.

Based upon the interbedding of sand and mud, *Unit 2* appears to be a proximal glaciolacustrine environment. A fining-upward sand lens in the lowest mud layer which pinches out is probably a turbidity flow. Shearing and deformation indicates rapid deposition from a fluctuating (?) ice margin.

Based on the similarity to *Unit 1*, *Unit 3* appears to be a subglacial diamicton, most likely originating as a meltout till. However, deformation and meltwater reworking have obscured much of the fabric.

Unit 4 is a laminated mud. Based upon the presence of sand and gravel inclusions (turbidity flows) and a striated, subrounded dropstone this appears to have been laid down in an ice marginal glaciolacustrine environment. *Unit 5*, is similar, but possesses non-striated, subangular distantly-derived clasts. It seems likely that this is a more distal ice-marginal glaciolacustrine environment, with finer particle size than *Unit 4*. The dropstones are probably from valleyside glacigenic deposits (supraglacial?).

3.2.12. Site 17

Based upon the lack of stratification, *Unit 1* appears to be a massive gravel which probably originated as a glacial diamicton, but has been subjected to meltwater resedimentation.

Bearing in mind the stratigraphic relation to *Unit 1* and based upon the presence of stratified, bedded gravel, a predominantly unimodal fabric and subrounded clasts, *Unit 2* appears to be of a moderately distal, ice marginal glaciofluvial origin. It was probably part of a tributary valley ice marginal delta.

3.2.13. Site 18

Based on the presence of laminated fine mud, and its stratigraphic relation to Site 17 and 19, this appears to have been deposited in an ice marginal glaciolacustrine environment. A lack of dropstones and a fine particle size suggests that it may have been located distally from the ice margin.

3.2.14. Site 19

Based on the presence in this diamicton of some fissility, a few striated bottom surfaces of subrounded clasts, stoss-lee features, a weakly bimodal fabric and some fine sand layers; *Unit 1* appears to be a lodgement till. Striae are preserved on the bottom surfaces, but a lack of upper surface striae suggests both passive deposition and meltwater smoothing. Fine sand layers indicate that water escape probably occurred along joints. Lodgement of a basal ice slab appears to have occurred followed by subglacial meltout deposition. Striae and stoss-lee

features suggest that some clast reorientation or settling may have occurred at this time.

Unit 2 possesses a roll-up feature, the particle size appears to fine upward, and subangular clasts have no visible striae or stoss-lee structures. Based on these criteria it appears that this unit is probably some form of valleyside debris flow feature, possibly being deposited into a glaciolacustrine environment (*Unit 3*). Based upon the presence of striated dropstones in a laminated mud, *Unit 3* would appear to be related to a moderately distal (fine particle size), ice marginal glaciolacustrine environment.

3.2.15. Site 20

This is a diamicton with a sand lens. It has a largely unidirectional fabric, little mud and subangular clasts with some striae. The presence of these features suggests that sediment has been transferred a short distance by ice, and that it was laid down in the form of subglacial meltout till. The sand lens suggests that meltwater activity was locally significant (the till possesses some sorting by water), and this may account for the lack of mud. However, the fabric appears to have been well-preserved permitting classification as a subglacial meltout till, although some clast reorientation or settling appears to have occurred, as shown by striae, stoss-lee and fabric data (Figure 2.1r).

3.2.16. Site 22

Stratigraphically situated in a major depositional sequence of Hicks Creek, and consisting of a laminated silty mud with rare local, subrounded dropstones, with non-parallel striae, this would appear to have been laid down in a distal ice marginal glaciolacustrine environment.

3.2.17. Site 23

Unit 1 is a stratified gravel, with few fines. Fabric is dispersed and weakly bimodal, the unit starts to pinch out, and subrounded clasts possess no visible striae or stoss-lee features. Based on the presence of these features, and its stratigraphic relation to overlying units, this unit would appear to be some form of gravity flow, probably resedimenting valleyside deposits following ice decay.

Based on the presence of a laminated mud with unstriated dropstones, *Unit 2* would appear to be a distal ice marginal glaciolacustrine environment. *Unit 3* has similar characteristics to *Unit 1* and is considered to be of similar origin.

3.2.18. Site 25

Based on the presence of a laminated sandy mud, small unstriated subangular dropstones, diamicton lenses with some mixing at their edges, and downwarped laminae beneath these lenses; this site appears to consist of deposits laid down in a moderately proximal ice marginal glaciolacustrine environment. Diamicton 'dropstones' appear to have been iceberg rafted, since the subangular

dropstones appear to emanate from the valleyside. The presence of a sandy mud suggests that the ice margin is sufficiently distant for laminae to develop.

3.2.19. Site 26

Unit 1 is similar to many other stratigraphic sections in Hicks Creek. It contains one distantly-derived dropstone, and because of its silty mud texture was probably formed in a relatively distal ice marginal glaciolacustrine environment.

Unit 2 is particularly significant because strong, unimodal fabric in this glaciofluvial sediment (well sorted, pebbly gravel with massive bedding, percussion marks on clasts) indicates flow into Chilliwack valley. Some clasts near the lower part of the unit have fine striae and fabric suggests that a subglacial diamicton has been reworked (*Unit 2b*). A dispersed clast fabric in the upper part of the unit suggests waning flows and clast rolling.

3.2.20. Site 28a

Unit 1 appears to have been laid down in a relatively proximal ice marginal glaciolacustrine setting (it is a laminated sandy mud with no dropstones), although a lack of dropstones suggests a more distal origin. *Unit 2* is discussed in Section 5.2.3. *Unit 3* appears to be a colluvial veneer.

3.2.21. Site 28b

Based upon the presence of a laminated sandy mud with no dropstones, and two small diamicton lenses with downwarping of the underlying laminae, it appears

that this unit was laid down in a proximal ice marginal glaciolacustrine setting. The diamicton lenses were probably deposited as frozen 'dropstones' from either an iceberg or the retreating ice margin (Dreimanis, 1990).

3.2.22. Site 30

Unit 1 is a grey, muddy diamicton. Based on the presence of subangular clasts with striae on their bottom surface (a slightly dispersed orientation), girdle-type bimodal fabric, shear planes in the top of the unit (infilled with clay), and water escape structures; this would appear to be a subglacial meltout till. Shear planes and water escape structures being conferred by *Unit 2.*

Based on the presence of predominantly subrounded clasts with basal striae, a mainly unimodal fabric, two sand lenses which grade into the surrounding diamicton associated with several transverse clasts, and a sand lens higher up in the unit which shows no indication of mixing with the surrounding diamicton, and many distantly-derived clasts; *Unit 2* appears to be a subglacial meltout till. Transverse clasts may have been oriented by compressive flow in the ice immediately downglacier of a possible riegel at the northeast end of Greendrop Lake (Section 4.2.2.). This unit seems to have been partially reworked by meltwater following deposition causing some breakdown in the fabric (transverse clasts and mixing). This deposit appears to have overloaded the underlying meltout till, perhaps by moving ice 'lodging' a stagnant ice mass into *Unit 1.*

3.2.23. Site 33

Based on the presence of a diamicton with gravel lenses (which pinch out) near the upper contact, subangular striated dropstones, bimodal fabric, sand inclusions, and some distantly-derived clasts, *Unit 1* appears to be a subglacial diamicton which possesses characteristics of tributary and main valley ice. Gravel lenses indicate active meltwater reworking, but coarse fabric (imbrications) does not appear to have been altered. It is difficult to infer depositional processes, but the presence of pinching out clay smudges suggests passive meltout as opposed to a more active subglacial regime. However, top surface striae appear to be oriented north-south and northeast-southwest, and there are no stoss-lee features or bottom surface striae. These data suggest lodgement (of debris-rich basal ice?) and subsequent reorientation by meltwater reworking while the underlying till was still viscous.

Unit 2 is a sandy mud. Bearing in mind the stratigraphic relation, it appears that finely striated subrounded dropstones near the base of the unit have probably been dropped from the base of stagnant ice. *Unit 1* shows indications of rapid ice melt, and *Unit 2* appears to be a proximal ice marginal glaciolacustrine environment. Ice margin decay and clast free fall from an ice roof or iceberg rafting may be responsible for dropstone presence (Dreimanis, 1990).

Based on the stratigraphic sequence, and the presence of a well sorted gravel with massive beds, and some bimodality of fabric, *Unit 3* would appear to be part of a distal glaciofluvial delta or valley sandur.

Unit 4 appears to be colluvium.

3.2.24. Site 34

Based on the presence of a diamicton with no dropstones, no mixing between sand lenses and the surrounding diamicton, pebble clusters and strong fabric in dominantly subrounded clasts; *Unit 1* appears to be a subglacial diamicton. Meltwater and perhaps gravity resedimentation have proffered new clast orientation and pebble clusters. Furthermore, resedimentation appears to have taken place in two phases. First, when the upper diamicton was frozen (?), meltwater created discrete sand lenses; second, strong fabric and pebble clusters suggest meltwater and gravity resedimentation. Since the mud content is still high, meltwater reworking must have been predominantly by surface winnowing.

3.2.25. Site 35

Based on the presence of large, subrounded, cobble clasts in a fine sand matrix, and similar fabric between *Units 1 and 2*, *Unit 1* appears to be of glaciofluvial origin. *Unit 2*, a diamicton with fine sand matrix, subangular clasts with striae on their bottom surfaces, a deformed lens of fine mud near the base, bimodal fabric, and stoss-lee features; appears to be a subglacial diamicton. *Unit 2* appears to have reworked some of the underlying unit and may have proffered fabric on *Unit 1*. Furthermore, the presence of deformed fine mud near the base of this unit suggests that subglacial meltwater has been active and that *Unit 1* may have been deposited subglacially.

It seems most likely that the deposit was laid down by meltout, with deformation of mud being caused by overloading by stagnant ice, this is inferred from the lack of upper surface striae and pervasive deformation structures.

3.2.26. Site 40

Based on the presence of interbedded sand and gravel, strong unimodal fabric, and the stratigraphic setting, *Unit 1* appears to be of glaciofluvial origin. *Unit 2*, a fine laminated mud, has no dropstones, and appears to be a distal ice marginal glaciolacustrine environment. *Unit 3*, another interbedded sand and gravel sequence, possesses rare clast imbrications and appears to be a less active glacio(?)fluvial regime than *Unit 1*.

3.2.27. Site 41

Based on the presence of interbedded sand and gravel, poorly-defined planar cross-bedding, weak bimodal fabric and deformation structures; *Unit 1* appears to be part of an aggrading (deformation structures) valley sandur/braided river sequence. *Unit 2* appears to have been laid down as a debris flow (fining upward sand, a layer of sub-rounded gravel forming an erosional contact with *Unit 1*, and the unit pinching out).

It is possible that the deposition of *Unit 2* is related to instabilities created by the formation of *Unit 3*, a distal ice marginal glaciolacustrine setting (fine, laminated mud with dropstones, some of distant origin). Based upon the presence of interbedded sand and gravel, crude bedding planes, unimodal fabric,

subrounded clasts, and some sandy channel fills; *Unit 4* appears to be part of a braided stream network.

3.2.28. Site 43

Interpretation of *Unit 1* is based upon the presence of interbedded sand and gravel, subrounded clasts, striae on the upper surfaces of larger clasts near the base of the unit, gently dipping beds, and a bimodal fabric. This appears to be a rapidly aggrading distal glaciofluvial environment. Striated clasts have been rapidly buried prior to smoothing of upper surfaces, with some clast reorientation as opposed to rolling. Fabric is strongly bimodal and the upper contact is gradational, suggesting a decline in stream competence. *Unit 2* indicates a correspondingly reduced level of meltwater activity (well sorted, fine sand). A reactivation appears to occur in *Unit 3* as fabric become distinctly unimodal and clast size increases.

3.2.29. Site 44

Based on similarities between Sites 43 and 44, *Units 1 and 2* appear to be of distal glaciofluvial origin. *Unit 2* is slightly more active, with larger grain size and a strong unimodal fabric.

3.2.30. Site 46

Based on the presence of gravel, random stone fabric, sand lenses near the base of the section, parallel sets of striae on the underside of several subrounded

clasts, and several non-striated subangular clasts near the base of the exposure; *Unit 1* appears to be of complex origin. It is situated on a topographical ridge on the east valleyside and appears to be of predominantly glaciofluvial origin. It is suggested that this is a kame terrace, which rapidly aggraded and buried striated, subrounded clasts. Sand lenses in the base of the unit are from meltwater seepage, and non-striated subangular clasts (often transverse or non-parallel orientation) appear to be from supraglacial sources.

3.2.31. Site 46

Based upon the presence of horizontally-bedded sand and gravel, bimodal fabric, clasts with percussion marks, and gently dipping bedding planes near the base of the unit; *Unit 1* appears to be of glaciofluvial origin (some finely-striated clasts), and was probably deposited in a moderately distal glaciofluvial deltaic environment.

3.2.32. Site 50

Unit 1 is a thick coarsening-upward gravel. Based upon the presence of coarse horizontal bedding, diamicton lenses with striated, bullet-shaped clasts, and bimodal fabric; the unit appears to have been laid down in a rapidly aggrading proximal glaciofluvial deltaic environment. Diamicton lenses appear to be glacigenic (striated clasts) and probably melted out of ice buried by rapid aggradation.

3.2.33. Site 53

Based upon the presence of 98.6 m of well sorted, interbedded sand and gravel, this site appears to have been laid down in a deltaic environment. All subunits possess similar features, *Unit 1c* for example, has foreset beds, clasts with percussion marks and poorly-preserved fine striae, pebble clusters of horizontally-imbricated stones, coarser clasts than overlying units. These features are indicative of an actively aggrading glaciofluvial regime in a proximal ice marginal delta. The angle of bedding and their vertical extent suggest a Gilbert-Type delta (Gilbert 1885, 1890).

3.2.34. Site 54

Based upon the presence of predominantly subangular clasts with no striae, unimodal fabric, and small clay lenses; *Unit 1* appears to be a diamicton. It is difficult to infer a depositional environment, although it may be resedimented valleyside material (subangular clasts, clay lenses) deposited as a turbidity flow at the base of *Unit 2*.

Based on the stratigraphic relation with *Unit 1*, *Unit 2* appears to be a distal, ice marginal glaciolacustrine deposit. It is a fine laminated mud with subrounded dropstones, many with clay drapes. Lack of striae and other glacial indicators suggest that this was deposited in distal ice marginal environment and that dropstones may have emanated from valleyside deposits destabilised by ice retreat.

3.2.35. Site 55

Based upon the presence of non-striated dropstones in a fine laminated mud, this site appears to be a similar depositional environment to Site 54, a distal, ice marginal glaciolacustrine setting. Since the dropstones are subangular, locally-derived, and have no striae, they appear to be from valley side freeze-thaw as opposed to ice-rafted clasts (Luckman, 1975).

3.2.36. Site 56

The site comprises a fine laminated mud with a sand and gravel lens (which is of variable thickness). The lens has subrounded clasts oriented perpendicular to the direction of thickening, and terminates in a roll-up structure. There are some distantly-derived clasts. Based on this information this appears to be a distal ice marginal glaciolacustrine setting, with a subaqueous mass movement feature of glacigenic origin.

3.2.37. Site 58

Based on the presence of a subrounded and subangular clast-supported sandy-gravel with a diamicton lens, dipping beds, bimodal fabric, pebble clusters, no striae, and many distantly-derived clasts; this unit would appear to have been deposited in a high energy, proximal glaciofluvial environment, perhaps even deltaic.

3.2.38. Site 61

Based upon the presence of dispersed subrounded clast orientation, striae and stoss-lee features (including one bullet-shaped clast), deformation structures (clay smears, water escape features), clay drapes, a fine sand and gravel lens with trough-fill cross-stratifications; *Unit 1* appears to be a partially meltwater-reworked subglacial meltout till.

Unit 2 overlies the meltout till and is a coarse sand and gravel with subrounded clasts and a weakly bimodal fabric. This appears to form a slight topographical ridge and while it is glaciofluvial, it may be a remnant of a kame terrace feature. Lack of striae, or other glacial indicators may be the result of meltwater smoothing.

3.2.39. Site 62

This appears to be an alluvial fan sequence associated with an ice marginal glaciofluvial environment. Fabric indicates a change in flow direction near the base of the site, and beds start to level out. It is inferred that the fan joins kame terrace flows at the base of the section.

3.2.40. Site 64

Based upon the presence of fine laminated mud with rare, small dropstones, this would appear to be a glaciolacustrine environment, distal from active ice.

3.2.41. Site 65

This site is composed of gravel with visible diamicton, sand, and mud lenses. Based upon the presence of weakly dispersed fabric, pebble clusters, a pinching out mud lens, and a diamicton lens, this site appears to have been laid down in a dead ice environment. Meltwater and gravity reworking appear to have destroyed the original fabric, although lenses of diamicton indicate that some has been preserved.

3.2.42. Site 68

Based upon ground surveys, aerial photography, and the presence of a diamicton, with discrete lenses of mud (deformed, laminated with rare dropstones), and coarse sand and gravel; dispersed fabric of subrounded clasts, no visible striae, and some distantly-derived clasts; this unit appears to be of similar origin to Site 65. It appears to have been laid down in a dead ice environment. Meltwater and gravity reworking appear to have destroyed the original fabric.

3.3. Interpretation of Diamictons

Diamictons at several sites have been classified as either lodgement or meltout tills, or with a qualifying prefix, based upon a group of observed and recorded criteria. These interpretations are compared with an additional criterion of three-dimensional analyses of diamicton clast fabric using eigenvalue data (see Dowdeswell *et al.*, 1985 for methodology). Eighteen units were classified as either tills or diamictons and the strengths of the a-axis and c-axis eigenvalues in the clast

fabric were calculated and plotted in Figure 3.1. All diamicton points are encompassed by the envelop fields defined by Dowdeswell *et al.* (1985) and Dowdeswell and Sharp (1986). It should be noted that these envelopes are only approximations of fabric fields, and that the debris-rich basal ice field was taken from contemporary ice masses. This field indicates strong fabric orientation prior to deposition, however it also approximates a fabric that could be conferred by meltwater resedimentation transverse or parallel to flow direction.

Site 2 (*Unit 2*) is classified as a meltout till above, although it appears just beneath the 'meltout' field (MF) in the 'debris-rich basal ice' envelope (DRBI). Fabric in part of this unit appears to have been slightly altered by the overlying unit.

Site 3 (*Unit 2*) is considered to be a transition between lodgement and meltout tills, but plots within the 'waterlain glacigenic sediment' field (WGS). It seems likely that a weaker than expected fabric was recorded because deposition took place close to the ice margin, reducing the strength of proffered orientation. Site 3 (*Unit 4*), a predominantly lodgement till, plots within the 'lodgement' field (LF) parameters. This suggests that deposition may have taken place farther behind the ice margin that *Unit 2*.

Site 11 (*Unit 1*) has been classified as a subglacial diamicton which has been reworked in the upper part of the unit by meltwater. This plots within the MF, and suggests that while meltwater reworking may be apparent, a meltout fabric has largely been preserved.

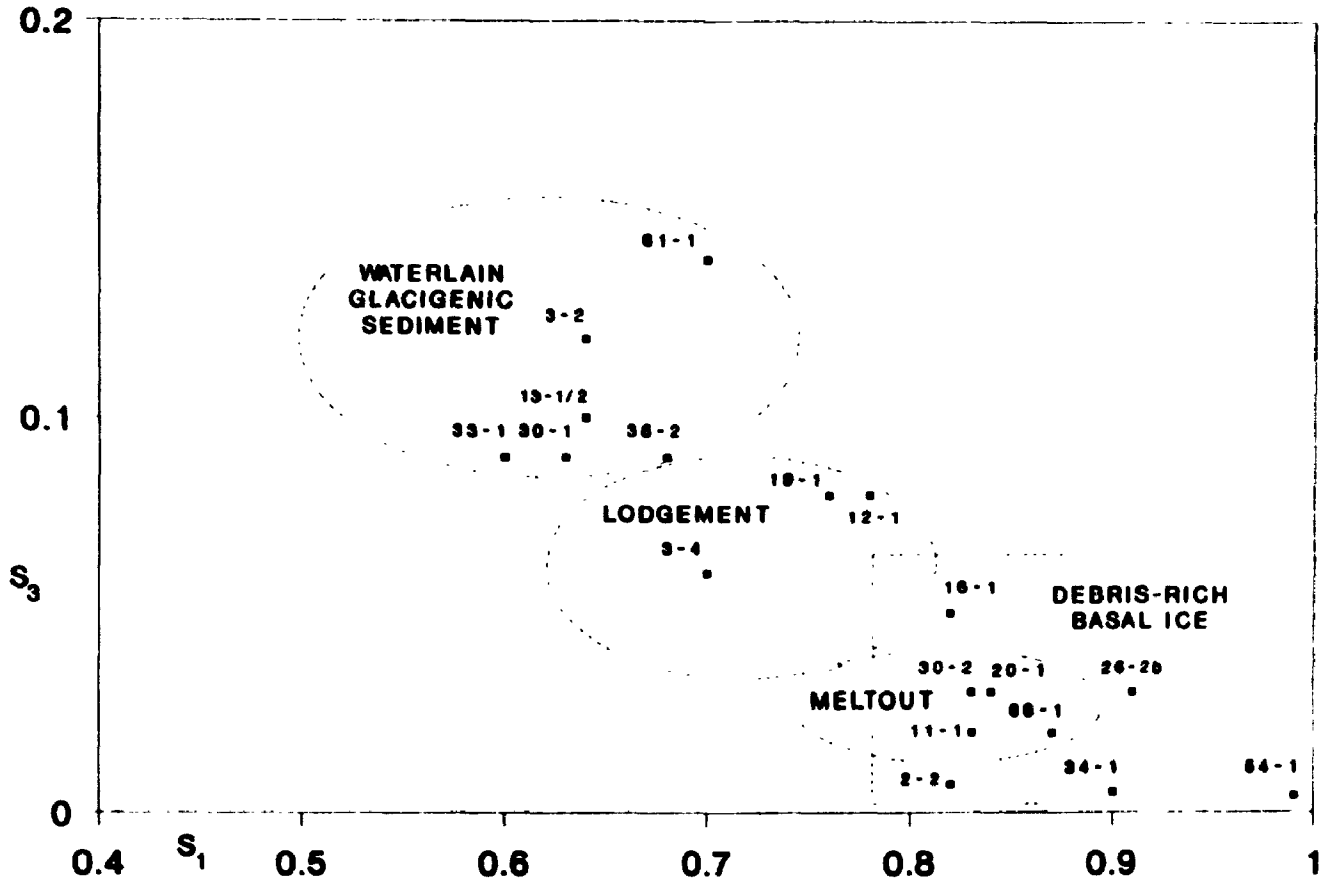

Figure 3.1 Eigenvalue Comparison of Fabrics from Diamictons (S_1 represents the strength of clustering about the mean axis V_1 (eigenvector representing the direction of maximum clustering); S_3 is inversely proportional to the strength of the preferred plane of the fabric). Dashed lines envelop fields of Dowdeswell *et al.*, 1985; and Dowdeswell and Sharp, 1986

Site 12 (*Unit 1*), a meltout till, plots as a lodgement till. Confinement of meltwater to discrete lenses and deposition near (?) the ice margin may explain a more dispersed fabric than would normally be expected.

Site 13 (*Units 1 and 2*) is considered to be a subglacial diamicton. It plots as a WGS with dispersed fabric. *Unit 1* has some fabric conferred by *Unit 2*, which in turn appears to be a mix of sediments from two different ice masses.

Site 16 (*Unit 1*) has been classified as a complex lodgement/meltout till and it plots just between these two fields in the DRBI envelope, which appear to most closely approximate the fabric recorded.

Site 19 (*Unit 1*) is categorised, and plots, as lodgement till. The position near the top of the field is probably related to a relatively dispersed fabric produced by delayed pore water dissipation creating a viscous (?) medium, leading to some settling and clast reorientation (i.e. subglacial flow till).

Sites 20 (*Unit 1*) and 30 (*Unit 2*) are both classified as meltout tills, and plot within this field. Both appear to possess the necessary criteria for this classification.

It is suggested that Sites 26 (*Unit 2b*) and 34 (*Unit 1*) are meltwater-reworked subglacial diamictons. They plot in the DRBI field and, as mentioned above, this could relate to clast realignment associated with meltwater activity.

Site 30 (*Unit 1*), a meltout till, plots in the WGS field. A more dispersed fabric than expected appears to have been proffered by the overlying unit.

Site 33 (*Unit 1*), like Site 13 (*Unit 2*) is classified as a subglacial diamicton, but appears to possess the characteristics of two ice masses. They both plot in similar positions in the WGS field.

It is suggested that Site 35 (*Unit 2*) is a subglacial diamicton. However, this plots just inside the WGS field. Dispersed fabric may be the result of partial reworking and incorporation of some of *Unit 1*.

Site 54 (*Unit 1*) is believed to be a diamicton which has been resedimented possibly as a turbidity flow. This plots within the DRBI field and possesses a strong fabric which would be expected by extensive turbidity/gravity resedimentation.

Meltwater reworking of Site 61 (*Unit 1*) appears to have placed the inferred meltout till in the WGS field. Fabric has apparently been reworked more than was apparent from field observations, although many features are still preserved.

Based upon many criteria, Site 68 (*Unit 1*) has been classified as a dead ice (meltout) diamicton resedimented by gravity and meltwater. The strong proffered fabric resulting from resedimentation places it to the far right of the meltout field.

Eigenvalue comparisons provide a useful additional criterion, but it is essential to consider other criteria in determining depositional environment. Site specific variations place many units in unexpected fields, and it appears that a further dimension, the degree of meltwater reworking, should be incorporated in eigenvalue comparisons. Similar data from future studies should help to show whether diamicton classifications can be improved by the addition of this further dimension. In Chapter Four, local and regional interpretations based on these classification are considered.

CHAPTER FOUR

INTERPRETATION OF LATE WISCONSINAN SEDIMENTATION

4.1. Overview

The apparent local and regional sedimentary history of Silverhope valley is interpreted in this chapter. During the discussion, the sedimentology of some units is briefly reviewed and reference is made to Chapter Two and the appendices. To aid the reader in following the text reference is made several times to Figure 4.1 which presents four stages of the inferred deglaciation in the valley (four paleogeographic maps).

It is difficult to infer the history of Silverhope valley prior to the late Wisconsinan, however drainage patterns and gross valley form indicate that it was complex. At some point in the past it seems likely that a watershed just north of Silver Lake was breached. This would have separated a much smaller north-flowing Silverhope Creek (possibly Eureka Creek) from a south-flowing creek which probably drained west through Post Creek into Chilliwack valley (Figure 1.1). With this in mind, it is possible that the steep cliff at the east end of Greendrop Lake is a relict waterfall (Section 4.2.2.). Another watershed would have existed between Klesilkwa River and the Silverhope Creek flowing out through Post Creek. This would probably have been situated just to the east of where the creek emanating from Clerf Lake enters the present day Klesilkwa River. A forked drainage pattern suggests that subsequent glacigenic deposits

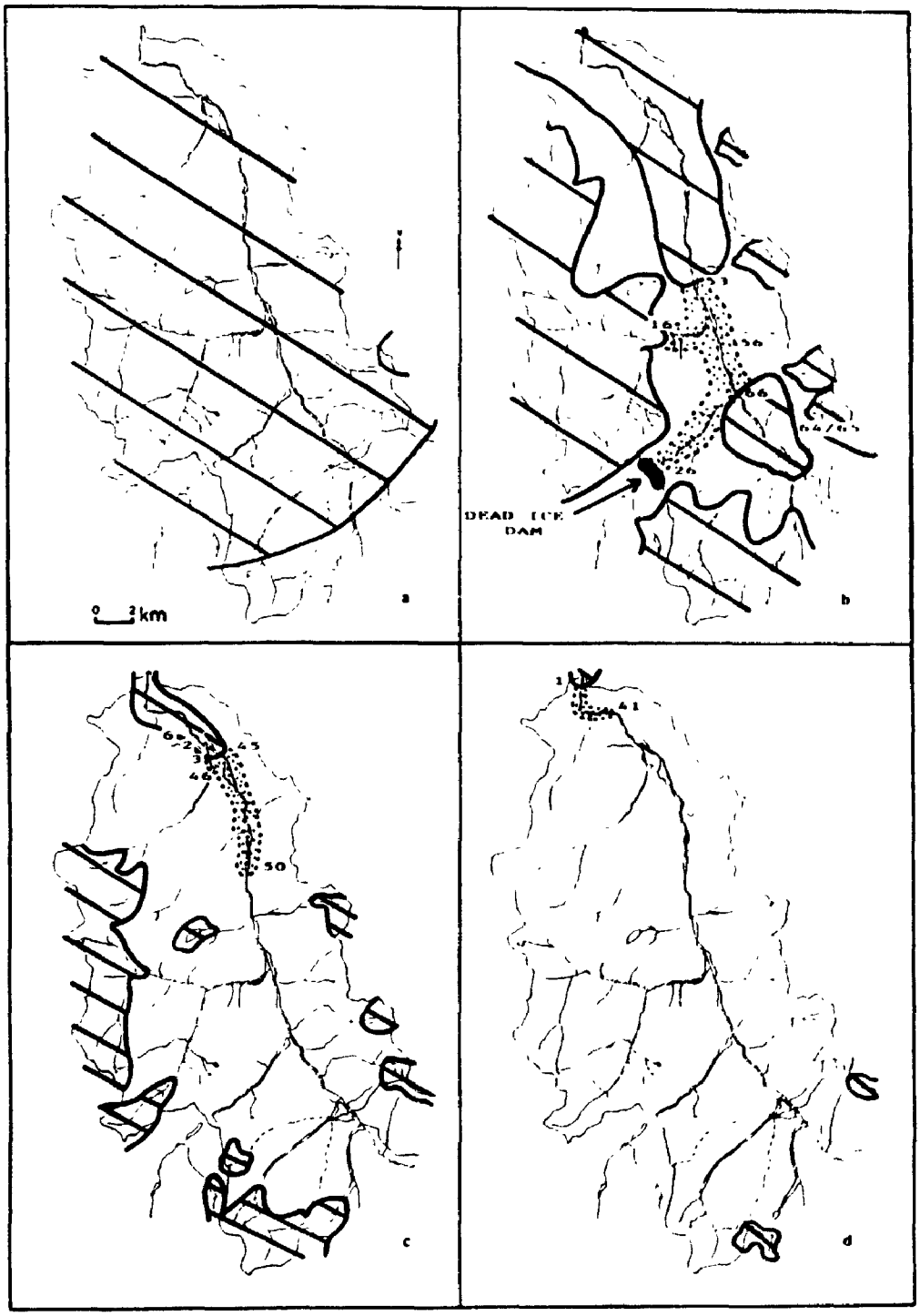

Figure 4.1 **SKETCHES OF THE GENERAL SEQUENCE OF EVENTS DURING DEGLACIATION: 11 500 - 11 000 BP (Relevant site locations, approximate ice positions and lake levels at the time of; a. Readvance at Site 68; b. Hicks Creek-Post Creek outburst, Glacial Lake Silverhope - Level 1; c. Standstill north of Silver Lake, GLS - Levels 9/10; d. Outburst at Site 1, GLS - Level 11)**

have diverted flow to the east. It is difficult to extend historical interpretation beyond these approximations.

Chronological interpretation of the recessional phase of late Wisconsinan glacial ice is constrained by the fact that the eastern Fraser Lowland and Fraser Canyon near Yale were ice-free by about 11 000 years BP. Paucity of dateable wood in Silverhope valley necessitates the adoption of a chronology based upon recorded events in the adjacent Chilliwack valley.

Saunders (1985) points out that valley glacier retreat in the Chilliwack valley may have been either slow or fast. Homogeneity of a thick till unit at Tamihi Scar suggests that there was no break in deposition between the Vashon and Sumas Stades (Saunders, 1985). However, the Chilliwack valley glacier could have experienced similar rapid retreat as those in Washington State (Crandell, 1965). Ice in the Silverhope valley had a predominantly distant source and, being near the margin of the Cordilleran Ice sheet, would have been more likely to experience rapid retreat, in response to climatic amelioration. Timing of the catastrophic outburst from Silverhope valley along Post Creek can been placed between 11 700 $\pm$ 100 years BP and about 11 000 years BP (Clague and Luternauer, 1982; Saunders *et al.*, 1987). High-energy deltaic sedimentation at the Slesse Creek section in Chilliwack valley (about 11 700 years BP) indicates rapid ice retreat, but by about 11 300 - 11 400 years BP (11 400 $\pm$ 140 years BP) glaciofluvial activity had diminished (Saunders *et al.*, 1987).

It is assumed that diminished glaciofluvial activity is associated with glacier standstill, since ice advance or retreat normally generates increased meltwater

activity (Maizels, 1976; 1979; Goff, in prep.). The only observed standstill in the Chilliwack valley is the end moraine which formed Chilliwack Lake when ice retreated about 11 000 years ago (Clague and Luternauer, 1982). Evidence suggests that Silverhope outburst sediments were deposited either against the snout of the Chilliwack Valley glacier or in a pond fronting the glacier (Clague and Luternauer, 1982), which would suggest that these events occurred early during the standstill period about 11 400 years BP.

Exposures in Silverhope valley can be linked with either pre- or post-outburst sedimentation. This places the majority of preserved deposits within a timeframe of approximately 400 years, although some sediments found to the south of the outburst area are probably older. Numerous ice-dammed lake levels were recorded in the Silverhope valley. Final drainage of the ice-dammed lake to the north into the main Fraser valley indicates that at least locally ice-free conditions must have existed there at this time. The Late Wisconsinan chronology ends at the time of ice-free conditions within the Silverhope valley. To aid interpretation of pre-outburst sediments, deposits in the upper reaches of the Klesilkwa and Chilliwack Rivers are also considered (Figure 1.1).

Where meltwater has resedimented till deposits they are referred to as diamicton unless otherwise stated; they could equally be referred to as sediment flow deposits (Dreimanis, 1990). The former definition is preferred because many of the environments discussed here concern '*in situ*' meltwater reworking and the term 'flow' could be misleading.

4.2. Pre-Outburst

4.2.1. Silverhope Creek - Klesilkwa River (Figure 4.1a)

The oldest sediments in the Silverhope Creek-Klesilkwa River valley are probably those of Site 68. The site is composed of large blocks (up to 15 m long) of locally-derived Chilliwack Batholith granodiorites overlying hummocky terrain. A local bedrock source suggests valley side mass movement onto dead ice subsequent to melting and passive deposition on top of dead ice or resultant hummocky terrain deposits. However, preferred orientation, smoothed stoss and plucked lee features indicate a subglacial origin. Complex meltwater, lacustrine and diamicton deposits in the underlying sediment are preserved in hummocks beneath clusters of boulders (boulder mounds).

Intermound areas, some occupied by lone blocks, are low lying, swampy and partially-occupied by shallow lakes (stereo triplet - Plate 4.1). This is a unique landsystem in the valley, to the south of which is flat, marshy valley-fill. This landsystem is probably the result of a minor ice readvance over a relict interfluve (between Masilpanik Creek and the Upper Klesilkwa River; note the abrupt change in channel orientation in the Upper Klesilkwa River, Figure 1.1) which sheared blocks of local bedrock and valley-fill material over previously-deposited dead ice. Subsequent high energy meltwater flows removed the matrix between the boulders, and much of the underlying material, depositing it downstream as valley-fill.

Between Site 68 and Hicks Creek there is an extensive deposit of hummocky terrain, overlain by a proglacial alluvial fan (which is partially covered

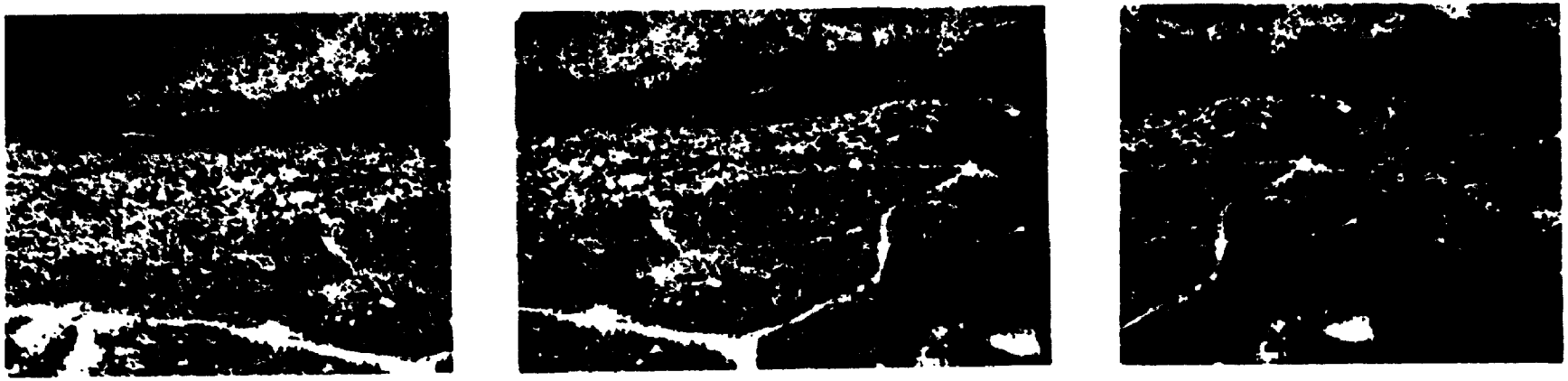

Plate 4.1 SITE 68: Stereo Triplet of Boulder Mound Terrain (upper reaches of Klesilkwa River)
(Approximate Scale, 1 : 2650)

by a more recent paraglacial fan) emanating from Upper Silverhope Creek. This fan represents the current drainage divide (Section 5.3.2.). Partially-infilled kettle holes are visible in the main valley adjacent to the confluence. Lacustrine deposits (Site 64) abutting the margins of dead ice material (Site 65) suggest that this area was occupied by a dead ice dam to a height of at least 797.0 m. However, in order for outburst waters to flow down Post Creek the lake level (Glacial Lake Silverhope (GLS), level one) must have risen above the elevation of the low pass (1015.0 m) between the Silverhope and Chilliwack valleys. The ice blockage in Silverhope valley must have been accompanied by another obstruction in the vicinity of the low pass.

4.2.2. Post Creek - Hicks Creek (Figure 4.1b)

Site 30, with a maximum elevation of 1150.0 masl, is the highest exposure of sediments. These appear to be of a subglacial meltout till origin. Paleomovement indicators and provenance show that ice moved west along Hicks Creek and overrode tributary valley ice emanating from the hanging valley of Flora Lake Creek. Till fabric suggests that ice from the east reworked some of the underlying till and was therefore still active after the decay of Flora Lake Creek ice. This concurs with the generally accepted model of Cordilleran Ice Sheet decay, in which high altitude valleys become ice-free first (Fulton, 1967; Ryder *et al.*, 1991).

Morphology of the Hicks Creek - Post Creek area provides further ice movement indicators. Preserved striae and stoss-lee features on both sides of the

valley indicate ice movement from the east. The flat pass between Hicks and Post Creeks has only a thin colluvial veneer, but is terminated abruptly by a 30 m cliff which forms the east shore of Greendrop Lake. A similar, less pronounced, feature is evident at the east end of Lindeman Lake. These appear to be analogous to riegels, althought they may be relict waterfalls. Lack of valley fill in Post Creek, and a marked transition from the U-shaped valley of Hicks Creek to a V-shaped valley to the west of Greendrop Lake suggests that a high energy meltwater regime was active here for some time. Site 30 has been preserved because of its location on the edge of the Flora Lake Creek hanging valley. It is suggested that during downwasting of the Cordilleran ice Sheet a large segment of Hicks Creek ice was isolated at the low pass, causing the initial ice dam (Figure 4.2).

4.2.3. Glacial Lake Silverhope (GLS). Level One: > 1015.0 masl

Exposures of high elevation lacustrine deposits are found in the Silverhope Creek valley and several of its tributaries. However, there are only two exposures above 1015.0 masl.

Site 26, located in the upper reaches of Hicks Creek, indicates lacustrine deposition up to a height of 1027.9 masl. It is a small exposure, but there appears to be continuity between this and underlying lacustrine sediments, since the deposit has only a slightly coarser particle size distribution. This coarseness was probably proffered from the overlying gravel. Particle size distribution, fabric and paleoflow features indicate that the gravel was laid down by a high energy

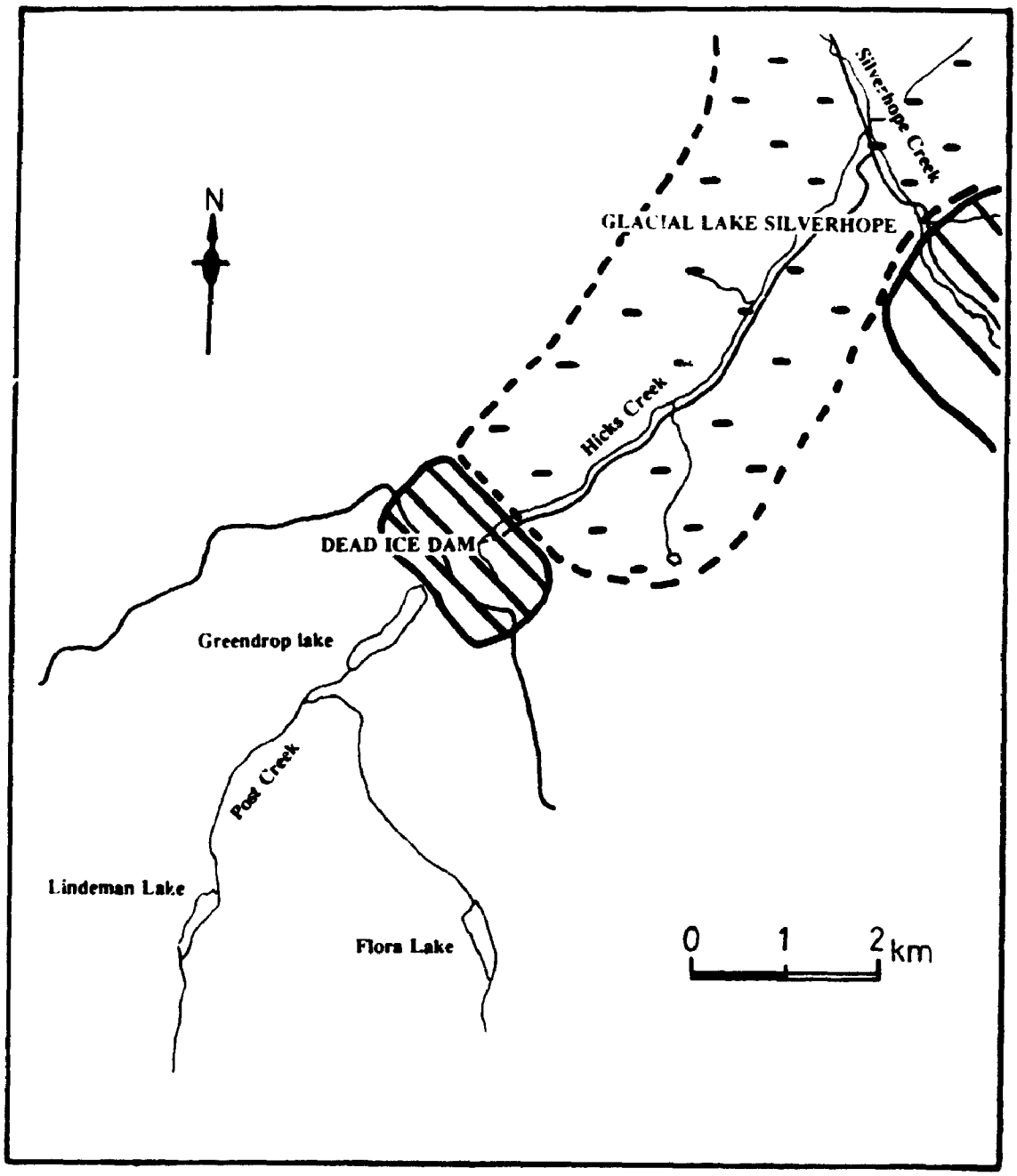

Figure 4.2 **HICKS CREEK-POST CREEK:** **Sketch of proposed location of dead ice dam in Hicks Creek**

meltwater regime from the northeast. For an erosional contact to form, the lake must have been lowered to permit such flow conditions, which can only have taken place during a catastrophic outburst. Preserved fine striae on some clasts indicate that this gravel lag incorporates a considerable amount of reworked glacigenic material.

Site 16 (*Unit 5*), 1017 - 1022.5 masl, is in Cantelon Creek and indicates the existence of a large ice-dammed lake within the Silverhope drainage basin. An absence of deformation structures and glacial indicators suggests that rapid meltwater inundation temporarily covered Cantelon Creek valley dead ice (Section 4.3.12.3.). At this time the northern extent of the retreating Silverhope ice margin was probably located near Site 53, where a massive Gilbert-Type delta was forming (Section 4.3.1.), possibly during a period of glacier standstill.

No other exposures of lacustrine sediments were found above 1015 masl, and there is no obvious evidence of lakeshore development. Given that deglaciation must have been rapid, it is unlikely that any preserved lakeshore would be found. However, the altitude of failure lines of three soft sediment mass movement features within the proposed lake limits in Silverhope Creek valley lie between 975 and 1040 masl.

Assuming that no major ice marginal, supra- or subglacial drainage conduits opened up following the initial catastrophic outburst into the Chilliwack valley, then lake levels would have been determined by the level of the low pass between Hicks and Post Creeks. As Silverhope ice retreated, and the dead ice

blockage decayed, the lake level would have slowly declined prior to stabilisation at the next inferred drainage point (928.8 masl).

Exposures in Hicks Creek between 1006.7 and 1004.0 masl, and in Silverhope valley between 935.0 and 932.0 masl indicate the existence of an ice marginal lake. At Site 28a, lacustrine sediments occur as laminated sandy-muds, but Site 28b possesses diamicton lenses which were probably frozen till blocks dropped from calving icebergs. Furthermore, on the east side of Silverhope valley instability is evident at Site 56 which contains a subaquatic mass movement feature in the lacustrine muds. Rapid resedimentation of valley side sediments appears to have been common.

Many exposures of lacustrine sediments located at intermediate altitudes (between inferred lake levels) were studied, and described in Chapter Two. Details of their fabric and particle size can also be found in Appendices II and III.

4.3. Post-Outburst - Ice-Free Conditions

4.3.1. Glacial Lake Silverhope. Level Two: approximately 920.0 masl

As Silverhope ice retreated, a kame terrace became established on the western side of the valley between 928.8 and 908.8 masl (Site 8 - Eureka Creek). This appears to have controlled GLS level two. This terrace is only preserved in the northwest section of the valley although it may have extended as far as Swanee Creek, adjacent to the Gilbert-Type delta at Site 53. The kame terrace forms a topographic ridge that extends for approximately 2 km from below Isolillock Peak to north of Eureka Creek. The presence of mud lenses, and a

high percentage of mud, particularly in the lower half of the unit indicate the reworking of frozen (ice marginal) lacustrine muds. Subangular and subrounded clasts are probably of supra- and subglacial origins, respectively.

Site 53 forms a concordant height with the kame terrace (Site 8). Interbedded sands and gravels related to fluctuating fluvial regimes can be traced to a height of 919.7 masl. Rare dropstones, some with preserved striae, are found in some of the fine sand beds indicating deposition from ice as opposed to meltwater sources. Other clasts have experienced smoothing in an active ice marginal delta and bear only percussion marks from frequent clast impact. A series of horizontal beds similar to topsets may have formed either as a result of drainage from a subglacial conduit or relate to a lateral flow pattern across the delta to an ice marginal drainage source, which could have been temporarily open at the time of outburst along Post Creek.

4.3.2. Glacial Lake Silverhope. Intermediate Stage: approximately 795.0 masl

In Section 4.2.1., lacustrine deposits of Site 64 abutting the margins of dead ice material at Site 65 were discussed. Site 65 appears to consist of meltwater reworked sediments oriented to the south. It seems that lake drainage by overtopping of the dead ice of the hummocky terrain has given the clasts a preferred orientation as opposed to a more random alignment. Dropstones at Site 64 seem to have a glacigenic origin (iceberg rafting ?). It is unlikely that this lake

level was stable, with rapid downwasting encouraged by an abundant supply of meltwater.

4.3.3. Glacial Lake Silverhope. Level Three: approximately 760.0 masl

A second kame terrace is visible on the west side of Silverhope Creek. The exposure is more extensive than the upper terrace, extending as a visible topographical ridge for 3 km between Sowerby and Eureka Creeks. Site 7 is aggradational with a coarser upper half. Clasts have a similar preferred orientation to the higher kame terrace, but particle size distribution suggests that this was not such a high energy regime. A high percentage of Mount Barr Batholith granodiorite indicates that much of the sediment transported probably came from a Sowerby Creek source. Ice marginal drainage may have been encouraged by meltwater flows from this tributary valley.

4.3.4. Glacial Lake Silverhope. Level Four: approximately 630.0 masl

Concordant elevations in the north and central hummocky terrain deposit (Sites 63 and 66 - hill a) appear to be remnants of an old erosion surface. Intervening sediments have subsequently been reworked to a lower level. Figure 4.3 depicts the approximate topography of the relevant section of hummocky terrain.

Site 66 consists of six hills and two terraces cut into their eastern and northern flanks. Ground surveying indicates concordant elevations to the south at Site 63. Analysis of aerial photographs reveals that meltwater flows appear to

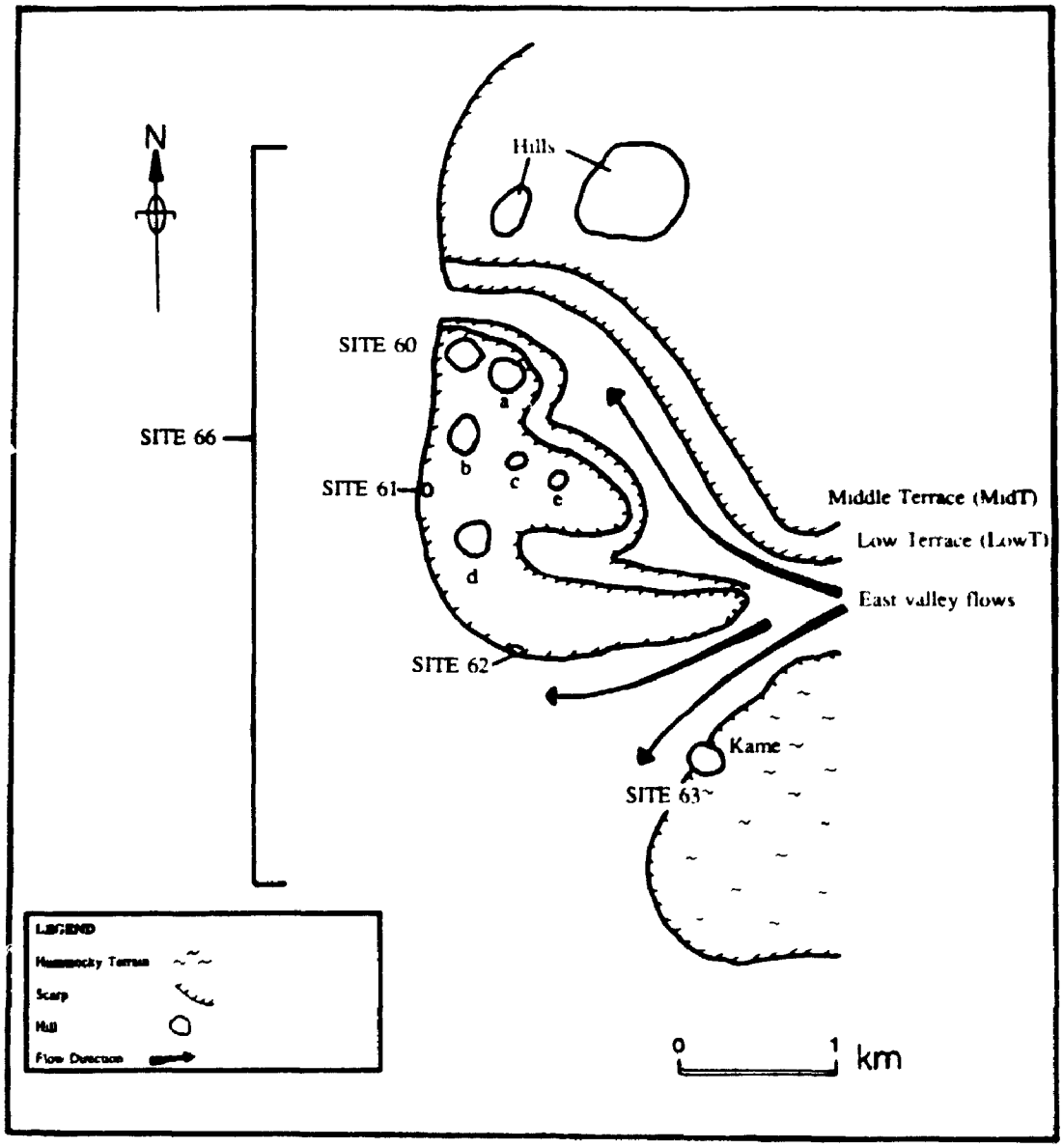

Figure 4.3 SKETCH OF HUMMOCKY TERRAIN TOPOGRAPHY IN SILVERHOPE VALLEY SOUTH OF HICKS CREEK

have emanated from an east valleyside tributary. Signs of glaciation are evident in the upper reaches of the tributary (e.g. cirque, arêtes) which forms a hanging valley. Ground surveys suggest that the glacier which occupied the valley did not extend far beyond the edge of the cirque, a position marked by an end moraine visible on aerial photographs. It is inferred that meltwater flows from this valley initially formed erosion surfaces, visible now as concordant heights, and indicative of periods of relatively stable lake levels. Additional evidence of further lake level indicators at these sites is discussed below.

4.3.5. Glacial Lake Silverhope. Level Five: approximately 615.0 masl

A series of concordant elevations between 618.6 and 614.0 masl in the north and central hummocky terrain are indicative of a lower lake level (Sites 60, 62, 63 and 66 - hills b-e). In addition to five distinct hills in the north (Sites 60 and 66 - hills b-e), there is an outwash terrace and associated deposits emanating from an unnamed east tributary valley (Sites 62 and 63). It is inferred that during deglaciation a small outburst occurred from a moraine-dammed lake in the east tributary cirque. There is no hard evidence for this other than aerial photographic interpretation which suggests that the end moraine has been eroded on the north side and now curves to the south. This suggests meltwater reworking and resedimentation. Ground surveys were unable to substantiate this further. An absence of fan delta or alluvial fan suggests that either the lake had drained to the west of the hummocky terrain, or that outburst flows were sufficient to destroy

any fan structure, leaving only a gravel lag on subsequent terraces and the outwash plain.

The outwash plain forms a terrace 11.9 m below the previously inferred lake level, incising through an isolated kame and hummocky terrain plateau (Plate 4.2). The plain is oriented southwest, but becomes buried beneath more recent alluvial fans within 1 km of its source. To the northwest of the tributary valley, concordant heights are formed by a series of low hills, suggesting the existence of a similar plain (Figure 4.3). To the west, an alluvial fan (Site 62) extended into what appears to have been a kame terrace outlet draining GLS alongside remnant dead ice. Paleocurrent indicators show a gradual merging of two flow directions from the east-southeast and southeast (Site 62, Figure 2.1bc). A lack of fine sands in the kame terrace is indicative of an active meltwater regime, which may be responsible for a weak (0.67) eigenvalue of clast orientation since many were transverse to the flow and others may have been rotated by lateral, alluvial fan flows.

A problem with clear interpretation is the relatively small exposure of the kame terrace section, in an area where flows were clearly influenced by outburst activity (a problem exacerbated by aggregate extraction). On aerial photographs the kame terrace can be traced for about 1 km north to the area of concordant hills in the hummocky terrain. This suggests that the kame terrace emanated from a point to the northwest of these hills where the lake abutted the dead ice deposit. The alluvial fan appears to merge with the kame terrace at about 601.3 masl, which coincides with altimetry measurements of a poorly-preserved outlier

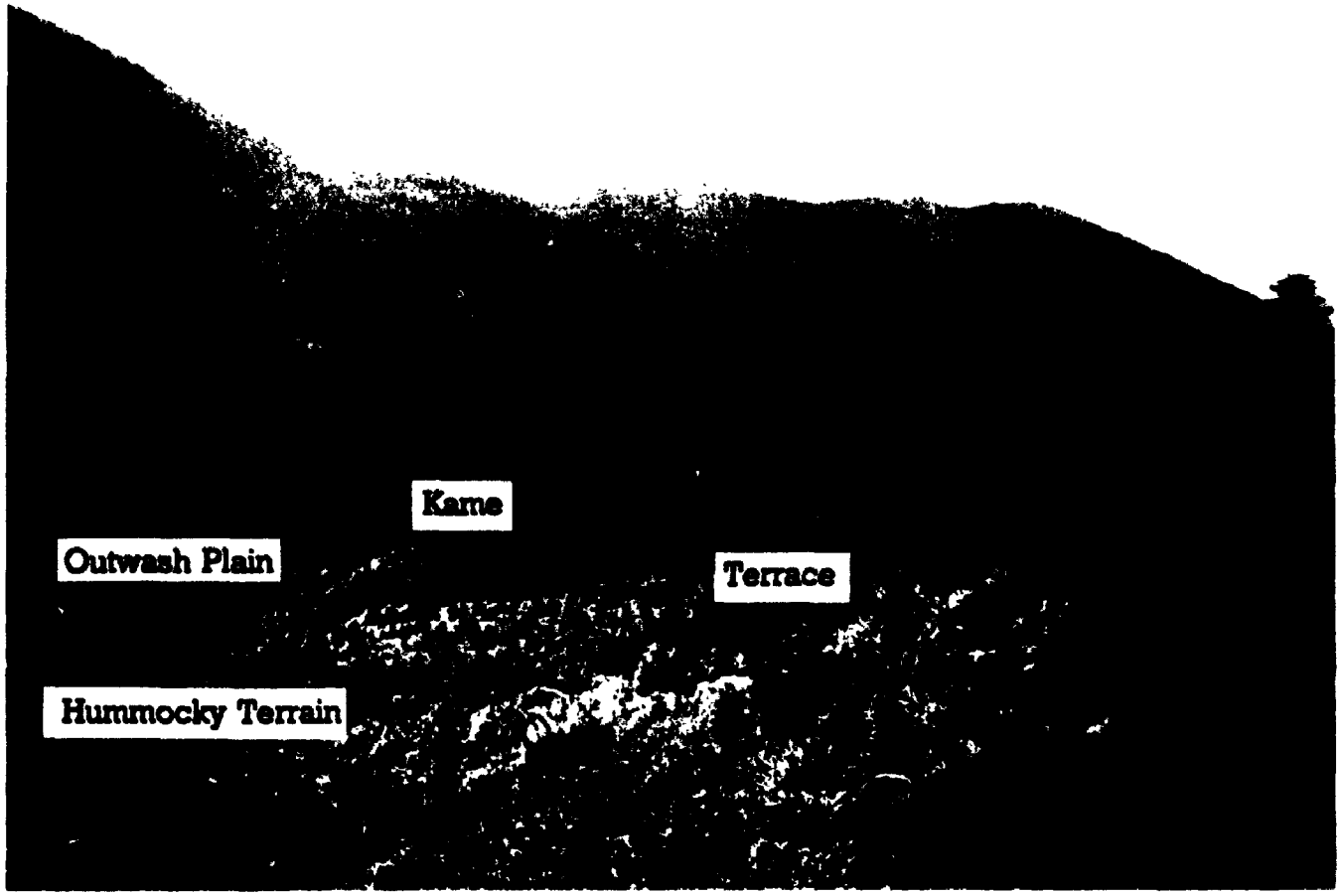

Plate 4.2 OUTWASH PLAIN INCISION OF KAME AND HUMMOCKY TERRAIN (Main Silverhope valley, south of Hicks Creek. Kame is approximately 13 m high)

of hummocky terrain deposit on the west side of Silverhope Creek valley (Site 59 - 601.1 masl), 0.5 km northwest of the low hills.

4.3.6. Glacial Lake Silverhope. Level Six: approximately 585.0 masl

GLS probably continued to drain south by kame terrace through the hummocky terrain/dead ice deposit. Evidence is sparse although concordant heights of meltwater features indicate sustained meltwater activity. A middle outwash terrace (60), with a gravel lag veneer, is preserved on the northern edge of the hummocky terrain (Figure 4.3) at an elevation of 582.1 masl. The terrace can be traced to the southeast, behind the series of low hills (Site 66) discussed above. Meltwater appears to have come from the unnamed east side tributary and breached the hummocky terrain to the northwest to a new base level (lake level).

A coincident elevation is found in an exposure about 1 km south (Site 61). Coarse sand and gravel with no apparent stratification indicates paleoflow to the northwest. However the eigenvalue is weak, clast settling has taken place following ice melt and orientations are scattered. It seems unlikely that flows could have travelled northwest, and clasts may have been oriented down massive beds which are not visible in this limited exposure. Aerial photographs show that this poorly-preserved low gravel ridge is parallel to, but slightly west of, the previous kame terrace (Section 4.3.5.), suggesting that the path of the kame terrace followed declining ice elevations.

At Site 61 the underlying diamicton still possesses paleomovement orientation to the southeast, but has been considerably reworked in the upper half of the unit. Meltwater and deformation structures have altered the original fabric of what appears to have been a subglacial meltout till.

4.3.7. Glacial Lake Silverhope. Level Seven: approximately 570.0 masl

A lower terrace (Site 60), with a gravel lag veneer, preserved on the northern edge of the hummocky terrain (Figure 4.3), has an elevation of 571.1 masl. This terrace can also be traced to the southeast (Section 4.3.6.) and to the east side tributary meltwater source. No concordant elevations could be matched with preserved features, but bearing in mind the morphological similarities between this and the upper terrace it is inferred that lake drainage continued to the south.

4.3.8. Glacial Lake Silverhope. Level Eight: approximately 555.0 masl

Level eight appears to represent the final control exerted on lake levels by the dead ice deposit at the south end of Silverhope valley. Concordant heights vary between 553.0 - 560.0 masl and are found at the north and south ends of the feature.

To the north, two sites, 60 and 58, indicate meltwater activity at a new base level. The former site represents the lowest level incised by the east tributary valley flows (Figure 4.3 - 'East valley flows'), and possessing a poorly-preserved gravel lag veneer. The latter, a dead ice outlier to the northwest of the main

feature, shows meltwater reworking of dead ice deposits. Beds dip gently south, but weak clast orientation (eigenvalue 0.55) suggests paleoflow to the north. Many clasts appear to be oriented along the bedding planes or have rolled transverse to main flow, which is to the south. No lower contact is evident in this unit, but aerial photographic data have been interpreted as showing the site to be part of the dead ice blockage. It appears to represent a truncated outlier which has been planed off by south-flowing meltwater. To the south, boulder mound and intermound channel elevations are concordant (Section 4.2.1.). Concordant boulder mound elevations appear to be accidental since it is unlikely that these meltwater flows could have redistributed such large blocks. Meandering intermound channels downstream of the main blockage suggest that a gentle slope had developed on the southern side of the hummocky terrain as meltwater flows declined and finer material was entrained.

No further breaches of the hummocky terrain by east valley flows are apparent other than the modern stream channel which drains southwest. Exposures to the north indicate a change in flow regime with lake levels and meltwater drainage being controlled by the downwasting and retreat of Silverhope ice.

4.3.9. Glacial Lake Silverhope. Level Nine: approximately 480.0 masl

Extensive talus deposits cover the east valley side to the northeast of Silver Lake. Between these colluvial deposits there is a poorly-preserved ridge trending northwest-southeast for about 100 m. A single exposure (Site 45) indicates that

the ridge is composed of glacigenic clasts reworked by an active meltwater regime. A low percentage of mud, diverse clast orientations (eigenvalue = 0.51), and the presence of subangular and subrounded clasts suggests that the kame terrace is some distance from its lacustrine source. Clast characteristics indicate that sub- and supraglacial material have been reworked by ice marginal flows. The existence of a kame terrace in this location indicates that there could have been an outlet for meltwater to the east of Silverhope Creek in the Fraser valley. This infers irregular downwasting of Fraser valley ice.

All talus-free areas were closely scrutinised, but it appears that this is a unique exposure on the east valley side. There is no further evidence of lake drainage by the east ice marginal path which infers that this was an unstable route.

4.3.10. Glacial Lake Silverhope. Level Ten: approximately 390.0 - 320.0 masl (Figure 4.1c)

Silverhope Creek becomes a steep gradient mountain stream to the north of Silver Lake and has deeply incised valley fill sediments. Under normal conditions it appears that the creek favours the west side of the valley where it follows the Ross Lake Fault. However, rapid deposition of a fan delta emanating from Sowerby Creek (Site 46 - see below) blocked the northwest exit of Silver Lake during ice retreat, and diverted flows to the east of the roche moutonnée (Site 10). A west side channel is reestablished approximately 2 km downstream.

This morphological arrangement has protected the surficial deposits on the west valley side. These show a dichotomy of depositional environments between the west and east valley sides. However, beneath 280.0 masl on the west valley side, the river either abuts the bedrock valley wall or has previously reworked surficial deposits. Fortuitously, because of the river's course, surficial deposits have been preserved on the east valley side between 324.0 and 209.0 masl.

Exposures indicate that the fan delta emanating from Sowerby Creek (Site 46) was probably diverted to the south side of the roche moutonnée because Silverhope ice blocked flow to the north. It appears that this peculiar truncated delta morphology was brought about by the rapid drainage of Sowerby Creek and the equally rapid formation of an ice-contact proglacial fan delta. Thick topsets are visible at Site 46, with a few foresets identifiable in the lower part of the unit. Transverse clasts and some preserved striae indicate that this deposit probably emanated from a proglacial source during high energy flow conditions.

The depositional record of Site 3 suggests that this and Site 46 probably represent ice oscillations/ standstills. This may have been caused by a delayed downwasting in the confined valley to the north, however oscillations in the ice margin may indicate a minor readvance. At Site 3, the stratigraphic column indicates two cycles of change from glaciolacustrine (*Units 1 and 3*) to till (*Units 2 and 4*). The contact between *Units 1 and 2* is deformed and flame structures appear to rise up from *Unit 1* into *Unit 2*. Flames appear to be forced into shear planes which dip north and suggest that active lodgement was occurring under ice advancing to the south. A gradation seems to take place into subglacial

meltout till (Section 3.2.3.), which suggests that reactivation of ice flow here was short-lived, and that it could have occurred near the ice margin.

Deformation of the underlying unit, possible clast rotation, local shear, and abundant meltwater provide evidence of potential ice streaming or surging ice advance in this area. Although deformation appears to be minimal beneath the contact (which may have been frozen), it may have occurred above the contact as subglacial deformation similar to the process described by Boulton (1979). Shears near the base of the unit infer that the lower section was frozen, but meltwater penetration (evidenced by fine sand inclusions) may have provided lubrication. Possible clast rotation suggests that at least some areas were experiencing deformation in a viscous medium, probably under high pore water pressure, similar to the process described by Hicock (1992). The above evidence indicates a complex subglacial regime and it is conceivable that minor surging could have occurred. This offers a possible explanation for the lack of major glacigenic deposits in Silverhope valley. If it was operating as an ice stream, or surging lobe, most sediment would have been rapidly transferred through this narrow valley into the Skagit Basin.

A return to ice marginal conditions is evident in *Unit 3* and an aggrading environment suggests that rapid downwasting was occurring. A similar ice advance appears to have taken place at the contact between *Units 3 and 4*, although an erosional contact was formed. This advance appears to have been in conjunction with well-defined subglacial meltwater drainage, perhaps lubricating the ice-bed interface. Deformation of and lodgement into the

subglacial meltwater material suggests that the second oscillation was equally as significant as the previous one. However, a gradational transition into subglacial meltout till again suggests that the ice stalled soon after overriding the site, perhaps due to valley widening.

Ice front oscillations caused fluctuations in the level of GLS and changes in drainage path, and the glaciolacustrine sediments also provide useful evidence of these changes. GLS appears to have abutted the ice margin during the oscillations, and is preserved beneath diamictons at Sites 2 and 3.

An almost continuous conformable record of deposition is recorded over 100 m of elevation between Sites 2, 3 and 6. Site 3 represents the lowest exposure of GLS on the west valley side. The lake has small dropstones with preserved fine striae. This suggests that there was minimal active meltwater reworking of the dropstones which may have been dropped from a floating ice margin. Some deformation has taken place at the upper contact with the overlying diamicton. A southerly paleomovement is indicated although it appears to have been a fairly passive readvance, perhaps lubricated by meltwater, since the contact is preserved. This also suggests that this is not simply the result of ice sheet grounding which would have caused more pervasive deformation.

The thickness of the overlying diamicton, preserved flame structures at the lower contact with the overlying diamicton, and rare sand-filled shear planes indicate that this was at least temporally, more than just a minor fluctuation of the ice margin (see above). However, the Sowerby Creek fan delta is most likely to have formed immediately after ice decay cleared the entrance to the tributary

valley and preservation of the original structure suggests that all ice readvances must have been spatially minor, at most extending 1 km south. In addition, the kame terrace ridge at Site 6 does not extend beyond Sowerby Creek.

Site 6 indicates that lake drainage was again by kame terrace. Preservation of this feature is rare because it has been used as a source of aggregate for the nearby logging road, although the ridge can be traced for several hundred metres. Meltwater flow from the east indicates that the terrace followed the valley side. For lake drainage to occur along the west valley side the kame terrace must have been flowing in a channel carved between the valley side and the ice. The origin of this channel was probably in the area of the truncated Sowerby Creek ice-contact proglacial alluvial fan delta. Near the base of Site 6, a thin sequence of laminated mud provides evidence of damming and the formation of a temporary ice marginal lake. Striated dropstones were probably deposited from ice melt, rapid deposition of kame terrace gravel following reestablishment of a drainage path induced diapiric dewatering structures to form in the underlying mud. Rapid aggradation is evident and indicative of an active meltwater regime. It is likely that damming merely diverted the drainage path and that the kame terrace continued to drain the lake. Poor-preservation along the valley side may, in part, infer that the kame terrace followed a meandering channel path along a decaying ice margin.

Site 2, approximately 150 m northwest of Site 3, indicates the presence of an ice marginal lake. The exposure is small, but the unit is situated between kame terrace and diamicton deposits which suggests that it is likely to be a valley

side, ice marginal lake adjacent to an advancing ice front. Readvancing ice appears to have reworked lacustrine and fluvial sediments, although no striae are present, suggesting that movement was either occurring in a viscous slurry, or that later meltwater activity during meltout may have removed them. Meltwater reworking is evident in the main body of the diamicton, with loading structures in the upper part of the unit induced by rapid ice decay. Interbedded sand and gravel laid down by meltwater following ice retreat has deformed the upper part of the diamicton indicating that water at this location was flowing south.

Exposures on the east valley side indicate an environment dominated by glaciofluvial activity. There is no further evidence of glacial advances in the valley, which suggests that retreat and downwasting were rapid. Meltwater deposits from 324.0 - 212.5 m on the east valley side all indicate paleoflow to the south (or locally eastward with topographic changes). Valley orientation suggests that rapid ice melt would have been asymmetrical with meltwater flowing along the east valley side. However, paleoflow indicators show meltwater found an exit on the west valley side. This exit, in the form of ice marginal kame terrace, is evident in the drainage of the lowest level of GLS. To the east, drainage was either impeded by unstable ice or remnants of Fraser valley ice farther north.

4.3.11. Glacial Lake Silverhope. Level Eleven: approximately 263.0 masl (Figure 4.1d)

The final drainage to a definable lake level appears to have occurred by outburst through a low pass in the interfluve between Silverhope Creek and

Fraser valley. Analysis of aerial photos of Site 1 indicate that there is a relict kame terrace feature forming a topographical ridge on the west valley side, just to the south of the low pass. However, this ridge appears to only extend along the valleyside for about 50 m and there are no visible exposures. This section of preserved kame terrace suggests that there was at least short term stability of drainage along the ice margin. On the Fraser valley side of the interfluve is a large outburst fan deposited by drainage of GLS. Recent highway construction has obscured the base of the fan, but on earlier aerial photos there is no obvious truncation at its lower elevations. Preservation of the outburst fan is important because it provides evidence of ice-free conditions in the Fraser valley at that time.

The first evidence for north flowing meltwater in Silverhope valley on the east valley side is at an elevation of 212.5 m. This may indicate final drainage of GLS out of the valley mouth over remnant dead ice, but may also represent subglacial drainage.

4.3.12. Tributary Valley Interactions

4.3.12.1. Upper Silverhope Creek

A glacier occupied this tributary valley and appears to have commenced downwasting prior to ice decay in the main valley. Meltwater appears to have reworked the diamicton in the lower part of the valley (Site 33) until an ice marginal lake backed up beyond the exposure. This temporary lake (no evidence for ice marginal lake at Site 34, but there is a thin lacustrine unit at Site 33) would

have been drained by breach of the dead ice in the main valley, presumably by flow to the south. Paleoflow indicators in all sections indicate ice flow from an upland valley source. In the highest exposure, Site 35, meltwater deposits are visible at the base of the diamicton unit. Site 35 has a bedrock base and thin exposure of meltwater sediments; these are probably subglacial in origin (Section 3.2.25). Drainage of the ice marginal lake is difficult to demonstrate, although meltwater flow from Klesilkwa Mountain (3 km NE of Paleface Mt. - Figure 1.1) appears to have moved freely at Site 33.

4.3.12.2. Hicks Creek

Most of the exposures in Hicks Creek have been discussed with reference to levels of GLS. The turbidity flows at Site 23 appear to have occurred during the existence of GLS and provides evidence of valley side instabilities brought about by ice retreat. This activity appears to have resedimented much of the valley side material prior to the drainage of GLS from Hicks Creek.

4.3.12.3. Cantelon and Yola Creeks

These creeks extend west from the main valley for over 10 km. In the lower reaches downstream of their confluence, the lowest altitude exposure (Site 16) is dominated by a large unit of sand and gravel. However, at the base of the section there is a small exposure of diamicton which appears to be laterally extensive, and indicates ice movement to the northeast. This diamicton has striated clasts from north of Silver Lake. These appear to have been transported

either by an ice sheet overriding interfluves, or by iceberg-rafting, or by main valley ice advancing southwest up Cantelon Creek. The latter seems unlikely since there is no evidence of such incursions in Cantelon Creek, whereas laminated muds in the same exposure contain some dropstones of similar provenance. The lacustrine muds relate to GLS, which appears to have occupied this valley since Level One (Section 4.2.3.), by which time Cantelon ice must have retreated to at least Site 16. Iceberg-rafting seems to be the most logical explanation for the presence of distantly-derived clasts.

The Cantelon valley ice margin was probably unstable at this time, advancing and retreating into the lake (buried dead ice may have been isolated from the main glacier), and the sand interbeds may well be subglacial in origin. Deposition was vigorous enough to deform the underlying diamicton. About 1.2 km east of this site, at a higher elevation, are lacustrine sediments with dropstones but no sand interbeds. This was evidently farther from the ice margin, but the dropstones are most likely from valleyside freeze-thaw (Section 3.2.35).

Unit 3 at Site 16, is a thin exposure of deformed diamicton. Ground survey of the valley side suggests that this is an isolated lens of diamicton. The unit contains some proximally-derived gabbro which is exposed in the main valley and appears to have been either transported west along Cantelon Creek by iceberg-rafting, or by ice sheet transfer across interfluves. In view of the apparent isolation of the diamicton unit, it seems likely that this is an iceberg-rafted deposit which has subsequently been reworked by meltwater, and consolidated by overlying lacustrine mud. Lacustrine mud comprises the remainder of Site 16 up

to an elevation of 1022.5 m. Provenance of some clasts indicate ice sheet movement south over interfluves. The lower diamicton unit in Yola Creek (Site 19) bears evidence of ice sheet overriding with clasts of intermediate provenance.

Sub-angular argillite dropstones in the upper unit (*Unit 5*) appear to bear no obvious signs of glaciation, suggesting a valleyside origin. Some valley side instability is indicated at the interface between diamicton and lacustrine deposits. Turbidity deposits emanating from the north valley side form a coarse sand and gravel layer which appears to have failed immediately following ice retreat.

Adjacent to the confluence of Yola and Cantelon Creeks, exposures on either side of the valley indicate that individual valley ice retreat probably occurred at different rates. Sites 15 and 17 appear to have experienced meltwater reworking following ice retreat, which at Site 17 developed into foreset beds of an ice marginal delta. Provenance of some clasts indicate that glacial sediments have been reworked. When ice occupied Cantelon Creek, Yola Creek ice appears to have retreated south, with a floating ice front and dead ice buried beneath a lake formed in the main valley by the Hicks Creek dead ice blockage. More rapid retreat of Yola Creek ice probably occurred because the local ice source is at a lower elevation than Cantelon Creek in a more southerly location.

4.3.12.4. Sowerby Creek

Sowerby Creek Ice retreat appears to have occurred later than in Cantelon Creek Initial ice retreat (Site 11) produced a shallow ice marginal lake when meltwater was unable to drain out immediately from the valley mouth. This

produced interbedded sand and mud, and turbidity flows from destabilised valleyside deposits. An exposure at Site 12 indicates similar activity farther to the west in the tributary valley at a similar elevation. Ice damming appears to have been short-lived, ice marginal deltaic deposits overlie the lacustrine sediments, indicating meltwater flow to the north, probably via kame terrace.

The one-sided, truncated ice-contact proglacial fan delta at the mouth of Sowerby Creek (Section 4.3.10., Site 46) appears to indicate that lake drainage occurred immediately following Silverhope ice retreat/decay north. It is possible that either a minor ice readvance or reactivation of the same ice occurred in the Sowerby Creek valley. Site 13 has two distinct diamicton units, with clasts in both oriented in the same direction, although they appear to be separated by a deformed contact. The lower diamicton seems to have been winnowed by meltwater in the upper part of the unit leaving a coarser layer. The upper diamicton is generally more compact and appears to be deformed down into the lower diamicton. The fabric appears most similar to lodgement till, with striac on the upper and lower surfaces of many clasts.

Comparison with ice margin fluctuations in Section 4.3.10. suggests that the ice readvance is most similar to the first one at Site 3, where ice overrode underlying deposits and advanced some distance downvalley. There are no further exposures to the west in the headwaters of Sowerby Creek. Aerial photographs indicate that there is possibly a moraine-dammed lake about 1.5 km west of Site 13. A small lake situated on the south side of the valley is located upstream of a crescentic ridge which is breached by the present day Sowerby

Creek. It is possible that this represents a glacial oscillation equivalent perhaps to the second readvance recorded at Site 3.

4.4. Regional Context

4.4.1. Introduction

There are a paucity of exposures in Silverhope valley mainly due to rapid meltwater reworking as ice retreated and an ice-marginal lake developed. The only major deposits are those left by the ice-marginal lake, glaciofluvial activity and ice front oscillation/readvance, necessitating the use of a discontinuous valleyside record to reconstruct late Wisconsinan deglaciation. Postglacial activity has both helped and hindered this research. Most of the valley side deposits have been resedimented by meltwater and mass movement activity, but landslide-damming of Silver Lake has created a new temporary headwater for the lower reaches of Silverhope Creek. Downcutting into glacigenic valley fill has created several exposures and road construction has had a similar effect.

A history of the deglaciation has been developed by combining exposures, morphology and macro-paleomovement indicators (e.g. bedrock striae, valley side stoss and lee features).

4.4.2. Comments

4.4.2.1. Ice Flow Direction

Considerable evidence has been reported supporting ice sheet movement to the south. However, Coates (1974) concluded that another ice sheet, the

Hozameen Ice Sheet, flowed north through Manning Provincial Park along the east side of the Silverhope - Coquihalla drainage divide. This was based upon erratics found on the east side of the Skagit River valley, northeast of Ross Lake.

There is some concern (Waitt, 1977; Waitt and Thorson, 1983) that erratics may have been incorrectly identified, because they cannot be traced. However, it is agreed that this section of the Skagit valley acted as a collecting area for ice moving down the Klesilkwa valley (southeast), Skagit valley (southwest), northeast and west down several tributary valleys north of Ross lake (Barksdale, 1941; Weis, 1969; Waitt, 1972). On the eastern side of the interfluve between Skagit and Manning Provincial Park, ice-diverted meltwater flowed west along Lightning Creek during deglaciation (Mathews, 1968) and probably found the lowest drainage point into the Skagit valley via Gibson Pass into Nepopekum Creek (Figure 4.4), and possibly farther north into Twentysix Mile Creek. Coates (1974) gave no details about clast morphology, but the complex drainage pattern in this area may account for the presence of 'erratics' from the south.

In addition, evidence for a general southeasterly ice sheet flow across the interfluve into the adjacent Manning Provincial Park was recorded at several low passes in Silverhope Creek (Section 4.4.2.4.). All recent evidence tends to suggest that Coates (1974) was mistaken.

4.4.2.2. Ice Front Oscillations

Two minor readvances were recorded in Chilliwack valley, 11 500 and 11 200 years BP (Saunders *et al.*, 1987). The second minor ice readvance might be

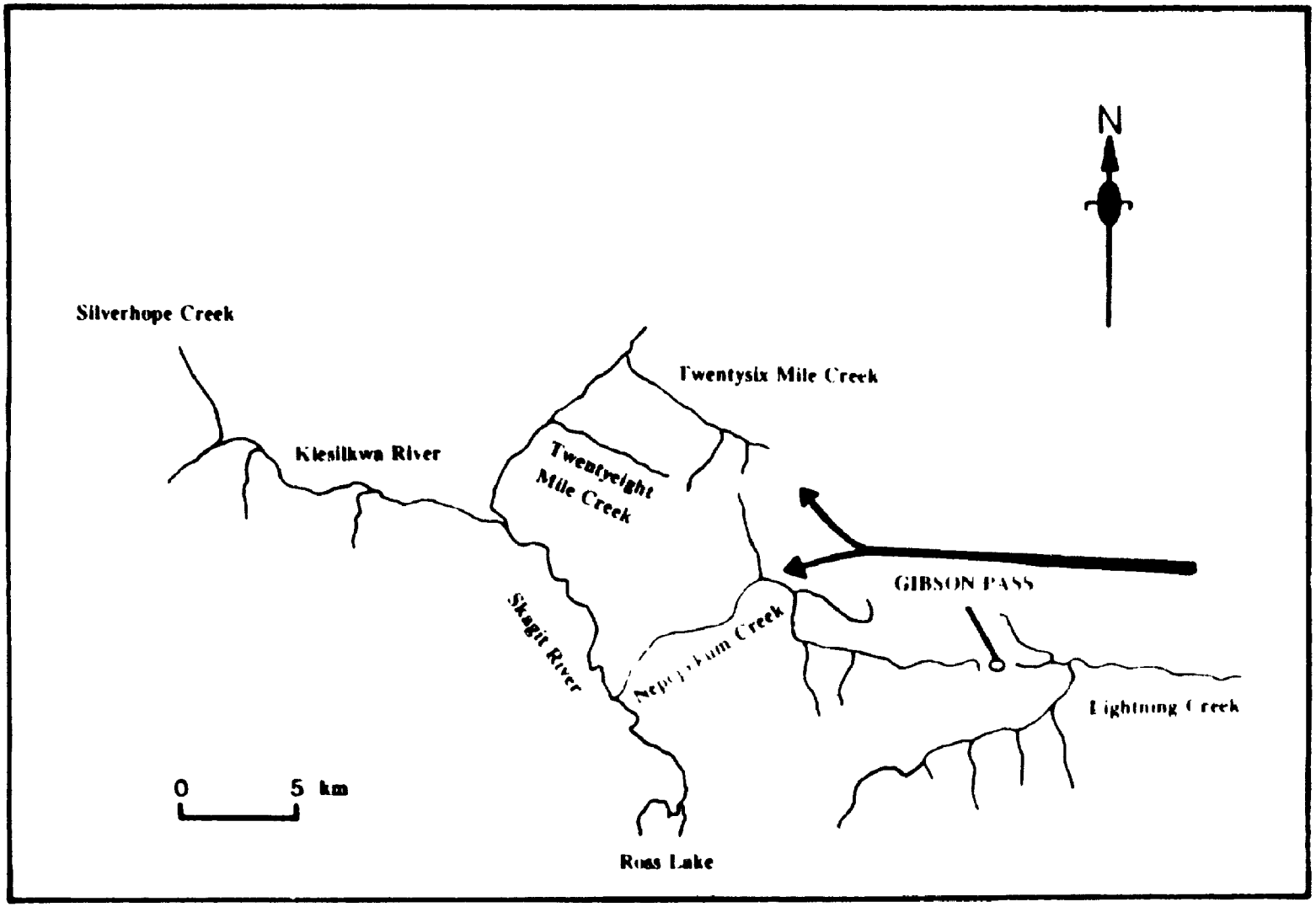

Figure 4.4 POSSIBLE TRANSFER PATHS FOR ERRATICS EMANATING FROM THE SOUTH IN SKAGIT BASIN

synchronous with the two small readvances/oscillations in Silverhope valley, the first Chilliwack readvance being concurrent with deposition of the boulder mounds to the south. These events were more obvious in Chilliwack valley because of rapid isostatically-induced phases of reemergence of low-lying areas from the sea, backing ice up in two stages into side valleys of the Fraser Lowland (Saunders *et al.*, 1987).

Waitt and Thorsen (1983) believed that Silverhope valley was the first valley in the Cascades Range adjacent to the Fraser Lowland, to not be influenced by late Wisconsinan sea level fluctuations and isostatic reemergence, although minor effects may have been manifested as small oscillations in the ice front. Alternatively, geothermal activity induced by the isostatic readjustments may have caused minor surges. Evidence for the centre of activity is suggested by anomalous localised glacier advances, such as those recorded in the Chilliwack valley, and proposed contemporaneous activity in the Silverhope basin. Related research by Ryder *et al.* (1991) suggests that glacial loading and unloading could trigger volcanism, and anomalous volcanic landforms (For example; flat topped volcanoes and esker-like lava flows) that may come from subglacial eruptions are found in other areas of B.C. (Mathews, 1951; 1958; Grove, 1974).

Harrison Hot Springs is an area of contemporary geothermal activity midway between Chilliwack and Silverhope valleys. Periods of intense geothermal activity, triggered by rapid isostatically-induced phases of reemergence of low-lying areas in the Fraser Lowland, could have generated subglacial ice melt. Chilliwack valley, downglacier of Harrison Hot Springs would

have experienced greater ice front oscillations than Silverhope valley, upglacier of the geothermal source. There is no direct evidence for this hypothesis, but the coincidence of ice front oscillations in Chilliwack and Silverhope valleys and the location of Harrison Hot Springs warrants its consideration. Lack of similar oscillations in peripheral Fraser Lowland tributaries suggests a more localised explanation than regional isostatically-induced phases of land reemergence.

4.4.2.3. Deglaciation

During deglaciation, ice sheet downwasting and retreat sometimes occurred in the direction of meltwater flow creating ice-dammed lakes (Davis and Mathews, 1944; Mathews, 1944; Fulton, 1969; Sawicki and Smith, 1992). Fulton (1969) reported that in the Nicola, Thompson, North Okanagan and Shuswap Basins, lake levels were controlled by interfluves, retreating ice (sometimes flowing across it), ice marginal drainage, glacial deposits, dead ice or isostatic adjustment. The deglacial history of the Silverhope valley appears to be less complex, with lake levels being controlled by interfluves, retreating ice, ice marginal drainage and dead ice deposits. There is no evidence of drainage over the ice front (although it probably occurred), and the proximity of Silverhope valley to the margin of the Cordilleran Ice Sheet margin may explain the lack of isostatic readjustment in the valley.

At the ice oscillation/readvance site just north of Silver lake, a substantial quantity of local shale was reworked and laid down in the ice marginal lacustrine and glacigenic deposits. This easily eroded bedrock outcrops near Hope and

provides a useful indicator of glacial transfer over short distances, and the depositional environment. Preservation of striae and fabric indicates lodgement or rapid subglacial meltout from stagnant ice. Lodgement may have occurred in some cases but only sporadically as few shears are recorded. However, subglacial meltout from stagnant ice or rapid subglacial meltout underlying moving ice can preserve clay smudges (Shaw, 1979; Edwards, 1986), which were found in numerous sites.

The oscillation/readvance site has rare flames preserved in the diamicton, these may be the result of either ice grounding in a lacustrine environment (e.g. Gravenor *et al.*, 1984), or actively retreating ice (Hart, 1990), or by a small, slow ice advance overriding the ice marginal debris (Shaw, 1985).

Rates of glacier advance are a function of sediment yield (drainage area, rates of glacial erosion & transportation & debris release), total sediment volume of grounding-line system (valley width, lake depth minus maximum water depth required for terminus stability, angle of repose of sediment), and sediment dispersal patterns (process of debris release and dispersal, type of sediment, lake currents). Thus, advance rate is normally slow because both a stable ice margin and sediment build up are required, whereas retreat is faster (Powell, 1991). Bearing in mind the suite of features preserved in the exposure it seems more likely that flame structures were caused by a small, slow ice advance overriding the ice marginal debris (Shaw, 1985), during a period of relatively rapid glacier retreat depositing sedimentary sequences similar to those discussed by Stewart (1991).

Grain size distributions of diamictons in Silverhope valley and the Sumas tills in adjacent Fraser Lowland (Armstrong, 1981) generally correspond (Figure 4.5). Points lying outside the zone delimited by Armstrong (1981) refer to units which experienced considerable amounts of resedimentation or winnowing of fines, but maintained sufficient structural and textural integrity to differentiate them generally from glaciofluvial or glaciolacustrine deposits. In the larger fraction percentages (gravel - sand -mud) differentiation is less clear and is only possible through fabric analysis (Figure 4.6).

4.4.2.4. Erosional Features

In the Silverhope drainage basin, several rounded, low passes in upland and lowland areas indicate that there was glacier overriding of interfluves. The low-lying drainage divide between Klesilkwa River and Silverhope Creek appears to have been a more substantial watershed prior to the Fraser glaciation (Waitt, 1977). Immediately southeast of the Upper Klesilkwa River, truncated spurs from both valley sides constrict the main valley to about 250 m in width. Large blocks of local granodiorite are found in mounds and then individually in diminishing concentrations over the next 2 km downglacier. This pass may have existed in the past, but morphological evidence suggests that it was substantially reshaped during the latter part of the Fraser glaciation. In addition, there appears to be a marked modification in the drainage pattern of the Upper Klesilkwa River. Where the river joins the main valley, flow direction changes from the north to the southeast. This suggests that prior to the Fraser glaciation the Upper Klesilkwa

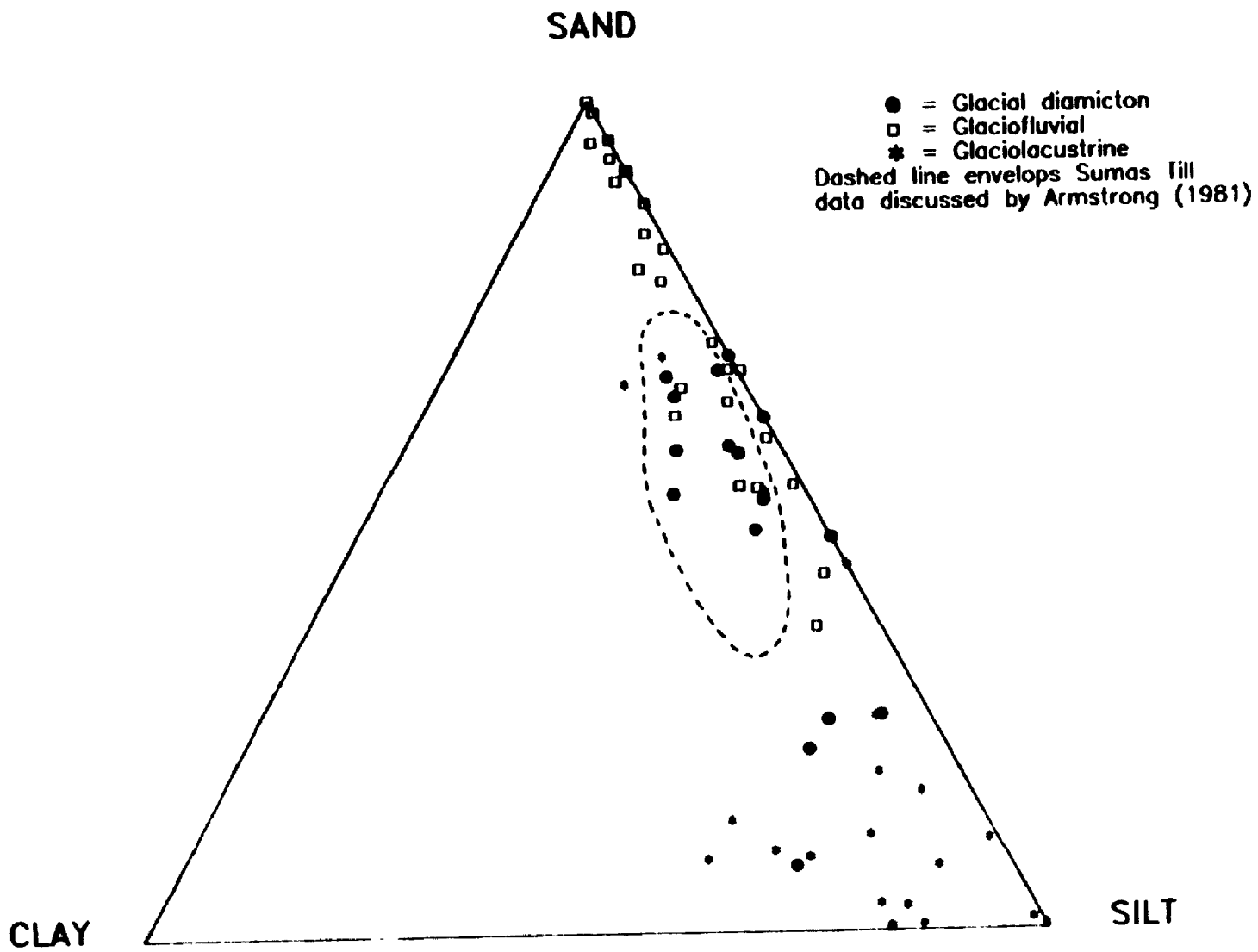

Figure 4.8 TEXTURAL TERNARY FOR MATRICES OF GLACIGENIC DEPOSITS

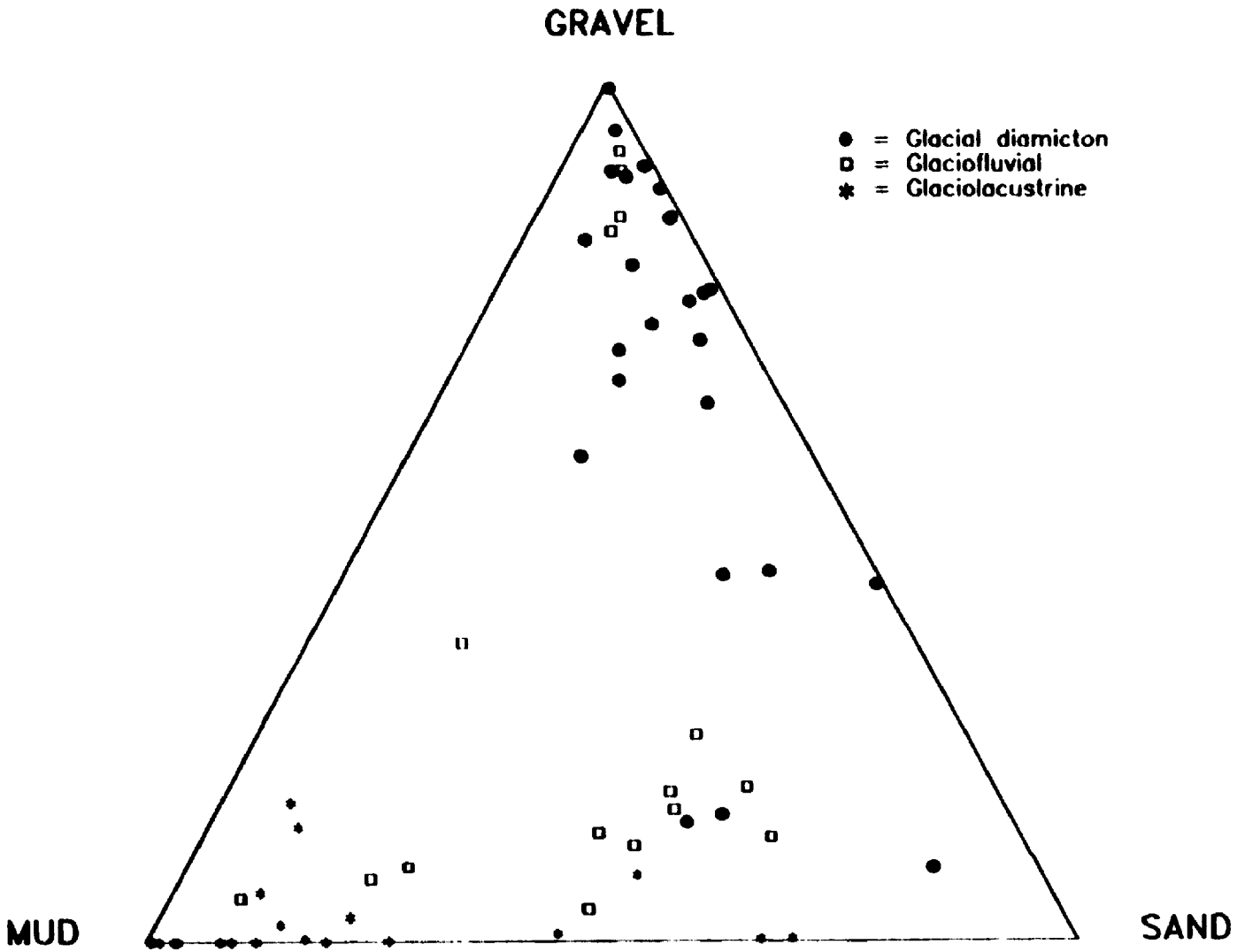

Figure 4.6 TEXTURAL TERNARY FOR WHOLE ANALYSES OF GLACIGENIC DEPOSITS

River formed the headwaters of Silverhope Creek, redirection probably being caused by the deposition of hummocky terrain immediately northwest of this breach.

Other glacial overrides appear to have lowered the altitude of interfluves as opposed to reorienting flow directions, the most notable of these being the Hicks Creek-Post Creek watershed. Ice appears to have flowed southwest and merged with Chilliwack ice in the adjacent valley. Other low, glaciated passes can be found; to the west into the Chilliwack River drainage basin (e.g. east of Paleface Mt., south and north of Mt. Northgraves), and to the east into the Coquihalla drainage basin (e.g. north and southeast of Wells Peak). North of Wells Peak (Figure 1.1), striae and valley side stoss-lee features indicate that ice flowed southeast from the Silverhope valley across the interfluve between Alexander and Berkey Creeks (in the Coquihalla drainage basin) at a height of about 1524.0 m. Similarly, to the southeast, on the flanks of Mt. Forddred (Section 2.2.55.), ice flowed south at a height of about 1877.5 m. although the peak appears to have been ice free at 1935.5 m. On the west side of the valley, Mt. Holden (Figure 1.1) shows signs of glaciation to a height of 1988.0 m which suggests asymmetrical ice coverage across the valley.

In such a narrow valley, climatic control of ice coverage seems unlikely, but the valley's proximity to the ice margin should be considered. Paraglacial sedimentation indicates similar conditions and the causes are discussed in more detail in Section 5.3.3.

Ryder *et al.* (1991) stated that in many alpine valleys of British Columbia, the downstream limit of significant erosion by former glaciers can be determined by an abrupt change from a "U"- to a "V"- shaped valley. This may either indicate the position of an ice margin during a time when glaciers were relatively stable, or the location where alpine glaciers merged with the ice sheet. Ryder's (1989) preliminary work in the Okanagan Range of the Cascade Mountains favours the former hypothesis. In Silverhope valley, the latter proposal appears to be more appropriate. At the confluence of each west side tributary with the main valley there is a distinct widening ("U"-shape) (Plate 1.1). Furthermore, there is a marked transition from a "V"- to "U"- shaped valley (as opposed to a "U" to "V" - shaped transition) south from the glacial oscillation/ readvance point at Silver Lake. This northern section of the valley is at the divergence between Fraser valley and Cascade Mt. ice where glacial erosion would presumably be high (as shown by bedrock erosion on the west valley wall).

It seems likely that an increase in the main valley ice mass by tributary ice creates the "beaded" valley shape. This widening attenuates downglacier (southward along the Silverhope valley) until additional tributary ice enters, creating another "bead". At the confluence between tributary and main valley ice, the two separate ice flows may or may not have merged immediately depending upon ice density and flow rates, but would in time (or distance) merge. Rather than rise up, ice could initially move laterally, widening the valley. It is proposed that gradual uplift of main valley ice caused a downglacier diminution in erosive power until the next input from tributary ice. Where ice emerged from high

hanging valleys (e.g. Swanee Creek) valley widening effects were mitigated because altitude adjustments occurred more rapidly.

4.4.2.5. Morphological Evidence of Silverhope Basin Deglaciation in Adjacent Valleys

Kame terrace drainage of GLS flowed northwest into Fraser valley. Regrettably the presence, or lack of ice in the Fraser valley cannot be confirmed by attempting to trace kame terrace deposits. Kame terrace deposits and their topographical expression are truncated by a series of gullies northwest of Eureka Creek.

The possibility exists that these kame terraces are actually ancient lake shorelines (e.g. Sissons, 1978; 1979). There are three main reasons for discounting this theory. First, there are no matching pairs on the east valley side. Second, the material incorporates many erratic clasts and there is no evidence of major till sources above the terraces to account for their presence in lake terraces (prior to kame terrace deposition this area was heavily scoured by ice removing the majority of valleyside deposits). Third, many clasts are subrounded and possess imbrication and paleoflow indicators of glaciofluvial origin.

Glacial outburst events have been found in two adjacent valleys, Chilliwack and Fraser. Morphology of the former event has been discussed in Clague and Luternauer (1982) and used in this study to determine the timing of deglaciation. The latter event marks the end of the glaciation of Silverhope valley. In the Fraser valley there are no lateral kame terrace deposits and there appears to have been

unconfined deposition of the alluvial fan. This suggests that the Fraser valley was ice-free when outburst occurred, and that Silverhope valley was probably blocked by dead ice.

Further study of the southern side of the Fraser valley and the tributary valleys between Hope and Chilliwack will help to resolve some of the questions concerning conditions at the end of the Fraser glaciation.

CHAPTEP FIVE

HOLOCENE SEDIMENTATION AND INTERPRETATION

5.1. Introduction

This chapter deals with evidence of Holocene sedimentation and its interpretation. Sedimentation is considered in three parts; valleyside sections, lake sediment cores taken from Silver Lake, and Silverhope Creek gravels. An interpretation, incorporating local and regional contexts, follows each description.

5.2. Valleyside Sections

5.2.1. Introduction

In the Silverhope drainage basin there are many debris fans visible on aerial photographs, although few possess exposed sections. Those that contain late Wisconsinan sediments were interpreted in Chapters Two and Three; the remainder are considered here. Annotated stratigraphic sections for each exposure are in the text (these have been completed in accordance with the criteria detailed in Tables 2.1, 2.2 and 2.3). Particle size and fabric data are given in Appendices II and III. Pebble source lithology information is given in Table 2.5.

5.2.2. Site 14

This site is located on the west side of Silverhope Creek on the north side of the confluence between Maimen and Silverhope Creeks. It is 11.8 m from the mouth of Silverhope Creek (Figure 5.1a).

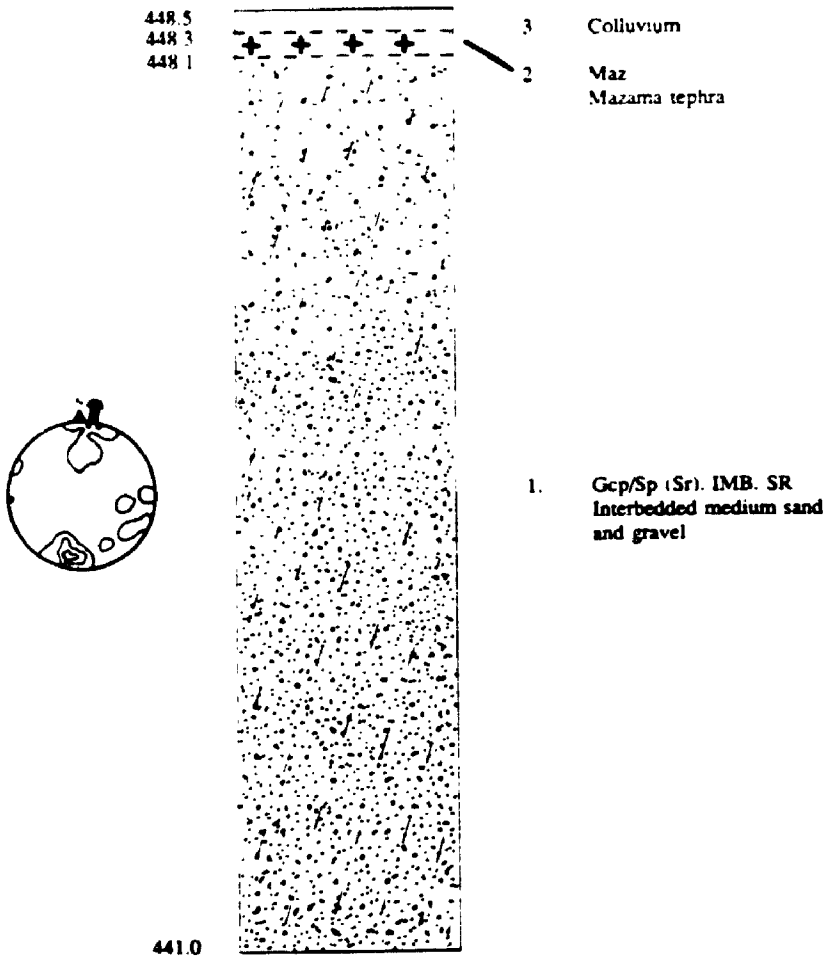

Figure 5.1a SITE 14

Unit 1 is about 7.1 m thick. It consists of non-compacted, interbedded medium sand and gravel. Weakly bimodal clast imbrication and pebble clusters indicate paleoflow from the south-southwest (an eigenvalue of 0.80). Planar cross-stratification is visible, with some sand interbeds possessing ripple features. Beds dip at about 2° to the north. Percussion marks are evident on some clasts. The upper contact appears to be conformable, and there is no visible lower one. Clast lithology is predominantly locally-derived pegmatitic granite gneiss (KTc) and pelite (PJH).

Unit 2, 0.2 m thick, consists of a non-compacted silty-sand tephra. There are no apparent structures and no large clasts or dropstones. The unit is draped over several clasts on the upper surface of *Unit 1*. The upper contact appears to be conformable.

Unit 3 is approximately 0.2 m thick. It appears to be a thin colluvial veneer which conformably overlies *Unit 2*. The unit was not analysed.

5.2.3. Site 28a

This exposure is located in a gully cut on the Hicks Creek logging road about 6.1 km from the junction with the main logging road (Figure 2.1v).

Unit 1, 0.7 m thick, consists of a grey, laminated sandy mud. This is discussed in Section 2.2.27. The upper contact appears to be conformable.

Unit 2, 0.3 m thick, appears to be a layer of non-compacted silty-sand tephra. Water seepage occurs at the contact with *Unit 1*. The unit appears to

have a similar structure and texture to Site 39 (Section 5.2.4.). The upper contact appears to be conformable.

Unit 3, about 0.5 m thick, appears to be a colluvial veneer and has not been studied.

5.2.4. Site 39

This site is located in a high altitude, partially water-filled depression. It is located approximately 30 m south of Hope Mountain summit. About 0.08 m beneath the surface peat is a layer of non-compacted silty-sand tephra which appears to overlie bedrock and is conformably overlain by peat. This unit is approximately 0.10 m in thickness.

5.2.5. Site 49

This site is located in a gravel pit adjacent to the main logging road, approximately 11.0 km south of the mouth of Silverhope Creek (Figure 5.1b).

Unit 1 is approximately 22.3 m thick, but is divided into two parts by a 0.10 m thick unit 2.3 m below the upper contact with *Unit 3*. It is composed of a stratified coarse gravel with beds dipping west at 10-15°. Lenses of fine mud and mud drapes are present in the middle part of the unit. Above these are medium sand channel-fill deposits with small trough cross-bedding and ripples, indicating a northwest paleoflow direction. Subangular and subrounded clasts are present, their fabric appears variable, with many appearing to be oriented transverse to the inferred southerly paleoflow (there is an eigenvalue of 0.62). No apparent striae

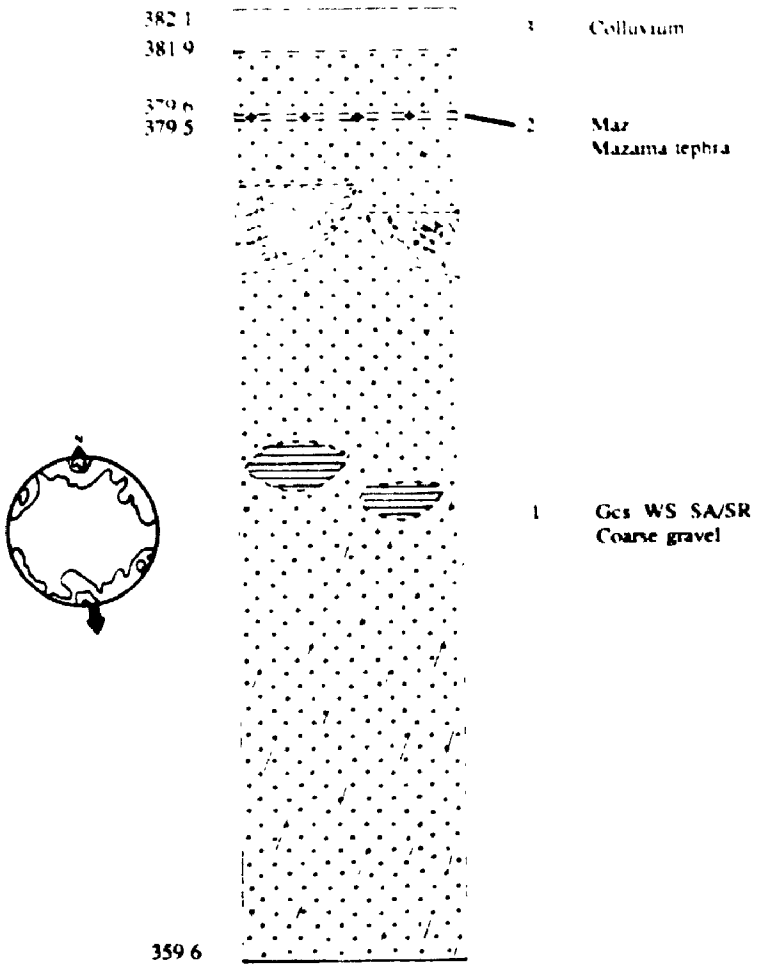

Figure 5.1b SITE 49

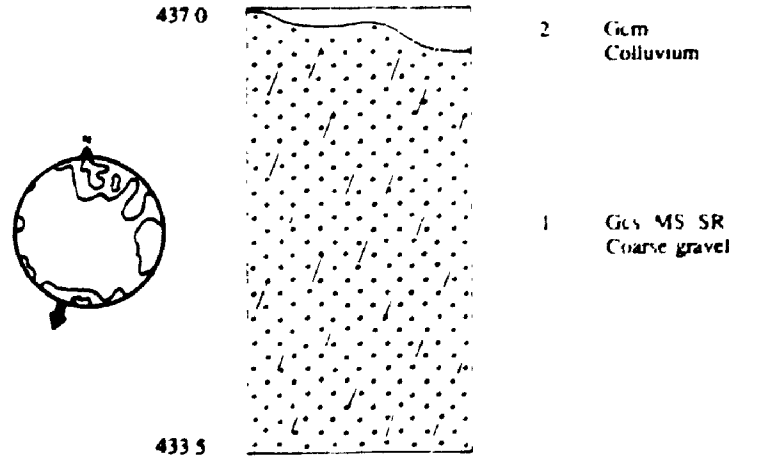

Figure 5.1c SITE 52

were observed on any clasts. The upper contact with *Unit 3* appears to be conformable. Clast lithology is mainly locally-derived pelite (PJH) and granodiorite (Ogd).

Unit 2 is 0.10 m thick. It is located 2.3 m from the top of *Unit 1*, and 2.5 m from the present surface elevation of the land. It is composed of a fine silty-clay tephra which appears to have upper and lower conformable contacts with *Unit 1*. It is differentiated from *Unit 1* because of particle size, structural and textural differences, although it appears to have been laid down concurrently. It appears to be a tephra deposit.

Unit 3 is about 0.2 m thick. It consists of a thin layer of colluvial material which appears to conformably overlie *Unit 1*. This unit was not studied.

5.2.6. Site 52

This site is situated on the east side of the main logging approximately 17 km from the mouth of Silverhope Creek (Figure 5.1c).

Unit 1 is about 3.1 m thick. It consists of a stratified, coarse gravel unit with poorly-defined bedding dipping west at 5-10°. There are no visible striae or imbrication structures, but there are numerous percussion marks. General clast orientation is bimodal, but paleoflow to the southwest is indicated (there is an eigenvalue of 0.70). The upper contact is apparently erosional. Clast lithology is mainly locally-derived pelite (PJH) and granodiorite (eTgd), with some distantly-derived diorite (Kd).

Unit 2 is approximately 0.4 m in thickness. The unit consists of a colluvial veneer which was not studied. It is thicker at the southern end of the exposure.

5.2.7. Site 67

This site is located on the north side of the Upper Silverhope Creek logging approximately 300 m from the junction with the main logging road (Figure 5.1d).

Unit 1 is approximately 1.0 m thick. It is composed of a non-compacted, interbedded coarse sand and subrounded gravel sequence. Beds dip at 5° to the north. Clasts lie on the slope of the bed and are well oriented in the opposite direction to inferred northerly paleoflow. Clast lithology appears to be locally-derived with rare pebbles of distant origin, although this was not studied in detail. There are no visible striae, but some clasts possess percussion marks. There is no apparent lower contact and the upper one seems to be erosional.

Unit 2, 0.5 m thick, consists of non-compacted, interbedded fine sand and medium gravel. Beds dip at 15° to the northwest, and paleoflow, although not studied in detail, appears to emanate from the Upper Silverhope valley. Clast lithology was not studied in detail but appears to be locally-derived with rare intermediate pebbles. The upper contact appears to be erosional.

Unit 3 attains a maximum thickness of 2.5 m of interbedded coarse sand and gravel. It is similar in structure and texture to *Unit 1* with beds dipping at 5° to the north/northwest. Weakly bimodal clast imbrication and pebble clusters indicate dominant paleoflow from the south (an eigenvalue of 0.85). Percussion

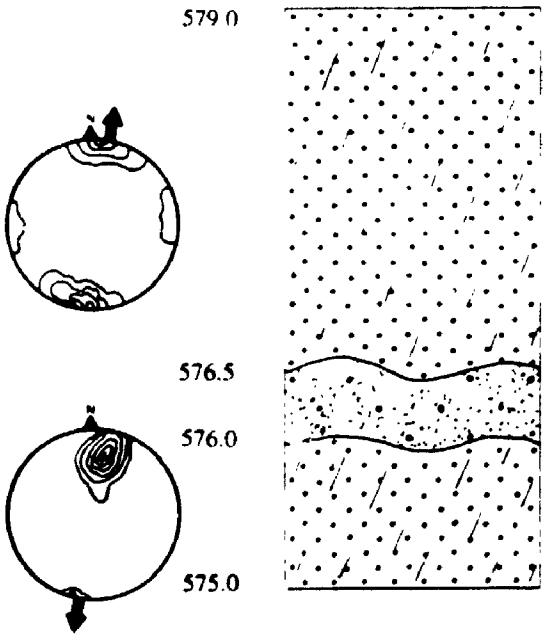

3. Gcp/Sp. IMB. SR. Interbedded coarse sand and gravel

2. Gcp/Sp. IMB. SR. Interbedded fine sand and medium gravel

1. Gcp/Sp. IMB. SR. Interbedded coarse sand and gravel

Figure 5.1d SITE 67

marks are visible on some clasts, but there appear to be no striae. Clast lithology is predominantly locally-derived pelitic schist (KTc) and granodiorite (Ogd), with rare pebbles of distant origin. There is an apparent erosional upper contact with a thin (<0.05 m) colluvial veneer.

5.3. Interpretation of Valleyside Sections

5.3.1. Introduction

There are too few exposures of paraglacial sediments to be able to reconstruct the complete history of the early Holocene in the valley. However, several exposures are located on clearly-defined morphological features that overlie earlier glacial deposits. Where possible, these morphologies will be considered in conjunction with exposures. Particle size and fabric data are given in Appendices II and III. Pebble source lithologies are detailed in Table 2.5. Figures 5.2 and 5.3 present results of textural analysis of Holocene valleyside exposures.

5.3.2. General Comments

In British Columbia, many researchers have shown that the majority of paraglacial sedimentation occurred between deglaciation and deposition of Mazama tephra (approximately 6 800 years BP):(e.g. Ryder, 1971a, 1971b; Church and Ryder, 1972). In many cases in western Canada, paraglacial deposition had finished within the first 1000 to 2000 years after deglaciation, and some studies in British Columbia have attributed complex responses during this period to climatic

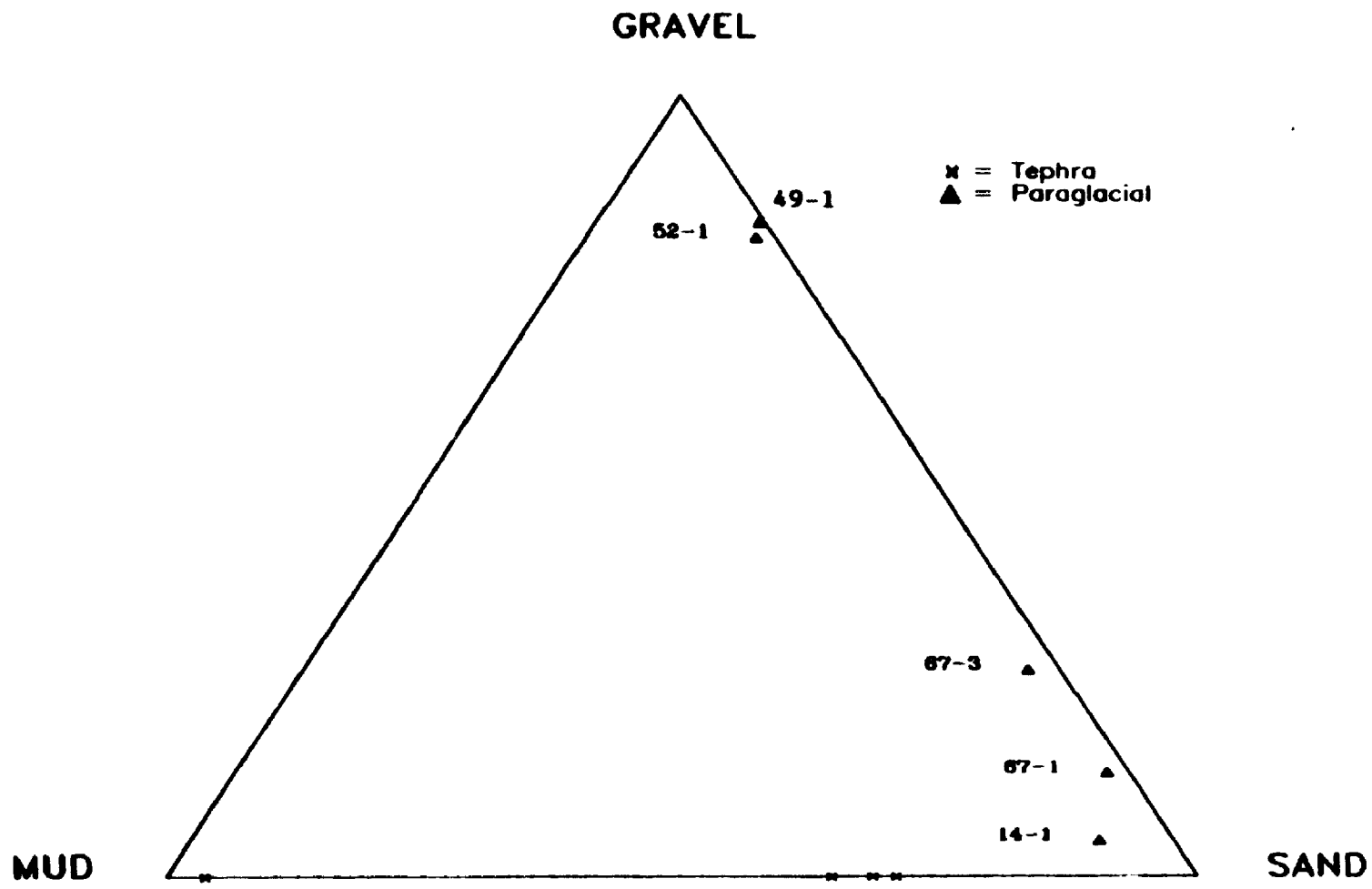

Figure 5.2 TEXTURAL TERNARY FOR WHOLE SAMPLES FROM HOLOCENE VALLEYSIDE EXPOSURES

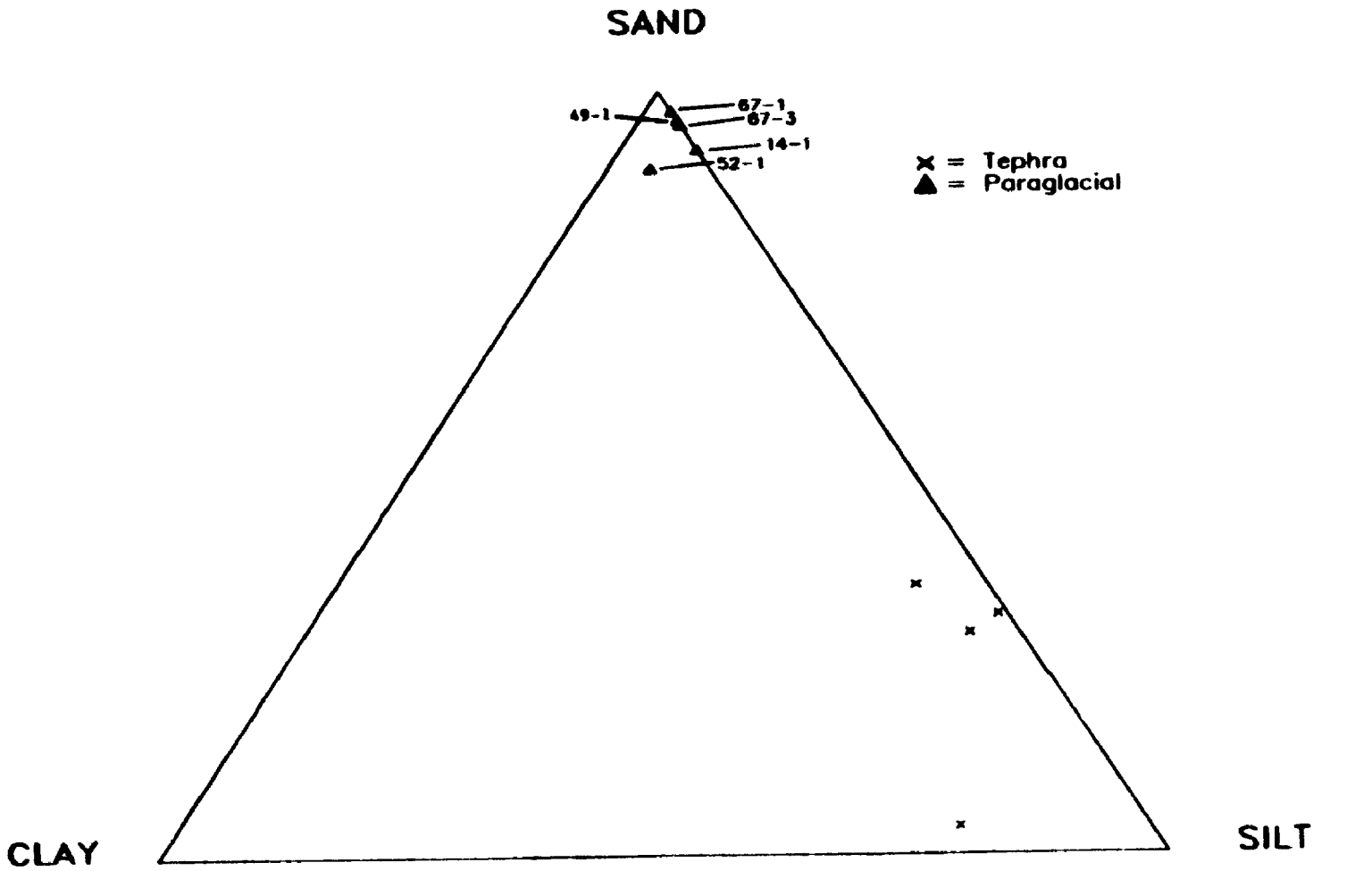

Figure 8.3 TEXTURAL TERNARY FOR MATRICES OF SAMPLES FROM HOLOCENE VALLEYSIDE EXPOSURES

change, base level fluctuations, and the increasing presence of vegetation (e.g. Smith, 1975; Jackson *et al.*, 1982, Souch, 1989). The deglaciation of Silverhope valley appears to have been independent of base level changes and there is no clear evidence for an early return of vegetation to the valley. This suggests that any changes in the rate of sediment supply may have been climatic in origin.

All the valley side exposures and morphological features observed on aerial photographs appear to be alluvial fans. These have issued from narrow confined valleys (albeit small on the east valley side) and approximate to the alluvial-fan delta morphology discussed by Nemec (1990). These are referred to as "paraglacial fans" below.

The exposure at the east end of Upper Silverhope Creek (Site 67) indicates that a paraglacial fan built out from this tributary valley into the main Silverhope valley. Flows were variable, from high energy with clasts avalanching down bedding planes in *Unit 1*, to more subdued flows (*Unit 2*), overlain by higher energy deposits in *Unit 3*. From aerial photographs and ground surveying it appears that this paraglacial fan overlies an older proglacial alluvial fan which flowed out of Upper Silverhope Creek onto dead ice. This compound fan forms the present drainage divide between Silverhope Creek and Klesilkwa River, and kettle holes situated on the fan indicate that either dead ice was buried by this feature or ice blocks rested in it. There are no exposures of the underlying proglacial alluvial fan, although a distinct break in slope at the site of Site 67 suggests that deposition was rapid, probably by an initial outburst (Section 4.3.12.1.) of a small ice-dammed lake. Following a hiatus, deposition of the

paraglacial fan appears to have taken place in a more restricted area covering about two-thirds of the older proglacial alluvial feature. The presence of rare intermediate and distal lithologies in the paraglacial fan indicates that some glacigenic sediments have been reworked. A high sand percentage (Figures 5.2 and 5.3) in the paraglacial fan suggests that the majority of coarser clasts were probably removed by outburst flooding.

A paraglacial fan emanates from the east main valley side adjacent to Upper Silverhope Creek. Unfortunately there are no exposures, although aerial photographs indicate that drainage of the partially-infilled kettle holes occurs northwest along the contact between the two fans (east valley side and the older proglacial alluvial fan emanating from Upper Silverhope Creek which extends across the whole valley floor).

Except for two Holocene exposures, the remainder possess tephra units. These tephra layers have been identified using their magnetite composition (Brewster and Barnett, 1979; Beaudoin and King, 1986), (Appendix IVa and Figure 5.4) as being of Mt. Mazama origin (approximately 6.8 ka years BP; Fulton, 1971).

In Hicks Creek, a small valley side exposure is topped by Mazama tephra which has a conformable upper contact with a thin (0.5 m) layer of colluvium (Site 28a). Mazama tephra overlies lacustrine sediments which, by elevation must have been laid down immediately prior to meltwater outburst into Chilliwack valley. Aerial photographs suggest that paraglacial activity in this upper part of Hicks Creek was minimal, and following tephra deposition only a thin layer of colluvium has developed.

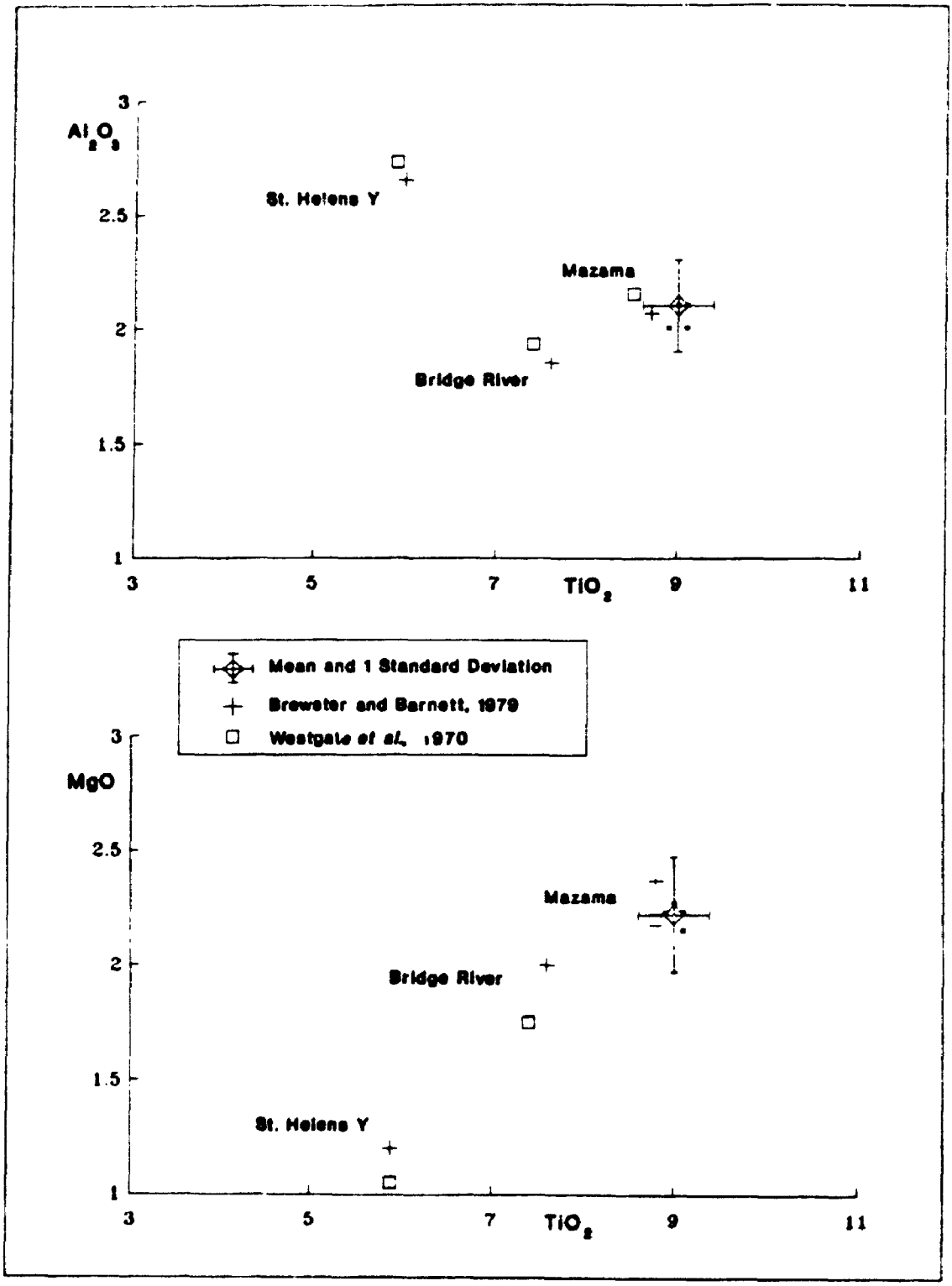

Figure 5.4 MAGNETITE COMPOSITION OF SILVERHOPE TEPHRAS (Binary plot of TiO_2 versus Al_2O_3 and MgO; modified after Brewster and Barnett, 1979)

Similarly, on the west valley side of the main Silverhope valley at Site 14, Mazama tephra is found 0.2 m beneath the present surface. At this site, *Unit 1* comprises paraglacial fan material. It is located on the north edge of the fan which emanates from Maimen Creek. One rare intermediate clast indicates reworking of glacigenic deposits, although most clasts are of local Maimer Creek origin. Rapid deposition is indicated although particle size distribution is relatively fine (high sand percentage); larger clasts may well be buried in the lower sections of the fan. There appears to be no break in deposition, with Mazama tephra conformably overlying the fan. Lack of subsequent deposition suggests that paraglacial activity had ceased by the time Mazama ash was deposited.

Site 49, on the east side of the main valley, is situated on a paraglacial fan which issued from an unnamed east valley side creek. Deposits indicate a gentler meltwater regime with channel-switching and ponded sediments. The exposure is situated on the southern side of the fan and paleoflow indicators reflect this orientation. Clast lithology suggests that it consists of reworked glacigenic sediments. 2.5 m beneath the present surface, and 2.3 m beneath a colluvial veneer, there is a thin unit of Mazama tephra. This is conformably sandwiched by the sand and gravel of *Unit 1*. The depth of burial of this tephra suggests that paraglacial activity on the east valley side continued beyond that of the west for some time. The only other east valley side exposure with preserved Mazama tephra was in a high-altitude peat deposit (Site 39). The Mazama was laid down directly on bedrock and is conformably overlain by 0.08 m of peat.

The final exposure which appears to be of paraglacial origin (Site 52), is again situated on the east valley side, and appears to have issued from another unnamed creek. Deposition seems to have been under high energy conditions as suggested by percussion marks on clasts. Intermediate clast lithology indicates that water has reworked glacigenic deposits. Mazama tephra was not present, and the upper part of the unit has been truncated by an overlying colluvium.

All exposures on the paraglacial fans were near the upper contact with the overlying colluvial cover, but Sites 49 and 52 are far coarser than the exposures on the west side of the drainage basin. This may represent higher energy glacial meltwater flushing of coarser sediments on the west side, and delayed reworking of material on the east side. Smaller drainage areas on the east valley side and lower precipitation rates may have delayed reworking of glacigenic sediments. The Mazama tephras are all of similar particle size distribution.

5.3.3. Discussion

There are clear topographical differences between the west and east sides of the Silverhope drainage basin. Regional glacial topography in the Skagit region and southern Coast Mountains indicates that western tributaries contributed ice to the main trunk valleys, but that eastern valley glaciers rarely extended beyond their cirques (Waitt, 1977; I.S. Evans, pers. comm., 1992). It is suggested that tributary glaciers on eastern valley sides have a higher equilibrium-line altitude, farther away from the Pacific source of moisture (Waitt, 1977).

Paraglacial and modern climatic asymmetry appear to reflect similar conditions. To the west of Ross Lake (on the US-Canada border, 30 km south of Silverhope valley) annual precipitation is 250-500 cm, but to the east it is only 130-250 cm (Foxworthy and Richardson, 1973). Recent studies of paraglacial activity in the North Cascades National Park suggest that this dichotomy was more extreme than previously suggested by Evans (J. Riedel, pers. comm., 1992), with sedimentation rates declining rapidly during the first 1000 years after deglaciation on the west side, but continuing at a steady (lower) rate for several thousand years on the east side. Silverhope valley is narrow and such dramatic fluctuations in sedimentation rates appear unusual. Evans (I.S. Evans, pers. comm., 1992) points out that the dominant wind direction in the area is from the south. Therefore it is possible that a combination of climatic asymmetry and wind direction have contributed to this local phenomenon.

Sedimentation rate is directly affected by the ability of meltwater to transport sediment. In the Silverhope valley, there are more and longer tributaries to the west and an unbalanced sediment supply would be expected. However, the arrangement of tributary valleys within the drainage basin appears to be indicative of climatic asymmetry, perhaps in conjunction with bedrock geology.

Palynological records in British Columbia show that cool, moist conditions succeeded glaciation, but that climatic amelioration followed (low precipitation and high temperatures) during the "early Holocene xerothermic interval" between about 10 and 7.5 ka years BP (Mathewes and Heusser, 1981). These conditions were later followed by a return to cool, moist conditions after 7 ka (Mathewes and

Heusser, 1981; Mathewes, 1985). This dry period may have reduced fluvial efficiency and encouraged vegetation, decreasing sediment supply to the valley floor (Souch, 1989). In Silverhope valley this drier period may have had a more significant affect on the east valley side, further slowing delayed paraglacial processes.

Evidence from the Silverhope valley concurs with this proposal. Mazama tephra is found in the upper one metre of two exposures on the west side of the drainage basin (although only one appears to have been affected by paraglacial activity), but is beneath 2.5 m of sediment on the exposure to the east. It is important to note though that because Silverhope valley is steep-sided, poor preservation of deposits is the norm. Climatic influences may have been minimal, but regional evidence for climatic asymmetry tends to be supported by the sedimentary record.

5.4. Silver Lake

5.4.1. Introduction

Silver Lake is situated approximately 8.0 km from the confluence of the Fraser River and Silverhope Creek (Figure 1.1.). Recent radiocarbon analysis of samples taken from drowned trees in Silver Lake gives an approximate age of the landslide-damming event of 890 $\pm$ 60 years BP (GSC-5444) and 1010 $\pm$ 100 years BP (GSC-5204) (Clague and Shilts, in press). As mentioned in Section 1.5.2., this event may possibly have been coeval with other paleoseismic evidence for a major earthquake beneath Seattle about 1100 years ago (Adams, 1992; Atwater

and Moore, 1992; Bucknam *et al.*, 1992; Karlin and Abella, 1992); and in particular with concurrent blockage of streams in the Olympic Mountains by landslide-damming events (Jacoby *et al.*, 1992; Schuster *et al.*, 1992). Radiocarbon ages tend to suggest that the landslide-damming of Silver Lake may actually be a slightly younger non-seismic event.

The lake is about 1.5 km long and up to 350 m wide. There are three deltas on the lakeshore, a relict fan delta to the northwest (Section 4.3.10.), and two at the south end. The delta on the southwest side has been inactive since 1946 when major logging of the valley started and Silverhope Creek flows were diverted to the east (this will be referred to as the 'old' delta). The delta to the southeast became active in 1946 (this will be referred to as the 'new' delta).

A CGRC - Freeze Sectioning Corer (RLII) ('frozen finger') was used to extract lake sediment cores (Goudie, 1981). The device (Plate 5.1) was filled with dry ice and released from the stern of a boat (Plate 5.2). After ensuring vertical penetration of the lake bed, the corer was lifted to the surface once freeze-on had taken place (approximately 20 minutes). The water-sediment interface was preserved at the top of each core, which allowed the actual depth of core retrieved to be measured.

Appendix V details information concerning the units sampled for particle size analysis, radiocarbon ages and caesium dating, and specifies lake depth and core length. Annotated stratigraphic logs for each core are detailed in Figure 5.5a, (these have been completed in accordance with the criteria detailed in Tables 2.1, 2.2 and 2.3). Radiocarbon ages and caesium dates are shown in

Plate 5.1 **C.G.R.C. FREEZE-SECTIONING CORER (RLII)** **(in use aboard M.V. Pilea. Corer approximately 2 m in length)**

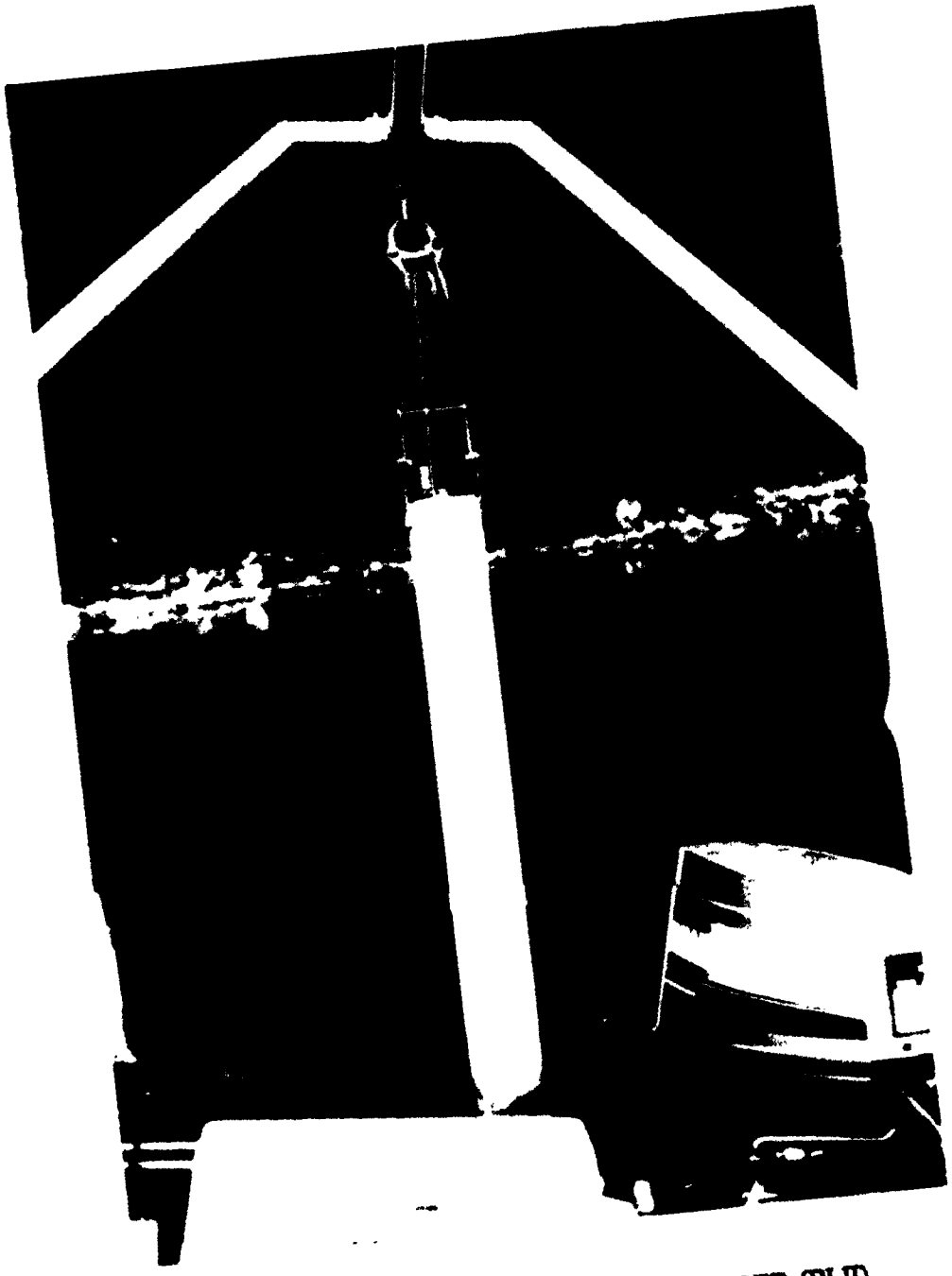

Plate 5.2 C.G.R.C. FREEZE-SECTIONING CORER (RLII)
(Immediately prior to release. Corer approximately 2 m in length)

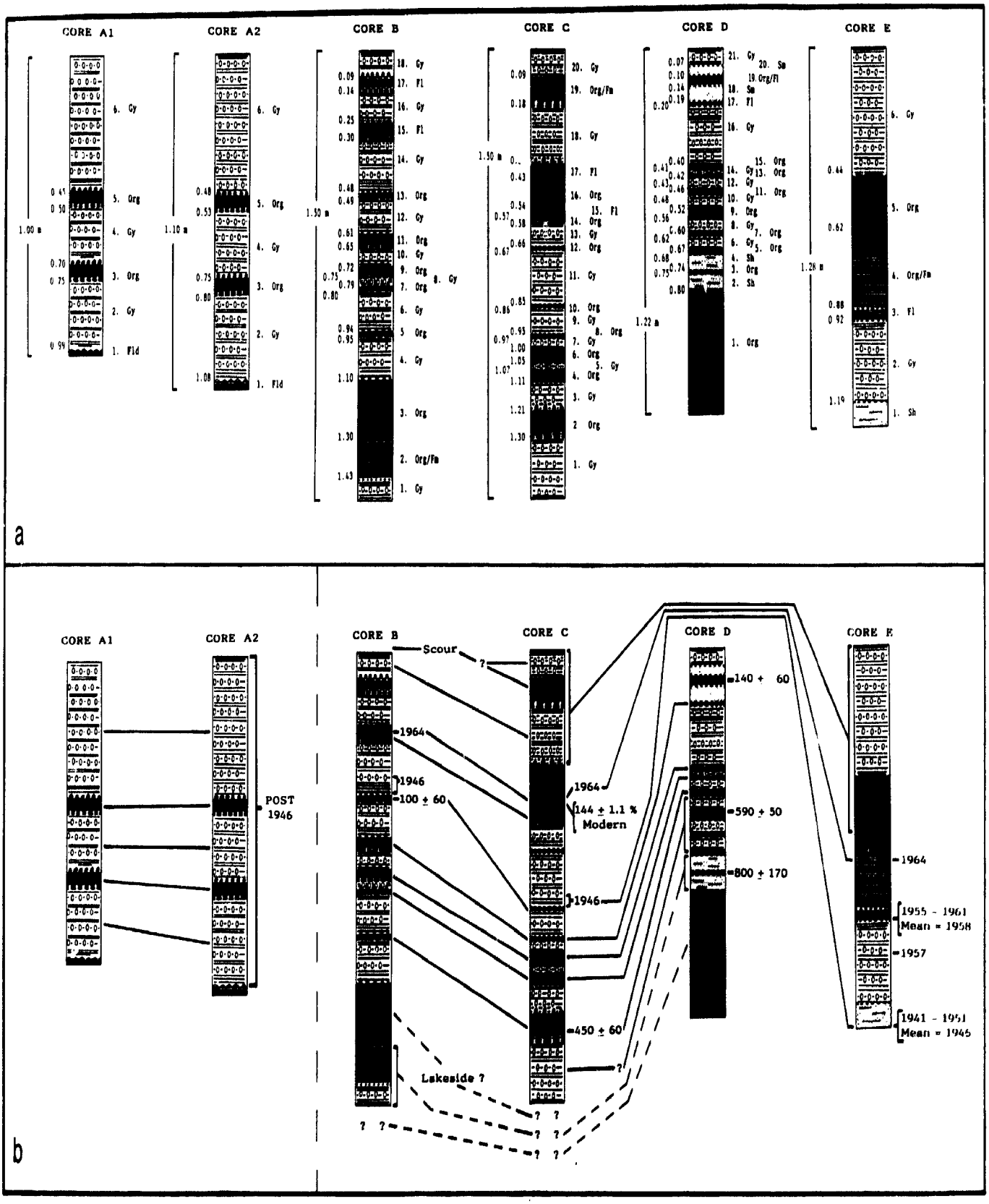

Figure 5.5 STRATIGRAPHIC LOGS OF SILVER LAKE CORES: a) Interpretation of Units, b) Inferred stratigraphic relationships (including radiocarbon and caesium data)

Figure 5.5b (and Appendices IVb and IVc respectively) together with the inferred stratigraphic relations between each core. Particle size data are given in Appendix III. Figure 5.6 shows a ternary plot of sand-silt-clay percentages. Core extraction sites are detailed in Figure 5.7 on a bathymetric map of Silver Lake (produced from SCUBA survey and seismic data). Sites were chosen to ensure that sediments from the new and old delta were adequately represented, and to obtain information from as near to the landslide dam as possible. Lake sections are described below (a Munsell Colour Code is given in patentheses).

5.4.2. Lake Sections

5.4.2.1. Section A1: (49°19.021'N, 121°24.810'W)

Unit 1 [5B 5/1] is 0.01 m thick. It is composed of a compact, grey, laminated mud with rare, subrounded dropstones. All dropstones are intermediate argillite, some appear to possess fine striae (all dropstones discussed in Section 5.4.2. possess associated features consistent with the criteria detailed in Section 2.1.). There is no apparent lower contact and the upper one seems to be erosional.

Unit 2 [5YR 3/1] is 0.24 m thick. It is composed of a non-compacted, structureless gyttja consisting mainly of fine-grained organic debris and mud. The upper contact appears to be deformed.

Units 3 and 5 are both 0.06 m in thickness. They are composed of non-compacted, deformed layers composed of fine- and coarse-grained organics. Both upper and lower contacts appear to be deformed.

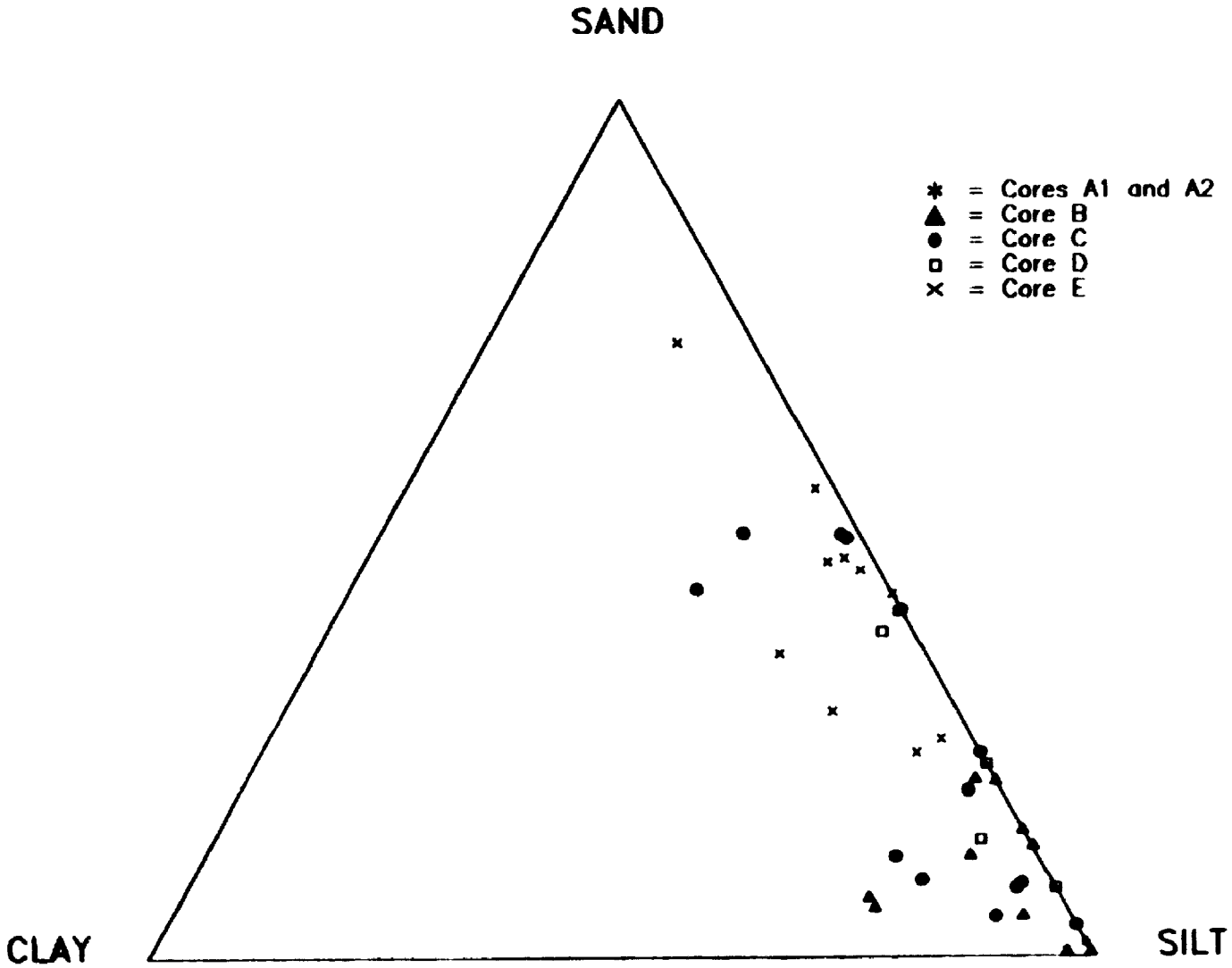

Figure 8.6 TEXTURAL TERNARY FOR MATRICES OF SAMPLES FROM SILVER LAKE CORES

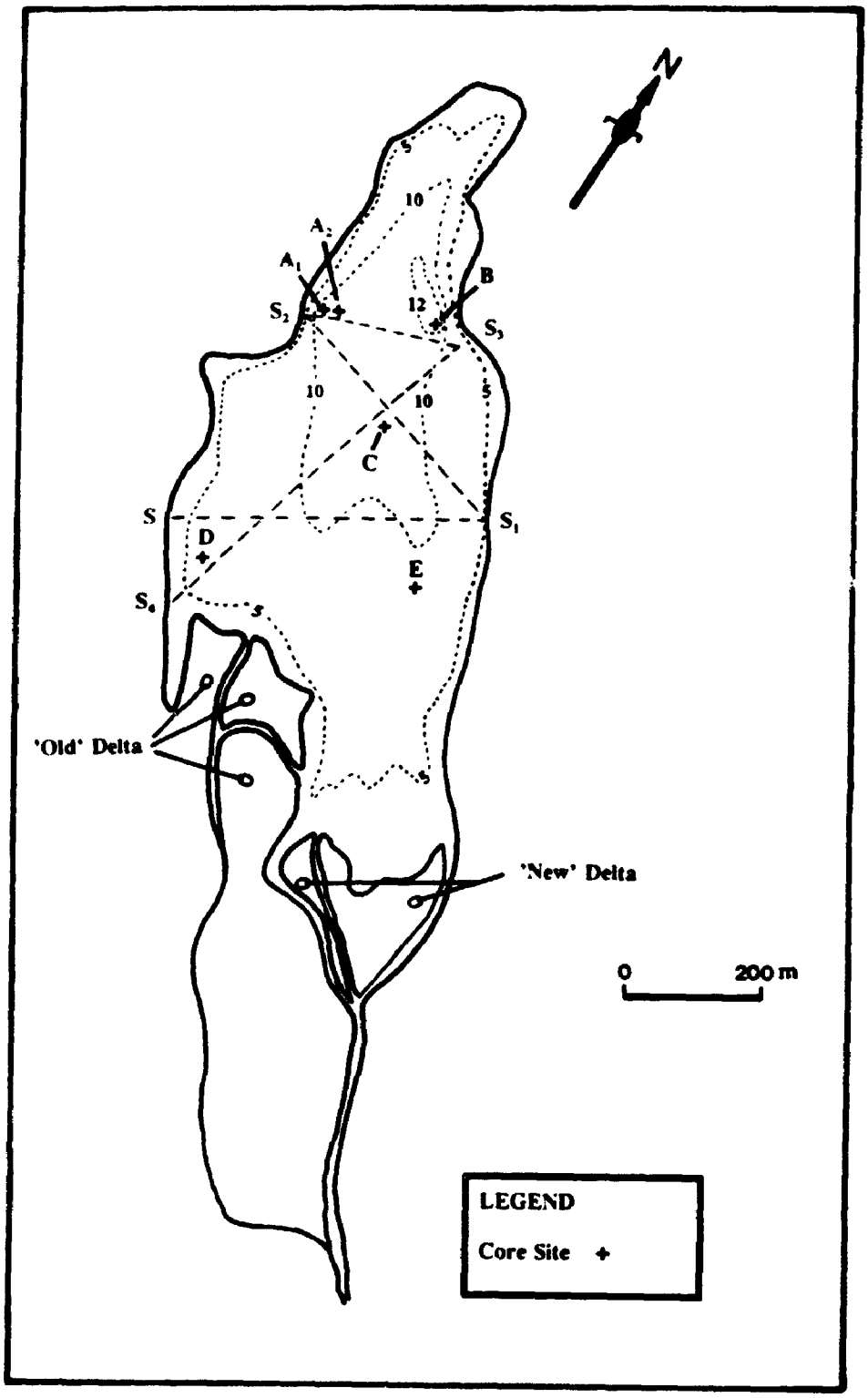

Figure 5.7 **SILVER LAKE: Bathymetry and Core Sites (Seismic profile S-S_4 shown in Figure 5.8, depth in metres)**

Unit 4 [5Y 2/1], 0.20 m thick, appears to be similar in composition to *Unit 2*, possibly with more sand-sized particles. Both upper and lower contacts appear to be deformed, but the unit otherwise seems to be structureless.

Unit 6 [5Y 2/1] is 0.45 m thick. The upper contact forms the lake bed. The unit appears to possess similar texture and structure to *Unit 4*.

5.4.2.2. Section A2: (49°19.020'N, 121°24.808'W)

Unit 1 [5B 6/1] is 0.02 m thick. It is composed of a compact, grey, laminated mud with rare, subrounded dropstones. All dropstones are intermediate argillite, some appear to possess fine striae. There is no apparent lower contact and the upper one seems to be erosional.

Unit 2 [5YR 3/1] is 0.28 m thick. It is composed of a non-compacted, structureless gyttja consisting mainly of fine-grained organic debris and mud. The upper contact appears to be deformed.

Units 3 and 5 are 0.05 m and 0.07 m thick respectively. They are composed of a non-compacted, deformed layer of fine- and coarse-grained organics. Both upper and lower contacts appear to be deformed.

Unit 4 [5Y 2/1], 0.20 m thick, appears to be similar in composition to *Unit 2*, possibly with more sand-sized particles. Both upper and lower contacts appear to be deformed, but the unit otherwise seems to be structureless.

Unit 6 [5Y 2/1] is 0.48 m thick. The upper contact forms the water-sediment interface. The unit appears to be similar to *Unit 4*.

5.4.2.3. Section B: (49°19.081'N, 121°24.705'W)

Unit 1 [5GY 4/1] is 0.07 m thick. It is composed of a non-compacted, structureless gyttja consisting mainly of fine-grained organic debris and silt-sized sediment. There is no visible lower contact, and the upper one appears to be conformable.

Unit 2 [5G 4/1], 0.13 m thick, is composed of interbedded organics (mainly fine-grained organics) and non-compacted, massive mud. There are thirteen visible beds of equal thickness (approximately 0.01 m). The upper contact appears to be deformed, and the uppermost mud interbed appears to possess some diapiric structures.

Units 3, 5, 7, 9, 11 and 13 are 0.20 m, 0.01 m, 0.01 m, 0.03 m, 0.04 m and 0.01 m thick, respectively. They are composed of a non-compacted, deformed layer of fine- and coarse-grained organics. Both upper and lower contacts appear to be deformed.

Unit 4 [5GY 3/1] 0.15 m thick, *Unit 6* [5B 3/1] 0.14 m thick, *Unit 8* [5B 4/1] 0.04 m thick, *Unit 10* [5YR 4/1] 0.07 m thick, *Unit 12* [5Y 4/1] 0.12 m thick, *Unit 14* [5YR 4/1] 0.18 m thick, and *Unit 16* [5Y 4/1] 0.11 m thick, appear to be similar in texture. They are composed of a non-compacted, structureless gyttja consisting mainly of fine-grained organic debris and silt- or clay-sized sediment. *Units 4 and 6* have a higher percentage of clay-sized fraction. *Unit 12* has no clay-sized fraction. The upper and lower contacts appear to be deformed.

Units 15 and 17 [5B 7/1], are both about 0.05 m thick. They are both composed of a compact, contorted, fine laminated mud. Laminae are

approximately 0.005 m in thickness. The upper and lower contacts seem to be deformed.

Unit 18 [5YR 3/1] is 0.09 m thick. It is composed of a non-compacted, structureless gyttja which appears to consist mainly of fine-grained organic debris and silt-sized particles. The lower contact appears to be deformed, and the upper contact is formed by the water-sediment interface.

5.4.2.4. Section C: (49°18.857'N, 121°24.597'W)

Unit 1 [5G 3/1], 0.20 m thick, is composed of a non-compacted, structureless gyttja which appears to consist mainly of fine-grained organic debris and silt- and clay-sized sediment. There appears to be no lower contact and the upper one seems to be deformed.

Unit 2 is about 0.09 m thick. It comprises a non-compacted, deformed layer of mainly fine-grained organic debris. Both upper and lower contacts appear to be deformed.

Unit 3 [Upper - 5G 5/1, Lower - 5G 4/1], 0.10 m thick, is composed of a non-compacted, structureless gyttja which appears to consist mainly of fine-grained organic debris and silt-sized sediment, there is no clay. The upper contact appears to be conformable.

Units 4, 6, 8, 10, 12 and 14 are composed of a non-compacted, deformed layer of mainly fine- and coarse-grained organic debris. Both upper and lower contacts appear to be conformable. They are 0.04 m, 0.05 m, 0.02 m, 0.01 m, 0.01 m and 0.01 m thick respectively.

Unit 5 [5GY 6/1] 0.02 m thick, *Unit 7* [5GY 5/1] 0.03 m thick, *Unit 9* [5G 4/1] 0.09 m thick, *Unit 11* [5GY 5/1] 0.08 m thick, and *Unit 13* [5G 5/1] 0.08 m thick, appear to be similar in texture. They are composed of a non-compacted, structureless gyttja which appears to consist mainly of fine-grained organic debris and silt-sized sediment. The upper and lower contacts appear to be conformable. *Unit 9*, the thickest, appears to have a significantly higher proportion of clay-sized particles than other units.

Unit 15 [5B 7/1] attains a maximum thickness of 0.03 m. It is composed of a compact, contorted, finely laminated mud. Laminae are approximately 0.005 m in thickness. The upper and lower contacts with organic units appear to be conformable.

Unit 16 is approximately 0.11 m thick. It comprises a compact, deformed layer of fine- and coarse-grained organic debris with some fine mud. The upper contact appears to be deformed, the lower, conformable.

Unit 17 [5B 7/1], is 0.06 m thick. It is composed of a compact, contorted, finely laminated mud. Laminae are approximately 0.005 m in thickness. The upper and lower contacts seem to be deformed.

Unit 18 [5GY 4/1], 0.19 m thick, is composed of a non-compacted, structureless gyttja which appears to consist mainly of fine-grained organic debris and silt-sized sediment. The unit appears to fine upwards. Both upper and lower contacts appear to be deformed.

Unit 19 [5GY 3/1] is about 0.09 m thick. It is composed of interbedded organics (coarse- and fine-grained organics) and non-compacted, massive mud.

Each interbed is approximately 0.005 m in thickness. A mud interbed forms the basal contact, and a thicker (0.01 m) organic layer, the upper one. The lower contact appears to be deformed, the upper one is conformable.

Unit 20 [5YR 3/1], 0.09 m thick, is composed of a non-compacted, structureless gyttja which appears to consist mainly of coarse-grained organic debris and sand- and silt-sized particles. The lower contact appears to be conformable, and the upper contact forms the water-sediment interface on the lake bed.

5.4.2.5. Section D: (49°18.745'N, 121°24.777'W)

Unit 1, 0.42 m thick, is composed of a compact layer of mainly coarse-grained organic debris. There is no apparent lower contact and the upper appears to be conformable.

Units 2 and 4 [5YR 1/1] are 0.05 m and 0.06 m thick respectively. They are composed of a non-compacted, horizontally stratified sandy-silt which appears to fine upward. Some fine-grained organics are visible in the upper parts of each unit, but separated from the overlying organic unit by silt. The upper and lower contacts appear to be conformable.

Units 3, 5, 7, 9, 11, 13 and 15 are composed of a non-compacted layer of mainly fine- and coarse-grained organic debris. Both upper and lower contacts appear to be conformable. They are 0.01 m, 0.01 m, 0.02 m, 0.04 m, 0.02 m, 0.01 m and 0.01 m thick respectively.

Unit 6 [5G 3/1] 0.05 m thick, *Unit 8* [5G 3/1] 0.04 m thick, *Unit 10* [5GY 4/1] 0.04 m thick, *Unit 12* [5GY 5/1] 0.03 m thick, *Unit 14* [5G 5/1] 0.01 m thick, and *Unit 16* [5GY 4/1] 0.20 m thick, appear to be similar in texture. They are composed of a non-compacted, structureless gyttja which appears to consist mainly of fine-grained organic debris, sand- and silt-sized sediment. The upper and lower contacts appear to be conformable.

Unit 17 [5B 6/1] attains a maximum thickness of 0.01 m. It is composed of a compact, laminated silt. Laminae are approximately 0.002 m in thickness, and three of the middle laminae appear to have some contortions. The upper and lower contacts appear to be conformable.

Units 18 and 20 [5Y 7/1] are 0.05 m and 0.03 m thick, respectively. They consist of a non-compacted, massive silty-sand. There is no clay present and the two units are separated by interbedded organics and laminated silt. Textures of both units appear to be similar and they fine upwards. There are no visible deformation structures. Upper and lower contacts appear to be conformable.

Unit 19 is approximately 0.04 m thick. It consists of interbedded fine- and coarse-grained organic debris with a compact, laminated silt. The latter appears to be similar in texture to *Unit 17*, and has the same Munsell colour. Beds are approximately 0.005 m thick and laminae are about 0.002 m in thickness. The upper and lower contacts appear to be conformable.

Unit 21 [5YR 3/1], 0.07 m thick, is composed of a non-compacted, structureless gyttja which appears to consist mainly of coarse-grained organic debris and sand- and silt-sized particles. The lower contact appears to be

conformable, and the upper contact forms the water-sediment interface on the lake bed.

5.4.2.6. Section E: (49°18.749'N, 121°24.524'W)

Unit 1 [5Y 5/1] is approximately 0.09 m thick. It consists of a non-compacted, horizontally stratified sandy-silt which appears to fine upward. In the upper part of the unit, it seems to be mainly composed of silty clay which appears to form a conformable upper contact with the overlying gyttja. There is no apparent lower contact.

Unit 2 [5G 3/1], 0.27 m thick, is composed of a non-compacted, structureless gyttja which appears to consist mainly of fine-grained organic debris and silt-sized sediment. The upper and lower contacts appear to be conformable.

Unit 3 [5B 7/1] attains a maximum thickness of 0.04 m. It is composed of a compact, laminated silty-sand. Laminae are approximately 0.005 m in thickness, and some laminae appear to possess some contortions. The upper and lower contacts appear to be conformable.

Unit 4 [Upper - 5GY 2/1, Middle - 5GY 4/1, Lower - 5GY 3/1] is about 0.26 m thick. It consists of interbedded organics (coarse-grained) and non-compacted, massive mud. Each organic interbed is approximately 0.02 m in thickness, the mud ones are about 0.01 m. The upper interbed, a mud, appears to be the most coarse, and there is a high clay percentage in the lowest unit, also a mud interbed. There are nine mud interbeds in all. The upper and lower contacts appear to be conformable.

Unit 5 attains a maximum thickness of 0.18 m. It is composed of a non-compacted layer of coarse-grained organic debris. Both upper and lower contacts appear to be conformable.

Unit 6 [Upper - 5YR 3/1, Upper Middle - 5G 3/1, Lower Middle - 5GY 2/1, Lower - 5GY 3/1] is 0.44 m thick. The unit is composed of a non-compacted, structureless gyttja which appears to consist mainly of coarse-grained organic debris and sand- and silt-sized particles. The lower contact appears to be conformable, and the upper contact forms the water-sediment interface on the lake bed.

5.5. Interpretation of Lake Sections

5.5.1. General Comments

The sedimentary record combines deposits from both the old and new deltas. Recent domination of the sedimentary environment by the new delta is evident, particularly in sections extracted from the central part of Silver Lake (Cores C and E). Stratigraphic continuity between Cores B, C, D, and E has been satisfactorily established (Figure 5.5b), based mainly on caesium dating and radiocarbon ages together with similarities between organic, gyttja and lacustrine facies in each core. Radiocarbon and caesium data (Appendices IVb, IVc and V, Tables 5.1 and 5.2 respectively) were also used to estimate sedimentation rates before and after 1946 (this marks the commencement of major logging activity and road construction in Silverhope valley).

Laboratory No.	Site No.	^{14}C date (years BP)	Calibrated Age[1] (A.D.)
Beta-56420	Core D - *Unit 9*	590 $\pm$ 60	1320 - 1370 (1290 - 1410)
Beta-56421	Core D - *Unit 3*	800 $\pm$ 170	1240 (1030 - 1370)
Beta-61040/CAMS-5488	Core B - *Unit 13*	100 $\pm$ 60	1710 - 1910 (1680 - 1950)
Beta-61041/CAMS-5489	Core D - *Unit 19*	140 $\pm$ 60	1690 - 1930 (1660 - 1950)
Beta-61042/CAMS-5490	Core C - *Unit 16*	144.0 $\pm$ 1.1 % of modern[2]	1962 - 1972
Beta-61043	Core C - *Unit 2*	450 $\pm$ 60	1440 (1420 - 1470)

[1] Calculated from dendrocalibrated data of Stuiver and Pearson (1986). The range in parentheses represents the 95% confidence interval based on 1 standard deviation error limits of the radiocarbon age.

[2] Radiocarbon was a by-product of nuclear bomb testing which began in the 1950's. This gradually diluted natural radiocarbon to almost 200% by 1963. A range of values is given for the calibrated age because the "bomb curve" has both a rising and falling limb (J.J. Stipp, pers. comm., 1993).

Table 5.1 Silver Lake Radiocarbon Ages

Site No.	^{137}Cs Data[1]		Estimated Post-1946 Sedimentation Rates[1] (cm/yr)
	Estimated Date	Depth (cm)	
Core A	N/A	N/A	N/A
Core B	1964	27.5	0.982 ± 0.089
Core C	1964	52.5	1.750 ± 0.126
Core D	DEAD	< 10.0	NONE
Core E	1957 1964	113.0 70.5	2.957 ± 0.272 2.517 ± 1.126[2]

N.B. 'Dead' means that there was no detectable ^{137}Cs (T. Hamilton, pers. comm., 1993).
[1] See Appendix IVc and V for further details.
[2] See Section 5.5.3.

Table 5.2 Summary of Caesium-137 Data

Cores A1 and A2 are anomalous. The basal unit appears to be composed of ice-marginal lacustrine sediments, similar in particle size to Site 22 (*Unit I*) (Sections 2.2.21. and 3.2.16.), deposited in a distal environment. These are unconformably overlain by gyttja and organic debris. The location of the core site is important to the interpretation of these deposits. It is near the constricted north end of the lake, abutting the roche moutonnée which forms the western shore. It appears that the basal unit was deposited during deglaciation, and that the subrounded, striated argillite clasts were deposited contemporaneously. These clasts form 'dropstone' features in the underlying laminae (downwarping) and overlying laminae drape the obstructions. It therefore seems unlikely that the clasts were deposited later from the side of the roche moutonnée after deglaciation; but that they were probably ice-rafted. This seems to provide additional evidence of the existence of an earlier Silver Lake (Glacial Lake Silverhope) occupying this site during the glacial standstill recorded to the northwest of the lake (Section 4.3.10.). Preservation of the unit is probably fortuitous because of its location near the lee side of the roche moutonnée, and its compactness.

Upper layers of Core B appear to be considerably thinner than those of other cores following the commencement of logging practices, with the exception of Core D. This appears to be the result of both quasi-channelised scouring of the lake floor and the redirection of flow drainage along the east side of the lake in front of the new delta.

Clague and Shilts (in press) interpret this irregular, hummocky lake bed, with a relief of several metres as rockfall or rock-avalanche debris derived from slopes to the northeast. However, the linear continuity of these depressions in the lakebed appear to be indicative of underflow currents retaining some channelised flow. Whether these "quasi-channels' are threaded through rockfall material is uncertain, although the more detailed seismic and SCUBA surveys carried out in this study were unable to detect any obvious blocky debris in this area either on or immediately under the lakebed. However, individual blocks indicative of landslide activity are found at several sites in and around the lake to the south.

Core B was taken from the deepest part of the lake and water flow to the north is evident up to 3 m above the lake bed. It seems likely that the basal unit in Cores A1 and A2 was scoured by flows emanating from the old delta and draining along the west side of the lake. Redirected flows are now scouring the east side in the vicinity of Core B and rapid deposition is taking place at the site of Cores A1 and A2. Comparison with the other cores suggests that the sedimentary record in Cores A1 and A2 may be incomplete (see below).

Core D, retrieved from the proximal zone of the old delta, appears to have the oldest sedimentary record (Figure 6.5b, Appendices IVb and V). Differences between units laid down at this site and other locations indicate the expected variations in the lake-wide depositional regime, as finer sediments are deposited with increasing distance from the input source. Based on radiocarbon data and stratigraphic correlation, it appears that at approximately the same time that coarse turbidity deposits were laid down in Core D (*Units 2 and 4*), gyttja and

fine, interbedded mud and organics were deposited on the distal lake bed in Core B (*Units 1 and 2*). There are some notable variations in the depositional regime at all core sites up until the time that logging commenced in the area. In Core D, and most of Core C, units appear to be conformably laid down, whereas in Core B all possess contorted contacts. A similar situation exists in the sediments of Cores A1 and A2, and this appears to be a function of their location. Cores A1, A2 and B were all retrieved from a quasi-channelised section with unstable banks. Deformed contacts appear to be indicative of this instability.

The most notable anomalies appear to be a function of location. Core B (*Unit 3*) does not appear to correlate with any other core units and may be the result of instabilities in lakeside sediments inputting organics into a site specific location. Similarly, a unit sequence in Core D (*Units 6 - 10*) appears to correlate with a single gyttja unit in both Cores C (*Unit 1*) and B (*Unit 4*). If this correlation is correct, it is likely that the organic units (*Units 7 and 9*) are well-defined because of proximity to the fluvial source.

Two laminated silty-sand units (*Units 15 and 17*) in Cores B and C indicate that there were two periods of relatively calm lacustrine deposition following the commencement of logging. In Core D, a similar depositional sequence (*Units 17 and 19*) is visible prior to 1946 (according to caesium data - Appendices IVc and V, Table 5.2). These units are situated in the upper 0.20 m and are separated by a coarse turbidity deposit. These are not found elsewhere in the lake, but appear to correlate with organic units in Cores B (*Units 11 and 13*) and C (*Units 8 and 10*) which are separated by gyttja deposits. This suggests that the main

distributary channel on the old delta did not flow in the vicinity of Core D at this time. Furthermore, thicker units are found in Core B, which suggests that the main distributary channel may have followed the west shore of the lake (Ross Lake Fault - Section 1.2.), transferring the majority of sediment beyond the vicinity of Core C.

The turbidity deposit in Core D (*Unit 18*) may be the result of instabilities caused by channel switching. Interbedding of organics in the lower part of the upper laminated unit in Core D (*Unit 19*) suggests that some organics were laid down at this site during high flows. In addition, *Unit 19* appears to be conformably overlain by another turbidity flow deposit which may signify similar instabilities (*Unit 20*), this time possibly as a result of channel diversion at the commencement of logging activities in the area. Records indicate that Silverhope Creek flowed into Silver Lake along the west valley side at the commencement of logging activity, necessitating channel diversion to the east valley side (McCombs and Chittenden, 1990; W. Chittenden, pers. comm., 1991). Lack of detectable caesium in the upper 10 cm of sediments in Core D suggests that this sequence of events may be correct, since little or no sedimentation has occurred at this site after the early fifties (Table 5.2).

Core E, extracted from the lake just north of the new delta, consists of sediments laid down after 1946 (Figure 5.5b and Section 5.5.3.). The basal unit consists of a turbidity deposit which appears to have either flowed off the side of the old delta, or off the front of the new delta, and probably reflects the commencement of the new delta formation (based upon inferred sedimentation

rates - Table 5.1, Section 5.5.3.). *Unit 3*, a laminated silty-sand, may be an amalgam of the two units found in Cores B and C. It indicates fairly passive deposition in a lacustrine environment following the commencement of new delta growth. Proximity to the delta front probably makes this a thicker, more discrete sequence of interbeds as opposed to Cores B and C. In Core B the two corresponding units (*Units 15 and 17*) are separated by gyttja (Figure 5.5b), which may represent resedimented fines emanating from the delta front. At Core C, *Units 15 and 17* are separated by a coarse organic layer, possibly showing initial resedimentation of organic material out of a turbidity flow, with fines being redeposited near Core B.

Figure 5.6 shows that the gyttja deposits of Core E are generally coarser than any other sediments analysed, indicating the proximity of the core site to the new delta, and an increased supply of coarser material to the flow regime.

Core C is the most similar in stratigraphy to Core E. *Unit 18* appears to be a turbidity flow (Section 5.4.2.4.), which probably originated from the old delta. Similar particle size distributions are found in Core D - *Units 18 and 20* which, together with the upper units of Core D (*Units 19 and 21*), may have been resedimented on the periphery of the old delta by flows emanating from the new one. The gyttja unit in Core C (*Unit 18*) may be a mixture of these resedimented units.

Interbeds of laminated mud and organics in Core C - *Unit 19* do not appear to correlate with those in Core E - *Unit 4*, and appear to have been deposited in approximately 1989 (based upon a sedimentation rate of 1.75 cm a^{-1} - Table 5.2),

correlating with Core E - *Unit 6*. The stratigraphic difference is possibly related to core location. However, the uppermost gyttja unit of Core C (*Unit 20*) has similar qualities to those in Cores B and E.

Cores A1 and A2 can be stratigraphically correlated with each other, but their sediment record differs from other cores. It is assumed that A1 and A2 deposits relate to post-1946 sedimentation because of the inferred change in quasi-channelised flow at the lake bed from west to east sides of the lake. This is less evident in seismic data (Figure 5.8), but can be observed by comparison between previous bathymetric data (Figure 5.9) and Figure 5.7. These data suggest that the deepest part of the lake is now nearer to the east bank. Readjustment in the lake bed between these two sites may have been induced by lake bed instabilities and oversteepening of the western channel. All contacts in Cores A1 and A2 are contorted, but there are no obvious signs of turbidity flow, except the slight offsetting of units between each core. This may simply be a function of different unit thickness on the lake slope, although Core A2 was extracted from a site to the east of Core A1, nearer to the possible source of turbidity flows and may explain differences in thickness. Some, or all, of the post-1946 sediments in these cores are therefore probably resedimented lake floor deposits and cannot be correlated with units from other cores.

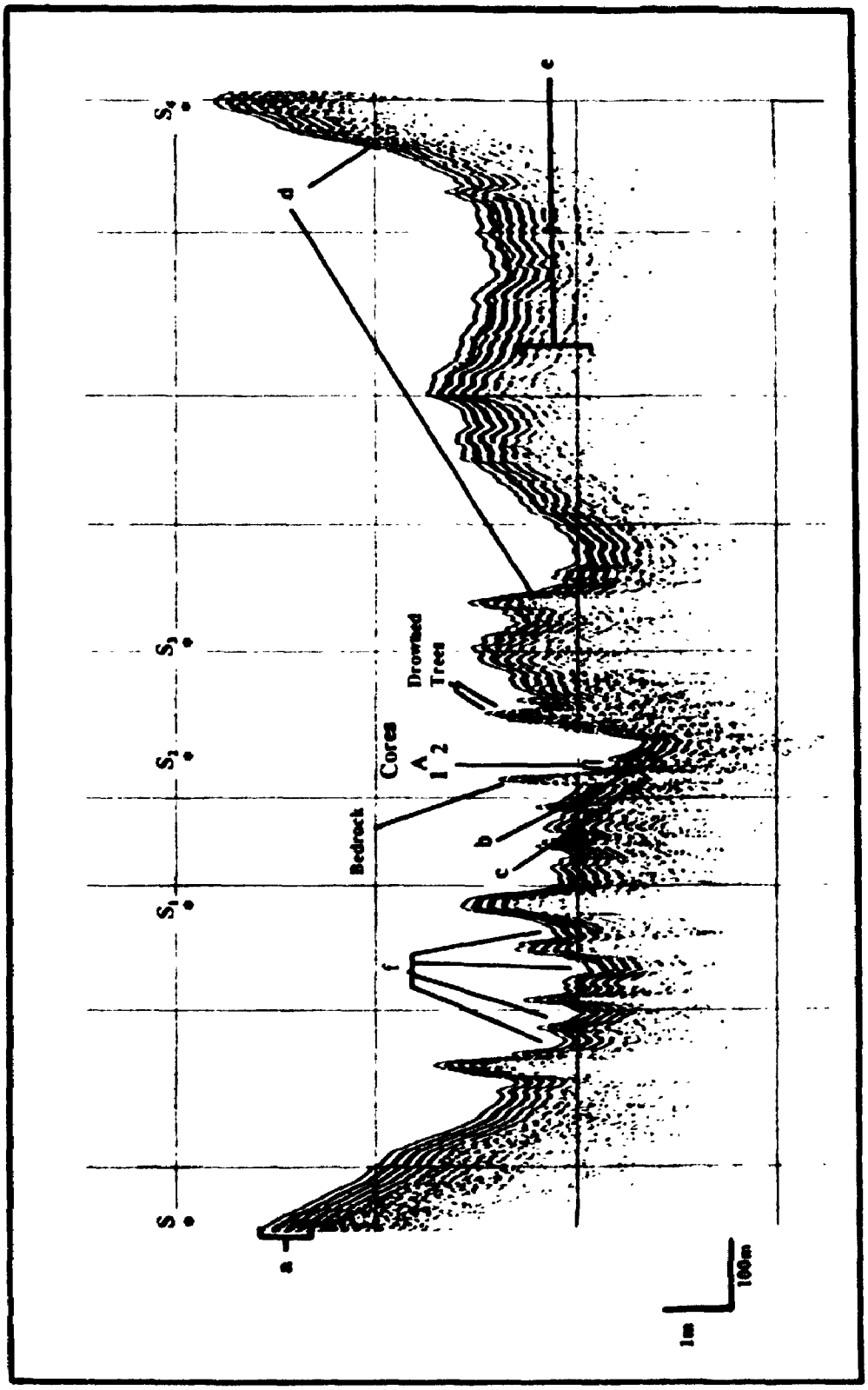

Figure 8.8 SILVER LAKE: Subbottom Acoustic Profile (3.5 kHz; Survey line in Figure 8.7, S-S$_4$)

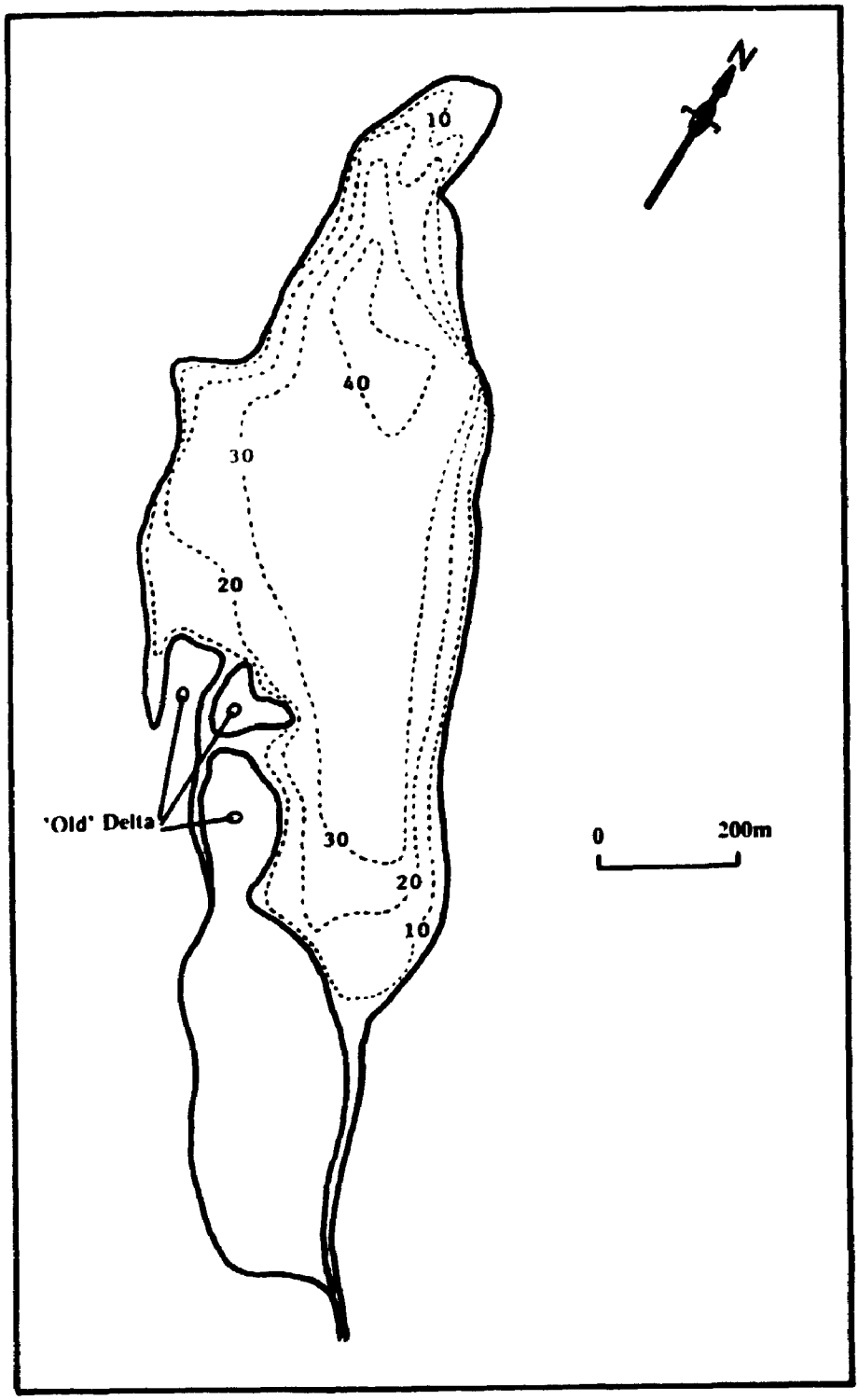

Figure 5.9 SILVER LAKE: 1976 Bathymetric Map (modified after Anon, 1975) (Depth in ft.)

5.5.2. Radiocarbon Ages

Radiocarbon data and calibrated ages are detailed in Table 5.1. Where necessary, brief reference is made to caesium dates, but they are discussed in detail in Section 5.5.3.

There appear to be no anomalous ages in the stratigraphic sequence which suggests that the carbon record is relatively undisturbed. Furthermore, the overlap between caesium and radiocarbon data in Core C (*Unit 16*) and the inferred stratigraphic continuity between these data in Cores B and D, tends to confirm this uniformity.

Clague and Shilts (in press) obtained radiocarbon data from two drowned trees (one by the west bank about midway down the lake, the other at the southeast end submerged in the new delta) in the lake. The results produce a range of ages (890 $\pm$ 60 - GSC-5444, 1010 $\pm$ 100 - GSC-5204) based on calendric ages (using Stuiver and Pearson, 1986; taking into account 2 standard deviation error limits as opposed to one in this study), from about 903 and 1223 A.D., with an overlap between 1033 and 1163 A.D. The oldest radiocarbon age obtained in this study from Core D (*Unit 3*) was 800 $\pm$ 170 (Table 5.1). This corresponds to a calendric age of 1240 (1030 - 1370), which overlaps with both of the ages detailed by Clague and Shilts (in press), although it may be slightly younger.

The base of Core D is marked by a thick (0.42 m) coarse-grained organic unit which might indicate the landslide-damming event discussed by Clague and Shilts (in press). Based on a mean calibrated calendric age of 1100 A.D. for their two radiocarbon ages (and an estimated sedimentation rate between 0.16 and 0.26

cm a^{-1} (Table 5.3) and assuming an age of 1240 A.D. (see below), this would place the event at an additional depth of between 0.22 and 0.37 m, or 0.96 - 1.11 m of total core length (assuming a top unit depth of 0.74 m for Core D - *Unit 3*). Sedimentation rate appears to increase with age in Core D, and it is inferred that the upper estimate of 1.11 m is more appropriate for this calculation. These calculations place *Unit 1* well within the age range of the landslide-damming event recorded by Clague and Shilts (in press); but they also indicate that this unit may be older and perhaps related to paleoseismic-generated mass movement activity. Therefore, Silver Lake may have been coeval with major seismic activity recorded in the Seattle area about 1100 years ago. It seems likely that Core D (*Unit 1*) represents the landslide-damming event, thus giving an almost complete sedimentary record for the lake.

A combination of stratigraphic relationships and calibrated ages has been used to estimate sedimentation rates (Table 5.3). Excluding the data from Core C (*Units 10-16*), since this is largely a transitional sedimentation rate spanning the 1946 period, estimated sedimentation rates appear to be vary between 0.07 and 0.26 cm a^{-1}. However, inclusion of a one standard deviation error limit extends the range from 0.06 to 21.0 cm a^{-1}. The upper limit is caused by an overlap between standard deviation error limits for radiocarbon ages recorded in Core D (*Units 3 and 9*). This suggests that deposition might have occurred over one year, or that mixing, contamination or delayed input of older carbon could have taken place.

In Cores B and C, estimated sedimentation rates prior to 1946 between calibrated ages and stratigraphic correlations, excluding the inferred match-up

Core Depth[1] (m)	Calibrated Age[2] (A.D.)	Estimated Sedimentation Rate[3] (cm/yr)
Core B (*Unit 13*): 0.48[t]	1710 - 1910 (1680-1960)	*Units 2-13*: 0.14 - 0.20 (0.10 - 0.30)
Core B (*Unit 5*): 0.945	1440 (1420-1470)	*Units 5-13*: 0.10 - 0.17 (0.09 - 0.22)
Core B (*Unit 2*): 1.43[b]	1240 (1030-1370)	*Units 2-5*: 0.24 (0.11 - 0.97) inc. *Unit 3*
		0.14 (0.06 - 0.57) excl. *Unit 3*
Core C (*Unit 16*): 0.43[t]	1962 - 1972	*Units 2-16*: 0.16 - 0.17 (0.16 - 0.18)
Core C (*Unit 10*): 0.855	1690 - 1930 (1660-1960)	*Units 10-16*: 0.15 - 1.34 (0.14 - 3.64)
Core C (*Unit 2*): 1.30[b]	1440 (1420-1470)	*Units 2-10*: 0.09 - 0.18 (0.08 - 0.23)
Core D (*Unit 19*): 0.10[t]	1690 - 1930 (1660-1960)	*Units 3-19*: 0.09 - 0.14 (0.07 - 0.18)
Core D (*Unit 9*): 0.64	1320 - 1370 (1290-1410)	*Units 9-19*: 0.07 - 0.14 (0.07 - 0.18)
Core D (*Unit 3*): 0.75[b]	1240 (1030-1370)	*Units 3-9*: 0.16 - 0.26 (0.06 - 21.0)

[1] To simplify calculations, estimated sedimentation rates are based on maximum radiocarbon-aged core lengths (from the base of the oldest unit (b) in which a radiocarbon aged sample is located, to the top of the youngest (t) in which a radiocarbon aged sample is located). Approximate ages for units outside these core lengths are based on the estimated sedimentation rates in the table. In the case of Core B, an estimated sedimentation rate has been based upon the inferred stratigraphic relationship between units in Cores B (*Units 5 and 2*, middle and base depths respectively), C (*Unit 2*) and D (*Unit 3*). Core B (*Unit 2*) is correlated with Core D (*Unit 3*) based on the presence of organics which are not found in Core C (*Unit 1*). In Core C, an additional rate has been calculated based on the stratigraphic correlation between Unit 10 (middle value) and Core D (*Unit 19*). In Core D, the middle value for *Unit 9* has been used to estimate two separate rates.

[2] See Table 5.2 for details about radiocarbon and calibrated ages.

[3] Estimates are based on inferred stratigraphic correlations (Figure 5.5b) and radiocarbon ages (Table 5.1). Estimates in parentheses are based on the one standard deviation range of calibrated ages, also in parentheses - column 2. In the text, ranges of estimated sedimentation rate have been narrowed, and explanations are given in the relevant discussion.

Table 5.3 Estimated Sedimentation Rates Based on Radiocarbon Ages

between Core B (*Unit 2*) and Core D (*Unit 3*) (Beta-56421: 800 $\pm$ 170 years BP), fall between 0.09 and 0.18 (0.08 - 0.23) cm a^{-1}. Inclusion of Core B (*Unit 2*) extends the upper limit to 0.24 (0.97) cm a^{-1}, however this includes an anomalous organic unit (*Unit 3*) absent in other cores. Without *Unit 3*, the rate becomes 0.14 (0.57) cm a^{-1}. These rates suggest a reasonably uniform sedimentation rate between about 0.09 and 0.18 cm a^{-1}. The large one standard deviation error limit for Beta-56421 is a result of small sample size, but bearing in mind the similarity in estimated sedimentation rates throughout the pre-1946 record, it is suggested that calibrated age of 1240 A.D. is a good approximation for the radiocarbon data.

Assuming that the estimated sedimentation rate in the lower units of Core B was approximately 0.14 cm a^{-1}, the corresponding rate in Core D still appears to be higher (Table 5.3: 0.16 - 0.26 cm a^{-1}). This is probably a function of two variables: proximity to the fluvial input point and delta growth, and a lag response to landslide-damming.

No caesium is recorded in the upper units of Core D (Section 5.5.3.), and it has been inferred that *Unit 20* may have been deposited as a result of channel diversion following the commencement of logging. It therefore seems probable that *Units 20 and 21* were laid down prior to 1953-1954 (Appendix IVc). Stratigraphic continuity between Core D (*Unit 19*), Core C (*Unit 10*) and Core B (*Unit 13*) has been inferred and appears to place the calibrated ages for Beta-61040/CAMS-5488 (1710 - 1910) and Beta-61041/CAMS-5489 (1690 - 1930) near the upper limit (less than the maximum one standard deviation maximum error). This assumption means that estimated sedimentation rates based on these ages are at

the upper end of the cited range (Table 5.3). Therefore, higher sedimentation rates are found in Cores B (0.17 cm a^{-1}) and C (0.18 cm a^{-1}) than in Core D (0.14 cm a^{-1}). This suggests that maximum deposition was taking place in the vicinity of Core C, and that the delta elongation had extended well beyond Core D.

Assuming both a maximum calibrated age range of 1910-1930 for Beta-61040/CAMS-5488 and Beta-61041/CAMS-5489 and stratigraphic correlation with Core C (*Unit 10*), these indicate that rapid sedimentation probably occurred between *Units 10 and 16*. Caesium data for Core C place an estimated age of 1964 between core depths of 0.49 and 0.56 m (*Units 15 and 16*). Furthermore, a radiocarbon age of 1962 - 1972 (Beta-61042/CAMS-5490) based on the "bomb curve" (J.J. Stipp, pers. comm., 1993) was obtained from wood at a depth of 0.52 m (*Unit 16*). The earlier radiocarbon age, 1962, appears to be more realistic based upon the rising limb of the bomb curve and the caesium date. This gives maximum sedimentation of 0.43 m over a 32 - 52 year time period, or 0.83 - 1.34 cm a^{-1}. The time period covered by the radiocarbon ages is a transitional period from immediately prior to logging to post-1946 sedimentation. However, these radiocarbon data alone suggest that there has been a dramatic increase in sedimentation rates at Core C over this period.

Results from Core B tend to confirm those from Cores C and D. Assuming even a maximum estimated sedimentation rate (note discussion of Beta-56421 above and its relevance to Ccre B) over the core length from *Units 2-13* of 0.20 cm a^{-1}, this is only slightly higher than those recorded in Cores C and D, and incorporates the anomalous *Unit 3* in the calculations.

Based upon six radiocarbon ages, inferred stratigraphic relationships and correlations with caesium data; estimated sedimentation rates prior to about 1930 (and no more recent that 1946) vary from about 0.09 to 0.26 cm a^{-1}. More specifically, in Core D the rates appear to have declined from a high in the region of 0.26 cm a^{-1} or greater following landslide-damming, to about 0.14 cm a^{-1} in about 1930. In Core C, rates appear to have been about 0.18 cm a^{-1}, with an increase over a transitional period (immediately pre- and post-1946) from about 1910/1930 - 1962 of between approximately 5-7 times or 0.83 - 1.34 cm a^{-1}. In Core B, estimated sedimentation rates appear to decline from the base upward, which largely seems to be a feature of an anomalous unit possibly caused by lakeside slumping. The norm seems to be in the region of 0.17 to 0.20 cm a^{-1}. No radiocarbon ages are available for Cores A1, A2 and E.

5.5.3. Caesium Dating

The sedimentation rate of recently deposited sediments can be measured using the radionuclide ^{137}Cs, and this technique has proved useful in the reassessment of recent sedimentation rates in Alaska (Stihler *et al.*, 1992). However, as a dating technique it has several potential problems (Appendix IVc), but still appears to yield good comparative results (Ritchie *et al.*, 1973; Stihler *et al.*, 1992). The results of caesium dating in Silver Lake are detailed in Appendices IVc and V, and are summarised in Table 5.2.

Post-1946 sediments appear to be preserved in all cores (it seems likely that Cores A1 and A2 are mainly composed of sediments reworked since 1946 -

but caesium dating was not possible due to poor sample preservation). Core E has the best post-1946 record. Conformable contacts tend to suggest that a complete record of post-1946 sedimentation has been preserved following the diversion of Silverhope Creek from the west to the east bank.

In 1946, the Core E site was about 0.6 km north of the new delta location and it appears to have received only organics and reworked lacustrine and fluvial deposits. If a sedimentation rate of 2.957 cm a^{-1} is assumed (Table 5.2), this would place the timing of the deposition of the base of the lowest unit somewhere between 1947 and 1951. At the slower rate of 2.517 cm a^{-1} the estimate is from 1941-1944 (an error of $\pm$ 1.125 cm a^{-1} is largely caused by poor caesium preservation in an organic interbed for which only a small sample size of fine sand could be analysed. Assuming continuity of deposition, which seems likely, errors are reduced to about $\pm$ 0.25 cm a^{-1}). A mean rate of about 2.75 cm a^{-1} yields a date of 1946 (Figure 5.5b). It seems reasonable to assume that *Unit I* probably represents the first depositional phase following creek diversion, although the complete unit may not be preserved in the core. If this is the case, then upon initial observations there appears to have been an increase in the sedimentation rate of between 10 to 20 times (based on a pre-1946 rate of between 0.14 - 0.26 cm a^{-1}, and a post-1946 rate of 2.75 cm a^{-1}).

Clear-cut logging on the valley floor immediately south of Silver Lake commenced in about 1955. Prior to this date, logging activities had been centred farther south along the valley in an attempt to clear all available timber in and around the newly-formed Ross Lake (McCombs and Chittenden, 1990). Logging

activity advanced northward, back up the road until timber supplies were exhausted by the end of 1955. Depending upon the interpretation of caesium data (2.517 or 2.957 cm a^{-1}), the upper contact of *Unit 2* appears to represent a time period between about 1955 and 1961, although it must be later than 1957 because of an underlying caesium date. The interpretation of the conformable change to laminated mud is difficult, but it may represent a delayed release of fines into Silverhope Creek following clear-cut logging. Subsequent deposition of interbeds of fines and organics may possibly represent the delayed impact of logging in close proximity to the lake.

A generally high sedimentation rate appears to be a reflection of the proximal position of the core site to the new delta. However, it should be borne in mind that the Core E site is currently relatively farther away from the new delta than core D is from the old one. At the time of lake formation, the core D site would have been farther from the old delta front than the present site for Core E and it therefore appears to represent a good average sedimentation rate for the old delta. This also suggests that Core E appears to be the best representative site for new delta sedimentation rates, as opposed to Core C.

Core C has a less complete caesium record, and sufficient grain size variation to complicate the interpretation and correlation to the fallout record. The measurements are as high as is typically measured for the 1963-1964 peak of fallout, and the lower samples all have higher concentrations than Core E. This is probably due to finer grain size and less dilution by inert sand (T. Hamilton, pers. comm., 1993). The highest readings appear in a sample taken between 0.49

and 0.56 m depth and a mid-point - 0.525 m is assumed to represent the 1964 peak, yielding a sedimentation rate of approximately 1.750 cm a^{-1} (Appendices IVc and V, Table 5.2). This correlates well with a radiocarbon age, taken to be 1962, at a depth of 0.52 m (Section 5.5.2.).

The highest values of caesium activity recorded in Core B (*Unit 15*) fall within the maximum values recorded in other fine grained samples and is therefore inferred to represent the 1964 peak. This suggests a sedimentation rate of approximately 0.982 cm a^{-1} (Appendices IVc and V, Table 5.2) and shows that sedimentation rates tend to decrease to the north-northwest away from the new delta. Furthermore, the maximum value for each core increases in a similar manner (Appendix IVb). This can be interpreted as, i) ^{137}Cs increasing as sedimentation decreases due to a higher proportion of fallout and less dilution effect, and ii) ^{137}Cs increases as mean grain size decreases due to less dilution by inert sand.

Post-1964 stratigraphic relationships between cores appear to be a function of distance from the fluvial input. Core E appears to comprise two thick units, one organic (*Unit 5*), the other gyttja (*Unit 6*). At a greater distance, Core C is separated into three units with interbedded organics and muds (*Unit 19*) suggestive of channel switching and by-passing of the core site. Both cores appear to have complete records in their upper units. In Core B the units appear to indicate a slower rate of deposition with more compressed units, although recent changes in lake depth in the vicinity of Cores A1, A2 and B suggest that scour has taken place. A lack of clear stratigraphic correlation between Core C

(*Units 19 and 29*) and upper units in Core B may be indicative of the extent of recent scour.

Comparison of caesium dating with radiocarbon ages suggests that initial sedimentation rates in Silver Lake following landslide-damming were higher in Core D than elsewhere. However, it appears that this became more uniform with time. Post-1946 sedimentation rates appear to be non-uniform across the lake and may indicate the initiation of an additional disequilibrium within the system. Presumably this rate will also gradually decline, although the cause of the disequilibrium seems to be ongoing. With this in mind it is interesting to note that there was only a slight decline of about 8% in the rate by 1964, which is reflected in the one core, Core E, and no significant decline over the past twenty years or more. Other than an anticipated decline in rates with distant from the sediment source, sedimentation rates in other cores appear to have stayed fairly constant through time, similar to the situation found in pre-1946 cores other than Core D. However, rates appear to have increased at both Cores B and C, by about 6-10 times respectively.

These figures are less than those between Cores D (pre-1946) and E (post-1946), but indicate a similar trend, which is probably best recorded in the spatially similar locations of cores of D and E. Here the initial observations of about a 20 times increase in the sedimentation rate appear to be borne out by the caesium and radiocarbon records in other cores.

5.5.4. Discussion

Silver Lake is one of many landslide-dammed lakes in Western Canada and the Pacific Northwest (Logan and Schuster, 1991; Clague and Shilts, in press). On average the total volume of Silver Lake water is flushed about every 1.5 days (Anon, 1951). The lake is stratified (because of the existence of an underflow plume (Smith and Ashley, 1985)), but has no hypolimnion (Anon, 1975).

Clague and Shilts (in press) suggest that the "bench" which occupies the southern third of the lake (the new delta) is perhaps a remnant of a pre-830 year-old floodplain or delta. The caesium data presented above show that this "bench" has actually been laid down over the past 50 years and does not relate to a previous lake level. However, evidence from late Wisconsinan sediments (Chapter Four) and Cores A1 and A2 indicate that previous lakes were present in the basin.

One acoustic facia (Figure 5.8 - *a*) occurs throughout almost all of the lake (Sangree and Widmier, 1979), except in the vicinity of Cores A1 and A2 at the north-west part of the lake where it is less well preserved, the side walls of the lake, and on the old delta in the south-west (Figure 5.8 - *b*, - *d*). The former occurs at a site underlain by ancient glaciolacustrine sediments (Figure 5.8 - *c*). The main facia is well stratified and attains a maximum thickness of about 2.0 m in low-lying areas situated to the east side of the lake. This thickening to the east indicates that either the input of sediment plumes to the lake is sufficiently concentrated to be influenced by the Coriolis effect; or that post-1946 sedimentation has favoured the east side following channel diversion to the new

delta. Sediment input is dominated by an underflow regime and coupled with high post-1946 sedimentation rates, it appears that preferential deposition along the east side of the lake floor is a more likely explanation of lake sediment distribution (e.g. Smith *et al.*, 1982). The sedimentary record for Cores A1 and A2 discussed above (Section 5.5.1.) suggests that the upper acoustic facia at this site mainly consists of deposits resedimented by either turbidity flows or slope failure. However, resedimentation appears to have infilled the previous thalweg and not created any ridged or similar topographical features (e.g. Desloges and Gilbert, 1991). Resedimentation has created fewer and thicker interbeds of gyttja and organics, similar to the process discussed by Doig (1991). This may account for the apparent thinning at the sites of Cores A1 and A2.

In some parts of the lake acoustic returns are sufficient to indicate that interbedded sediments may exist to the depth of another metre (Figure 5.8 - *e*) beneath the main acoustic facia, but in the vicinity of Cores A1 and A2 this is not apparent. This lack of return may be indicative of a discrete area of ice marginal sediments preserved on the valley side, since the pattern suggesting deeper interbedding is soon reestablished. Lower sediments or bedrock cannot be inferred from these data.

If the ratio of bedload to suspended load is high then a steep delta front of 30-35° is expected, and although these conditions are normally expected in glacier-fed lakes (Gilbert, 1975; Pickrill and Irwin, 1983), the snowmelt dominated regime of Silverhope Creek appears to produce similar conditions. Sediment input to the lake is coarse (91.14% gravel at the sampling site upstream of Silver

Lake) and the new delta front has an angle of repose of about 32°. However, the old delta (comprised of similar, but finer material) has an angle of repose of approximately 37° which suggests that oversteepening has taken place. Both the new and old deltas are elongate in form, mainly because of distributary channel stability across the delta surface (Smith and Ashley, 1985), but in the case of the new delta, rapid sediment input is an additional influence on the rate of progradation.

Delta elongation is accentuated by a lack of wave action. Furthermore, wave action aids sediment dilution in a dominant underflow environment (Smith and Ashley, 1985). In the spring particularly, suspended sediment-rich meltwater input is much denser than lake water (high Richardson Number) which ensures that the plume retains its integrity within the lake as a discrete density current. Fine sediments are transferred out from the delta into the more distal sections of the lake and are probably responsible for infilling most of the original thalweg (c.f. Gilbert and Shaw, 1981). The structureless nature of the lake sediments suggests that there is a considerable amount of mixing at the water-bed interface which is probably caused by rapid flushing of the lake and the maintenance of several quasi-channelised drainage paths emanating from the new delta visible in the seismic data (Figure 5.8 - *f*).

A concentration of these quasi-channels near the narrow, north end of the lake appears to be responsible for the scouring reported above (Section 5.5.1.). Thicker beds, especially Core E - *Unit 6*, appear to be the result of either extended periods of strong underflow triggered by anomalously high suspended

sediment input independent of any change in discharge, or to a single event (Core C - *Unit 18*) such as bank collapse or human disturbance (Weirich, 1986).

Silver Lake has a forested mountain catchment. Recent logging activities and road construction commenced in 1946 and appear to have had a considerable effect on the sedimentation within the lake and Silverhope Creek (Section 5.7.1. and 5.7.2.). These effects are discussed below in Section 5.8. (However, it should be remembered that over the past twenty years climatic changes have resulted in a general increase in precipitation (B. Thompson, pers. comm., 1993). Increased sedimentation in Silver Lake may therefore not be solely due to clear-cut and patch-cut logging practices).

5.6. Silverhope Creek Channel Deposits

5.6.1. Introduction

Silverhope Creek drains a total area of about 320 km^2 (241 km^2 upstream from Silver Lake), and discharge is generally 1 - 2 m^3s^{-1} (Anon, 1975).

In-channel bulk samples were taken every kilometre down the length of Silverhope Creek (Figure 5.10). Sampling commenced on the Upper Silverhope Creek alluvial fan immediately downstream of the watershed between Klesilkwa River and Silverhope Creek waters. Four sites were omitted from the survey; SH1, SH8, SH9 and SH10. Site SH1, one kilometre south of the mouth of Silverhope Creek is in an area where the creek flows through an artificial channel with reinforced banks and a straightened channel. Sites SH8 - 10 are in the vicinity of Silver Lake, SH8 is located at the base of the landslide dam, SH9 is in Silver Lake,

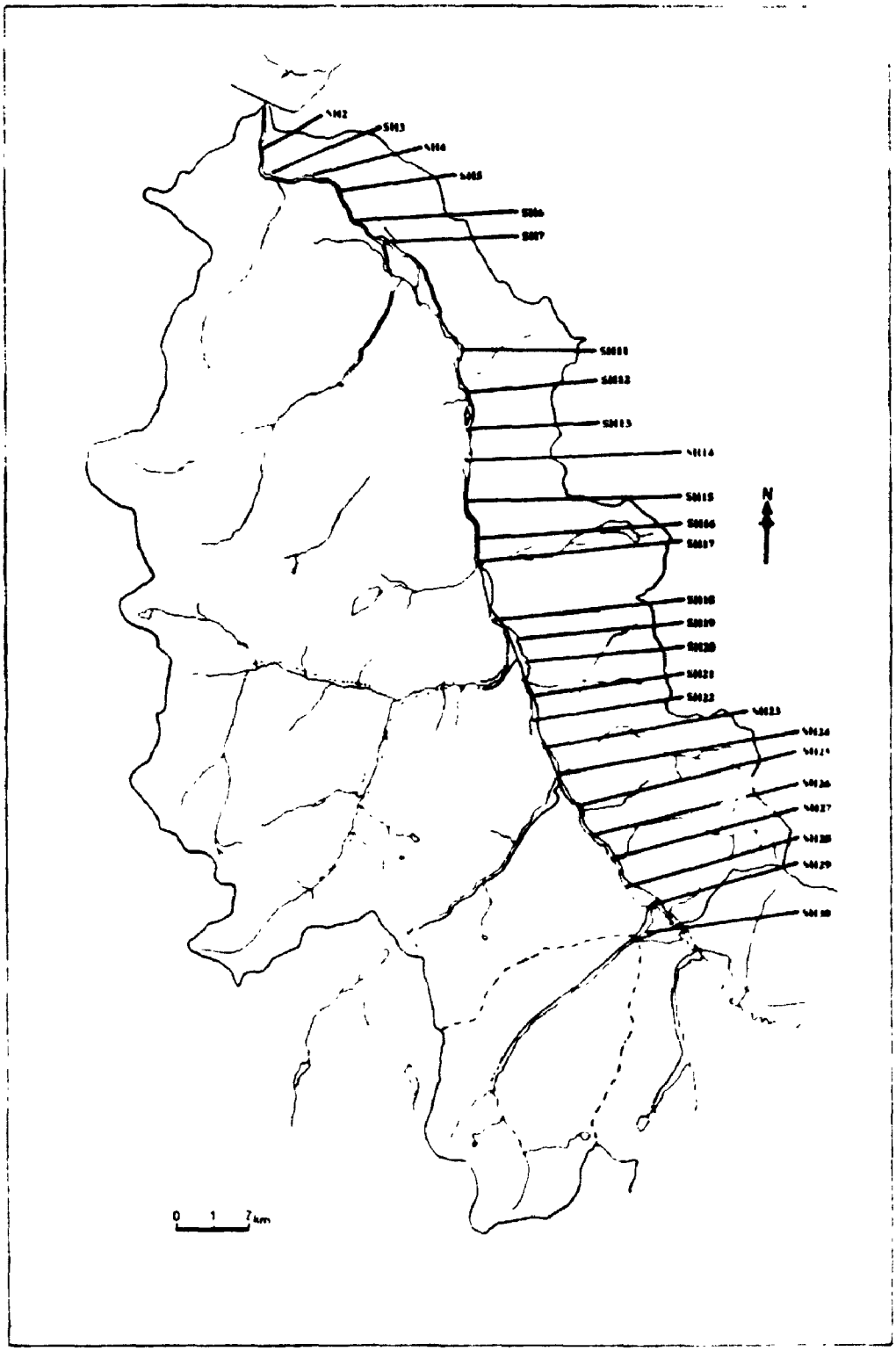

Figure 5.10 SILVERHOPE CREEK: In-Channel Gravel Sample Sites

and SH10 is on the edge of the new delta where no representative sample location could be identified.

Appendix II details the criteria for bulk sampling, sieve and hydrometer analyses, and specifies particle size data (major fraction percentages and moment statistics). Samples were taken immediately upstream of a bar head. This location is likely to feature the maximum particle size being actively transported (or as channel lag), and is a relatively uniform depositional environment along the length of the creek. This gives a reasonable consistency to the interpretation of changes in downstream bed sediment distribution. A veneer of bed sediment was removed from the channel to the depth of the largest clast. Samples were obtained by transferring sediment immediately from the bed onto tarpaulins on the bank for drying. Particle size distribution percentiles (D_{84} - coarse fraction, D_{50} - mean, and D_{16} - fine fraction) and major fraction percentages (Gravel-sand-mud and sand-silt-clay) are used to describe the downstream changes in channel deposits.

5.6.2. Downstream Changes in Particle Size Distribution

5.6.2.1. Percentiles

5.6.2.1.1. *D_{84} and D_{50}*

Fluctuations in the D_{84} and D_{50} percentiles are similar (Figure 5.11), but downstream fining is interrupted in at least two places, 10 km and 25 km from the confluence with Klesilkwa River. The D_{16} percentile has more extreme fluctuations (Figure 5.11), which appear to be superimposed on the general pattern affecting

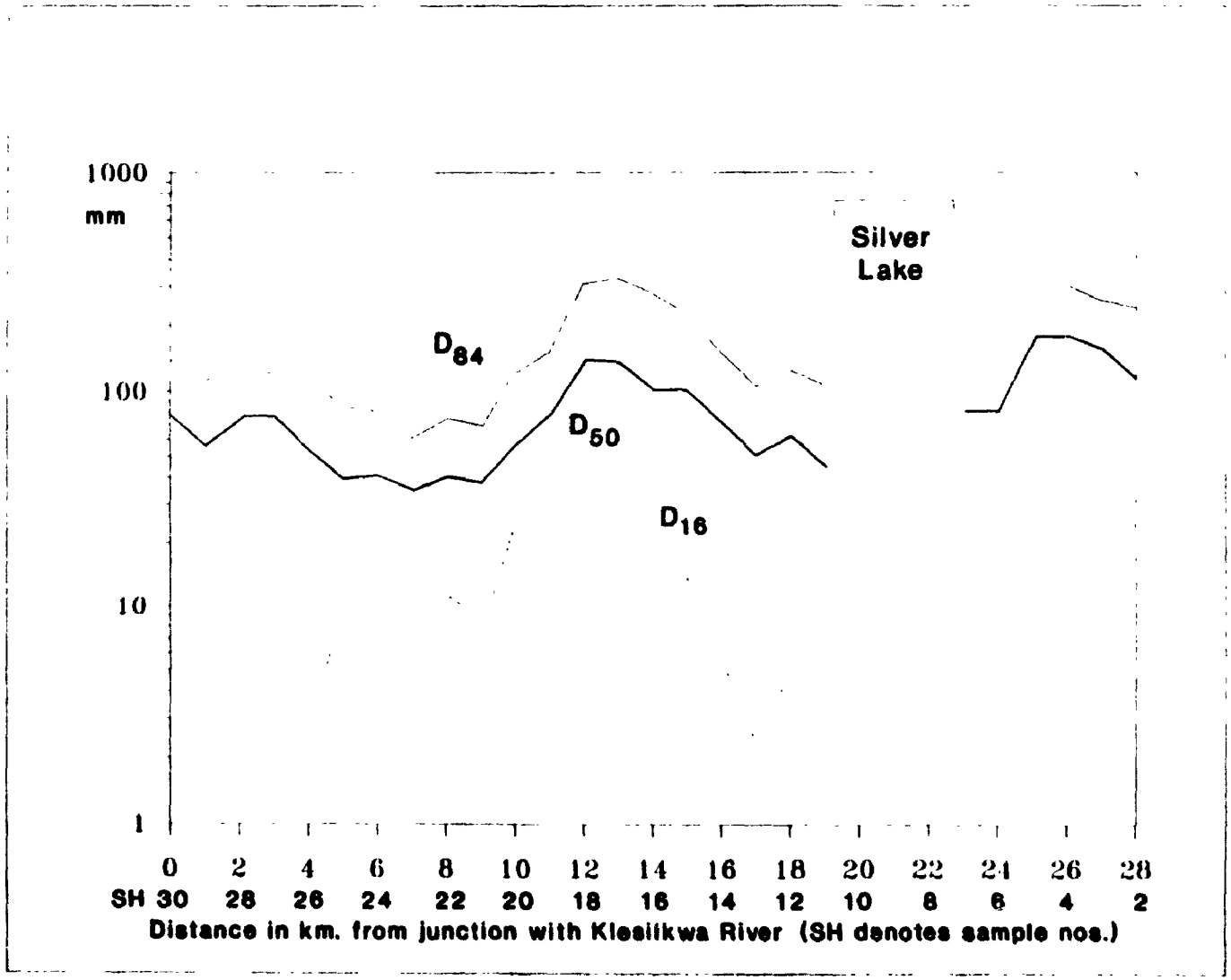

Figure 8.11 SILVERHOPE CREEK IN-CHANNEL GRAVELS: Downstream changes in moment statistics

D_{84} and D_{50}. This suggests that there may be more than one factor affecting fluctuations in downstream particle size distribution.

D_{84} and D_{50} percentiles generally decline from the confluence of Silverhope Creek and Klesilkwa River to the 10 km point. There are two minor size increases at 2 and 8 km, more noticeable in the D_{50} percentile. The former occurs at a site adjacent to the south end of the hummocky terrain deposit, the latter is situated in a marshy area of Silverhope Creek, immediately downstream of a small, ancient mass movement feature on the east valley side. More substantial increases in particle size take place between 10 and 12 km. This covers the area from a point adjacent to the mouth of Cantelon Creek and an east valley side alluvial fan (10 km) to a site immediately downstream of the present confluence between Cantelon and Silverhope Creeks (course diverted in 1985 - it used to enter upstream of the 11 km site).

Subsequent diminution in sediment size is delayed in D_{84} beyond 13 km, immediately downstream of the confluence between Swanee and Cantelon Creeks, but then continues to 19 km with only one further increase at 18 km (see below). The D_{50} percentile declines from 12 km to 19 km with minor breaks at 16 km, immediately downstream of a mass movement feature on the west valley side, and 18 km. The 18 km site is situated just downstream of the confluence between Maimen and Silverhope Creeks. At 19 km the values of both percentiles are lower than at 0 km.

North of Silver Lake, immediately downstream of the confluence between Sowerby and Silverhope Creeks (23 km), there is a distinct increase in both D_{84}

and D_{50}. Downstream increases continue to 26 km, through a sharp rise at 25 km where the valley narrows. Downstream diminution is reestablished from this point to the end of the reach, although the values of both percentiles are higher at 28 km than at 0 km.

5.6.2.1.2. *D_{16}*

Fluctuations in the D_{16} percentile are more varied. There is a general decrease in particle size between 0 and 19 km, a marked decline at 23 km, but the final value at 28 km is higher than at 0 km. Increases and decreases are equally extreme. Increases occur at 2, 5, 6, 8, 10, 11, 12, 15, 18, 19, 25 and 26 km. Sites at 2, 8, 10-12, 15, 18, and 24-26 km are identified in Section 5.6.2.1.1. The 5 km site is situated adjacent to the north edge of the hummocky terrain at a confluence between a small east side tributary and Silverhope Creek, the 6 km site is immediately downstream of the Hicks and Silverhope Creek confluence, and the 19 km site is adjacent to an alluvial fan emanating from a small east side valley between Maimen Creek and Silver Lake.

Sharp declines in D_{16} are also evident, the most extreme occurring at 4, 17, and 23 km. The 23 km location is identified in Section 5.6.2.1.1. At 4 km, the site is adjacent to the north end of the hummocky terrain, and the 17 km location is just south of the confluence between Maimen and Silverhope Creeks.

5.6.2.2. Major Fraction Percentages

5.6.2.2.1. *Introduction*

Ternary plots of gravel-sand-mud and sand-silt-clay indicate the fluctuations in the major fraction percentages (Figures 5.12 and 5.13). Variations are more evident in the gravel-sand-mud, although there are some important changes in the sand-silt-clay fractions.

5.6.2.2.2. *Gravel-Sand-Mud (Figure 5.12 and Appendix III)*

The majority of samples possess percentages between about 85-95% gravel, 5-15% sand, and 0-5% mud. The sand fraction remains reasonably stable throughout the study reach, with the main fluctuations occurring between gravel and mud. At ten sites the mud content is greater than 21%, with the gravel fraction falling as low as 45%. Mud fractions are generally higher in the study reach from 12-28 km, and fall into two groups, 12-15 km and 23-28 km. The former is located between the confluence of Cantelon and Silverhope Creeks and downstream of a mass movement feature on the west main valley side. The latter is situated between the confluence of Sowerby and Silverhope Creeks and the end of the study reach. From 12-15 km the mud percentage gradually declines, but between 23 and 28 km the trend is less clear, although the percentage does decline over the total subreach.

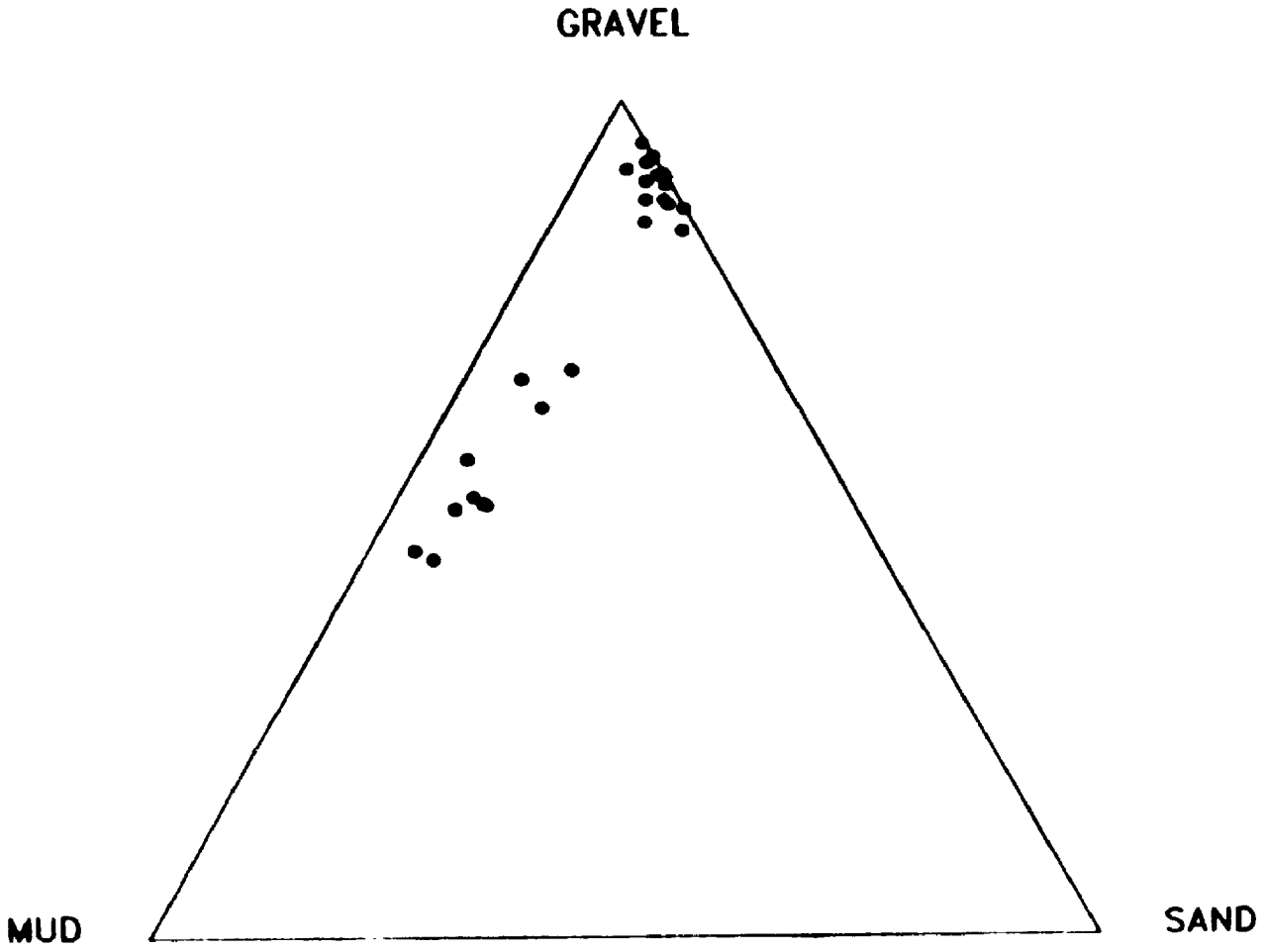

Figure 8.12 TEXTURAL TERNARY FOR WHOLE SAMPLES FROM SILVERHOPE CREEK IN-CHANNEL GRAVELS

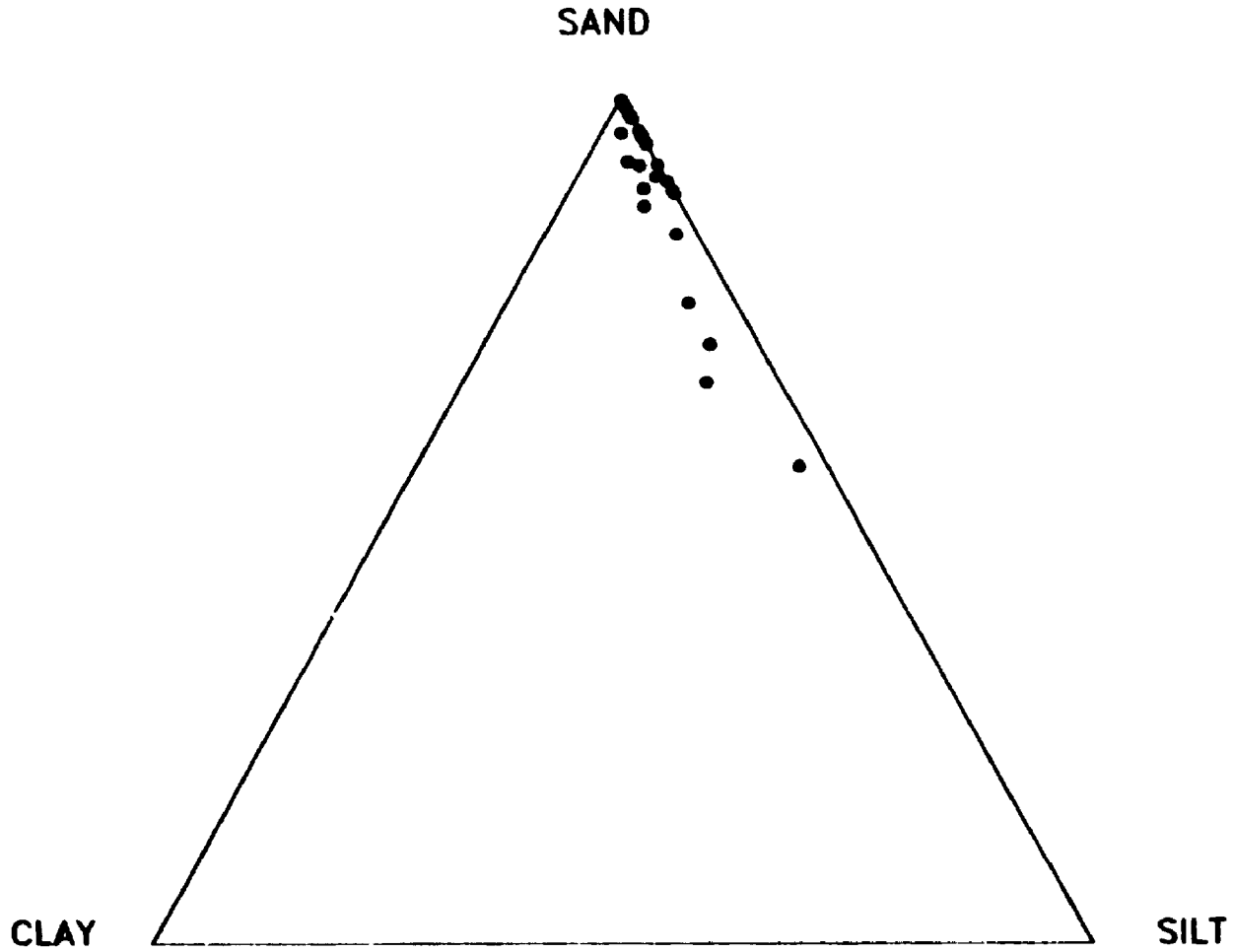

Figure 6.13 TEXTURAL TERNARY FOR MATRICES OF SAMPLES FROM SILVERHOPE CREEK IN-CHANNEL GRAVELS

5.6.2.2.3. *Sand-Silt-Clay (Figure 5.13 and Appendix III)*

Most samples have from 87-100% sand, 0-12% silt, and 0-8% clay. As opposed to the gravel-sand-mud fractions it is the middle fraction, silt, which increases at the expense of the upper one, while clay remains fairly constant. There appear to be five cases where silt is greater than 12%, and at three of these the clay fraction is equal to or greater than 5%. The five sites are located at 0, 9-11, and 16 km. At 0 km, a sample was taken on the present Upper Silverhope Creek alluvial fan immediately downstream of the confluence between Silverhope Creek and Klesilkwa River. From 9-11 km Silverhope Creek flows through a marshy area adjacent to the mouth of Cantelon Creek (5% clay fraction at 10 km, 5.2% at 9 km). At 16 km, the site is about 3 km north of the confluence between Swanee and Silverhope Creeks.

5.7. Interpretation of Silverhope Creek Channel Deposits

5.7.1. General Comments

In general, one would expect to record a downstream diminution of sediment size, and this relationship has been observed by many researchers (Yatsu, 1959; Church, 1972; Maizels, 1979; Frostick and Reid, 1980; Dawson, 1988). This is not the case in the Silverhope valley where the D_{84}, D_{50} and D_{16} all increase over the total distance studied.

D_{84}, D_{50} and D_{16} percentile size increases occur adjacent to relict glacial deposits at 2, 5 (D_{16} only - additional fine sediment input from a tributary passing through the hummocky terrain and winnowing out remnant silt), and 25 km. The

latter occurs where channel incision into glacial valley fill has removed the majority of fines. Size increases are also evident adjacent to mass movement features (8 and 15 km), alluvial fans (10 and 11 km), downstream from tributary input sites 6 (D_{16} only - the majority of coarse material possibly being removed by outburst flows during deglaciation), 12, 13, 18 and 23 km.

Size increases at 19 km occur in the D_{16} percentile only. This is adjacent to a small alluvial fan and immediately downstream of the confluence between a small unnamed east valley side creek and Silverhope Creek. Since there are no corresponding increases in D_{84} and D_{50} percentiles, it seems likely that either the material from the alluvial fan or small creek are the cause of this increase. Landslide-damming of Silver Lake (Section 5.4.1.) has caused the fluvial system to aggrade. It is possible that fines have been selectively entrained by an aggrading system, coarsening the D_{16} percentile.

Relatively large declines in D_{16} occur at three sites, one of which is associated with a relict glacial deposit (4 km), which may be an expression of the bimodality of the sediment. In addition, the area has recently been logged (1984-1986; Ministry of Forests, 1992 (MOF, 1992) and increased fines input may accentuate the bimodal distribution. At 17 km, there are no apparent features to account for the decline in D_{16}, although the clay fraction percentage dramatically increases at 16 km (from 0% at 15 km to 7.8% at 16 km). The 16 km site is adjacent to a recent log cut (1988-1989; MOF, 1992) on the east valley side, and may account for fines input at both sites.

The final site, 23 km, is associated with a significant bimodal distribution. Situated just downstream of the confluence between Sowerby and Silverhope Creeks, this site receives fines from Silver Lake, Sowerby Creek (logged 1976-1985; MOF, 1992) and repeated road construction on the adjacent highway. Coarse fractions are input from Silverhope and Sowerby Creeks. It seems likely that the majority of fines are being input by construction on the logging road which follows the river bank at this point. The road climbs steeply up the side of the landslide dam through which Silverhope Creek has incised. There is evidence of abundant runoff. Winter outbursts from Silver Lake have also provided a significant source of fines. Preferential deposition of fines at 23 and 24 km has resulted from bridge replacement on the Silver Lake campground logging road in 1992. Water ponded upstream of the construction site during relatively high spring flows, but following completion, flows declined due to waning meltwater supplies. Infiltration of fines into the coarse gravel bed structure appears to have delayed entrainment. Downstream of the construction site, increased sediment input and lower flows produced similar local conditions.

Landslide-damming of Silver Lake has caused the northern part of Silverhope Creek to adjust to a new source level, resulting in rapid incision of mass movement and relict glacial debris. This has significantly increased the size of the coarse fraction at 23 km. The interim headwaters imposed by landslide-damming has produced a second phase of downstream fining. Adjustment to the new regime is evident at 25 km, and downstream fining appears to follow a more conventional pattern from this point.

Changes in mud fraction percentages suggest that tributary input is a significant factor in the increase of fines, although this appears to only be pertinent to two major tributaries, Cantelon and Sowerby Creeks (Section 5.6.2.2.2.). Bearing in mind that both D_{84} and D_{90} increased downstream of the confluences with these creeks, it seems likely that material released by recent logging activity within these valleys (Cantelon Creek, 1980-1987, Sowerby Creek, 1981-1985; MOF, 1992) and road construction in Silverhope valley, were the principle contributors.

Fluctuations in silt-clay fractions are indicative of more subtle influences, as discussed above at the 16 km site. Upper Silverhope Creek was logged between 1986 and 1988 (MOF, 1992), but there is little slope instability and no evidence of major sediment input into the creek. It seems most likely that the high silt fraction at 0 km on the alluvial fan is indicative of a cumulative effect of fines input over a period of years during and after logging. In the absence of a brief excess of sediment supply, these fines are now being removed. From 9-11 km, silt and clay contents are high, but gradually diminish through the subreach. This appears to be the result of a coincidence in morphology and human activity. Patch-cut logging (in 1989; MOF, 1992) of the east valley side adjacent to 21 km appears to have contributed fines to a shallow-sloped section of Silverhope Creek. Excess sediment supply over flow competence has delayed downstream transport, although some downstream transfer through the area is apparent.

5.7.2. Discussion

Numerous studies have shown that the basic premise of downstream fining is too generalised. Among the key variables disrupting this trend are, past glaciations (Fahnestock, 1963; Bradley *et al.*, 1972), an aggrading or degrading system (Bradley *et al.*, 1972; Shaw and Kellerhals, 1982), tributary input (Church and Kellerhals, 1978; Kellerhals, 1982; Shaw and Kellerhals, 1982), and lithology (Church and Kellerhals, 1982). At least three of these variables, past glaciation, an aggrading or degrading system, and tributary input, appear to have a significant influence on particle size distributions in Silverhope Creek. The final variable, lithology, is an unreliable indicator in this area because of previous glacial activity. This activity introduced a wide variety of exogenic clasts which possess a form and structure related to glacial processes. Therefore it is valid to infer the influences of relict glacial activity on the acquired characteristics of downstream fining, but invalid to extend this to lithologic interpretations. Human activity appears to be locally significant, and seems to have a noticeable influence, particularly on the quality and quantity of tributary input.

For the Silverhope valley, it is convenient to discuss the relative effects of these three variables in a hierarchical framework of disequilibrium. First, past glaciation appears to have had a pervasive influence on Silverhope valley (Section 4.3.2.4.). Second, disequilibriums imposed by downstream changes in aggradation and degradation are superimposed upon the pervasive glacial disequilibrium. Third, landslide-damming of Silver Lake has imposed a general

trend towards upstream aggradation and downstream degradation from the slide site (Section 1.2.).

The scale of disequilibrium conferred by tributary input is more local than either of the others; and causes particle size fractions to both increase and decrease. Quantities of tributary input appear to be enhanced by logging activities within some of the valleys; the effects apparently declining rapidly over 5-12 years. The quality of the input is affected in a similar manner; fines increase, accentuating the bimodality of tributary input. Tributary input from valleys logged prior to 1980, and unlogged valleys (for example: Maimen Creek, 1965-1971; Swanee Creek, due to be logged in 1993; MOF, 1992) appear to be less significant than more recently logged areas (for example; Cantelon Creek, 1980-1987; Hicks Creek, 1979-1987), Sowerby Creek, 1976-1985; MOF, 1992).

Human activity is again evident in highway construction. Individual cases of locally imposed disequilibriums are generally short term (for example; tens of years in the case of channel diversion or bridge construction), but repeated maintenance and rebuilding programs have extended the effects of these practices from about 10 to 50 years (Section 5.7.1.). Major channel diversion by dykes has occurred above the 11 km site (1984; P. Hartell, YRB Road Management, pers. comm., 1992)(Cantelon and Silverhope Creeks now join just upstream of 18 km) and adjacent to the 12 km area (1987; P. Hartell, YRB Road Management, pers. comm., 1992), and bridge construction at 23 km (Spring 1992; P. Hartell, YRB Road Management, pers. comm., 1992) in particular. Corresponding downstream increase in coarse fraction percentages are evident.

5.7.3. Persistent Passive Disequilibrium?

Brown (1990) and Ferguson (1981) discuss the theory of 'persistent passive disequilibrium', which refers to a spatial control of Holocene fluvial processes inherited from glaciation. Gross valley form and boundary sediments are directly or indirectly (paraglacial) related to previous glaciations. This concept is too confining for the 'disequilibriums' being experienced in the Silverhope valley which appears to be affected by a hierarchy of disequilibriums, both passive and active. The nature of remnant glacial features (persistent passive disequilibrium) has imposed recurrent active disequilibriums upon the fluvial system.

First is the control of gross aggradation and degradation inherited by landslide-damming of Silverhope Creek. Upstream of Silver Lake the creek is slowly adjusting to the new base level by aggradation, and downstream it has downcut from recently-acquired interim headwaters. (There are still local reaches which appear to have acquired characteristics from the previous glaciation (at 2-5 km, and 25 km).

Second, superimposed upon the gross entrainment regime, are changes in downstream fining brought about by tributary input and road construction. The former appears to have been modified by logging activities in many cases and this has affected the quality and quantity of sediment input. It appears that this modification is relatively short-lived in the Silverhope valley and that effects ameliorate significantly after about 12 years (the original particle size distribution prior to commencement of major logging activities in 1946 is unknown). Road construction commenced at the same time as logging, but its apparent effects can

only be separately identified in site-specific locations where recent road construction (including dykes and bridges) has taken place on the channel sides. All evidence suggests that the effects of road construction below Silver Lake are quickly dissipated (23 km site), but above Silver Lake considerable sediment storage times may be involved (11 km site). Long term monitoring of particle size distributions are required.

5.8. A Model of Holocene Sedimentation in Silverhope Valley

Holocene sedimentation in British Columbia has been modeled by several researchers (e.g. Church and Slaymaker, 1989; Jordan and Slaymaker, 1991). A general model proposes that the greatest denudation occurs in the smallest headwater tributaries (Vanoni, 1975). However, Church and Slaymaker (1989) believe that for glaciated mountain landscapes this is not the case, and that sediment yield increases downstream. Jordan and Slaymaker (1991) produced an alternative model which applies specifically to the Lillooet River and recognises that sediment inputs are highly episodic on several timescales. They include two additional episodes of sediment input, from volcanic and neoglacial activity, but state that further examination of the model is needed to assess the full significance of human activity in accelerating sediment yield. A model for Silverhope Creek (Figure 5.14), an upland stream (which is currently unglaciated), indicates that sediment yield is both episodic (lake-forming mass movement event and human impact) and subject to climatic asymmetry (Section 5.3.3.).

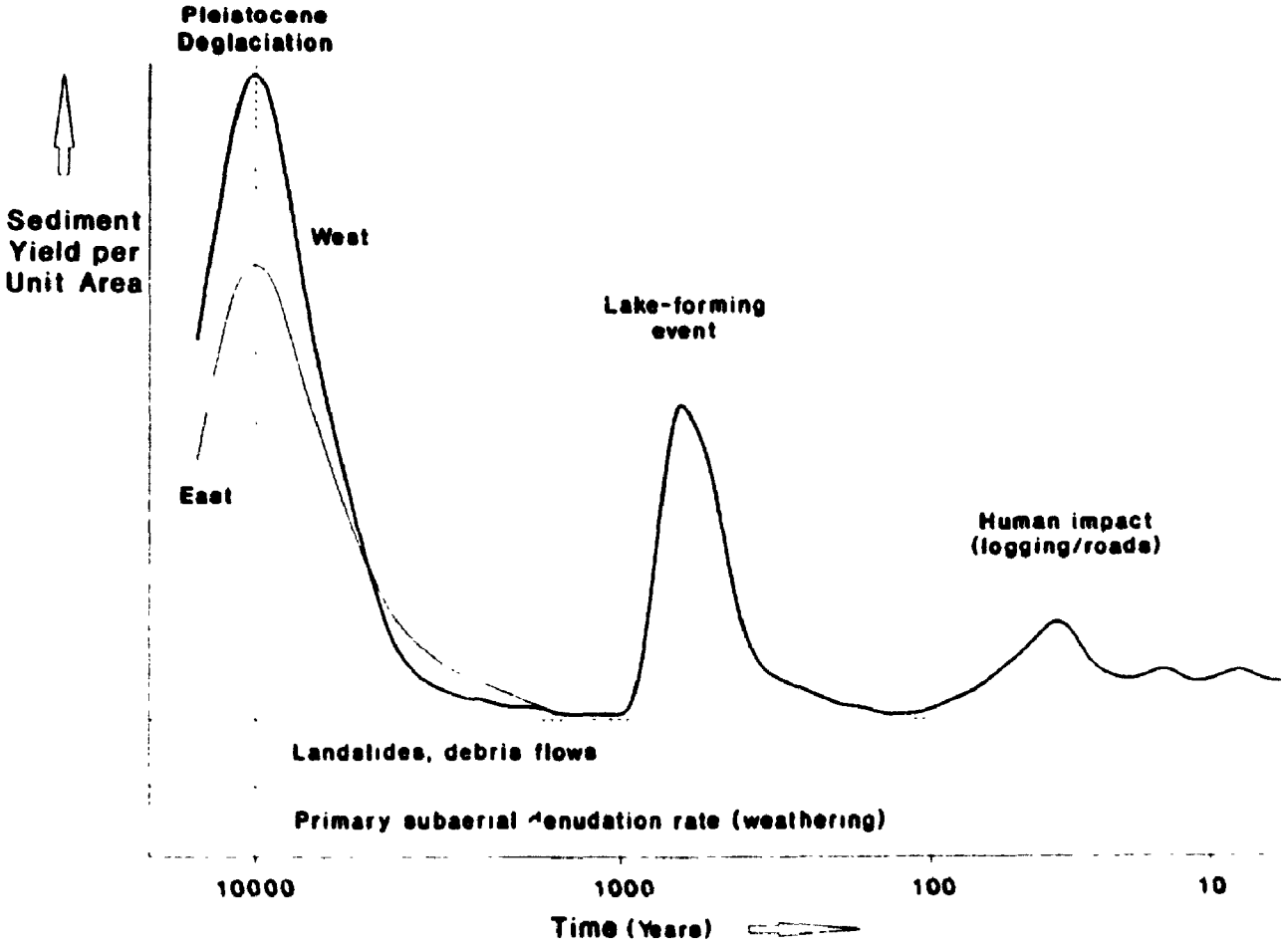

Figure 8.14 SILVERHOPE CREEK: **A Model of Holocene Sedimentation (showing the effects of episodic sediment inputs on sediment yield, modified after Jordan and Slaymaker, 1991)**

In mountain valleys of British Columbia, climatic asymmetry is an important variable of sediment supply (Waitt, 1972; 1977; I.A. Evans, pers. comm., 1992), and landslide-damming events are recognised as common (Costa and Schuster, 1988; Logan and Schuster, 1991; J.J. Clague, pers. comm., 1991). Creek gravels and lake sediments indicate that human impact can also be significant.

5.9. The Effects of Recent Human Disturbance on the Silverhope Drainage Basin

5.9.1. Fish Habitat

There has been an increasing interest in the effects of human activity on salmonid fish, mainly because of the revenue generated from recreational fishing permits, but also as indicators of river quality and biota (Mosley, 1985). Growing concern about the possible future effects of global warming on salmon populations in the Fraser River drainage basin has led to the defining of specific goals for sustainable fisheries development (Levy, 1992). Goals include the 'avoidance of irreversible human changes to fish-producing habitats'.

Fish are ectotherms and as such are sensitive to changes in ambient water temperature. Increased runoff generated by logging activity tends to lead to an increase in stream temperatures, adversely affecting the life cycle of salmonids (Holtby, 1988; Levy, 1992) Temperature increases of up to 3.2°C have been recorded and while these adversely affect the salmonid life cycle they can also lead to significant population increases (e.g. 7% for the coho salmon - Holtby, 1988). However logging activity appears to have a more immedi e affect on

river quality which can negate population growth and even reverse it by degenerating fish-producing habitats.

In Section 5.7.1. brief reference is made to the apparent quantitative effects of human disturbance (logging activities and road construction) on the fluvial sediment regime. However, qualitatively the effects seem to be considerably more dramatic. It has been shown that human activity in the Silverhope valley appears to have produced high suspended solid loads ('fines'). These sediments may either settle in gravel spawning-grounds, infilling the interstices; or become part of increased suspended sediment input into Silver Lake, reducing the ability of fish to travel upstream (Carling, 1987).

In Silverhope valley, salmonid fish such as salmon and trout tend to bury their eggs in channel gravels 8-30 cm below the bed surface (Milner *et al.*, 1981). Scouring flows, crushing, burial, declining oxygen supply and food sources generated by increased in-channel deposition are often serious causes of egg mortality (McNeill, 1966; Elliott, 1976). Moderate flows often winnow fines from interstices, but not to great depth unless the gravel is mobilised (Carling, 1984). Where flows are highly variable, excessive gravel mobility or scour is detrimental to fish-spawning grounds, and thus any imbalance in the sediment load has serious implications for river biota.

In a management context, the imposition of an altered sediment and discharge regime often leads to channels adjusting their overall dimensions by scour or deposition. In Silverhope valley, this situation is exacerbated by the inherited disequilibrium of the landslide-damming of Silver Lake. Fines cannot be

winnowed out of the gravel framework except by flows which exceed bankfull and disrupt the sediments (Milner *et al.*, 1981). Regrettably, in Silverhope valley such events merely transfer fines into Silver Lake and further reduce water quality.

Evidence in Silverhope valley of declining river quality or biota is indirect, but can be found in salmonid fish stock data, and from observations of deteriorating riparian environments. In 1951 and 1975, fish surveys revealed six species of salmonid; *Onocorhynchus kisutch* ('Coho'), *O. tshawytscha* ('Chum'), *O. gorbuscha* ('Pink'), *Salmo gairdneri* ('Steelhead': anadromous, 'Rainbow Trout': non-anadromous), *Salvelinus malma* ('Dolly Varden'), and *O. nerka kennerlyi* ('Kokanee'); (Anon, 1951; Anon, 1975). Between 1960 and 1974 the anadromous salmonid population history was recorded in Silver Lake (this covers the period during which logging activity commenced in tributary valleys following exhaustion of timber supplies in the main Silverhope valley - Section 5.5.2.). Of the four species, Coho, Chum, Pink and Steelhead, populations declined by 84%, 17%, 20%, and 43% respectively (Anon, 1975). There were fluctuations in population, and brief dramatic increases were experienced in the populations of Chum, Pink and Steelhead. A survey carried out in Silver Lake in 1992 (in conjunction with representatives of BC Hydro) found only one anadromous salmonid species, Steelhead; and one non-anadromous, Dolly Varden. Furthermore, numbers of Steelhead appear to have declined by about 50% since 1974 (J. DeLair, pers. comm., 1992). No physical barriers to fish migration appear to have been emplaced downstream, and the most likely cause of the decline seems to be deteriorating river and spawning ground quality.

Riparian land has been seriously affected by road construction (Section 5.7.1.). Dyke and bridge construction in particular seem to have increased the supply of suspended load to the river. Quantitatively there are no data available, however based on the requirements of highway maintenance work, bank instability has become increasingly problematic over the past 10 years, and has led to the temporary postponement of a project to pave the main logging road from the mouth of Silverhope Creek to Ross Lake (P. Hartell, YRB Road Management, pers. comm., 1992).

5.9.2. Sedimentation

It is generally accepted that even controlled logging in forested catchments increases sediment yield and peak discharge significantly. Some researchers believe that the effects may be relatively short-lived if forest regrowth is rapid (Sopper & Lynch, 1973; Langford, 1976). However the 46 year record since the beginning of major logging activity (and road construction) in Silverhope valley shows that sedimentation rates have increased, although declining slightly from a rate of 2.97 to 2.52 cm/yr by 1964 (Section 5.5.3.). Rapid forest regrowth *per se* does not appear to be the major problem, but rather the qualitative coverage of regrowth.

Forest vegetation in the Silverhope valley is dominated by *Alnus rubra* (Red Alder), *Acer glabrum var. douglasii* (Douglas Maple), *Thuja plicata* (Western Red Cedar), *Betula papyrifera commutata* (Western White Birch), and *Pseudotsuga menziesii* (Douglas Fir). Ground cover and shoreline vegetation generally

consists of *Acer circinatum* (Vine Maple), *Rubus spectabilis* (Salmonberry), and *Spiraea douglasii* (Hardhack).

A ground and aerial photograph survey of mass movement features in a recently-logged (Hicks Creek; logged 1979-1987; MOF, 1992) and a previously-logged (Maimen Creek, 1965-1971; MOF, 1992) tributary valley of the Silverhope drainage basin indicates that tree regrowth is delayed in areas of slope instability. Slope failures ending at the banks of tributary stream channels appear to be the last features to be stabilised, primarily because of continued reactivation by undercutting. In Maimen Creek, 11 out of 15 are still active; in Hicks Creek, 21 out of 22 slope failures reaching the channel are still active. Other failures have stabilised more rapidly; 2 out of 17, and 7 out of 19 are still active respectively. These results imply that sediment input may initially decline fairly rapidly with regrowth, but that a significant amount of material is still fed into the drainage system by open transfer routes.

In this study, the size of each slope failure was not considered in detail, excepting a subjective observation that it is mainly the larger features that remain active. Percentage calculations therefore provide a lower boundary estimate. Since 1971, in Maimen Creek 59% of slope failures have stabilised, the majority (47% of the total) not being connected by a direct sediment pathway to the creek. Of the creek-contact failures, 73% are still active. In Hicks Creek (since 1987), 32% of slope failures have stabilised (only one or 3% is creek-contact), 95% of the creek-contact failures are still active. In 16 years (1971 - 1987) between the termination of logging activity in each valley, there has only been an additional

22% decline in active creek-contact failures, but non-contact failures have declined rapidly.

The results of this study (lacustrine and fluvial sediments, and slope failures) suggest that there is probably a significant base level of sediment input generated by logging activity (the above sections detail the qualitative measurement) which declines slowly over an extended period of tens of years. There seems to be an initial rapid drop in the rate of sediment input over the first few years after logging, but subsequent input appears to take place at a higher base level than previously recorded. Patch-cutting (rare in Silverhope valley) ameliorates these problems, but is more expensive and rarely adopted (Beschta, 1978). The implications for improved erosion control measures are evident. Logging activities may appear to have a relatively minor impact on the fluvial sediment regime (although qualitative considerations are important), a considerable amount of fines add to increased sediment input in the lacustrine record. Over a period of tens of years this is having a significant effect upon the sedimentary regime of Silverhope valley, longer term effects are unpredictable.

Preliminary results from ongoing research in the contiguous Klesilkwa River drainage basin (Figure 1.1) suggest that the effects of recent logging activity are less obvious. Gross valley form, inherited disequilibriums and biomass distribution appear to be the major controlling factors. This suggests that fairly rudimentary geologic, geomorphologic, sedimentologic and ecosystem criteria can be developed for use in an environmental impact assessment to estimate drainage basin respons to logging activity in this area of the north Cascades.

CHAPTER SIX

SUMMARY AND CONCLUSIONS

6.1. Summary

6.1.1. Introduction

Studies of late Wisconsinan and Holocene deposits within the Silverhope Creek drainage basin were carried out over a period of two years. It appears that the sedimentary history of the basin is dominated by three phases of disequilibrium; deglaciation, landslide-damming of Silver Lake, and human disturbance (logging activity and road construction).

6.1.2. Late Wisconsinan Sedimentation

Paucity of exposures in Silverhope valley made it necessary to adopt a relative chronology for deglaciation based upon dateable events in adjacent valleys. Most deglaciation in the valley is believed to have taken place between about 11 400 and 11 000 years BP, although research was extended south into the upper reaches of the Klesilkwa River where deposits are believed to date from about 11 500 years BP.

Glacial paleomovement indicators (e.g. striae, stoss-lee, and fabric analysis) support the general consensus that ice mainly flowed south through this section of the north Cascade Mountains. However, local ice flow crossed the divides between Silverhope Creek and the Chilliwack and Coquihalla drainage basins. The most significant overflow was probably into Chilliwack valley. During

downwasting and retreat of the Hicks Creek - Post Creek ice tongue, an ice block formed a barrier to meltwater flow to the west. The origin of this blockage had been debated by several researchers (Gourlay, 1976; Clague and Luternauer, 1 .2; Saunders *et al.*, 1987), but sedimentologic and structural data indicate that it was of Silverhope origin.

Timing of glaciation and comparison with previous research suggest that the diamicton deposits are Sumas equivalent. These deposits are mainly reworked subglacial meltout till (although lodgement till is evident) and could be termed "sediment flow deposits" (Dreimanis, 1990). In general, meltwater reworking appears to have winnowed fines from the matrix in an ice marginal lacustrine environment, preservation of diamicton clasts in more active meltwater flows was less common, but observed.

During deglaciation the ice sheet downwasted and retreated northward in the direction of meltwater flow creating Glacial Lake Silverhope (GLS). Eleven levels for GLS have been proposed supported by evidence of topographic control, height of retreating ice, ice marginal drainage (kame terraces, valley sandurs, and deltas (inc. a Gilbert-type delta)) and dead ice/glacial deposits. During ice retreat there appears to have been one minor readvance and two less extensive oscillations. The site of the former is marked by boulder mounds superimposed on hummocky terrain in the Upper Klesilkwa River valley, the readvance shearing bedrock up from a previously ice-breached ancient interfluve. The site of the oscillations/readvances is visible as a distinct morphological

change from "V"- to "U"- shaped valley, and is also preserved in the sedimentary record.

Two minor readvances were recorded in Chilliwack valley, 11 500 and 11 200 years BP (Saunders *et al.*, 1987) and it is suggested that fluctuations in the ice front in Silverhope valley are synchronous. Differences in the magnitude of these events (the two minor oscillations/readvances coincide with the second Chilliwack readvance) in each valley may be the result of variations in ice sheet response to rapid isostatically-induced phases of reemergence of low-lying areas of the Fraser Lowland. Alternatively, the magnitude of these events may differ in response to periods of intense local geothermal activity, triggered by land reemergence.

Morphology indicates that west tributary valley ice input generally contributed to a distinct widening ("U"-shape) of the main Silverhope valley establishing a "beaded" valley form. Subsequent to initial lateral erosion gradual uplift of main valley ice caused a downglacier diminution in erosive power until the next tributary ice input. Valley asymmetry is discussed below (Section 6.1.3.1.).

6.1.3. Holocene Sedimentation

6.1.3.1. Paraglacial Sediments

There are clear topographical differences between the west and east sides of the Silverhope drainage basin. Glacial topography in the Silverhope region indicates that western tributaries contributed ice to the main trunk valley, but that

eastern valley glaciers rarely extended beyond their cirques. It appears that tributary glaciers on the east valley sides have a higher equilibrium-line altitude, away from the Pacific source of moisture (Waitt, 1972; 1977). Aerial photographs and the areal extent of paraglacial activity suggests that Holocene climatic asymmetry reflects similar conditions. The largest paraglacial fans are found on the west valley side and one, which overlies dead ice deposits, forms the present drainage divide between Silverhope Creek and Klesilkwa River.

In British Columbia, many researchers have shown that the majority of paraglacial sedimentation occurred between deglaciation and deposition of Mazama tephra. Indicator beds of Mazama tephra in Silverhope valley suggest that climatic asymmetry has played an important part in delaying paraglacial sedimentation on the east side of the valley. Tephra is exposed near the upper surface of paraglacial deposits on the west side of the drainage basin, but is beneath 2.5 m of sediment on the east side.

6.1.3.2. Silver Lake

A radiocarbon age and caesium dating chronology has been established from the lake sediments. The landslide-damming of Silver lake may have taken place up to 1100 years ago in an event coeval with major seismic activity recorded in the Seattle area, with major human disturbance (logging activity and road construction) commencing in 1946. Both dates are significant because they establish a time for the initiation of 'old' and 'new' delta formation, respectively.

Six cores, up to 1.5 m in length, were retrieved. Evidence of GLS was found in two adjacent cores, but analysis of seismic data and comparison with other cores suggests that these deposits are an isolated unit. The presence of local quasi-channelised flow indicates that some scouring and resedimentation has probably occurred, particularly at the north end of the lake. Prior to the commencement of major human disturbance in the valley there appears to have been a fairly uniform stratigraphy of gyttja and organic units, with some notable exceptions (e.g. Core B -*Unit 3*). Core data indicate that there have been some periods of turbidity (particularly following the landslide-damming event, and around 1946). The presence of an upper turbidity deposit in Core D (*Unit 20*) immediately prior to 1946, may be indicative of initial instabilities created by human disturbance.

Domination of the post-1946 sedimentary environment by 'new' delta deposits is evident, and variations in the lake-wide depositional regime indicate that thicker deposits are found along the east side of the lake. Changes in sedimentation rate are striking; in the most reasonable comparison (between Cores D and E) sediments appear to have accumulated at an average estimated rate of about 2.75 cm/yr since 1946, as opposed to an estimated pre-1946 rate of about 0.14 cm/yr.

6.1.3.3. Silverhope Creek Channel Deposits

Silverhope Creek suffers from a hierarchical pattern of passive and superimposed active disequilibriums, the most significant being the passive

control of gross aggradation and degradation inherited by the formation of Silver Lake by landslide-damming. Active disequilibriums are superimposed upon this regime, and changes in downstream fining are brought about by, a) tributary input (which in turn appears to be influenced by logging which affects the quality and quantity of sediment input) and, b) road construction and the redistribution of boundary sediments.

D_{84}, D_{50} and D_{16} percentile sizes increase adjacent to relict glacial deposits, mass movement features, alluvial fans, and downstream from tributary input sites. D_{16} was also affected by selective entrainment, brought about by aggradation upstream from Silver Lake. Dramatic decreases in D_{16} are associated with areas that have either been recently logged (as opposed to older logging sites), or are adjacent to current road construction sites.

Landslide-damming of Silver Lake has caused the northern part of Silverhope Creek to adjust to a new source level, causing rapid incision of mass movement and relict glacial debris. This has significantly increased the size of the coarse fraction downstream, establishing a second, more conventional, phase of downstream fining.

Tributary input exerts a localised influence on downstream fining, although quantities of sediment input appear to be enhanced by logging activities within some of the valleys, the effects appear to decline rapidly over 5-12 years (valleys logged prior to 1980, and unlogged valleys exert less influence on downstream fining). Quality of input appears to be affected in a similar manner, fines increase, accentuating the bimodality of tributary input. Road construction commenced at

the same time as logging, but its apparent effects can only be separately identified in site-specific locations where recent road construction (including dykes and bridges) has taken place on the channel sides.

6.1.3.4. Model

A model of Holocene sedimentation for Silverhope Creek has been produced and shows that sediment yield is episodic (mass movement and human impact) and subject to climatic asymmetry *and* drainage-modifying events.

The past glaciation of Silverhope valley and landslide-damming of Silver Lake exert passive qualitative and quantitative controls over sedimentation. However, the 46 year record of lacustrine sedimentation since the beginning of major human disturbance in the valley is of particular significance. It shows that sedimentation rates have increased by about 20 times (Section 5.5.3.) and may have diminished by only about 8%-15 between 1957 and 1964, with no significant decline in the past twenty years (logging activities have been strictly controlled over the past ten years to selected patch-cuts and tributary valleys - J. DeLair, pers. comm., 1992). Observations of mass movement activity suggest that it is the percentage of tree regrowth coverage which effectively stabilises slopes that is a significant factor in controlling tributary sediment input, not just regrowth.

Analysis of Holocene sedimentation processes (lacustrine, fluvial, and slope failures) suggests that human disturbance and logging activities may appear to have a relatively local impact on the fluvial sediment regime, but a considerable amount of fines add to increased sediment input in the lacustrine regime. Over

a period of tens of years the effects upon the sedimentary regime of Silver Lake are significant, and there are indications that the effects of aggradation are extending upstream into Silverhope Creek.

6.1.3.5. Relevance of Silverhope valley to studies of late Wisconsinan and Holocene Sedimentation

Silverhope valley provides an important basin-wide analysis of sedimentation. Late Wisconsinan deposits tend to support Saunders' (1985) evidence of two minor readvances in the adjacent Chilliwack valley. There is a possibility that Silverhope valley may have been associated with ice streaming, which may account for unusual gross valley form.

Holocene deposits provide significant evidence about the effects of human disturbance (logging acuvity and road construction) on sedimentation in mountain valleys of SW British Columbia. In this respect the writer believes that it represents a unique study of the effects of logging on both fluvial and lacustrine environments. This highlights the importance of studying basin-wide environments as opposed to individual processes, and has charted the effects of logging from inception to date. The results indicate that these effects can be significant and may provide an important model for similar catchments in the Pacific northwest.

6.2. Conclusions

The late Wisconsinan and Holocene sedimentation history in the Silverhope drainage basin spans about 11 500 years. It is punctuated by two major and one

relatively minor event, namely; glaciation/deglaciation, landslide-damming of Silver Lake, and recent human activities (logging and road construction). The following conclusions can be drawn.

1) Silverhope Creek suffers from a hierarchical pattern of passive and superimposed active disequilibriums through time. Passive disequilibriums are imposed by the landslide-damming of Silver Lake and past glaciation. Active disequilibriums (tributary input and road construction) bring about local changes in downstream fining.

2) In most of the Silverhope basin, rapid deglaciation appears to have taken place between about 11 400 and 11 000 years BP, based upon the radiocarbon chronology of the Chilliwack valley and Fraser Lowland.

3) One possible minor readvance and two probable ice front oscillations were recorded. The former about 11 500 years BP into the upper reaches of the Klesilkwa River, and the latter two, just to the north of Silver Lake during glacier standstill, may be synchronous with that recorded in Chilliwack valley about 11 200 years BP.

4) During ice retreat, ice-dammed Glacial Lake Silverhope experienced at least eleven recorded levels controlled by interfluves, dead ice/hummocky terrain and ice marginal drainage.

5) Radiocarbon ages and stratigraphic correlations indicate that the landslide-damming of Silver Lake may have occurred up to 1100 years ago and be coeval with paleoseismic activity recorded in the Seattle area. Prior to 1946, sedimentation and stratigraphy were fairly consistent to the west side of the lake. These were dominated by delta formation along the west margin of the lake, and by quasi-channelised flow toward the northwest end.

6) Radiocarbon ages and caesium dates indicate that sedimentation rates in Silver Lake may have increased by about 20 times since 1946 (although statistically this could be as low as 2 times). Deposition has been concentrated in delta formation along the east side, with a change in quasi-channelised flow to the northeast side.

7) Sedimentation rates have not subsided significantly and infer that possible long term effects of logging activities in particular, on sedimentation can not be interpreted by studying the fluvial regime alone. A basin-wide approach needs to be adopted.

8) Particle size distributions of fluvial gravels, and data from lake cores indicate that logging activity and highway construction have probably contributed significantly to a deterioration in water quality and fish-spawning grounds. Evidence from salmonid fish stocks concur.

9) Further quantitative work should be carried out on contiguous catchments to ascertain whether sedimentation is being similarly affected by human activity.

APPENDICES

APPENDIX I

ALTIMETRY DATA

Elevations were measured using an American Paulin Micro Surveying Altimeter Model MDM-5, in conjunction with benchmarks located throughout the study area (Map Sheets: 92 H/6 - 92 H/3 - 92 H/5 - 92 H/4). Where benchmarks were not available, secondary points were established (temperature fluctuations were taken into account).

At each section the altimeter, which is accurate to 0.1m, was used to determine the elevation above sea level of all contacts and the top and bottom of the exposure. A 30m measuring tape was also used to measure the section and record contacts. Altimetry measurements were repeated several times over the course of two field seasons. With repeated altimetry measurements it is estimated that an uncertainty of +/- 0.1m has been achieved.

LEGEND	
a/b/c/d/e/lower	Hill identification referred to in text
LowT	Low terrace
MidT	Middle terrace
m	Boulder mound
vfl	Valley floor

STUDY SITES:

SITE	HEIGHT (m)		SITE	HEIGHT (m)	
1	Max.	263.8	13	Max.	417.5
	Min.	79.6		---	416.0
				Min.	415.5
2	Max.	391.5			
	---	388.0	14	Max.	448.5
	---	385.5		---	448.3
	Min.	384.5		---	448.1
				Min.	441.0
3	Max.	351.6			
	---	347.1	15	Max.	791.0
	---	320.7		Min.	767.0
	---	309.7			
	---	297.8	16	Max.	1022.5
	Min.	288.8		---	1017.0
				---	631.0
4	---	536.1		---	584.8
				---	583.8
6	Max.	371.1		---	543.8
	---	365.2		---	504.3
	---	364.7		Min.	503.8
	Min.	362.7			
			17	Max.	721.5
7	Max.	760.2		---	717.5
	Min.	756.0		Min.	713.0
8	Max.	928.8	18	Max.	754.0
	Min.	908.8		Min.	752.0
10	---	405.7	19	Max.	936.5
				---	929.5
11	Max.	412.0		---	927.5
	---	406.9		Min.	925.5
	---	406.3			
	---	405.7	20	Max.	988.0
	---	404.2		Min.	980.0
	Min.	402.5			
			21	---	603.5
12	Max.	402.5			
	---	401.5	22	Max.	822.6
	Min.	400.0		Min.	792.5

STUDY SITES (cont.):

SITE	HEIGHT (m)	
23	Max.	743.5
	---	742.5
	---	738.5
	Min.	737.5
24	---	858.0
25	- -	743.5
26	Max.	1029.1
	---	1027.9
	Min.	1027.1
27	---	1280.0
28a	Max.	1007.5
	---	1007.0
	---	1006.7
	Min.	1006.0
28b	---	1006.0
	---	1004.5
29	---	1051.5
30	Max.	1150.0
	---	1132.0
	Min.	1124.0
31	---	1295.5
32	---	1988.0
33	Max.	722.2
	---	715.8
	---	714.6
	---	713.6
	Min.	700.8
34	Max.	904.0
	Min.	898.0

SITE	HEIGHT (m)	
35	Max.	979.0
	---	977.5
	Min.	977.0
36	---	1463.0
37/38	---	1448.0
39	---	1829.0
40	Max.	263.1
	---	244.0
	---	239.0
	Min.	233.5
41	Max.	237.0
	---	215.0
	---	213.0
	---	212.5
	Min.	209.0
42	---	1082.3
43	Max.	285.7
	---	280.7
	---	280.2
	Min.	248.0
44	Max.	323.9
	---	272.4
	Min.	260.0
45	Max.	490.5
	Min.	480.0
46	Max.	392.7
	Min.	390.2
47	---	415.8

STUDY SITES (cont.):

SITE	HEIGHT (m)	
48	---	1312.2
49	Max.	382.1
	---	381.9
	---	379.6
	---	379.5
	Min.	359.6
50	Max.	535.7
	Min.	529.7
51	N/A	-----
52	Max.	437.0
	Min.	433.5
53	Max.	919.7
	---	901.5
	---	651.0
	---	601.2
	---	599.7
	Min.	552.4
54	Max.	440.0
	---	439.1
	Min.	438.0
55	Max.	577.5
	Min.	574.5
56	Max.	935.0
	Min.	932.0
57a	Max.	1877.5
57b	Min.	1935.5
58	Max.	567.7
	Min.	563.5
59	---	600.1

SITE	HEIGHT (m)	
60	Max.	617.5
	---	582.1
	---	573.6
	Min.	554.0
61	Max.	593.0
	---	590.0
	Min.	584.5
62	Max.	618.3
	---	606.9
---	---	606.3
	Min.	601.3
63	Max.	631.5
	Min.	618.6
64	Max.	775.0
	Min.	772.5
65	Max.	797.0
	Min.	793.0
66	a	630.0
	b	617.0
	c	616.5
	d	615.0
	e	614.0
	MidT	580.5
	LowT	571.1
67	Max.	579.0
	---	576.5
	---	576.0
	Min.	575.0
68	m1	559.5
	m3	561.0
	m9	567.0
	m11	566.0
	vf1	563.0

SITE	HEIGHT (m)
m2	559.0
m4/8	560.0
m10	559.0
m12	566.0

LAKE LEVELS

Site No.	Elev.	Significance	Level No.
26	1027.9	OUTBURST PARTIALLY DRAINED DEAD ICE DAMMED LAKE	- LEVEL ONE
8	928.8 - 908.8	KAME TERRACE OUTLET FLOWED N.W. PARTIALLY DRAINING DEAD ICE DAMMED LAKE	- LEVEL TWO
65	797.0 - 793.0	WATER OVERSPILLED S. PARTIALLY DRAINING DEAD ICE DAMMED LAKE	- Intermediate
7	760.2 - 756.0	KAME TERRACE OUTLET FLOWED N.W. PARTIALLY DRAINING DEAD ICE DAMMED LAKE	- LEVEL THREE
63	631.5	HUMMOCKY TERRAIN SET LAKE LEVEL	- LEVEL FOUR
66	630.0	hill (a)	
63	618.6	HUMMOCKY TERRAIN HEIGHT SET LAKE LEVEL	- LEVEL FIVE
60	617.5	lower hill	
66	617.0	hill (b)	
66	616.5	hill (c)	
66	615.0	hill (d)	
66	614.0	hill (e)	
60	582.1	HIGH TERRACE INDICATES FORMER LAKE LEVEL	- LEVEL SIX
66	580.5		
60	573.6	LOW TERRACE INDICATES FORMER LAKE LEVEL	- LEVEL SEVEN
66	571.1		
68	560.0 - 553.0	OUTWASH TERRACE, BOULDER MOUNDS, AND	
58	557.7 - 553.5	PLANED-OFF HUMMOCKY TERRAIN INDICATE	
60	554.0	FORMER LAKE LEVEL	- LEVEL EIGHT
45	490.5 - 480.0	KAME TERRACE OUTLET FLOWED N.E. PARTIALLY DRAINING ICE DAMMED LAKE	- LEVEL NINE
2-3	391.5 - 320.7	ICE MARGIN OSCILLATION CAUSING FLUCTUATING LAKE LEVEL, AND KAME TERRACE OUTLET FLOWING N.W. PARTIALLY DRAINING ICE DAMMED LAKE	- LEVEL TEN
1	263.8 - 79.6	OUTBURST FLOWED N.W. DRAINING ICE DAMMED LAKE	- LEVEL ELEVEN

APPENDIX I:

SUMMARY OF PALEODIRECTION INDICATORS

Graphic interpretation of granulometric analyses were prepared using Planperfect 5.0. Data from fabric analyses were amalgamated with additional measurements of stoss and lee, striae, and chattermark paleodirectional indicators. A base diagram incorporating fabric data was prepared using Stereo software (McEachran, 1988). This plot represents equal area, lower hemisphere spherical projections of points plotted within 10% density areas.

A full data set can be found on the enclosed diskettes (these have the suffix '.PAS' and can be read on ROCKWARE - STEREO). Rose diagrams summarised in the text are recorded at the end of this appendix.

LEGEND:

N	=	No. of trend/plunge measurements
A	=	Azimuth of principal eigenvector
S	=	Strength of principal eigenvector
Nt	=	No. of striae measurements on top surface
Nb	=	No. of striae measurements on bottom surface
Ns	=	No. of stoss/lee measurements

Other features (no. in brackets)

Bm	=	Boulder mounds
C	=	Chatter marks
Cs	=	Clay smudges
Fs	=	Flame structures (not on rose diagrams)
Pc	=	Pebble clusters (included in spherical projections)
Ru	=	Roll-up features (not on rose diagrams)
S	=	Shear planes (included in spherical projections)

Site no.		Density Plots N	A (°)	S	Rose Diagrams Nt	Nb	Ns	Other
1		18	171.2	0.88	0	0	0	Pc(5)
2	*Unit 2*	50	330.8	0.82	0	0	0	Fs(5)
2	*Unit 3*	52	325.4	0.82	0	0	0	0
3	*Unit 2*	55	352.2	0.66	44	0	2	S(3)
3	*Unit 3*	55	352.2	0.55	0	0	0	S(5)
3	*Unit 4a/b*	53	3.4	0.70	75	8	8	S(3)
4		5	-----	----	28	0	5	C(2)
5		0	-----	----	20	0	5	C(2)
6	*Unit 1*	52	288.5	0.73	0	22	0	S(1)
6	*Unit 3*	50	259.9	0.73	0	0	0	0
7	*Unit 1*	51	157.8	0.77	0	0	0	0
8	*Unit 1*	50	128.4	0.66	0	0	0	0
9		0	-----	----	7	0	2	0
10		0	-----	----	32	0	2	C(2)
11	*Unit 1*	53	182.7	0.83	0	0	0	0
11	*Unit 3*	51	165.7	0.82	0	0	0	0
11	*Unit 5*	52	169.7	0.77	0	0	0	0
12	*Unit 1*	50	183.2	0.78	0	15	6	Cs(7)
13	*Unit 1*	51	194.1	0.64	0	0	0	Fs(12)
13	*Unit 2*	51	194.1	0.64	16	14	15	S(12)

Site no.	Density Plots N	A (°)	S	Rose Diagrams Nt	Nb	Ns	Other
14 *Unit 1*	51	191.7	0.80	0	0	0	Pc(4)
15 *Unit 1*	51	259.5	0.65	18	0	4	Pc(3)
16 *Unit 1*	54	246.2	0.82	0	0	0	S(2)
17 *Unit 2*	56	299.1	0.75	0	0	0	0
19 *Unit 1*	52	211.2	0.76	0	4	5	0
20 *Unit 1*	52	231.0	0.84	0	6	6	0
23 *Unit 1*	50	347.7	0.73	0	0	0	Pc(7)
23 *Unit 3*	53	345.2	0.74	0	0	0	Pc(5)
24	0	-----	----	0	0	0	Ru(1) S(1)
26 *Unit 2a*	53	31.3	0.68	0	0	0	0
26 *Unit 2b*	52	12.2	0.91	0	0	0	0
27	0	-----	-----	9	0	4	0
29	0	-----	----	9	0	2	0
30 *Unit 1*	56	137.4	0.66	0	8	0	S(3)
30 *Unit 2*	65	74.0	0.83	0	20	0	0
31	0	-----	-----	5	0	3	0
32	0	-----	----	5	0	3	0
33 *Unit 1*	53	88.6	0.60	42	0	0	0
33 *Unit 3*	53	199.2	0.74	0	0	0	0
34 *Unit 1*	25	189.0	0.89	0	0	0	Pc(1)

Site no.	Density Plots N	Density Plots A (°)	Density Plots S	Rose Diagrams Nt	Rose Diagrams Nb	Rose Diagrams Ns	Other
38 *Unit 2*	50	185.4	0.68	0	5	5	0
36	0	-----	----	3	0	3	0
37/38	0	-----	-----	7	0	1	0
39	0	-----	----	5	0	1	0
40 *Unit 1*	16	343.6	0.98	0	0	0	0
41 *Unit 1*	51	170.6	0.78	0	0	0	0
41 *Unit 3*	30	358.9	0.68	0	0	0	S(4)
41 *Unit 4*	27	8.1	0.79	0	0	0	0
42	0	-----	----	10	0	2	0
43 *Unit 1*	51	240.2	0.71	16	0	0	0
43 *Unit 3*	51	267.7	0.82	0	0	0	0
44 *Unit 2*	8	330.5	0.99	0	0	0	0
45 *Unit 1*	50	209.1	0.51	0	30	0	Pc(2)
46 *Unit 1*	52	359.2	0.73	0	0	0	0
47	0	-----	----	28	0	2	0
48	0	-----	----	10	0	3	0
49 *Unit 1*	53	354.0	0.62	0	0	0	0
50 *Unit 1*	52	355.3	0.74	0	0	0	0
51	0	-----	----	10	0	2	0
52 *Unit 1*	49	22.6	0.70	0	0	0	0

Site no.	Density Plots N	A (°)	S	Rose Diagrams Nt	Nb	Ns	Other
53 *Unit 1a*	56	174.2	0.76	0	0	0	0
53 *Unit 1b/c*	101	352.0	0.77	0	0	0	C
54 *Unit 1*	26	11.2	0.95	0	0	0	0
56 *Unit 1a*	14	203.5	0.77	0	0	0	Ru(1)
57a	0	-----	----	3	0	2	0
58 *Unit 1*	50	153.8	0.55	0	0	0	Pc(9)
61 *Unit 1*	23	301.9	0.70	0	10	3	0
61 *Unit 2*	33	101.7	0.64	0	0	0	0
62 *Unit 1a*	51	101.5	0.74	0	0	0	0
62 *Unit 1b*	53	90.9	0.75	0	0	0	0
62 *Unit 1c*	52	143.6	0.67	0	0	0	0
65 *Unit 1*	24	348.6	0.76	0	0	0	Pc(5)
67 *Unit 1*	26	10.8	0.97	0	0	0	0
67 *Unit 3*	51	194.0	0.85	0	0	0	Pc(3)
68 *Unit 1*	15	32.3	0.87	0	0	0	0
68	53	273.4	0.61	0	0	0	Bm(12)

Rose diagrams for units in which paleocurrent data was diagrammatically summarised in Chapter Two:

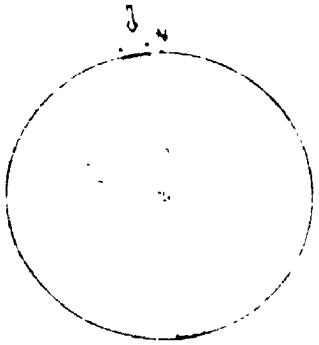

Site 3 - *Unit 2* (Nt = 44)

(Nt = 75)
Site 3 - *Unit 4a/4b* (Nb = 8)

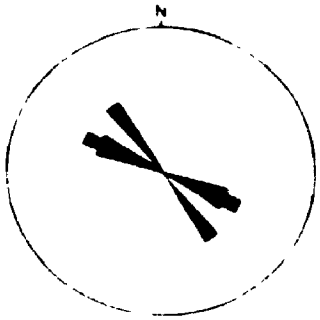

Site 6 - *Unit 1* (Nb = 22)

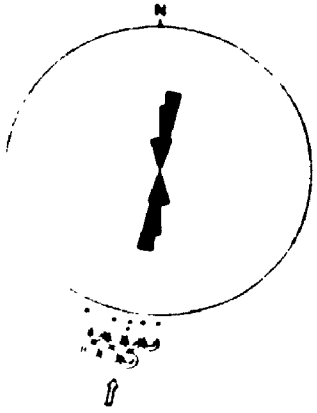

Site 12 - *Unit 1* (Nb = 15)

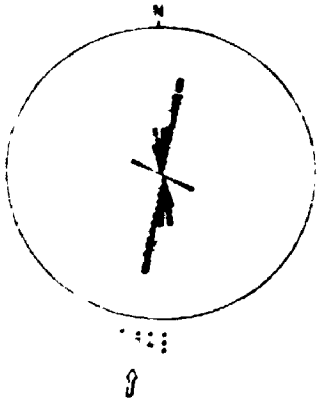

(Nt = 16)
Site 13 - *Unit 2* (Nb = 14)

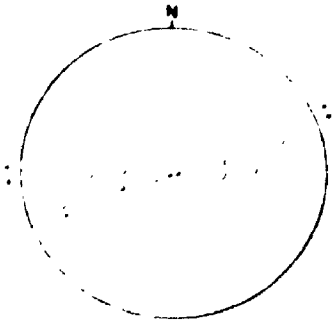

Site 15 - *Unit 1* (Nt = 18)

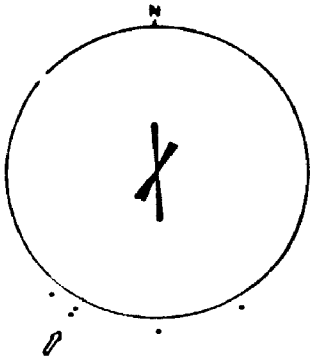

Site 19 - *Unit 1* (Nb = 4)

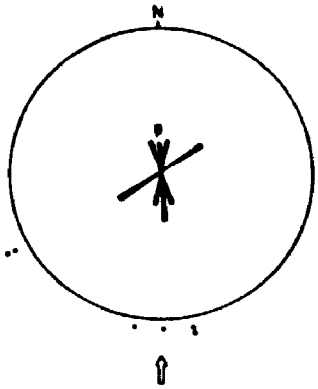

Site 20 - *Unit 1* (Nb = 6)

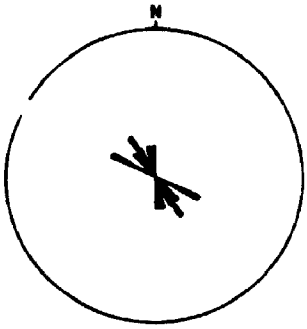

Site 30 - *Unit 1* (Nb = 8)

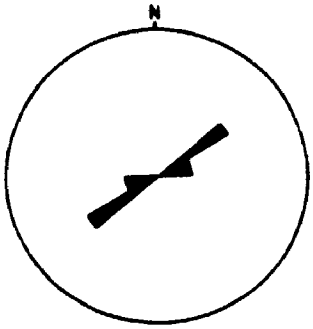

Site 30 - *Unit 2* (Nb = 20)

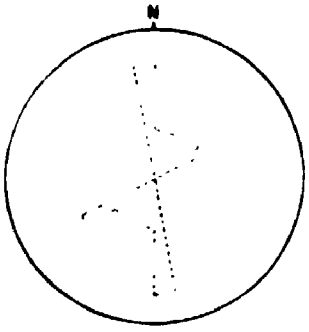

Site 33 - *Unit 1* (Nt = 42)

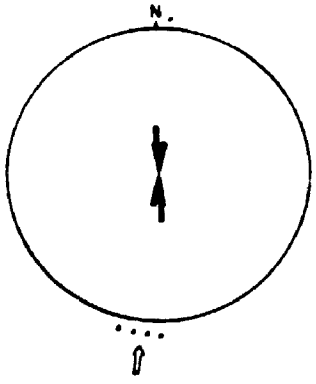

Site 35 - *Unit 2* (Nb = 5)

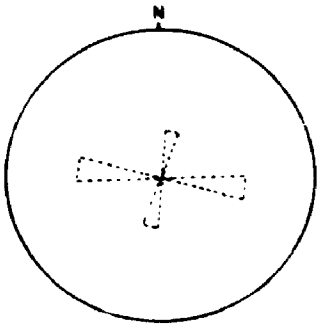

Site 43 - *Unit 1* (Nt = 16)

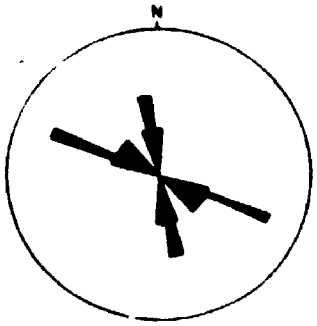

Site 45 - *Unit 1* (Nb = 30)

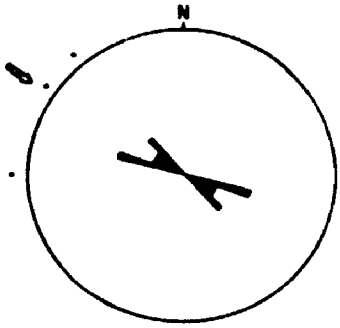

Site 61 - *Unit 1* (Nb = 10)

APPENDIX III

SUMMARY OF PARTICLE SIZE ANALYSIS

Particle size was determined using the Wentworth Classification. Laboratory analysis was carried out by the combined sieve and hydrometer method (ASTM, 1972). For samples with large clasts, field sieving was carried out on the coarse fraction greater than 8 mm. Samples were dried on tarpaulins and measurements were taken using a particle size template (256 mm - 8 mm) and weighed on field scales accurate to the nearest tenth of a gram. Sample sizes for sieve and hydrometer analysis were based on the following criteria:

a) < 2 mm size fraction - 100 g samples were analysed by hydrometer.

b) > 2 mm size fraction - sample weights were based on bulk sampling standards discussed in Church *et al.* (1987), and Yuzyk (1986). However, logistical constraints prohibited statistically significant weights to be gathered for samples with a largest particle size varying from 180-256 mm (180-400 kg), although samples in excess of 100 kg were analysed in each case.

Data were analysed on a Lotus 1-2-3 spreadsheet, and particle size distributions were produced for sand-silt-clay and gravel-sand-mud comparisons. Individual phi-size percentage distributions were also produced.

A full data set can be found on enclosed diskettes (suffix '.PLN - can be read with either PLANPERFECT 5.0 or imported into LOTUS 1-2-3 (version 2.1. or higher)).

Site/Unit no.		1: Tot. Sample % (Gravel	Sand	Mud)	2: < 2 mm 100 g % (Sand	Silt	Clay)
2	*Unit 2*	3.77	45.62	50.61	47.40	52.60	0.00
2	*Unit 3*	8.59	80.16	11.24	87.70	12.30	0.00
3	*Unit 2*	82.55	9.08	8.38	52.00	42.90	5.10
3	*Unit 3*	13.31	9.71	76.98	11.20	87.80	1.00
3	*Unit 4a*	94.41	3.67	1.92	65.60	27.20	7.20
3	*Unit 4b*	84.24	9.22	6.54	58.50	35.90	5.60
6	*Unit 1*	75.42	22.49	2.09	91.50	8.50	0.00
6	*Unit 2*	0.00	0.60	99.40	0.60	99.40	0.00
6	*Unit 3*	71.84	18.78	9.38	66.70	32.70	0.60
7	*Unit 1*	89.63	5.57	4.80	53.70	45.30	1.00
	Sample 2	70.05	24.80	5.15	82.20	17.20	0.00
8	*Unit 1*	89.00	7.46	3.54	67.80	31.20	1.00
	Sample 2	42.59	40.82	16.59	71.10	27.90	1.00
11	*Unit 1*	68.90	16.67	14.43	53.60	39.50	6.90
11	*unit 2*	0.30	65.90	33.80	66.10	20.70	13.20
12	*Unit 1*	17.40	47.58	35.02	57.60	37.40	5.00
12	*Unit 2*	0.40	69.12	30.48	69.40	23.20	7.40
13	*Unit 1*	17.96	55.54	26.50	67.70	30.20	2.10
13	*Unit 2*	24.00	47.12	28.88	62.00	38.00	0.00
14	*Unit 1*	4.65	88.10	7.25	92.40	7.60	0.00
14	*Unit 2*	0.00	29.30	70.70	29.30	65.70	5.00
15	*Unit 1*	42.99	45.55	11.46	79.90	15.50	4.60

Site/Unit no.		1: Tot. Sample % (Gravel	Sand	Mud)	2: < 2 mm 100 g % (Sand	Silt	Clay)
16	*Unit 1*	62.73	29.22	8.05	78.40	18.70	2.90
16	*Unit 5*	5.76	9.42	84.82	10.00	64.80	25.20
17	*Unit 2*	87.54	11.84	0.62	95.00	2.90	2.10
18	*Unit 1*	0.00	8.00	92.00	8.00	83.80	8.20
19	*Unit 1*	12.59	42.30	45.10	48.40	43.80	7.80
19	*Unit 3*	0.00	1.50	98.50	1.50	97.50	1.00
20	*Unit 1*	12.17	61.04	26.79	69.50	30.50	0.00
22	*Unit 1*	0.11	0.80	99.09	0.80	85.70	13.5
23	*Unit 3*	16.13	7.55	76.32	9.00	57.90	33.10
25	*Unit 1*	0.00	19.30	80.70	19.30	71.60	9.10
26	*Unit 1*	0.08	25.98	73.94	26.00	68.00	6.00
26	*Unit 2a*	91.96	5.39	2.65	67.00	24.90	8.10
26	*Unit 2b*	89.68	6.66	3.66	64.55	26.95	8.50
28a	*Unit 2*	0.00	35.60	64.40	35.60	57.30	7.10
28b	*Unit 1*	0.95	43.68	55.37	44.10	55.90	0.00
30	*Unit 1*	11.18	46.81	42.01	52.70	32.70	14.60
30	*Unit 2*	11.18	46.81	42.01	52.70	32.70	14.60
33	*Unit 1*	65.37	18.47	16.16	53.33	41.57	5.10
33	*Unit 2*	0.33	16.94	82.73	17.00	77.40	5.60
34	*Unit 1*	8.73	23.82	67.45	26.10	68.60	5.30
35	*Unit 2*	15.33	49.11	35.56	58.00	30.40	11.60

Site/Unit no.		1: Tot. Sample % (Gravel	Sand	Mud)	2: < 2 mm 100 g % (Sand	Silt	Clay)
39	*Unit 1*	0.00	31.60	68.40	31.60	67.40	1.00
41	*Unit 1*	41.50	57.74	0.76	98.70	1.30	0.00
41	*Unit 2*	81.63	6.73	11.63	36.67	56.23	7.10
41	*Unit 3*	0.00	0.60	99.40	0.60	82.30	17.10
41	*Unit 4*	0.00	11.80	88.20	11.80	74.40	13.80
43	*Unit 1*	78.70	13.27	8.03	62.30	28.10	9.60
45	*Unit 1*	74.52	21.43	4.05	84.10	14.10	1.80
46	*Unit 1*	75.85	23.02	1.14	95.30	4.70	0.00
49	*Unit 1*	83.58	15.81	0.62	96.25	3.75	0.00
49	*Unit 2*	0.00	3.70	96.30	3.70	77.50	18.80
50	*Unit 1*	56.57	18.67	24.75	43.00	53.90	3.10
52	*Unit 1*	81.70	16.44	1.87	89.90	4.20	6.00
53	*Unit 1a*	84.03	14.64	1.33	91.70	8.30	0.00
53	*Unit 1b/c*	90.17	8.88	0.95	90.30	7.90	1.80
54	*Unit 1*	7.29	20.49	72.22	22.10	62.60	15.30
54	*Unit 2*	0.00	9.20	90.80	9.20	69.00	21.80
55	*Unit 1*	2.06	13.42	84.52	13.70	58.20	28.10
56	*Unit 1*	0.00	3.10	96.90	3.10	82.80	14.10
56	*Unit 1a*	7.76	48.85	43.50	52.90	42.60	4.50
58	*Unit 1*	14.76	54.47	30.77	63.90	33.10	3.00
61	*Unit 1*	34.66	16.73	48.61	25.60	63.00	11.40

Site/Unit no.		1: Tot. Sample % (Gravel	Sand	Mud)	2: < 2 mm 100 g % (Sand	Silt	Clay)
61	*Unit 2*	14.76	54.47	30.77	63.90	33.10	3.00
62	*Unit 1a*	84.22	14.69	1.09	93.10	5.90	1.00
62	*Unit 1c*	99.49	0.51	0.00	100.00	0.00	0.00
64	*Unit 1*	0.00	3.40	96.60	3.40	79.70	16.90
66	*Unit 1*	13.87	51.16	34.97	59.40	39.60	1.00
66	*Unit 1a*	34.66	16.73	48.61	25.60	63.00	11.40
67	*Unit 1*	13.40	84.43	2.16	97.50	2.50	0.00
67	*Unit 3*	26.67	70.17	3.16	95.70	4.30	0.00
68	*Unit 1*	5.06	7.69	87.25	8.10	68.10	23.80
SILVER LAKE SECTIONS:							
CORE A1		0.00	0.80	99.20	0.80	96.70	2.50
CORE A2		0.00	1.60	98.40	1.60	98.40	0.00
CORE B4a		0.00	0.60	99.40	0.60	99.40	0.00
CORE B4b		0.00	0.60	99.40	0.60	96.90	2.50
CORE B5a		0.00	5.00	95.00	5.00	90.00	5.00
CORE B5b		0.00	15.20	84.80	15.20	84.80	0.00
CORE B5c		0.00	12.20	87.80	12.20	80.80	7.00
CORE B6a		0.00	21.00	79.00	21.00	77.00	2.00
CORE B6b		0.00	7.20	92.80	7.20	72.60	20.20
CORE B7a		0.00	6.00	94.00	6.00	73.80	20.20

Site/Unit no.	1: Tot. Sample % (Gravel	Sand	Mud)	2: < 2 mm 100 g % (Sand	Silt	Clay)
CORE B7b	0.00	13.20	86.80	13.20	86.80	0.00
CORE B7c	0.00	20.80	79.20	20.80	79.20	0.00
CORE C3a	0.00	49.40	50.60	49.40	48.60	2.00
CORE C3b	0.00	19.60	80.40	19.60	76.90	3.50
CORE C3c	0.00	8.80	91.20	8.80	87.90	3.30
CORE C4a	0.00	4.80	95.20	4.80	87.20	8.00
CORE C4b	0.00	9.20	90.80	9.20	77.20	13.60
CORE C4c	0.00	8.20	91.80	8.20	87.70	4.10
CORE C5	0.00	24.00	76.00	24.00	76.00	0.00
CORE C6a	0.00	49.60	50.40	49.60	38.20	12.20
CORE C6b	0.00	49.00	51.00	49.00	49.40	1.60
CORE C6c	0.00	3.75	96.25	3.75	96.25	0.00
CORE C7	0.00	43.00	57.00	43.00	36.60	20.40
CORE C8	0.00	40.60	59.40	40.60	59.40	0.00
CORE C9	0.00	12.00	88.00	12.00	73.00	15.00
CORE D4a	0.00	8.20	91.80	8.20	91.80	0.00
CORE D4b	0.00	14.00	86.00	14.00	81.00	5.00
CORE D5	0.00	38.00	62.00	38.00	58.70	3.30
CORE D6a	0.00	40.40	59.60	40.40	59.20	0.40
CORE D6b	0.00	22.60	77.40	22.60	77.40	0.00
CORE E3	0.00	24.00	76.00	24.00	69.30	6.70

Site/Unit no.	1: Tot. Sample % (Gravel	Sand	Mud)	2: < 2 mm 100 g % (Sand	Silt	Clay)
CORE E4a	0.00	25.60	74.40	25.60	71.10	3.30
CORE E4b	0.00	35.50	64.50	35.50	49.10	15.40
CORE E4c	0.00	46.20	53.80	46.20	48.80	5.00
CORE E4d	0.00	28.80	71.20	28.80	58.00	13.20
CORE E5a	0.00	45.20	54.80	45.20	52.80	2.00
CORE E5b	0.00	54.80	45.20	54.80	43.20	2.00
CORE E5c	0.00	46.60	53.40	46.60	50.40	3.00
CORE E5d	0.00	42.50	57.50	42.50	57.50	0.00
CORE E8	0.00	71.80	28.20	71.80	20.20	8.00
SILVERHOPE CREEK GRAVELS (distance in km from Klesilkwa River/Silverhope Creek confluence in brackets):						
SH 2 (28km)	66.70	27.23	6.07	92.50	4.50	3.00
SH 3 (27)	57.10	37.75	5.16	89.20	7.80	3.00
SH 4 (26)	45.32	47.25	7.44	95.90	2.10	2.00
SH 5 (25)	46.39	48.67	4.94	90.60	8.40	1.00
SH 6 (24)	52.67	39.34	7.99	99.70	0.30	0.00
SH 7 (23)	51.29	41.97	6.74	97.60	2.40	0.00
SH 11 (19)	91.14	8.85	0.01	99.90	0.10	0.00
SH 12 (18)	87.49	11.08	1.43	88.60	11.40	0.00
SH 13 (17)	84.34	14.11	1.55	90.10	9.90	0.00
SH 14 (16)	85.33	9.72	4.94	66.30	25.90	7.80

Site/Unit no.	1: Tot. Sample % (Gravel	Sand	Mud)	2: < 2 mm 100 g % (Sand	Silt	Clay)
SH 15 (15)	67.81	10.73	21.45	96.10	3.90	0.00
SH 16 (14)	63.32	9.86	26.82	98.00	2.00	0.00
SH 17 (13)	51.91	9.42	38.67	90.10	9.90	0.00
SH 18 (12)	51.72	9.81	38.47	95.40	4.60	0.00
SH 19 (11)	92.49	6.29	1.22	83.80	14.00	2.20
SH 20 (10)	90.23	7.39	2.37	75.70	19.30	5.00
SH 21 (9)	88.06	8.45	3.49	70.80	24.00	5.20
SH 22 (8)	90.99	8.29	0.72	92.00	6.00	2.00
SH 23 (7)	88.07	10.39	1.54	87.10	8.90	4.00
SH 24 (6)	92.66	6.53	0.81	89.00	11.00	0.00
SH 25 (5)	89.82	9.63	0.55	94.60	5.40	0.00
SH 26 (4)	94.85	4.74	0.41	92.10	7.90	0.00
SH 27 (3)	90.75	9.20	0.05	99.50	0.50	0.00
SH 28 (2)	93.24	6.68	0.08	98.80	1.20	0.00
SH 29 (1)	86.94	13.00	0.05	99.60	0.40	0.00
SH 30 (0)	91.67	4.69	3.64	56.30	40.70	3.00

APPENDIX IV

a) TEPHRA ANALYSIS

Tephra analysis was carried out by electron microprobe at the University of Western Ontario, Department of Geology. Samples were analysed for their magnetite chemical composition to determine the origin of the tephra deposits. Al, Mg, Fe, Ti and Mn oxide concentrations were determined. Volcanic ash identification is possible by the examination of Al_2O_3, TiO_2, and MgO (Westgate *et al.*, 1970; Brewster and Barnett, 1979). See Figure 5.4 for comparison with Westgate *et al.* (1970) and Brewster and Barnett (1979).

Site No.	Oxide Concentrations		
	TiO_2	Al_2O_3	MgO
14 *Unit 2*	8.91	2.04	2.23
28a *Unit 2*	9.14	2.12	2.23
39 *Unit 1*	9.02	2.11	2.27
49 *Unit 2*	9.05	1.95	2.15
Mean:	9.03	2.06	2.22

N.B. See diskette 2 for complete data - file name 'Mazama.WK1'.

b) RADIOCARBON AGES

There are two specific problems associated with radiocarbon dating in lacustrine environments. First, old carbon can become incorporated from solution into the tissue of living organisms. Their eventual addition to the lake sediment produces a ^{14}C age estimate older than the deposit (Olsson, 1974). Second, old carbon can be input from sources in the surrounding drainage basin. In lake samples this is most common with the commencement of human activity around the perimeter (Dickson *et al.*, 1978). In the case of Silver Lake, significant disturbance of the land surface draining to the lake does not appear to have taken place prior to 1946, except during discrete mass movement events. Downward-migrating humic acids, penetration of large organic material through several depositional units, and variable ^{14}C production in the upper atmosphere (DeVries effect) can cause age ranges of hundreds of years on samples which differ in calendar years by only decades (Stuiver and Pearson, 1986; Nelson, 1992). Stratigraphic continuity and associated radiocarbon ages tend to suggest that these possible causes of discordant ages have had minimal affect on Silver Lake samples.

Radiocarbon analyses were carried out at Beta Analytic Incorporated (Beta), Florida. This company was chosen for their reliability and speed of analysis. AMS measurements were made in the Lawrence Livermore National Laboratory in California (CAMS), with chemical pretreatments being done at Beta. In view of the small sample sizes extracted, either extended counts were carried

out to obtain the best age estimates, or analysis was carried out by Accelerator Mass Spectrometer technique.

Samples were first boiled/washed free of all adhering mineral matter and examined for any noncontemporaneous carbonaceous matter. Subsequent treatment was carried out by repeated soakings in dilute hot acid and alkali solutions to remove any carbonate or humic acid contaminants. Final rinsings to neutrality were done using hot distilled water. Large samples were dried, synthesised to benzene and counted for radiocarbon content.

The three very small samples (Beta-61040, 61041 and 61042) measured by AMS were combusted to CO_2, purified and reacted with hydrogen on cobalt catalysts to produce graphite. The reported ages have been adjusted by ^{13}C. The half-life of radiocarbon is taken to be 5568 years.

c) CAESIUM DATING

Caesium-137 is an artificial radio-isotope, and is the result of fallout from atomic-bomb testing and the occasional nuclear accident. It has a half-life of 30.2 years. Detectable concentrations can be dated to 1953-1954, and the peak of activity to 1963-1964, although other peaks can sometimes be resolved (e.g. 1956-1957, 1986-1987: Chernobyl - not recorded in Canada to date; Stihler *et al.*, 1992). A time lag of six to twelve months has been observed between fallout and deposition in sediments. Some corrections need to be made, such as variations in rainfall and delays in hemispheric exchange. Bioturbation and mixing of sediments introduce errors into dating, and there is evidence for ^{137}Cs migration in the sediment column (McHenry *et al.*, 1973; Pennington *et al.*, 1973). However, recent research suggests that it is fairly immobile in some lacustrine environments (Wan *et al.*, 1987). Delayed input from ^{137}Cs-enriched catchment surfaces (soils) offers an additional source of uncertainty, but provided that catchment characteristics are evaluated, the technique can be a useful dating tool. It is a non-destructive dating technique (McHenry *et al.*, 1973; Pennington *et al.*, 1973).

Counting the concentration of ^{137}Cs in sediments is by correlation as opposed to the conventional dating technique based on half-lives. Variations in concentration versus depth is compared to the fallout record with time, the best correlations coming from closely-spaced samples (Clague *et al.*, submitted).

Dried samples from known depths were counted on a gamma ray spectrometer using the procedures after the method of Lewis (1974). ^{137}Cs concentrations are measured in picocuries per gram (pCi/g) of freeze dried

sediment (see Appendix V). Counting errors were about 10% and concentrations of up to 1.73 picocuries per gram of freeze dried sediment were recorded.

Sedimentation rates based on the variable concentrations of ^{137}Cs in the sediment cores have been calculated based upon data shown in graphs below and in the detailed core section descriptions in Appendix V (complete data can be found on diskette 2 - file name 'Caesium.WK1').

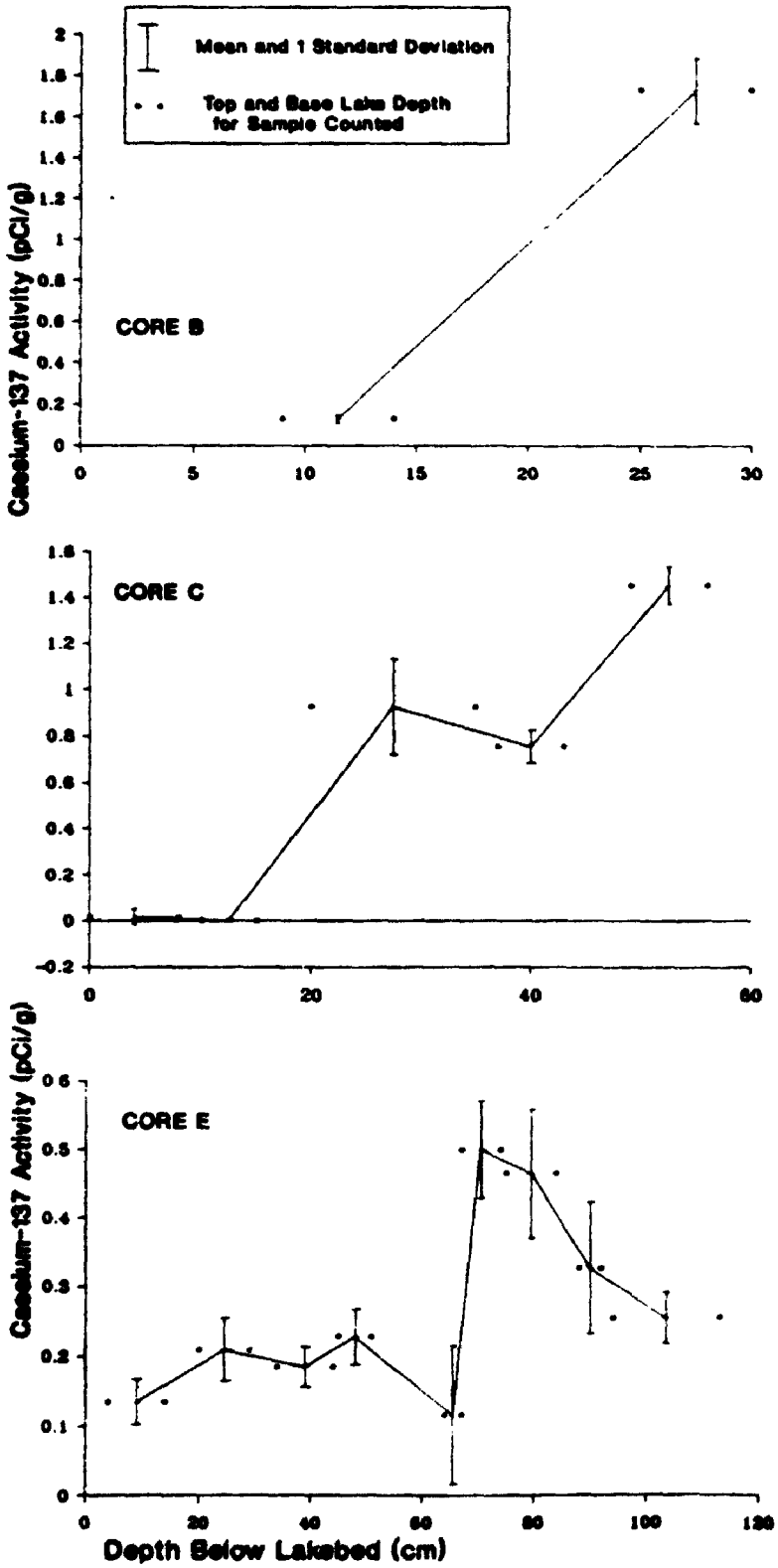

Concentration of ^{137}Cs versus Core Depth Below Lakebed (Cores B, C and E)

d) MAPS AND AERIAL PHOTOGRAPHS

Maps of the surficial sediments, interpretations of morphology and morphological changes, were made using a series of aerial photographs and topographical maps.

Flight Line (Nos.)	Year Flown	Approx. Scale
BC211 (5 - 25) BC334 (100 - 110) BC335 (1 - 22) BC339 (12 - 16) BC340 (98 - 106)	1947	1:50 000
BC7473 (120 - 140) BC7476 (160 - 180)	1973	1:25 000
BC87098 (147 - 152) BCC563 (1 - 99)	1987	1:70 000 1:10 000
BC88073 (218 - 222) (235 - 241) BC88078 (263 - 268) BC88079 (2 - 7)	1988	1:70 000
BCB91079 (90 - 93) BCB91157 (158 - 163)	1991	1:70 000

Map	Scale
NTS series: 92 H/3 (Skagit River) 92 H/4 (Chilliwack) 92 H/5 (Harrison Lake) 92 H/6 (Hope)	1:50 000

APPENDIX V

SILVER LAKE CORE DESCRIPTIONS

Section — Field Description (depth (m) - distance down core in brackets (), psd = particle size data sample, * = radiocarbon date recorded in 'years BP' or as '% of modern', + = ^{137}C activity: pCi/g - estimated date).
N.B. In recording ^{137}Cs activity, Dead = cannot be not distinguished from background radiation.

A1

Depth: Water - 11.19
Section - 1.00
Total - 12.19

Sample 1 - core section (0.99-1.00)
psd 1 - (0.99-1.00)

A2

Depth: Water - 11.19
Section - 1.10
Total - 12.29

Sample 2 - core section (1.08-1.10)
psd 2 - (1.08-1.10)

B

Depth: Water - 12.28
Section - 1.50
Total - 13.78

Sample *1 - wood (0.48-0.49) **Beta-81040/CAMS-5488: 100 ± 60 years BP**

2 - contaminated
3 - contaminated
4 - core section (0.00-0.34)
\+ psd 4a - (0.09-0.14) : **0.12820 pCi/g - N/A**
\+ psd 4b - (0.25-0.30) : **1.73020 pCi/g - 1964**
5 - core section (0.34-0.69)
psd 5a - (0.34-0.46)
psd 5b - (0.49-0.60)
psd 5c - (0.65-0.69)
6 - core section (0.69-0.98)
psd 6a - (0.76-0.78)
psd 6b - (0.80-0.94)
7 - core section (1.05-1.45)
psd 7a - (1.05-1.10)
psd 7b - (1.30-1.35)
psd 7c - (1.43-1.45)

C

Depth: Water - 10.67
Section - 1.50
Total - 12.17

Sample *1 - wood (0.43-0.54) **Beta-61042/CAMS-5490: 144.0 ± 1.1 % of modern**

*2 - wood (1.21-1.30) **Beta-61043: 450 ± 60 years BP**

3 - core section (0.00-0.36)

\+ psd 3a - (0.00-0.08) **: 0.12620 pCi/g - N/A**

\+ psd 3b - (0.10-0.15) **:-0.00040 pCi/g - N/A**

\+ psd 3c - (0.20-0.35) **: 0.92620 pCi/g - 1964**

4 - core section (0.37-0.70)

\+ psd 4a - (0.37-0.43) **: 0.78460 pCi/g - N/A**

\+ psd 4b - (0.49-0.56) **: 1.46380 pCi/g - N/A**

inc. organics

psd 4c - (0.60-0.65)

5 - core section (0.70-0.85)

psd 5 - (0.70-0.75)

6 - core section (0.97-1.15)

psd 6a - (0.97-1.00)

psd 6b - (1.05-1.07)

psd 6c - (1.11-1.14)

7 - core section (0.85-0.97)

psd 7 - (0.86-0.94)

8 - core section (1.09-1.34)

psd 8 - (1.15-1.20)

9 - core section (1.34-1.50)

psd 9 - (1.40-1.50)

D

Depth: Water - 4.88
Section - 1.22
Total - 6.10

Sample *1 - wood (0.10-0.14) **Beta-61041/CAMS-5489: 140 ± 60 years BP**

*2 - wood (0.52-0.56) **Beta-56420: 590 ± 50 years BP**

*3 - wood (0.74-0.75) **Beta-56421: 800 ± 170 yrs BP**

4 - core section (0.00-0.22)

Section 0.00 - 0.14 poorly preserved, analysed for caesium only

\+ (0.00-0.14) **: Dead**

\+ psd 4a - (0.15-0.19) **: Dead**

\+ psd 4b - (0.19-0.20) **: Dead**

5 - core section (0.25-0.55)

\+ psd 5 - (0.30-0.39) **: Dead**

Section 0.40 - 0.60 poorly preserved - not analysed

6 - core section (0.55-0.99)

psd 6a - (0.62-0.67)

psd 6b - (0.70-0.80 excl. 0.74-0.75)

E

Depth: Water - 9.14
Section - 1.28
Total - 10.42

Sample 1 - contaminated
2 - contaminated
3 - core section (1.10-1.28)
psd 3 - (1.20-1.28)
4 - core section (0.63-1.03)
+ psd 4a - (0.69-0.74) **0.80012 pCi/g - 1964**
+ psd 4b - (0.75-0.84) **0.46680 pCi/g - N/A**
+ psd 4c - (0.88-0.92) **0.32910 pCi/g - N/A**
+ psd 4d - (0.94-1.13) **0.25610 pCi/g - 1967**
5 - core section (0.20-0.67)
+ psd 5a - (0.20-0.29) **0.20930 pCi/g - N/A**
+ psd 5b - (0.34-0.40) **0.18480 pCi/g - N/A**
+ psd 5c - (0.40-0.44) **0.18480 pCi/g - N/A**
+ psd 5d - (0.64-0.67) **0.11610 pCi/g - N/A**
6 - core section (0.00-0.20)
+ psd 6 - (0.04-0.14) **0.13420 pCi/g - N/A**

REFERENCES

Adams, J. (1981) Earthquake-dammed lakes in New Zealand, **Geology, 9,** 215-219.

Adams, J. (1992) Paleoseismology: A search for ancient earthquakes in Puget Sound, **Science, 258,** 1592-1593.

Allaby, A. and Allaby, M. (1991) (eds.) **The concise Oxford dictionary of earth sciences** (Oxford University Press, Oxford), 204.

American Society for Testing and Materials (1972) Standard method for particle-size analysis of soils, **American National Standard, ASTM D 422-63,** 112-122.

Anon (1951) **Silver Lake - Lake survey data,** B.C. Environment, Fish and Wildlife Branch, Victoria, 5pp.

Anon (1975) **Silver Lake - Lake survey data,** B.C. Environment, Fish and Wildlife Branch, Victoria, 17pp.

Armstrong, J.E. (1960) Surficial geology of Sumas map-area, British Columbia, **Geological Survey of Canada, Paper,** 59-9, 27pp.

Armstrong, J.E. (1981) Post-Vashon Wisconsin glaciation, Fraser Lowland, British Columbia, **Geological Survey of Canada, Bulletin 322,** 34pp.

Armstrong, J.E., Crandell, D.R., Easterbrook, D.J. and Noble, J.B. (1965) Late Pleistocene stratigraphy and chronology in southwest British Columbia and northwest washington, **Geological Society of America Bulletin, 76,** 321-330.

Armstrong, J.E., Mathews, W.H., and Sinclair, A.J. (1971) Use of trend surfaces in till fabric analysis: discussion, **Canadian Journal of Earth Sciences, 8,** 1163-1167.

Atwater, B.F. and Moore, A.L. (1992) A tsunami about 1000 years ago in Puget Sound, Washington, **Science, 258,** 1614-1617.

Barksdale, J.D. (1941) Glaciation of the Methow valley, Washington, **Journal of Geology, 49,** 721-737.

Beaudoin, A.B. and King, R.H. (1986) Using discriminant function analysis to identify Holocene tephras based on magnetite composition: a case study from the Sunwapta Pass area, Jasper National Park, **Canadian Journal of Earth Sciences, 23,** 804-812.

Beschta, R.L. (1978) Long term patterns of sediment production following road construction and logging in the Oregon Coast Range, **Water Resources Research, 14,** 1011-1016.

Boulton, G.S. (1979) Processes of glacier erosion on different substrata: **Journal of Glaciology, 23,** 15-38.

Boulton, G.S. and Paul, M.A. (1976) The influence of genetic processes on some geotechnical properties of glacial tills, **Quarterly Journal of Engineering Geology, 9,** 159-194.

Bradley, W.C., Fahnestock, R.K. and Rowekamp, E.T. (1972) Coarse sediment transport by flood flows on Knik River, Alaska, **Geological Society of America Bulletin, 83,** 1261-1284.

Brewster, G.R. and Barnett, R.L. (1979) Magnetites from a new unidentified tephra source, Banff National Park, Alberta, **Canadian Journal of earth Sciences, 16,** 1294-1297.

Broecker, W.S. and Kulp, J.L. (1957) Lamont natural radiocarbon measurement IV, **Science, 126,** 1324-1334.

Brooks, G.R. and Hickin, E.J. (1991) Debris avalanche impoundment of Squamish River, Mount Cayley area, southwestern British Columbia, **Canadian Journal of Earth Sciences, 28,** 1375-1385.

Brown, A.G. (1990) Holocene floodplain diachronism and inherited downstream variations in fluvial processes: a study of the river Perry, Shropshire, England, **Journal of Quaternary Science, 5,** 39-51.

Bucknam, R.C., Hemphill-Haley, E. and Leopold, E.B. (1992) Abrupt uplift within the past 1700 years at southern Puget Sound, Washington, **Science, 258,** 1611-1614.

Butler, D.R., Malanson, G.P. and Oelfke, J.G. (1991) Potential catastrophic flooding from landslide-dammed lakes, Glacier National Park, Montana, USA, **Zeitschrift fur geomorphologie, S.B. 83,** 195-209.

Cairnes, C.E. (1924) Reconnaissance of Silver Creek, Skagit and Similkameen Rivers, Yale District, British Columbia, **Canadian Geological Survey, Summary Report, Part A,** 46-114.

Carling, P.A. (1984) Deposition of fine and coarse sand in an open-work gravel bed, **Canadian Journal of Fisheries and Aquatic Sciences, 41,** 263-270.

Carling, P.A. (1987) Bed stability in gravel streams, with reference to stream regulation and ecology, in Richards, K.S. (Ed.) **River Channels: Environment and Process** (Special Publication of the Transactions of the Institute of British Geographers, Blackwell Scientific Publications, Oxford), 321-347.

Church, M. (1972) Baffin Island sandurs: a study of Arctic fluvial processes, **Geological Survey of Canada Bulletin, 216,** 208pp.

Church, M. and Gilbert, M. (1975) Proglacial fluvial and lacustrine environments, in Jopling, A.V. and McDonald, B.C.(Eds.) **Glaciofluvial and glaciolacustrine sedimentation** (Society of Economic Paleontologists and Mineralogists, Special Publication No. 23), 22-100.

Church, M. and Kellerhals, R. (1978) On the statistics of grain size variation along a gravel river, **Canadian Journal of Earth Sciences, 15,** 1151-1160.

Church, M., McLean, D.G. and Wolcott, J.F. (1987) River bed gravels: sampling and analysis, in Thorne, C.R., Bathurst, J.D. and Hey, R.D.(Eds.) **Sediment transport in gravel-bed rivers** (John Wiley and Sons Limited, Chichester), 43-78.

Church, M. and Ryder, J. (1972) Paraglacial sedimentation: a consideration of fluvial processes conditioned by glaciation, **Geological Society of America Bulletin, 83,** 3059-3072.

Church, M. and Slaymaker, O. (1989) Disequilibrium of Holocene sediment yield in glaciated British Columbia, **Nature, 337,** 452-454.

Clague, J.J. (1981) Late Quaternary geology and geochronology of British Columbia, Part 2., **Geological Survey of Canada, Paper 80-35,** 41pp.

Clague, J.J. (1986) The Quaternary stratigraphic record of British Columbia - evidence for episodic sedimentation and erosion controlled by glaciation, **Canadian Journal of Earth Sciences, 23,** 885-894.

Clague, J.J. (1989) Quaternary geology of the Canadian Cordillera (Chapter 1), in Fulton, R.J.(Ed.) **Quaternary geology of Canada and Greenland** (Geological Survey of Canada, Geology of Canada, No. 1 and Geological Society of America, The Geology of North America, v.K-1), 17-96.

Clague, J.J., Bobrowsky, P.T. and Hamilton, T.S. (submitted) Documentation of a tsunami origin for a sand sheet at Port Alberni, British Columbia, by ^{137}Cs analysis, **Journal of Coastal and Estuarine Science.**

Clague, J.J., Evans, S.G., Fulton, R.J., Ryder, J.M. and Stryd, A.H. (1987) **Quaternary geology of the southern Canadian Cordillera** (XIIth Inqua congress field excursion A-18) 67pp.

Clague, J.J. and Luternauer, J.L. (1982) **Excursion 30A: Late Quaternary sedimentary environments, southwestern British Columbia** (11th International Congress on sedimentology (Hamilton), field excursion guide book).

Clague, J.J. and Shilts, W.W. (in press) Two landslide-dammed lakes in the Cascade Mountains, Southwestern British Columbia, **GSC Current Research**.

Clague, J.J., Shilts, W.W. and Linden, R.H. (1989) Application of subbottom profiling to assessing seismic risk of Vancouver Island, British Columbia, **Geological Survey of Canada, Current Research, Part E, Paper 89-1E**, 237-242.

Coates, J.A. (1974) Geology of the Manning Park area, British Columbia, **Geological Survey of Canada, Bulletin 238**, 177pp.

Costa, J.E. and Schuster, R.L. (1988) The formation and failure of natural dams, **Geological Society of America Bulletin, 100**, 1054-1068.

Crandell, D.R. (1965) The glacial history of western Washington and Oregon, in Wright, H.E. Jr. and Frey, D.G.(Eds.) **The Quaternary of the United States** Princeton University Press, Princeton, N.J.), 341-353.

Daly, R.A. (1912) Geology of the North American Cordillera at the forty-ninth parallel, **Geological Survey of Canada, Memoir 38 (3 parts)**, 857pp.

Davis, N.F.G. and Mathews, W.H. (1944) Four phases of glaciation with illustrations from southwestern British Columbia, **Journal of Geology, 52**, 403-413.

Dawson, M.J. (1988) Sediment size variation in a braided reach of the Sunwapta River, Alberta, Canada, **Earth Surface Processes and Landforms, 13**, 599-618.

Desloges, J.R. and Church, M. (1987) Channel and floodplain facies in a wandering gravel-bed river, in Ethridge, E.F., Flores, R.M. and Harvey, M.D.(Eds.) **Recent developments in fluvial sedimentology** (Society of Economic Paleontologists and Mineralogists, Special Publication No. 39), 99-109.

Desloges, J.R. and Gilbert, R. (1991) Sedimentary record of Harrison Lake: implications for deglaciation in southwestern British Columbia, **Canadian Journal of Earth Sciences, 28**, 800-815.

Dickson, J.H., Stewart, D.A., Thompson, R., Turner, G., Baxter, M.S., Drndarsky, N.D. and Rose, J. (1978) Palynology, palaeomagnetism and radiometric dating of Flandrian marine and freshwater sediments of Loch Lomond, **Nature, 274,** 548-553.

Doig, R. (1986) A method for determining the frequency of large magnitude earthquakes using lake sediments, **Canadian Journal of Earth Sciences, 23,** 930-937.

Doig, R. (1990) 2300 yr history of seismicity from silting events in Lake Tadoussac, Charlevoix, Quebec, **Geology, 18,** 820-823.

Doig, R. (1991) Effects of strong seismic shaking in lake sediments, and earthquake recurrence interval, Témiscaming, Quebec, **Canadian Journal of Earth Sciences, 28,** 1349-1362.

Dowdeswell, J.A., Hambrey, M.J. and Wu, R. (1985) A comparison of clast fabric and shapes in late Precambrian and modern glacigenic sediments, **Journal of Sedimentary Petrology, 55,** 691-704.

Dowdeswell, J.A. and Sharp, M. (1986) Characterization of pebble fabrics in modern terrestrial glacigenic sediments, **Sedimentology, 33,** 699-710.

Dreimanis, A. (1989) Tills: Their genetic terminology and classification, in Goldthwait, R.P. and Matsch, C.L.(Eds) **Genetic Classification of Glacigenic Deposits** (A.A. Balkema, Rotterdam), 17-83.

Dreimanis, A. (1990) Formation, deposition and identification of subglacial and supraglacial tills, in Kujansuu, R. and Saarnisto, M.(Eds.) **Glacial indicator tracing** (A.A. Balkema, Rotterdam), 35-60.

Edwards, M. (1986) Glacial environments, in Reading, H.G. (Ed.) **Sedimentary Environments and facies** (2nd Edition, Blackwell Scientific Publications, Oxford), 445-470.

Eisbacher, G.H. (1979) First order regionalization of landslide characteristics in the Canadian Cordillera, **Geoscience Canada, 6,** 69-79.

Eisbacher, G.H. and Clague, J.J. (1984) Destructive mass movements in high mountains: hazards and management, **Geological Survey of Canada, Paper 84-16.**

Elliott, J.M. (1976) The downstream drifting of eggs of brown trout, *Salmo trutta L.*, **Journal of Fish Biology, 9,** 45-50.

Evans, S.G. and Brooks, G.R. (1991) Prehistoric debris avalanches from Mount Cayley volcano, British Columbia, **Canadian Journal of Earth Sciences, 28,** 1365-1374.

Eyles, N., Eyles, C.H. and Miall, A.D. (1983) Lithofacies types and vertical profile models; an alternative approach to the description and environmental interpretation of glacial diamict and diamictite sequences, **Sedimentology, 30,** 393-410.

Fahnestock, R.K. (1963) Morphology and hydrology of a glacial stream - White River, Mount Ranier, Washington, **United States Geological Survey Professional Paper, No. 422-A,** 70pp.

Ferguson, R.I. (1981) Channel form and channel changes, in Lewin, J.(Ed.) **British rivers** (Allen and Unwin Limited, London), 90-125.

Foxworthy, B.L. and Richardson, D. (1973) Climatic factors related to land-use planning in the Puget Sound basin, Washington, **U.S. Geological Survey, Folio of the Puget Sound Area, I-851-A.**

Frostick, L.E. and Reid, I. (1980) Sorting mechanisms in coarse-grained alluvial sediments: fresh evidence from a Basalt gravel plateau, Kenya, **Journal of the Geological Society of London, 129,** 431-441.

Fulton, R.J. (1967) Deglaciation studies in Kamloops region, an area of moderate relief, British Columbia, **Geological Survey of Canada, Bulletin 154,** 36pp.

Fulton, R.J. (1969) Glacial lake history, southern Interior Plateau, British Columbia, **Geological Survey of Canada, Paper 69-37,** 14pp.

Fulton, R.J. (1971) Radiocarbon geochronology of southern British Columbia, **Geological Survey of Canada, Paper 71-37,** 28pp.

Fulton, R.J. and Smith, G.W. (1978) Late Pleistocene stratigraphy of south-central British Columbia, **Canadian Journal of Earth Sciences, 15,** 971-980.

Gallino, G.L. and Pierson, T.C. (1985) Polallie Creek debris flow and subsequent dam-break flood of 1980, East Fork Hood River basin, Oregon, **United States Geological Survey, Water Supply Paper 2273.**

Gardiner, V. and Dackombe, R. (1983) **Geomorphological field manual** (George Allen and Unwin, London), 254pp.

Gilbert, G.K. (1885) The topographical features of lake shores, **Annual Report of the United States Geological Survey, 5,** 75-123.

Gilbert, G.K. (1890) Lake Bonneville, **Monographs of the United States Geological Survey, 1,** 438pp.

Gilbert, R. (1975) Sedimentation in Lillooet Lake, British Columbia, **Canadian Journal of Earth Science, 12,** 1697-1711.

Gilbert, R. and Desloges, J.R. (1992) The late Quaternary sedimentary record of Stave Lake, south-western British Columbia, **Canadian Journal of Earth Sciences, 29,** 1997-2006.

Gilbert, R. and Shaw, J. (1981) Sedimentation in proglacial Sunwapta Lake, Alberta, **Canadian Journal of Earth Sciences, 18,** 81-93.

Goff, J.R. (in prep.) Bed load sediment budget of a proglacial stream during a period of rapid glacier retreat, **Ontario Geography.**

Goudie, A.(Ed.)(1981) **Geomorphological techniques** (George Allen and Unwin Limited, London), 395pp.

Gourlay, A. (1977) Valley train alluvial fan development by a Pleistocene jökulhlaup, Chilliwack valley, British Columbia, unpublished B.Sc. thesis, University of British Columbia, 46pp.

Gravenor, C.P., Von Brunn, V. and Dreimanis, A. (1984) Nature and classification of waterlain glaciogenic sediments, exemplified by Pleistocene, Late Paleozoic and Late Precambrian deposits, **Earth Science Review, 20,** 105-166.

Grove, E.W. (1974) Deglaciation - a possible triggering mechanism for recent volcanism, **International Association of Volcanology and Chemistry of the Earth's Interior** (Proceedings of the symposium on Andean and Antarctic volcanology problems, Santiago, Chile), 88-97.

Hart, J.K. (1990) Proglacial glaciotectonic deformation and the origin of the Cromer Ridge push moraine complex, North Norfolk, England, **Boreas, 19,** 166-180.

Heusser, C.J. (1973) Environmental sequence following the Fraser advance of the Juan de Fuca Lobe, Washington, **Quaternary Research, 3,** 284-306.

Hicock, S.R. (1992) Lobal interactions and rheologic superimposition in subglacial till near Bradtville, Ontario, Canada, **Boreas, 21,** 73-88.

Hicock, S.R. and Armstrong, J.E. (1985) Vashon Drift: definition of the formation in the Georgia Depression, southwest British Columbia, **Canadian Journal of Earth Sciences, 22,** 748-757.

Hicock, S.R., Hobson, K. and Armstrong, J.E. (1982) Late Pleistocene proboscideans and early Fraser glacial sedimentation in eastern Fraser Lowland, British Columbia, **Canadian Journal of Earth Sciences, 19,** 899-906.

Holtby, L.B. (1988) Effects of logging on stream temperatures in Carnation Creek, British Columbia, and associated impacts on the coho salmon (*Oncorhynchus kisutch*), **Canadian Journal of Fisheries and Aquatic Sciences, 45,** 502-515.

Hope Chamber of Commerce (1991) **Hope and area** (Hope Chamber of Commerce, Hope, B.C.), 32pp.

Jackson, L.E. Jr. and Clague, J.J. (1991) The Cordilleran Ice Sheet: one hundred and fifty years of exploration and discovery, **Géographie Physique et Quaternaire, 45,** 269-280.

Jackson, L.E. Jr., MacDonald, G.M. and Wilson, M.C. (1982) Paraglacial origin for terraced rived sediments in Bow Valley, Alberta, **Canadian Journal of Earth Sciences, 19,** 2219-2231.

Jacoby, G.C., Williams, P.L. and Buckley, B.M. (1992) Tree ring correlation between prehistoric landslides and abrupt tectonic events in Seattle, Washington, **Science, 258,** 1621-1623.

Jordan, P. and Slaymaker, O. (1991) Holocene sediment production in Lillooet River basin, British Columbia: a sediment budget approach, **Géographie Physique et Quaternaire, 45,** 45-57.

Karlin, R.E. and Abella, S.E.B. (1992) Paleoearthquakes in the Puget Sound region recorded in sediments from Lake Washington, U.S.A., **Science, 258,** 1617-1620.

Kellerhals, R. (1982) Effects of river regulation on channel stability, in Hey, R.D., Bathurst, J.C. and Thorne, C.R.(Eds.) **Gravel-bed rivers** (John Wiley and Sons Limited, Chichester), 685-715.

Langford, K.J. (1976) Change in yield of water following a bushfire in a forest of *Eucalyptus Regnans*, **Journal of Hydrology, 29,** 87-114.

Levy, D.A. (1992) Potential impacts of global warming on salmon production in the Fraser River watershed, **Canadian Technical Report of Fisheries and Aquatic Sciences 1869,** 96pp.

Lewis, T. (1974) Heat production measurement in rocks using a gamma ray spectrometer with a solid state detector, **Canadian Journal of Earth Sciences, 11,** 526-532.

Logan, R.L. and Schuster, R.L. (1991) Lakes divided: the origin of Lake Crescent and Lake Sutherland, Clallam County, Washington, **Washington Geology, 19,** 38-42.

Lowdon, J.A. and Blake, W. Jr. (1973) Geological Survey of Canada radiocarbon dates XIII, **Geological Survey of Canada, Paper 73-7,** 61pp.

Lowdon, J.A. and Blake, W. Jr. (1975) Geological Survey of Canada radiocarbon dates XV, **Geological Survey of Canada, Paper 75-7,** 32pp.

Luckman, B.H. (1975) Drop stones resulting from snow-avalanche deposition on lake ice, **Journal of Glaciology, 14,** 186-188.

Maizels, J.K. (1976) A comparison of present day and Pleistocene proglacial environments, with particular reference to geomorphology and sedimentology, unpublished Ph.D. thesis, University of London, 675pp.

Maizels, J.K. (1979) Proglacial aggradation and changes in braided channel patterns during a period of glacial advance: an Alpine example, **Geografiska Annaler, 61A,** 87-101.

Mathewes, R.W. (1985) Paleobotanical evidence for climatic change in southern British Columbia during late glacial and Holocene times, in Harington, C.R.(Ed.) **Climatic change in Canada. 5. critical periods in the Quaternary climatic history of North America** (Syllogeus, 55), 397-422.

Mathewes, R.W., Borden, C.E. and Rouse, G.E. (1972) New radiocarbon dates from the Yale area of the Lower Fraser River canyon, British Columbia, **Canadian Journal of Earth Sciences, 9,** 1055-1057.

Mathewes, R.W. and Heusser, L.E. (1981) A 12,000 year palynological record of temperature and precipitation trends in southwestern British Columbia, **Canadian Journal of Botany, 59,** 707-710.

Mathewes, R.W. and King, M. (1989) Holocene vegetation, climate, and lake level changes in the Interior Douglas-fir Biogeoclimate zone, British Columbia, **Canadian Journal of Earth Sciences, 26,** 1811-1825.

Mathews, W.H. (1944) Glacial lakes and ice retreat in south-central British Columbia, **Royal Society of Canada, Transactions, 38, sec. IV,** 39-57.

Mathews, W.H. (1951) The Table, a flat-topped volcano in southern British Columbia, **American Journal of Science, 249,** 830-841.

Mathews, W.H. (1958) Geology of the Mount Garibaldi map-area, southwestern British Columbia, Canada. Part II: geomorphology and Quaternary volcanic rocks, **Geological Society of America Bulletin, 69,** 179-198.

Mathews, W.H. (1968) Geomorphology of Lightning Creek valley, Manning Park, southwestern British Columbia, **Syesis, 1,** 65-79.

Mathews, W.H., Fyles, J.G. and Nasmith, H.W. (1970) Postglacial crustal movements in southwestern British Columbia and adjacent Washington state, **Canadian Journal of Earth Science, 7,** 690-702.

Mathews, W.H. and McTaggart, K.C. (1978) Hope rockslides, British Columbia, Canada, in Voight, B.(Ed.) **Rockslides and avalanches, 1: natural phenomena** (Elsevier Press, Amsterdam), 259-275.

McCombs, A.M. and Chittenden, W.W. (1990) **The Fraser valley challenge** (Treeline Publishing, British Columbia), 176pp.

McEachran, D.B. (1988) **Stereo: orientation analysis and plotting** (Rockware Inc, Wheat Ridge, Colorado), 204pp.

McHenry, J.R., Ritchie, J.C. and Gill, A.C. (1973) Accumulation of fallout Caesium-137 in soils and sediments in selected watersheds, **Water Resources Research, 9,** 676-686.

McNeill, W.J. (1966) Effects of the spawning bed environment on reproduction of pink and chum salmon, **Bulletin of the US Fish and Wildlife Services Fisheries, 65,** 495-523.

McTaggart, K.C. and Thompson, R.M. (1967) Geology of part of the Northern Cascades in southern British Columbia, **Canadian Journal of Earth Studies, 4,** 1199-1228.

Meade, R.H. (1982) Sources, sinks and storage of river sediment in the Atlantic drainage of the United States, **Journal of Geology, 90,** 235-252.

Miall, A.D. (1978) Lithofacies types and vertical profile models in braided river deposits: a summary, in Miall, A.D.(Ed.) **Fluvial sedimentology** (Canadian Society of Petroleum Geologists, Memoir No. 5), 597-604.

Milner, N.J., Scullion, J., Carling, P.A. and Crisp, D.T. (1981) The effects of discharge on sediment dynamics and consequent effects on invertebrates and salmonids in upland rivers, **Advances in Applied Biology, 6,** 153-220.

Ministry of Forests (1992) **Silverhope stand survey: Silverhope Creek and selected tributaries** (Ministry of Forests, British Columbia), 33pp.

Monger, J.W. (1989) **Geology, Hope, British Columbia** (Geological Survey of Canada, Map 41-1989), 1:250,000.

Mosley, M.P. (1985) River channel inventory, habitat and instream flow assessment, **Progress in Physical Geography, 9**, 494-523.

Munshaw, E. (1976) The geomorphology of the Chilliwack River valley, unpublished B.Sc. thesis, University of British Columbia, 48pp.

Nelson, A.R. (1992) Discordant ^{14}C ages from buried tidal-marsh soils in the Cascadia Subduction Zone, southern Oregon coast, **Quaternary Research, 38**, 74-90.

Nemec, W. (1990) Deltas - remarks on terminology and classification, in Colella, A. and Prior, D.B. (Eds.) **Coarse-grained deltas** (Special Publication No. 10, International Association of Sedimentologists. Blackwell Scientific Publications, Oxford), 3-12.

Olsson, I.U. (1974) Some problems in connection with the evaluation of ^{14}C dates, **Geologiska Föreningens i Stockholm Förnhandlingar, 96**, 311-320.

Østrem, G. (1966) The height of the glaciation limit in southern British Columbia and Alberta, **Geografiska Annaler, 48A**, 126-138.

Pennington, W., Cambray, R.S. and Fisher, E.M. (1973) Observations on lake sediments using fallout ^{137}Cs as a tracer, **Nature, 242**, 324-326.

Pickrill, R.A. and Irwin J. (1983) Sedimentation in a deep glacier-fed lake, Lake Tekapo, New Zealand, **Sedimentology, 30**, 63-75.

Pierce, R.S., Hornbeck, J.W., Likens, G.E. and Bormann, F.H. (1973) Effect of elimination of vegetation on stream water quantity and quality, in **Results of research on representative and experimental basins** (IASH/UNESCO, Proceedings of the Wellington Symposium, 1970, Volume 1), 311-328.

Powell, R.D. (1991) Grounding-line systems as second order controls in fluctuations of tidewater termini of temperate glaciers, in Anderson, J.B. and Ashley, G.M.(Eds.) **Glacial marine sedimentation; paleoclimate significance** (Geological Survey of America, Boulder, Colorado, Special Paper No. 261), 75-93.

Richmond, G.M., Fryell, R., Neff, G.E. and Weis, P. (1965) The Cordilleran Ice Sheet of the northern Rocky Mountains, and related Quaternary history of the Columbia plateau, in Wright, H.E. Jr. and Frey, D.G.(Eds.) **The Quaternary of the United States** (Princeton University Press, Princeton, N.J.), 231-242.

Ritchie, J.C., McHenry, J.R. and Gill, A.C. (1973) Dating recent reservoir sediments: **Limnology and Oceanography, 18,** 254-263.

Roberts, M.C. and Mark, D.M. (1970) The use of trend surfaces in till fabric analysis, **Canadian Journal of Earth Sciences, 7,** 1179-1184.

Ryder, J.M. (1971a) The stratigraphy and morphology of paraglacial alluvial fans in south-central British Columbia, **Canadian Journal of Earth Sciences, 8,** 279-298.

Ryder, J.M. (1971b) Some aspects of the morphometry of paraglacial alluvial fans in south-central British Columbia, **Canadian Journal of Earth Sciences, 8,** 1252-1264.

Ryder, J.M. (1989) Glacial history of the southern Okanagan Range, in **Glacial and post-glacial processes and environments in montane and adjacent areas, Program and Abstracts** (Canadian Quaternary Association Conference, Edmonton, Alberta), 44.

Ryder, J.L., Fulton, R.J. and Clague, J.J. (1991) The Cordilleran Ice Sheet and the glacial geomorphology of southern and central British Columbia, **Géographie Physique et Quaternaire, 45,** 365-377.

Sangree, J.B. and Widmier, J.M. (1979) Interpretation of depositional facies from seismic data, **Journal of Geophysics, 44,** 131-160.

Saunders, I.R. (1985) Late Quaternary geology and geomorphology of the Chilliwack River valley, British Columbia, unpublished M.Sc. thesis, Simon Fraser University, 185pp.

Saunders, I.R., Clague, J.J. and Roberts, M.C. (1987) Deglaciation of Chilliwack River valley, British Columbia, **Canadian Journal of Earth Sciences, 24,** 915-923.

Sawicki, O. and Smith, D.G. (1992) Glacial Lake Invermere, upper Columbia River valley, British Columbia: a paleogeographic reconstruction, **Canadian Journal of Earth Sciences, 29,** 687-692.

Schuster, R.L. and Costa, J.E. (1986) A perspective on landslide dams, in Schuster, R.L.(Ed.) **Landslide dams: processes, risk and mitigation** (American Society of Civil Engineers, Geotechnical Special Publication 3), 1-20.

Schuster, R.L., Logan, R.L. and Pringle, P.T. (1992) Prehistoric rock avalanches in the Olympic Mountains, Washington, **Science, 258,** 1620-1621.

Shaw, J. (1979) Genesis of the Sveg tills and Rogen moraines of central Sweden: a model of basal melt out, **Boreas, 8,** 409-426.

Shaw, J. (1983) Forms associated with melt-out till, in Evenson, E.B., Schlüchter, Ch. and Rabassa, J.(Eds.) **Tills and related deposits** (Proceedings of the INQUA symposium on the genesis and lithology of Quaternary deposits, USA 1981, Argentina 1982. A.A. Balkema, Rotterdam), 3-12.

Shaw, J. (1985) Subglacial and ice marginal environments, in Ashley, G.M., Shaw, J. and Smith, N.D.(Eds.) **Glacial sedimentary environments** (Society of Paleontologists and Mineralogists, Tulsa, Ok., SEPT Short Course, No. 16), 7-84.

Shaw, J. and Kellerhals, R. (1982) **The composition of recent alluvial gravels in Alberta river beds** (Alberta Research Council, Edmonton, Bulletin 41), 151pp.

Sims, J.D. (1975) Determining earthquake recurrence interval from deformation structures in young lacustrine sediments, **Tectonophysics, 29,** 141-152.

Sissons, J.B. (1978) The parallel roads of Glen Roy and adjacent glens, Scotland, **Boreas, 7,** 229-244.

Sissons, J.B. (1979) The later lakes and associated fluvial terraces of Glen Roy, Glen Spean and vicinity, **Transactions of the Institute of British Geographers, 4,** 12-29.

Slaymaker, O. and McPherson, H.J. (1977) An overview of geomorphic processes in the Canadian Cordillera, **Zeitschrift für Geomorphologie, 21,** 169-186.

Smith, N.D. (1975) Sedimentary environments and late Quaternary history of a 'low energy' mountain delta, **Canadian Journal of earth Sciences, 12,** 2004-2013.

Smith, N.D. and Ashley, G.M. (1985) Proglacial lacustrine environments, in Ashley, G.M., Shaw, J. and Smith, N.D.(Eds.) **Glacial sedimentary environments** (Society of Paleontologists and Mineralogists, Tulsa, Ok., SEPT Short Course, No.16), 135-216.

Smith, N.D., Vendl, M.A. and Kennedy, S.K. (1982) Comparison of sedimentation regimes in four glacier-fed lakes of western Alberta, in Davidson-Arnott, R., Nickling, W. and Fahey, R.D.(Eds.) **Geomorphological research in glacial, glaciofluvial and glaciolacustrine systems** (Proceedings of the 6th Guelph Symposium, Ontario), 203-238.

Sopper, W.E. and Lynch, J.A. (1973) Changes in water yield following partial forest cover removal on an experimental watershed, in **Results of research on representative and experimental basins** (IASH/UNESCO, Proceedings of the Wellington Symposium, 1970, Volume 1), 369-389.

Souch, C. (1989) New radiocarbon dates for early deglaciation from the southeastern Coast Mountains of British Columbia, **Canadian Journal of Earth Sciences, 26,** 2169-2171.

Stewart, T.G. (1991) Glacial marine sedimentation from tidewater glaciers in the Canadian high Arctic, in Anderson, J.B. and Ashley, G.M.(Eds.) **Glacial marine sedimentation; paleoclimate significance** (Geological Survey of America, Boulder, Colorado, Special Paper No. 261), 95-105.

Stihler, S.D., Stone, D.B. and Beget, J.E. (1992) "Varve" counting vs. tephrochronology and ^{137}Cs and ^{210}Pb dating: A comparative test at Skilak Lake, Alaska, **Geology, 20,** 1019-1022.

Stuiver, M. and Pearson, G.W. (1986) High-precision calibration of the radiocarbon time scale, AD 1950 - 500 BC, **Radiocarbon, 28,** 805-838.

Swanson, F.J., Oyagi, N. and Tominaga, M. (1986) Landslide dams in Japan, in Schuster, R.L.(Ed.) **Landslide dams - processes, risk, and mitigation** (American Society of Civil Engineers, Geotechnical Special Publication 3), 131-145.

Swanson, T.W. and Pankaj, S. (1992) Chlorine-36 ages for the Puget and Okanogan lobes of the Cordilleran Ice Sheet and Cascade alpine glaciers of western Washington: Implications for the nature and timing of deglaciation, **Geological Society of America Abstracts with Programs** (Cordilleran Section, 88th Annual Meeting, May 11-13, 1992. Eugene, Oregon), 84.

Trenhaile, A.S. (1990) **The geomorphology of Canada** (Oxford University Press, Oxford), 240pp.

Trimble, S.W. (1975) Denudation studies: can we assume steady stream state?, **Science, 88,** 1207-1208.

Trimble, S.W. and Lund, S.W. (1982) Soil conservation and the reduction of erosion and sedimentation in the Coon Creek Basin, Wisconsin, **U.S. Geological Survey Professional Paper No. 1234.**

Vanoni, V.A.(Ed.)(1975) **Sedimentation engineering** (American Society of Civil Engineers, Manual and Reports on Engineering Practice, No. 54), 748pp.

Waitt, R.B. Jr. (1972) Geomorphology and glacial geology of the Methow drainage basin, eastern North Cascade Range, Washington, unpublished Ph.D. thesis, University of Washington, 154pp.

Waitt, R.B. Jr. (1977) Evolution of glaciated topography of upper Skagit drainage basin, Washington, **Arctic and Alpine Research, 9,** 183-192.

Waitt, R.B. Jr. and Thorson, R.M. (1983) The Cordilleran Ice Sheet in Washington, Idaho and Montana, in Porter, S.C.(Ed.) **Late-Quaternary environments of the United States, Volume 1. The late Pleistocene** (University of Minnesota Press, Minneapolis), 53-70.

Wan, G.J., Stantschi, P.H., Sturm, M., Farrenkothen, K., Lueck, A., Werth, E. and Shuler, Ch. (1987) Natural (^{210}Pb, ^{7}Be) and fallout (^{137}Cs, $^{239, 240}$Pu, ^{90}Sr) radionuclides as geochemical tracers of sedimentation in Greifensee, Switzerland, **Chemical Geology, 63,** 181-196.

Weirich, F.H. (1985) Sediment budget for a high energy glacial lake, **Geografiska Annaler, 67A,** 83-99.

Weis, P.L. (1969) Glacial drainage divide in the Skagit valley, Washington, **U.S. Geological Survey Professional Paper 650-C,** C71-C74.

Westgate, J.A., Smith, D.W.G. and Tomlinson, M. (1970) Late Quaternary tephra layers in southwestern Canada, in Smith, R.A. and Smith, J.W. (Eds.) **Early man and environments in northwest North America** (Proceedings of the Second Annual Paleoenvironmental Workshop, University of Calgary Archaeological Association, The Student's Press, Calgary, Alberta), 13-34.

Wolman, M.G. (1977) Changing needs and opportunities in the sediment field, **Water Resources Research, 7,** 1383-1392.

Yatsu, E. (1959) On the discontinuity of grain size frequency distribution of fluvial deposits and its geomorphological significance, **Reports of the Faculty of Engineering,** Chuo University, G-1, No. 27.

Yuzyk, T.R. (1986) **Bed material sampling in gravel-bed streams** (Sediment Survey Section, Water Survey of Canada, Environment Canada - IWD-HQ-WRB-SS-86-8), 63pp.